The Epigenetic Effects of Prenatal Alcohol Exposure in Human Autopsy Brain Tissue

By

Jessica S Jarmasz

A Thesis submitted to the Faculty of Graduate Studies

of The University of Manitoba

in partial fulfilment of the requirements of the degree of

DOCTOR OF PHILOSOPHY

Department of Human Anatomy and Cell Science

Max Rady College of Medicine

Rady Faculty of Health Sciences

University of Manitoba

Winnipeg

ABSTRACT

Fetal alcohol spectrum disorder (FASD) is 100% preventable, yet is the leading cause of developmental disability. Many *in vivo* studies in animals have established the effects of prenatal alcohol exposure (PNAE) on epigenetic processes in the developing brain. However, no studies directly assess epigenetic processes such as DNA and histone modifications in human brains. Therefore, I hypothesized that PNAE is associated with changes to epigenetic modifications in human brain cells. To test the hypothesis, I first identified a cohort of PNAE / FASD individuals that had undergone autopsy. Descriptive epidemiology and neuropathological findings were summarized for 174 cases. The brain abnormalities included: micrencephaly in 31, neural tube defects in 5, hydrocephalus in 6, corpus callosum defects in 6, prenatal ischemic lesions in 5, and minor subarachnoid heterotopias in 4. I then evaluated the effects of post-mortem delay (PMD) on the stability of epigenetic marks in mouse, pig, and human brain using Western blots and immunohistochemistry. I found all DNA cytosine modifications and most histone methylation marks were stable $\geq$72 hours. Histone acetylation marks varied, but the majority were stable $\geq$48 hours. A subset of the PNAE autopsy cases including fetuses and infants (21 weeks gestation to 7 months postnatal; N=18) were selected along with age-, sex- and PMD-matched controls to assess epigenetic modifications in brain previously shown in the experimental literature to be affected by PNAE. I also studied brain samples from a monkey model of PNAE. In human temporal lobe (7 specific regions), I found statistically significant increases in 5mC, 5fC, H3K27me3, H3K36me3, H3K9ac, H3K14ac and H3K27ac, decreases in 5mC, 5caC, H3K4me3, H3K27me3, H3K36me3, H3K9ac, H3K14ac, H3K27ac, H4K5ac, H4K12ac, and H4K16ac, and no change in 5hmC. Overall, H3K4me3 (active transcriptional mark) demonstrated a consistent decrease in 5 of the 7 brain regions studied. Among the macaques, the ependyma showed

statistically significant decreases among epigenetic marks 5fC, 5caC, H3K9ac, H3K9me2 / K9me3, and H3K36me3. Comparison of the human infant and macaque brain findings shows overlap in H3K9ac (ependyma- decreased in PNAE) and H3K36me3 (white matter – decreased in PNAE). In conclusion, I demonstrate that changes to specific epigenetic modifications on DNA and on histones occur in association with PNAE in the developing human brain. Human autopsy brain tissue is worth exploring in the context of epigenetics to understand the pathogenesis of FASD.

ACKNOWLEDGEMENTS

DEDICATION

To my father – this is my "Eroica"

TABLE OF CONTENTS

LIST OF TABLES AND FIGURES

ABBREVIATIONS

Δp: proton motive force

μg: microgram

μm: micrometer

μl: microliter

2-OG: 2-oxoglutarate

5caC: 5-carboxylcytosine

5fC: 5-formylcytosine

5hmC: 5-hydroxymethylcytosine

5hmU: 5-hydroxymethyluracil

5mC: 5-methylcytosine

9-THC: 9-tetrahydrocannabinol

A: adenine

Ac: acetylation

AceCS: Acetyl-CoA Synthetase

ACTH: adrenocorticotropic hormone

ADD: ATRX-DNMT3-DNMT3L domain

ADH: alcohol dehydrogenase

ADP: adenosine diphosphate

AHCY/SAH: S-adenosylhomocysteine hydrolase

AKR: Aldo-keto reductase family

AKT1: RAC-α serine / threonine-protein kinase

ALDH: acetaldehyde dehydrogenase

ALKBH5: Alpha-Ketoglutarate-Dependent Dioxygenase AlkB Homolog 5

AMPA: 2α-amino-3-hydroxy-5-methyl-4-isoxazolepropionic acid

AP: apurine / apyramidine

APEX1: AP endonuclease 1

ARBD: Alcohol-Related Birth Defects

ARC: arcuate nucleus

ARND: Alcohol-Related Neurodevelopmental Disorder

ASCL2: Achaete-Scute Family BHLH Transcription Factor 2

ATP: adenosine triphosphate

AUD: alcohol use disorders

AZA: 5-azacytidine

BAC: blood alcohol concentration

Bp: base pairs

BBB: blood-brain-barrier

BCO: beta-carotene oxygenase

BDNF: brain-derived neurotrophic factor

BER: base excision repair system

BHMT: Betaine-homocysteine *S*-methyltransferase

β-LPH: β-lipotropin

BMP: bone morphogenetic protein 4

BNST: bed nucleus of the stria terminalis

BrD / BRM: bromodomain

BSA: bovine serum albumin

C: cytosine

CA: Canada

CA1-4: *Cornu ammonis* 1, 2, 3 or 4

Ca2+: calcium

CADASIL: cerebral autosomal dominant arteriopathy with subcortical infarcts and leukoencephalopathy

CAF-1: Chromatin Assembly Factor 1

CaMKII: Ca2+/calmodulin-dependent protein kinase II

cAMP: adenosine monophosphate

CB1R / 2R: Gi-coupled cannabinoid type 1 / type 2 receptor

CBP: CREB binding protein

CBS: Cystathionine-β-synthase

CFS: child and family services

ChIP: Chromatin immunoprecipitation

Cl- : chloride

CNS: central nervous system

CoA: Coenzyme A

CpG: cytosine-phosphate-guanine

CR: Cajal-Retzius

CRABP: Cellular retinoic acid-binding protein

CRF: corticotropin-releasing factor

CSE: Ɣ-cystathionase

CSF: cerebrospinal fluid

CTCF: 11-zinc finger protein / CCCTC-binding factor

CX: temporal cortex

CXXC: Cys-X-X-Cys chromatin-associated binding domain

CYP: CP450 family of enzymes

DAB: diaminobenzidine

DG: dentate gyrus

DGAT: Diacylglycerol O-acyltransferase

DGCR8: Drosha and DiGeorge syndrome critical region gene 8

DHFR: Dihydrofolate reductase

DLK1: Delta-like 1 homolog

DLX: Distal-less homeobox

DMP: DNA methylation program

DMR: differentially methylated region

DNA: deoxyribonucleic acid

DNMT: DNA methyltransferase

DORV: double outlet right ventricle

DSH (DVL): dishevelled

DSM-5: Diagnostic and Statistical Manual of Mental Disorders

DTT: ditiothretol

e- : electron

EDTA: ethylenediaminetetraacetic acid

ELISA: enzyme-linked immunosorbent assay

EMX: empty spiracles homeobox

ESCs: embryonic stem cells

EtG: ethyl glucuronide

EtOH: ethanol / alcohol

EtS: ethyl sulfate

FAEE: fatty acid ethyl esters

FAS: Fetal Alcohol Syndrome

FASD: Fetal alcohol spectrum disorder

Fe2+: ferrous

FFPE: formalin-fixed paraffin-embedded

FGF: fibroblast growth factor

FOX01: Forkhead box protein 01

FTO: Alpha-Ketoglutarate-Dependent Dioxygenase FTO

g/mol: grams per mole (molar mass)

g: grams

G: gestational day

GABA: gamma-aminobutyric acid

GABBR1: Ɣ-aminobutyric acid type B receptor subunit 1

GABRG2: Ɣ-aminobutyric acid (GABA) A receptor Ɣ-2

GAD67: Glutamate decarboxylase

GCN5 / PCAF: histone acetyltransferase

GFAP: glial fibrillary acidic protein

GlyR: glycine receptor

GNA15: G protein subunit Alpha 15

GNMT: Glycine N-methyltransferase

GPCR: G protein-coupled receptor

GPX: glutathione peroxidase

GSH: reduced glutathione

GSS: Glutathione synthetase

GSSP: glutathione-protein mixed disulfide

GTL2: maternally expressed gene 3, MEG3

H+: hydrogen

H&E: hematoxylin and eosin Y

H_2O: water

H_2O_2: hydrogen peroxide

H3panAc: pan-acetyl histone H3

H4panAc: pan-acetyl histone H4

HAT: histone acetyltransferase

HCl: hydrochloric acid

HDAC: histone deacetylase

HDM: histone demethylase

HMT: histone methyltransferase

HPA: hypothalamic-pituitary-adrenal

hr: hour

HpaII: *Haemophilus parainfluenzae* methyltransferase restriction endonuclease

HRP: horseradish peroxidase

hrs: hours

HSC: Health Sciences Centre

ICR: imprint control region

Id2: inhibitor of differentiation 2

IF: immunofluorescence

IGF2: Insulin-like growth factor 2

IQ: intelligence quotient.

IV: intravenous

IHC: immunohistochemistry

IZ: intermediate zone

JMJD3: Jumonji domain 2

K+: potassium

KAT: lysine acetyltransferase

Kb: kilobase

Kd: kilodalton

kg: kilograms

KLH: keyhole limpet hemocyanin

L: litre

lncRNA: long non-coding ribonucleic acid

LRAT: Lecithin retinol acyltransferase

LSD: lysine demethylate

m6a: N6-methyl-adenosine

MAP: mitogen-activated protein

MAT: Methionine adenosyltransferase

MBD: methyl-CpG binding domain

Me: methylation

MeCP2: methyl binding protein

MeDIP-ChIP: Methylated DNA immunoprecipitation

Mef2C: Myocyte Enhancer Factor 2C

METTL: methyltransferase like

mg: milligrams

Mg2+: magnesium

mGluR: G-protein coupled receptor

miRNA: micro ribonucleic acid

ml: milliliters

mm: millimeter

mM: millimole

mol: mole

MR: magnetic resonance

MRI: magnetic resonance imaging

mRNA: messenger ribonucleic acid

MS: Methionine synthase

mtDNA: mitochondrial deoxyribonucleic acid

MTHFR: 5,10-methylenetetrahydrofolate reductase

MTR: 5-methyltetrahydrofolate-homocysteine methyltransferase

MYST: lysine acetyltransferase 8

MZ: marginal zone

NAc: nucleus accumbens

NaChIP: native chromatin immunoprecipitation

nAChRs: nicotinic acetylcholine receptors

NAD+ / NADH: nicotinamide adenine dinucleotide

ND-PAE: Neurobehavioral Disorder associated with Prenatal Alcohol Exposure

nm: nanometers

NMDA: N-methyl-D-aspartate

NMDAR: N-methyl-D-aspartate receptor

NO•: nitric oxide

NOO^- : peroxynitrite

NPCs: neural precursor / progenitor cells

NTDs: neural tube defects

NVU: neurovascular unit

O_2 : oxygen

O_2- : superoxide

OH: hydroxyl group

OLIG: oligodendrocyte transcription factor

OTX: orthodenticle homeobox

P: postnatal day

p300/CBP: E1A binding protein p300 / CREB-binding protein

p53: tumor suppressor protein 53

PAX: paired box

PBS: phosphate-buffered saline

PC: post-conception

PCR: polymerase chain reaction

PDA: patent ductus arteriosus

PEth: phosphatidyl ethanol

pFAS: partial FAS

PGC: primordial germ cell

PGC-1α: peroxisome proliferation-activated receptor ɣ coactivator 1α

pH: potential hydrogen (acidity level)

PHD: plant homeodomain

PHF8: PHD finger protein 8

Pi: inorganic phosphate

PIC: preinitiation complex

PKA: protein kinase A

PKC: protein kinase C

PLGF: placental growth factor

PMD: post-mortem delay

PMSF: phenylmethylsulfonyl fluoride

PNAE: prenatal alcohol exposure

POMC: proopiomelano-cortin

PP: transient preplate

PRDM9: PR domain zinc finger protein 9

PTM: post-translational modification

PTSD: post-traumatic stress disorder

PVDF: polyvinylidene difluoride

PVN: paraventricular nucleus

PWWP: Pro-Trp-Trp-Pro domain

QC: Quebec

QH_2 : Coenzyme Q

RALDH: retinaldehyde dehydrogenase

RAR: RA receptors

RDH: Retinol dehydrogenase

RNA: ribonucleic acid

ROS: reactive oxygen species

RT-PCR: reverse transcription polymerase chain reaction

RTT109: fungal-specific histone acetyltransferase

RXR: retinoid X receptors

Rzrβ: retinoic acid receptor related orphan beta

SAM: S-adenosylmethionine

SAMDC: S-adenosylmethionine decarboxylase

SDHAP3: succinate dehydrogenase complex flavoprotein subunit A pseudogene 3

SDS: sodium dodecyl sulfate

SDS-PAGE: sodium dodecyl sulfate–polyacrylamide gel electrophoresis

SEM: standard error of the mean

SES: socioeconomic status

SET: lysine methyltransferase

SHH: sonic hedgehog

SHMT: serine hydroxymethyltransferase

SIDS: sudden infant death syndrome

SIRT: sirtuin

SN: substantia nigra

SOD: superoxide dismutase

SOX: sex determining region Y-box

SP: subplate

snRNA: small nuclear ribonucleic acid

ssRNA: single stranded ribonucleic acid

STI: sexually transmitted infection

SUDI: sudden unexplained death of an infant

SVZ: subventricular zone

SWI / SNF: mating-type switching / sucrose non-fermenting pathway

T: thymine

TAAR: Trace amine-associated receptor

TBE: Tris-borate-EDTA

TBS: Tris-buffered saline

TDG: thymine DNA glycosylase

TE: temporal ependyma

TET: ten-eleven translocation methylcytosine dioxygenase

TGF (BMP): Transforming growth factor-beta bone morphogenic protein

TIP60: histone acetyltransferase KAT5

tRNA: transfer ribonucleic acid

TS: transcription start site

TSA: Trichostatin A

UHRF: ubiquitinases

UPD6: uniparental disomy of chromosome 6

UTR: untranslated region

UTX: Ubiquitously transcribed tetratricopeptide repeat, X chromosome

VACTERL: vertebral defects, anal atresia, cardiac defects, tracheo-esophageal fistula, renal anomalies, and limb abnormalities

VGCC: voltage-gated Ca2+ channels

Vs: versus

VSD: ventricular septal defect

VTA: ventral tegmental area

VZ: ventricular zone

w: weeks

WD40: Trp-Asp (W-D) beta-transducin repeats

WM: white matter

WNT: wingless-related integration site

WTAP: Pre-mRNA-splicing regulator

ZIC: zic family member proteins

ZFP57: KRAB zinc finger protein

CHAPTER 1: LITERATURE REVIEW

The licit drug, alcohol (ethanol) is the primary subject of this thesis. Alcohol consumption has a widespread dose-dependent effect on the body and brain, and is a toxic substance. In adults, alcohol consumption contributes to the development of many pathologies. Prenatal alcohol exposure (PNAE) can affect the development, growth and function of the placenta (Behnke, & Smith, 2013; Carter, Wainwright, Molteno, et al., 2016; Wang, Tikellis, Sun, et al., 2014). It can affect brain development, cause birth defects, neural tube defects (NTDs), and is associated with Fetal Alcohol Spectrum Disorder (FASD) (Bailey, & Sokol, 2011; Chih-Ping Chen, 2008; Senturias, 2014). To understand the pathogenesis of FASD, several bodies of knowledge must be combined. These include an understanding of: human brain development, the effects of alcohol in the adult brain as well as the developing human brain, animal model studies of FASD, epigenetics, and epigenetic studies in the context of FASD. It is these topics that will be primarily discussed in this thesis. In particular, I explore how ethanol influences epigenetic modifications and how those changes impact the organism with regard to development. A general overview of alcohol consumption and its biological and social consequences are summarized in **Figure 1.1**. In addition, a substantial part to this thesis work is attempting to bridge animal model results to the human condition through the use of human autopsy tissue. Therefore, the final section to the thesis introduction addresses the use of human autopsy material.

Figure 1.1. The impact of alcohol consumption and metabolism (blue) on biological systems (green), and the health and social (pink / orange) consequences.
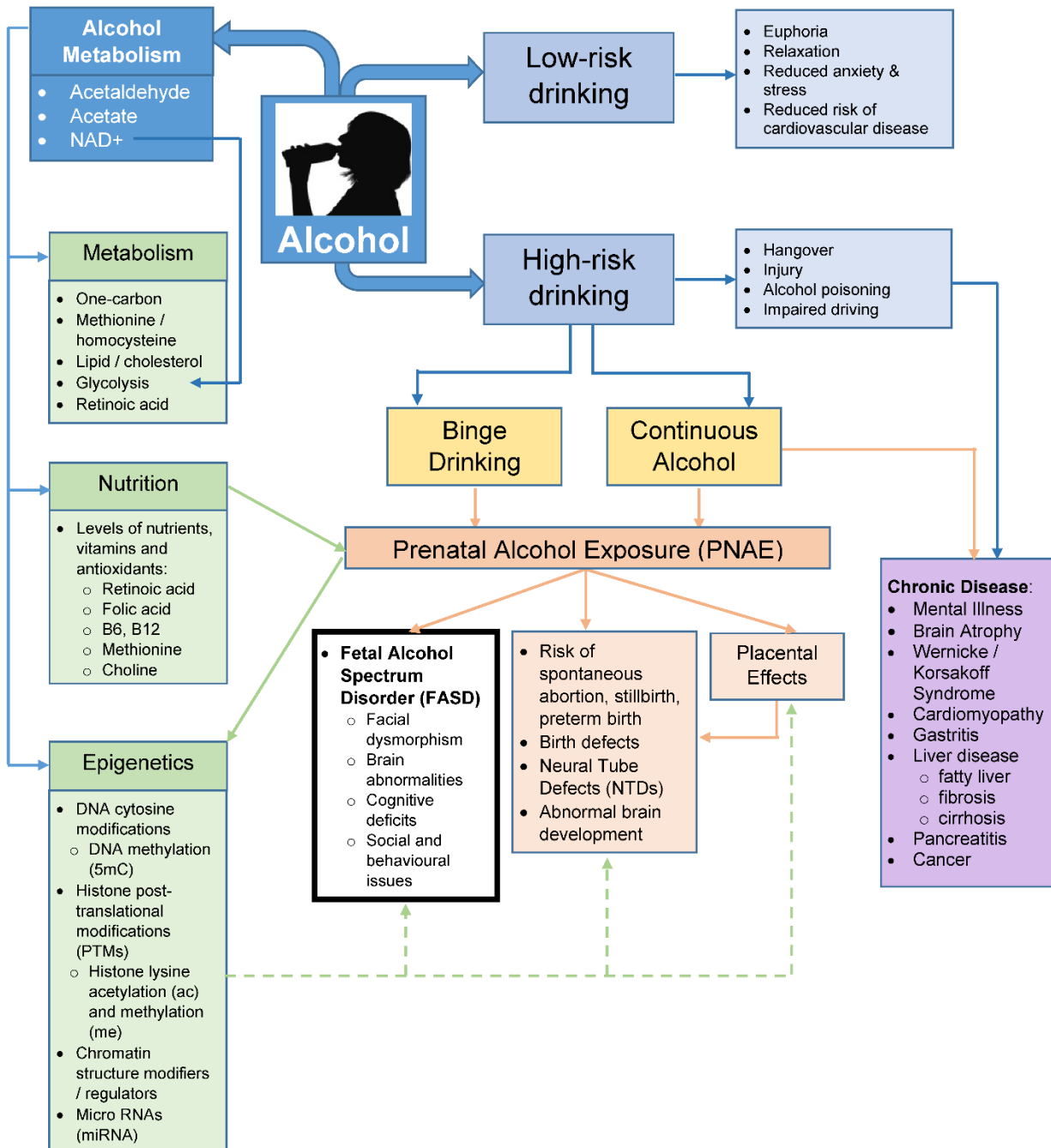
Human Brain Development

Primary Neurulation

Normal human development begins post fertilization at the start of the third week of gestation (Sadler, 2005). In the developing embryo, neurulation (the development of the neural tube), overlaps gastrulation (the formation of the ectoderm, mesoderm and endoderm) (**Figure 1.2**). The central nervous system (CNS) (brain and spinal cord) and epidermis form from the ectoderm. During the third week of gestation, the midline and anterior-posterior axes surface, guided by the movement of the primitive streak (mesenchymal cells along the midline). This occurs in the caudal region of the embryo which marks the start of gastrulation. This leads to formation of the notochord when the ectoderm undergoes invagination. The notochord initiates the differentiation of most ectodermal cells to neuronal precursor / progenitor cells (NPCs), which in turn establishes the neural plate (just above it) and signals the start of neurulation (Purves, Augustine, Fitzpatrick, et al., 2004; Sadler, 2005; Stiles, & Jernigan, 2010). A gradient of signalling molecules and transcription factors guides this process, resulting in the induction and suppression of various genes. These molecules include retinoic acid and various peptide hormones encoded by: *WNT, FGF, TGF (BMP), SHH*, and *DSH (DVL)* genes, as well as transcription factors encoded by: *DLX, EMX, OTX*, and *PAX* genes (Purves, Augustine, Fitzpatrick, et al., 2004; Stiles, & Jernigan, 2010; ten Donkelaar, 2000). The neuronal groove forms once the neural plate elongates and begins to fold. During the end of the third week and the start of the fourth week of gestation, the neural folds meet and fuse, eventually forming a tubular structure called the neural tube. The cranial / rostral (anterior) and caudal (posterior) parts of the neural tube (termed neuropores) close shortly after; anterior neuropore closure is around gestational day 24 / 25, and posterior closure is around day 27 / 28

(Purves, Augustine, Fitzpatrick, et al., 2004; Sadler, 2005; Stiles, & Jernigan, 2010). During neurulation, the neural crest cells (which are located dorso-lateral to the neural tube) migrate and differentiate into the sensory and sympathetic ganglia cells, adrenal neurosecretory cells and the enteric nervous system cells. The neural floorplate (ventral to the neural tube) gives rise to the motor neurons and determines the polarity of the neural tube. The remaining ectodermal cells differentiate into the epidermis and the neural tube gives rise to the entire CNS (Purves, Augustine, Fitzpatrick, et al., 2004; Sadler, 2005; Stiles, & Jernigan, 2010).

Figure 1.2: The differentiation of human embryonic stem cells (ESCs) into the three cellular layers that form the human body and CNS.
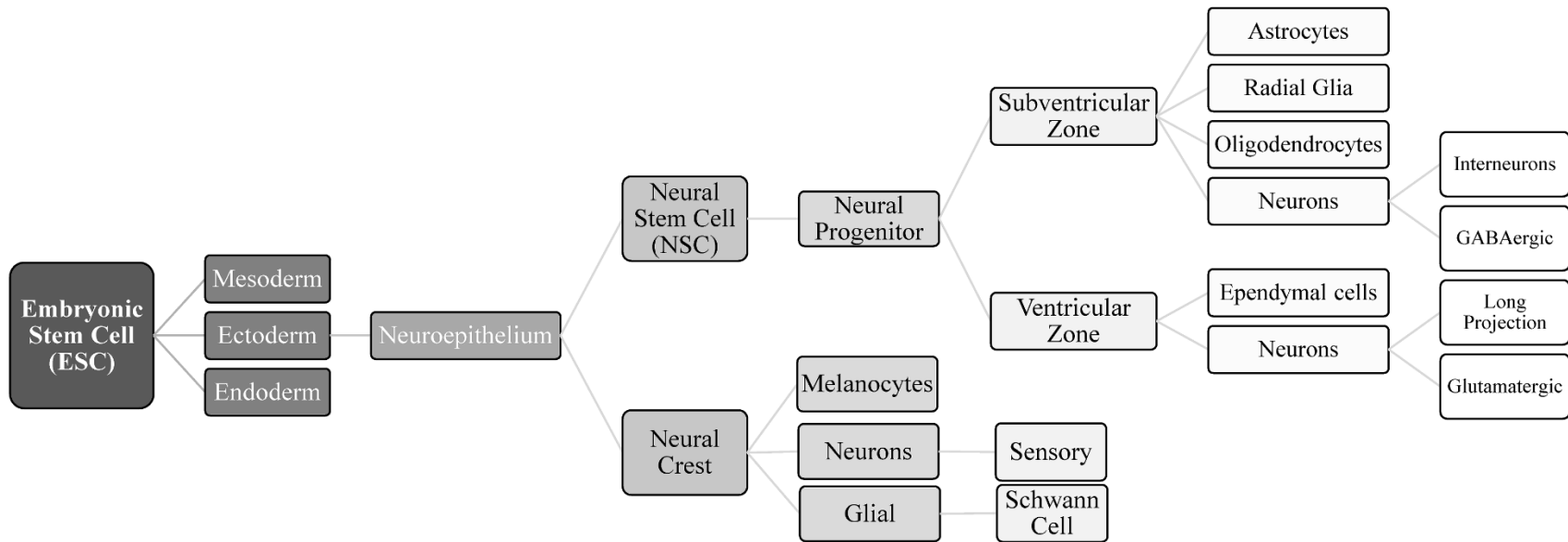
Brain Cell Development.

Neuronal precursors (derived from the neuroepithelium) of the neural tube commence the patterning of the major structures of the brain during the fourth week of gestation via various signalling molecules and gene expression gradients. The neural floorplate, which is the ventral aspect of the neural tube, gives rise to motor neurons. It starts at the primary vesicles, followed by the rise of ganglionic / ventricular eminences (germinal matrix) and the establishment of the prosencephalon (forebrain), the mesencephalon (midbrain), and the rhombencephalon (hindbrain). Further differentiation leads to the formation of the telencephalon and diencephalon (from the prosencephalon) as well as metencephalon and myelencephalon (from the rhombencephalon). Neuron production starts during the sixth week of gestation in the proliferative ventricular zones. By the eighth week of gestation, which is the end of the embryonic period in humans, the major compartments of the CNS and peripheral nervous systems are defined (Purves, Augustine, Fitzpatrick, et al., 2004; Stiles, & Jernigan, 2010).

The NPCs proliferate, migrate and differentiate into neurons and glial cells. The rudiments of most major brain regions are formed by the 12th week of gestation, except for the corpus callosum and cerebellum (Stiles, & Jernigan, 2010). The telencephalon gives rise to the cerebral cortex, the hippocampus, the basal ganglia, and the olfactory bulbs. The diencephalon gives rise to the hypothalamus, thalamus and optic cups (retinas). The metencephalon gives rise to the pons and cerebellum (Purves, Augustine, Fitzpatrick, et al., 2004; ten Donkelaar, 2000). The corpus callosum, which consists of axons that connect the two hemispheres, develops between 12 and approximately 16-20 weeks gestation (Rakic, & Yakovlev, 1968). From the 20th to the 36-38th week, as brain volume increases, folds develop on the surface and they invaginate to form the gyri and sulci. During the third trimester, myelination of axons by differentiated

oligodendrocytes begins in the spinal cord and brainstem. The thalamocortical and corticothalamic tracts are established by the 26th week of gestation. At full term the human brain is approximately a third of its adult volume and weight. Most cell proliferation is complete in the cerebrum, although it continues in the cerebellum until approximately nine months postnatal. The brain doubles in size during the first year of life. Early life experiences determine the number of connections that remain (and become myelinated) through complex processes, which are also influenced by the environment. Maturation of cells, including synaptogenesis and myelination, continues for years (Stiles, & Jernigan, 2010; ten Donkelaar, 2000). During this period, neuronal cell body expansion associated with synaptogenesis and the accumulation of myelin accounts for the increased size. By the age of 6, the brain reaches approximately 90% of the total adult volume. By age 10, the brain has reached its full size, however frontal lobe synaptic circuitry and myelination are not complete until approximately 25-30 years of age (Stiles, & Jernigan, 2010; ten Donkelaar, 2000). For an overview of human brain development, please see **Figure 1.3**.

Specific Brain Region Development

The primary brain regions of interest in this thesis are the temporal cerebrum and hippocampus. Therefore, the development of these brain structures along with the blood brain barrier, are discussed in greater detail below.

Figure 1.3: Proposed developmental timeline of human brain cell proliferation, migration, differentiation and maturation from implantation to adulthood.

Timeline headers: First Trimester | Second Trimester | Third Trimester | Birth | Childhood | Adolescence | Adulthood

Week/age markers: 1 … 12 | 13 … 24 | 25 … 38 | 1 … 5 … 30

First Trimester			Second / Third Trimester	Childhood–Adulthood
Neuru-lation	Brain regions	Prosencephalic Development	Neural cell maturation, organization, synaptogenesis, and early axonal myelination	Synaptogenesis, continued myelination
		Neural proliferation (High)	Neurogenesis (Low)	Neurogenesis (very low) - only in dentate gyrus and cortex
		Neural migration		
		Gyrification		
			Myelination (Low) – Brainstem, Spinal Cord, Visual Pathways	Myelination (High) / Myelination (Low)
	Radial Glia	Early gliogenesis	High Gliogenesis	
		Early Synaptogenesis	High Synaptogenesis & Pruning	Minimal Synaptogenesis & Pruning

The Germinal Matrix

Located next to the lateral ventricles, the germinal matrix gives rise to all the neurons and glial cells of the brain. Neurogenesis begins at around the sixth week of gestation, and by the 12th week of gestation, neurons and glia migrate radially outward from the germinal matrix towards the cerebral cortex and subsequently to all other regions of the brain (Adle-Biassette, Harding, & Golden, 2018; ten Donkelaar, 2000). The germinal matrix is broken down into the ventricular zone (VZ) and the subventricular zone (SVZ). The VZ contains radial glial cells, and progenitors that give rise to glutamatergic neurons as early as 8 weeks gestation. These glutamatergic neurons use radial glia to migrate out into the neocortex to give rise to the 6 layers of the cortical mantle. Post-mitotic neurons born later in the SVZ migrate in a non-radial manner and eventually form the GABAergic inhibitory interneurons that have only short, local connections. The SVZ also gives rise to precursors of astrocytes and oligodendrocytes. The size of the SVZ peaks between 23–25 weeks gestation, however NPC proliferation in the SVZ peaks between 20–26 weeks, and then begins to resolve by 30–32 weeks. The cerebral SVZ largely involutes by approximately 32-34 weeks gestation, by which time most neuronal and glial cells have been generated. The caudal ganglionic eminence generates GABAergic interneurons for the nucleus accumbens, hippocampus and amygdala, continuing to approximately 35 weeks gestation. The medial ganglionic eminence produces GABAergic interneurons for the neocortex and thalamus, continuing to approximately 27 weeks gestation (Arshad, Vose, Vinukonda, et al., 2016). Glial cells mature largely during the first half of postnatal life, and make up almost 90% of total brain cells, owing to the large volume of white matter in the human brain. Glial precursors and NPCs persist in small quantities in the SVZ into adulthood. These are capable of later differentiating,

often in response to brain injury (Adle-Biassette, Harding, & Golden, 2018; Arshad, Vose, Vinukonda, et al., 2016; Stiles, & Jernigan, 2010).

The Blood-Brain-Barrier (BBB)

The blood-brain-barrier (BBB) exists throughout the brain except in the small circumventricular organs and the choroid plexus. The BBB of the spinal cord forms before that of the telencephalon (Risau, & Wolburg, 1990). The BBB develops by embryonic (E) days 15 /16 in rats which, is roughly equivalent to E57-65 in humans (~8-9 weeks gestation) (Goasdoué, Miller, Colditz, et al., 2017; Risau, & Wolburg, 1990). The BBB matures during the rest of human gestation and occurs postnatally in rodents, where interendothelial tight junctions gradually "tighten". In rats, this peaks by postnatal (P) day 5-9, which is approximately equivalent to late third trimester in humans (Risau, & Wolburg, 1990). The developing BBB is said to be more permeable in order to keep up with the biochemical demands of the developing brain (Goasdoué, Miller, Colditz, et al., 2017; Saunders, Liddelow, & Dziegielewska, 2012). Pericytes wrap around the endothelial layer and maintain the integrity of the capillaries. Astrocytic "endfeet" are in direct contact with the BBB and are essential for the later stages of development as well as maintenance of the barrier. Microglia and basement membrane components also contribute to the BBB. Together this is the neurovascular unit (NVU), which is increasingly being used to reflect all the functional and associative components of the BBB (Goasdoué, Miller, Colditz, et al., 2017; Saunders, Liddelow, & Dziegielewska, 2012). The mature NVU blocks the passage of hydrophilic drugs, toxins, pathogens, and xenobiotics thereby protecting the nervous system and maintaining brain homeostasis. The brain has other barrier mechanisms in place. The arachnoid is a barrier between cerebrospinal fluid (CSF) and the dura,

the glia limitans between CSF and the extracellular fluid of the brain, and the CSF-blood barrier in the epithelial cells of the choroid plexus (Ek, Dziegielewska, Habgood, et al., 2012; Saunders, Liddelow, & Dziegielewska, 2012).

The Hippocampus

The general structure of the hippocampus, which is part of the archicortex (phylogenetically the oldest region of the brain), is seen by 15 weeks gestation. The dentate gyrus (DG) and hippocampus proper (*Cornu ammonis* (CA3, CA2 and CA1)) are present along with the subiculum. By 32 weeks gestation, the CA4 region appears. At term, the hippocampus cytoarchitecture resembles the adult hippocampus, however at age two, full hippocampal cytoarchitecture is present. The hippocampal pyramidal neurons of the CA are generated by 24 weeks gestation, but even at term, the neurons remain small and immature in appearance (especially in the CA1 sector) and enlarge thereafter. Granule neurons of the dentate gyrus are generated as early as 11 weeks, and continue with moderate frequency throughout gestation into the first postnatal year (Arnold, & Trojanowski, 1996; Yang, Zhang, Shi, et al., 2014). Recent evidence indicates that postnatal generation is rare in childhood and negligible after 13 years of age (Sorrells, Paredes, Cebrian-Silla, et al., 2018). This is contrary to previous claims that neurogenesis continues well into adulthood, particularly among granule cells of the dentate gyrus in the VZ of the lateral ventricle, but at considerably lower levels (Boschen, & Klintsova, 2017).

The Neocortex

The cerebral cortex comprises almost 80% of total human brain volume. The cortical lamina (the 6 cortical layers; **Figure 1.4**) begin to develop around the sixth week of gestation,

where most neurons with long projections (contralateral, brainstem, spinal cord) are produced up until the 18th week of gestation. During the embryonic period, the first wave of migrating neurons from the VZ extend across the intermediate zone (IZ) to form the transient preplate (PP) in the developing neocortex (pallium). The second wave of migrating neurons divide the PP into the marginal zone (MZ) and the subplate (SP). The MZ (including the Cajal-Retzius (CR) neurons) contribute to the superficial cortical laminae and the SP gives rise to the deeper laminae. CR cells in the MZ regulate the inside-out pattern of neuronal migration by secreting reelin. Meaning, the deepest cortical lamina (layers 6-4) form before the superficial layers (3-1). The first set of migrating neurons from the VZ settle between the MZ and SP, subsequently forming the cortical plate and layer 6 (eventual white matter) of the cortical lamina by 12 weeks gestation, followed by another wave of migrating neurons to form the following cortical layer by the 14th week (layer 5; internal pyramidal layer). The second and third layers form by the 27th week of gestation, and the final layer (outer layer) closer to term. The corpus callosum is comprised of axons from neurons of the external pyramidal layer. In the maturing cerebral cortex, the MZ and SP "boundaries" essentially disappear by the late fetal period, and the IZ becomes the white matter of the cerebrum (Stiles, & Jernigan, 2010; ten Donkelaar, 2000).

Figure 1.4: Human neocortical lamination.
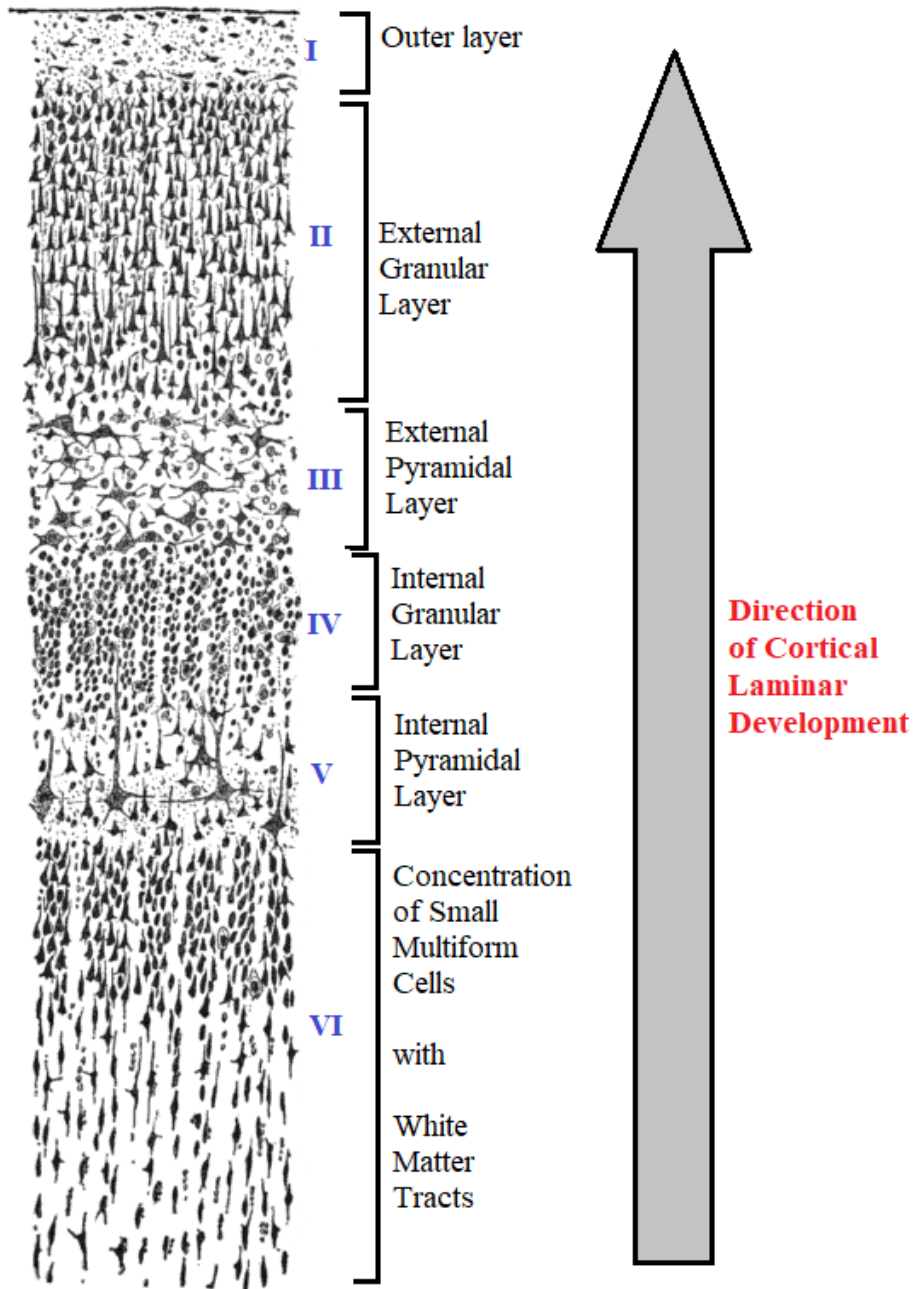
Image modified and taken from:

Abnormal Human Brain Development

The primary brain developmental events are: VZ proliferation, radial migration of neuronal precursors (long projections), SVZ proliferation, non-radial migration of inhibitory interneuron and glial progenitors, organization, and maturation (including axon elongation, synaptogenesis, myelination). In any given region of the brain, this occurs sequentially, but because different regions of the CNS mature at different times, all of these processes occur simultaneously. Various genes, transcription factors, and proteins guide proper brain development (**Table 1.1**). Differentiated brain cells will even produce signalling molecules or secrete proteins to help guide the differentiation or maturation of other brain cells (e.g settled Purkinje cells secrete sonic hedgehog (SHH) protein which in turn triggers the expansion of granule cell progenitors (ten Donkelaar, Lammens, Wesseling, et al., 2003)). Abnormal brain development leads to a variety of neurodevelopmental disorders which can be linked to interference of these processes at any neurodevelopmental time point (**Table 1.2**) (Ernst, 2016; Volpe, 2000). Genetic mutations (**Table 1.1**), nutritional effects, or toxins can affect different regions in different ways, even with a single exposure.

Comparative Inter-Species Brain Development

Excluding human specific features, much of what we have learned about the molecular aspect of brain development has come from animal models. The duration of mammalian gestation roughly reflects the lifespan and mature brain size, with the added factor of behavioural adaptation to the environment. Mice and rats have short gestations of 18 and 20 days (respectively), very immature newborns, and lifespans of approximately 2 and 3 years (respectively). Human gestation is 270 days (40 weeks) with a lifespan of approximately 80-90

years, and ambulation (walking) begins around one year of age. Higher level non-human primates have shorter gestations, mature earlier, and have shorter lifespans than humans. Elephants have a gestation of approximately 665 days (95 weeks) and a lifespan of approximately 50-80 years. However, elephant newborns (as well as those of a wide range of herbivores) are able to walk within minutes of birth because their brains are relatively more mature than those of newborn human and non-human primates (Herculano-Houzel, 2009).

Rodents have been suitable experimental subjects for elucidating the basic principles of brain development, but the timing of brain development, and the cytoarchitecture are very different from humans (**Figure 1.5**). For example, the average adult human brain weighs ~1,500g and contains ~86,000 million neurons, whereas the rat brain weighs ~1.8g and contains ~200 million neurons. That makes the human brain ~800X larger than the rat brain and contains ~430X more neurons (Herculano-Houzel, 2009). In humans, the corpus callosum begins to develop at the beginning of the second trimester (12 weeks) and is completed by the 20th week, while in mice and rats, the corpus callosum begins on embryonic day 17 and 19 (respectively) and finishes by postnatal days 7 / 8 (Stiles, & Jernigan, 2010). There are many differences between human and mouse neocortex as well. In humans, neuronal density is lower but dendritic and axonal branching is higher. Cortical maturation is also much longer, surpassing puberty and adolescence (Geschwind, & Rakic, 2013). Because higher order mammals have large brains, the surface folds to form gyri and sulci. This allows a larger number of neurons to be packed into a given volume. Rodent brains, in contrast, are small with smooth surfaces (lissencephalic) (Rajagopalan, Scott, Habas, et al., 2011). Because of the considerable differences in brain development and structure, rodent models to study the teratogenic effects of drugs and alcohol might not be entirely representative of the human situation (Knight, 2007).

Table 1.1: Examples of proteins and transcription factors that play a role in brain development[A].

Mutations / alterations in these genes have been associated with Fetal Alcohol Spectrum

Disorder (designated by an asterisk*).

Proteins and transcription factors essential for brain development	Role	Mutation / defect consequences	Associated disorders
Sonic hedgehog (SHH)	Patterning of the ventral neural tube, the anterior-posterior limb axis, and the ventral somites; Purkinje migration	Holoprosencephaly*, Preaxial polydactyly	VACTERL* (vertebral defects, anal atresia, cardiac defects, tracheo-esophageal fistula, renal anomalies, and limb abnormalities)
Reelin	Extracellular matrix protein thought to control cell-cell interactions critical for cell positioning and neuronal migration during corticogenesis	Lissencephaly*, Cerebellar hypoplasia*	Schizophrenia, autism, bipolar disorder, major depression, temporal lobe epilepsy
SRY-box 2 (SOX2)	Required for stem-cell maintenance in the central nervous system	Optic nerve hypoplasia*, Microphthalmia*	
Zic family member proteins (ZIC1, ZIC2, ZIC4, ZIC5)	Important for proper neural crest and granule cell development	Medulloblastoma, Dandy-Walker malformation*	X-linked visceral heterotaxy, Holoprosencephaly type 5
Oligodendrocyte transcription factor 2 (OLIG2)	Ventral neuroectodermal progenitor cell fate		T-Cell acute lymphoblastic leukemia, Down syndrome
Bone morphogenetic protein 4 (BMP4)	Regulates heart development and adipogenesis	Orofacial cleft* and microphthalmia*	
Notch3	Neural development		Cerebral autosomal dominant arteriopathy with subcortical infarcts and leukoencephalopathy (CADASIL)
Orthodenticle homeobox 2 (OTX2)	Brain, craniofacial, and sensory organ development; influences the proliferation and differentiation of dopaminergic neuronal progenitor cells during mitosis	Microphthalmia*	Medulloblastoma

[A] information for this table was taken from the https://www.ncbi.nlm.nih.gov/gene/ website by searching for gene symbol

Table 1.2: Resulting malformations and disorders of improper brain development.

Primary neurulation (neural tube) disorders	Prosencephalic Development Disorders	Neuronal Proliferation & Migration	Neuronal Organization	Myelination Disorders
• Craniorachischisis totalis • Anencephaly • Encephalocele • Myelomeningocele	• Holoprosencephaly • Agenesis of the corpus callosum of septum pellucidum	• Micro- and macro-cephaly • Lissencephaly • Heterotopias • Partial or full agenesis of the corpus callosum	• Cortical dysplasia • Mental retardation (including Trisomy 21, Fragile-X etc.)	• Demyelination

Figure 1.5: How human gestation aligns with other species.
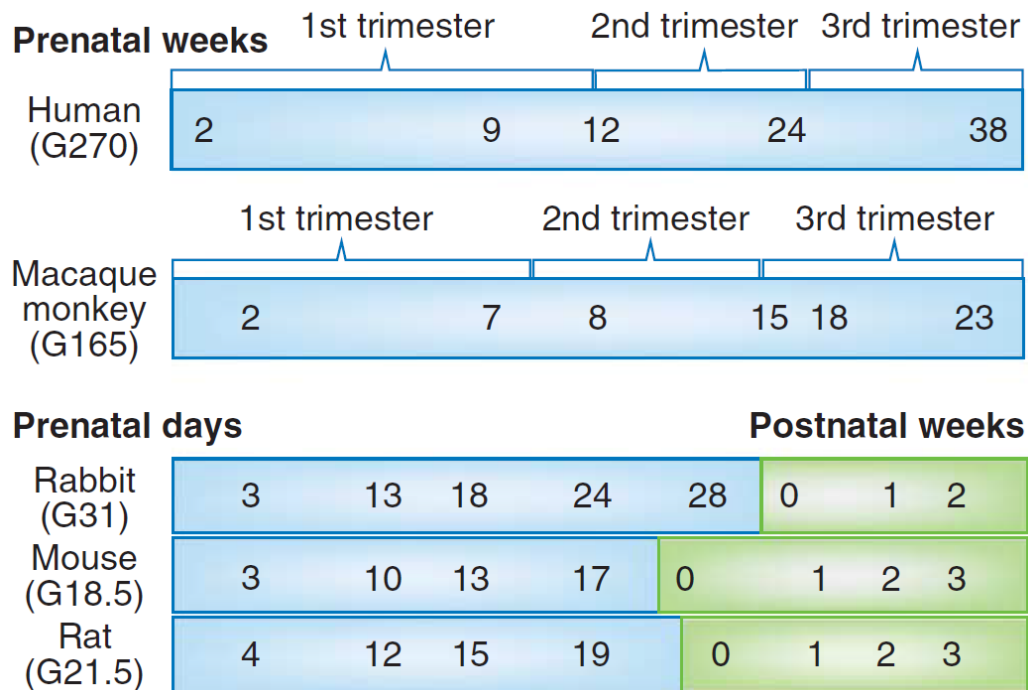
Figure taken directly from Ross *et al*. 2014. *Neuropsychopharmacology Reviews* (2015) 40, 61–

87. Permission to re-use figure obtained on March 29, 2018.

16

Alcohol

What is Alcohol?

Alcohols are organic compounds with a hydroxyl group (-OH) bound to a saturated carbon. Unless otherwise specified, in this thesis the term "alcohol" refers to ethanol, whose chemical formula is C_2H_5OH. Alcohol is classified as a psychoactive drug that has a widespread dose-dependent multisystemic effects on the body and brain. An alcoholic beverage is a drink that contains 3-40% of total alcohol. In Canada, one standard alcohol consumption unit contains 14g of ethanol (17ml) which is either one 355ml beer, 148ml wine, 89ml fortified wine or 44ml hard liquor (e.g. gin, vodka, whiskey etc.). Depending on family history (e.g. genetics), light to moderate use of alcohol can decrease the risk of cardiovascular disease (CPHO, 2015; Hannuksela, Liisanantti, & Savolainen, 2002). In higher doses (high-risk drinking), alcohol acts as a depressant and causes intoxication, which can lead to stupor, speech and motor delay, or unconsciousness. People around the alcohol abuser can experience violence, abuse, or familial conflict. Alcohol abusers are at risk for poor decision making, such as driving under the influence. Impaired driving injures or kills innocent people (World Health Organization, 2014). In Canada, 72,039 impaired driving incidents were reported by police in 2015, where 0.2% of incidents resulted in death and 0.8% caused bodily harm (Perreault, 2016).

Low-risk drinking in men and women differ due to bodyweight, particularly among the ratios of body water volume and body fat. Low-risk drinking in men is 2-3 standard drinks per day, up to a maximum of 14 drinks per week (196g of ethanol per week). Low-risk drinking in women is 1-2 standard drinks per day, up to a maximum of 9 drinks per week (126g of ethanol per week). High-risk drinking is defined as 5 or more standard drinks in one sitting ($\geq$70g of ethanol) which is also called "binge" drinking. High-risk / binge drinking can lead to the

development of alcohol use disorder, which is when an individual becomes dependent on alcohol and suffers from withdrawal when alcohol consumption ceases, creating a negative feedback loop which reinforces the need for that person to drink (CPHO, 2015; Crabbe, Harris, & Koob, 2011). This, as well as the consequences of alcohol use, is discussed later.

Statistics on Consumption

In 2013 / 14, Canadians spent an estimated $20.5 billion dollars on alcoholic beverages. The most popular alcoholic beverage in Canada is beer (51% of alcoholic beverages by volume consumed), followed by distilled spirits (27%), then wine (22%). In 2012, 22 million (almost 80%) of Canadians (age 15+) drank alcohol. The proportion of the Canadian population that partook in heavy drinking in 2014 was 17.9% (men 22.7%, women 13.2.%). In 2010, the costs related to impaired driving alone was estimated at $20.6 billion a year. In 2012, 5.9% of all global deaths were attributable to alcohol consumption; higher in men (7.6%), than in women (4%) (CPHO, 2015).

Distribution of Alcohol Throughout the Body

When alcohol is consumed, it enters the alimentary canal through the mouth, flows down the esophagus and enters the stomach. Most alcohol will move to the small intestine if no food is present in the stomach. If food is present, the pyloric sphincter closes in order to facilitate proper digestion of the food, which in turn slows the absorption of alcohol. Alcohol is absorbed by passive diffusion through the gastro-intestinal mucosa which is lined with epithelial cells. Ethanol, which is a small (46 g/mol) polar lipophilic molecule, readily crosses lipid bilayers of cells. The stomach absorbs ~20% of ethanol and the small intestine ~80%. Alcohol passively

diffuses into capillaries, then into the portal vein via the left and right gastric veins and the

inferior and superior mesenteric veins. The portal vein drains into the liver where ~90% of

alcohol is metabolically eliminated in hepatic cells. The hepatic vein takes the remaining blood-

borne alcohol into the inferior vena cava, through the right heart (atrium and ventricle), and

lungs (by way of the pulmonary artery), and eventually into the general circulation. At this point,

alcohol can travel to the brain by way of the aorta and carotid arteries (Abdel-Misih, &

Bloomston, 2014; K. L. Moore, Agur, & Dalley, 2011), and passes through the NVU because it

is small and lipophilic. It is postulated that the choroid plexus is the main barrier mechanism in

the developing fetal brain. CSF production and extracellular fluid turnover are low in the

developing fetal brain. Therefore alcohol can remain longer in the fetal brain than in the adult

brain (Ek, Dziegielewska, Habgood, et al., 2012).

Metabolism and Toxic Consequences

Five percent of alcohol is removed from the body through non-metabolic pathways such

as sweat, breath, urine, and feces. The liver metabolizes (through oxidation) ~90% of alcohol in

hepatocytes primarily by alcohol dehydrogenase (ADH), and to a lesser extent by enzymes of the

Cytochrome P450 (CP450) family (CYP2E1, 1A2, and 3A4) and catalase (Cederbaum, 2012).

This elimination path (**Figure 1.6**) is the rate-limiting step to alcohol metabolism, and is

dependent on the blood alcohol concentration (BAC) (Cederbaum, 2012). The greater the BAC

level, the more saturated the elimination pathway becomes. It also depends on the rate of gastric

emptying, available nutrients and the type of alcohol beverage consumed. Women and men

metabolize alcohol differently. Women generally metabolize alcohol at a slower rate than men,

leading to higher BACs. This is because women have a combination of low body water volume

and higher body fat levels in comparison to men (Cederbaum, 2012). A small fraction (~5%) of alcohol is also oxidized in the gastrointestinal tract, the kidneys and the brain. The enzymes responsible in the brain are catalase (~60% of all metabolism), CYP2E1 (~20% of all metabolism), and ADH (~20% of all metabolism) (Cederbaum, 2012).

Once alcohol is oxidized by ADH, it produces nicotinamide adenine dinucleotide (NADH) and acetaldehyde, which is a highly reactive and toxic by-product of ethanol metabolism (Zakhari, 2006). Acetaldehyde is the product responsible for the negative feeling of intoxication (nausea, vomiting, hypotension and tachycardia) (Cederbaum, 2012; Wall, Luczak, & Hiller-Sturmhöfel, 2016), as well as a contributing factor to the "hangover" (Swift, & Davidson, 1998). Acetaldehyde is further oxidized into acetate and NADH by acetaldehyde dehydrogenase (ALDH) 1 and 2. Acetate is then metabolized to acetyl coenzyme A (Acetyl-CoA) (Cederbaum, 2012; Zakhari, 2006).

Figure 1.6: Alcohol metabolism and the effects of its metabolites are exhibited in various metabolic and cellular processes. Green boxes and arrows demonstrate the resulting cellular functions. Symbols – Inhibits ━━━━━❙ ;Stimulates / Activates ━━━━━●; Enzyme Abbreviations - AceCS: Acetyl-CoA Synthetase; ADH: Alcohol Dehydrogenase; ALDH2: Acetaldehyde dehydrogenase 2; CoA: Coenzyme A; CYP2E1: Cytochrome P450 2E1; Fox01: Forkhead box protein 01; HATs: Histone Acetyltransferases (now lysine acetyltransferase; KATs); p53: tumor suppressor protein 53; PGC-1α: Peroxisome proliferation-activated receptor ɣ coactivator 1α; NAD / NADH: Nicotinamide adenine dinucleotide; SIRT1: NAP-dependent deacetylase sirtuitin-1.
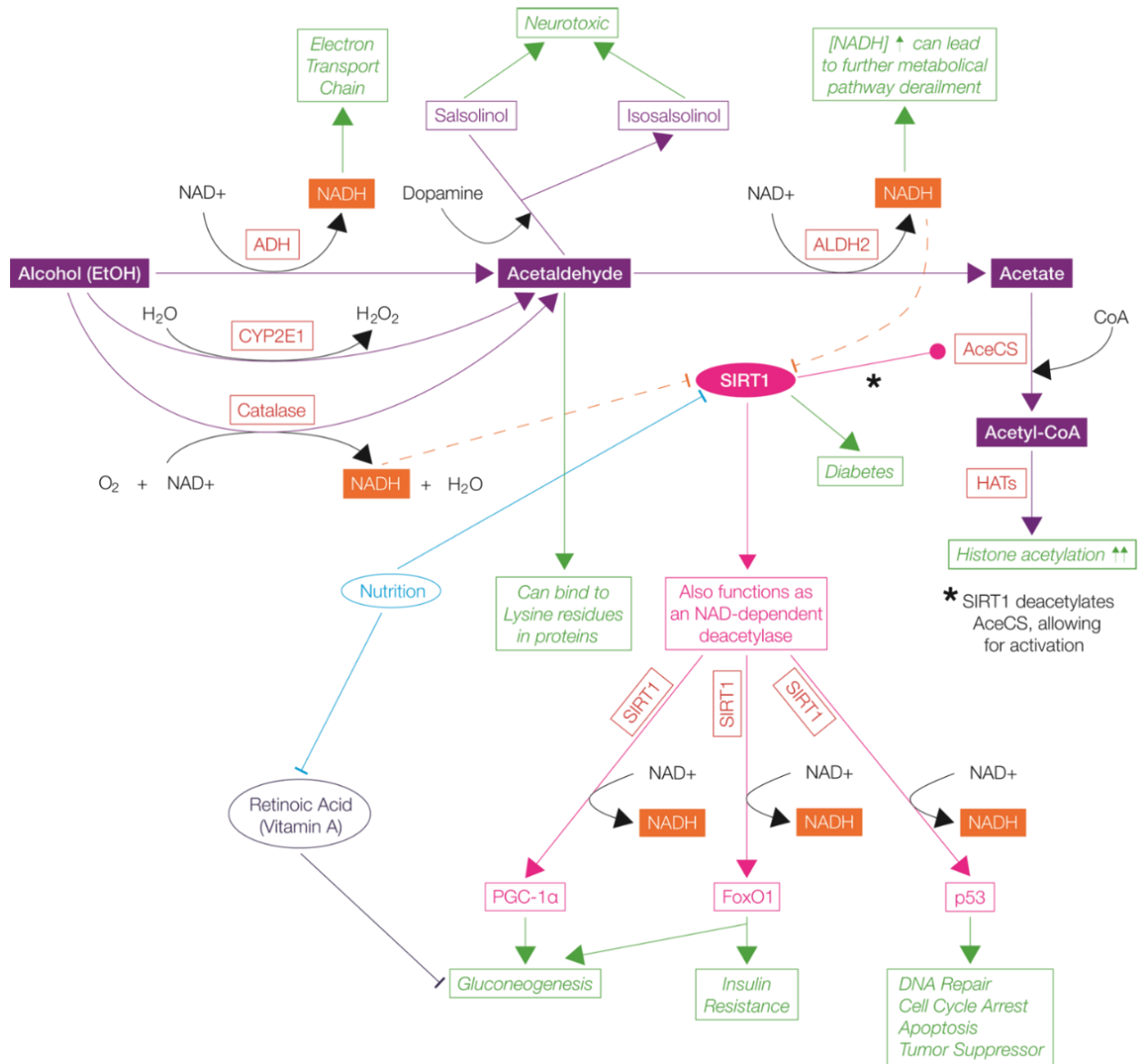
Taken from Liyanage & Jarmasz, *et al*. *Biology* 2014, *3*(4), 670-723. Used under Creative
Commons Attribution 4.0 International (CC BY 4.0).

Polymorphisms of Alcohol Metabolizing Enzymes

Genetics determine one's capacity to metabolize alcohol. ADH is encoded by many
different genes and is organized into five classes. Class 1 contains 6 different ADH isozymes
encoded by genes ADH1A, ADH1B and ADH1C, while the other 4 classes only contain 1 in

each. There are a few genetic variants of ADH1B and ADH1C, which contribute to different rates of ethanol metabolism, through varied levels of enzyme activity. The occurrence of these genetic variants (polymorphisms) varies among human populations. For example, genetic variant ADH1B*1 is predominantly found in Caucasians, while variant ADH1B*2 is predominantly found in Asian populations. Being heterozygous or homozygous for certain ADH alleles will either greatly enhance or greatly diminish alcohol metabolism which in turn determines susceptibility to alcohol dependence (Zakhari, 2006). For example, ADH1B*2, ADH1B*3, and ADH1C*1 are associated with lower rates of alcohol dependence (Wall, Carr, & Ehlers, 2003; Wall, Luczak, & Hiller-Sturmhöfel, 2016). Maternal genotypes with at least 1 ADH1B*3 allele was also associated with a lower incidence of FASD, due to less frequent alcohol consumption (Kobor, & Weinberg, 2011).

There are only two ALDH enzymes - 1 and 2. ALDH2 has two variants, ALDH2*1 and ALDH2*2; ALDH2*2 has decreased enzymatic activity and was shown to be associated with a reduced risk of alcohol dependence because acetaldehyde accumulates and causes negative symptoms. This creates a positive feedback loop, since it most likely encourages that individual to make a negative association with alcohol use (Wall, Luczak, & Hiller-Sturmhöfel, 2016; Zakhari, 2006).

Catalase primarily metabolizes hydrogen peroxide but functions as a peroxidase when metabolizing alcohol. All 245 single nucleotide polymorphisms of the catalase gene have decreased catalase activity and are associated with chronic disease (asthma, malnutrition, diabetes, rheumatoid arthritis, osteonecrosis) (Kodydková, Vávrová, Kocík, et al., 2014). One study did show in human male alcoholics that the -262C/T polymorphism was associated with alcohol-dependent subjects (Plemenitas, Kastelic, Porcelli, et al., 2015).

CYP450 family of enzymes metabolize all legal, illicit and prescription drugs. Isoforms CYP2E1, 1A2, and 3A4 specifically metabolize alcohol. CYP2E1 is the most studied isoform in the context of alcohol. Polymorphisms have been associated with a risk of alcoholism (Plemenitas, Kastelic, Porcelli, et al., 2015). However, one study demonstrated no statistical association of CYP2E1 polymorphisms with alcoholism in the Colombian population (Méndez, & Rey, 2015). The human fetal brain has lower levels of CYP2E1 than in adult brain (Brzezinski, Boutelet-Bochan, Person, et al., 1999). Fetal metabolism of alcohol is discussed in section "Alcohol delivery to the fetus" and "Fetal Metabolism of Alcohol" (pages 43-44).

Metabolic Products of Alcohol: Direct Effects, Mitochondria and Oxidative Stress

Ethanol can directly react with a range of molecular compounds including fatty acids and fatty acyl-CoA to produce fatty acid ethyl esters (FAEEs), phosphatidyl choline to produce phosphatidyl ethanol (Zakhari, 2006), and glucuronic acid as well as sulfuric acid to produce ethyl glucuronide and ethyl sulfate. Alcohol metabolism can lead to oxidative stress, particularly in mitochondria, as a result of increased production of reactive oxygen species (ROS) via the electron transport chain (because of the oxidation of NADH to NAD+) (**Figure 1.7**). ROS molecules can then cause DNA, protein, lipid and mitochondrial damage, which in turn can contribute to cell death, tissue damage, cancer, inflammation, and various chronic diseases (Brocardo, Gil-Mohapel, & Christie, 2011; Hannuksela, Liisanantti, & Savolainen, 2002; Hoek, Cahill, & Pastorino, 2002; Zakhari, 2006). Alcohol itself, as well as its metabolic by-products, have been shown (in humans) to alter mitochondrial structure and function (e.g. impairment of adenosine triphosphate (ATP) synthesis), particularly in the liver and in the heart, as well as affect nutrition and other metabolic processes (Hoek, Cahill, & Pastorino, 2002; Manzo-Avalos,

& Saavedra-Molina, 2010). Ethanol has been shown to adversely affect absorption of folic acid (vitamin B9), retinoic acid (vitamin A), vitamins B1, B6 and B12, choline and the amino acid methionine (Ballard, Sun, & Ko, 2012; Clugston, & Blaner, 2012; Gibson, Woodside, Young, et al., 2008; Kobor, & Weinberg, 2011; Thomson, 2000). Ethanol also affects lipid / cholesterol metabolism, glycolysis, the Krebs Cycle, one carbon metabolism, and the homocysteine / methionine metabolism pathway (**Figure 1.8**) (Kobor, & Weinberg, 2011; Kruman, & Fowler, 2014; Zakhari, 2013). This in turn affects a variety of cellular processes, including RNA and DNA synthesis, DNA repair, purine and pyrimidine biosynthesis, salvage of cellular adenine and methionine synthesis, and oxidative stress protection. It also greatly effects gene expression regulation by affecting mitogen-activated protein (MAP) kinases, histone H3 acetylation, H3 methylation, DNA methylation levels, as well as the enzymes responsible for these epigenetic modifications (e.g. methyltransferases) (Kobor, & Weinberg, 2011; Kruman, & Fowler, 2014; Shukla, Velazquez, French, et al., 2008; Zakhari, 2013). High concentrations of alcohol can also modify neurotransmitters (e.g., gamma amino butyric acid (GABA)A, N-methyl-D-aspartate (NMDA), NMDA-receptor (NMDAR) subunits) (Israel, Rivera-Meza, Karahanian, et al., 2013; Shukla, Velazquez, French, et al., 2008). Acetaldehyde can bind lysine residues in structural proteins (e.g. tubulin in microtubules). Acetaldehyde can convert the neurotransmitter dopamine to salsolinol and isosalsolinol (Israel, Rivera-Meza, Karahanian, et al., 2013; Zakhari, 2006), which may negatively regulate dopaminergic neurons and has been associated with alcoholism and Parkinson's disease (Naoi, Maruyama, & Nagy, 2004).

Figure 1.7: An example of ethanol's effects on the electron transport chain in mitochondria. Ethanol increases ROS production which can result in direct mitochondrial damage (e.g. phospholipids, proteins, and mitochondrial DNA (mtDNA), and can affect glutathione enzymes as we well as ATP production. Abbreviations: adenosine diphosphate (ADP), adenosine triphosphate (ATP), electron (e-), hydrogen (H+), oxygen (O_2), superoxide (O_2-), water (H_2O), hydrogen peroxide (H_2O_2), proton motive force (Δp), inorganic phosphate (Pi), superoxide dismutase (SOD), nitric oxide (NO•), peroxynitrite (NOO-), hydroxy radical (OH•), Coenzyme Q (QH_2), nicotinamide adenine dinucleotide (NADH / NAD+), glutathione peroxidase (GPX), reduced glutathione (GSH), glutathione-protein mixed disulfide (GSSP). ROS can damage mitochondrial constituents, such as phospholipids, proteins, and mitochondrial DNA (mtDNA) (Hoek, Cahill, & Pastorino, 2002).
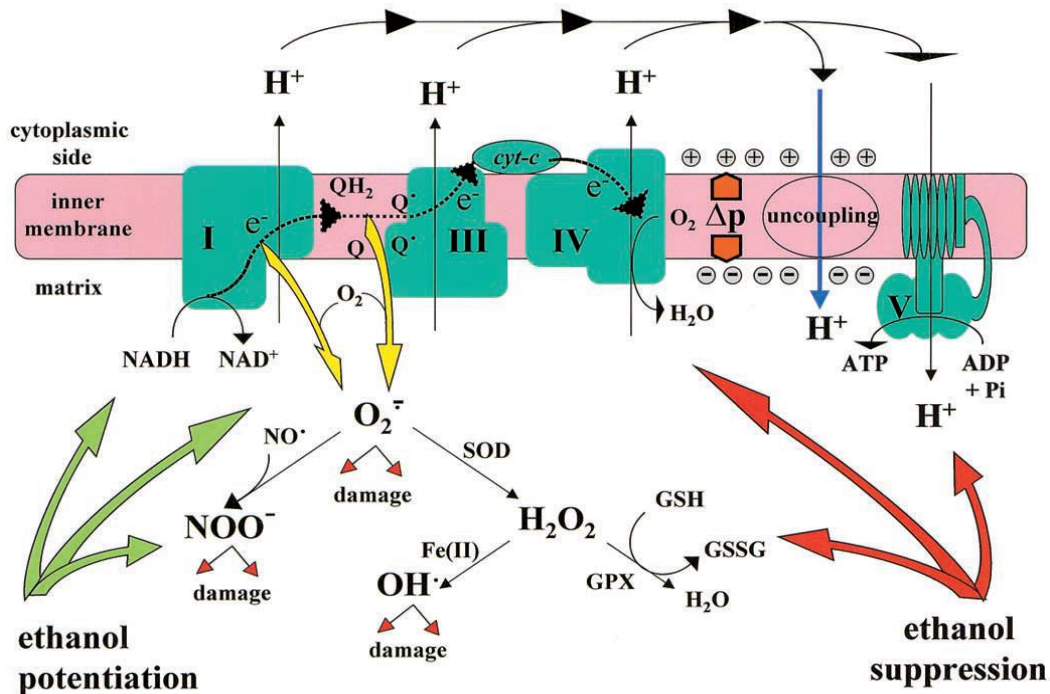
Reprinted from Gastroenterology 2002;122, Hoek *et al*. Alcohol and Mitochondria: A Dysfunctional Relationship, Copyright (2018), with permission from Elsevier through Rightslink obtained on June 29, 2018.

Figure 1.8: One carbon metabolism and the effects of alcohol (EtOH) and nutrition throughout the metabolical pathway. Green boxes and arrows demonstrate the resulting cellular functions. Symbols – Inhibits ————I ;Stimulates / Activates ————•; Enzyme Abbreviations – AHCY / SAH: *S*-adenosyl-L-homocysteine hydrolase; BHMT: Betaine-homocysteine *S*-methyltransferase; CBS: Cystathionine-β-synthase; CSE: Ɣ-cystathionase; DHFR: Dihydrofolate reductase; DNMTs: DNA methyltransferases; GCS: Ɣ-Glutamyl cysteine synthetase; GNMT: Glycine *N*-methyltransferase; GSS: Glutathione synthetase; HMTs: Histone methyltransferases; MAT: Methionine adenosyltransferase; MTHFR: 5,10-methylenetetrahydrofolate reductase; MTR: 5-methyltetrahydrofolate-homocysteine methyltransferase; MS: Methionine synthase; SAMDC: *S*-adenosylmethionine decarboxylase; SHMT: Serine hydroxymethyltransferase; TS: Thymidylate Synthetase.
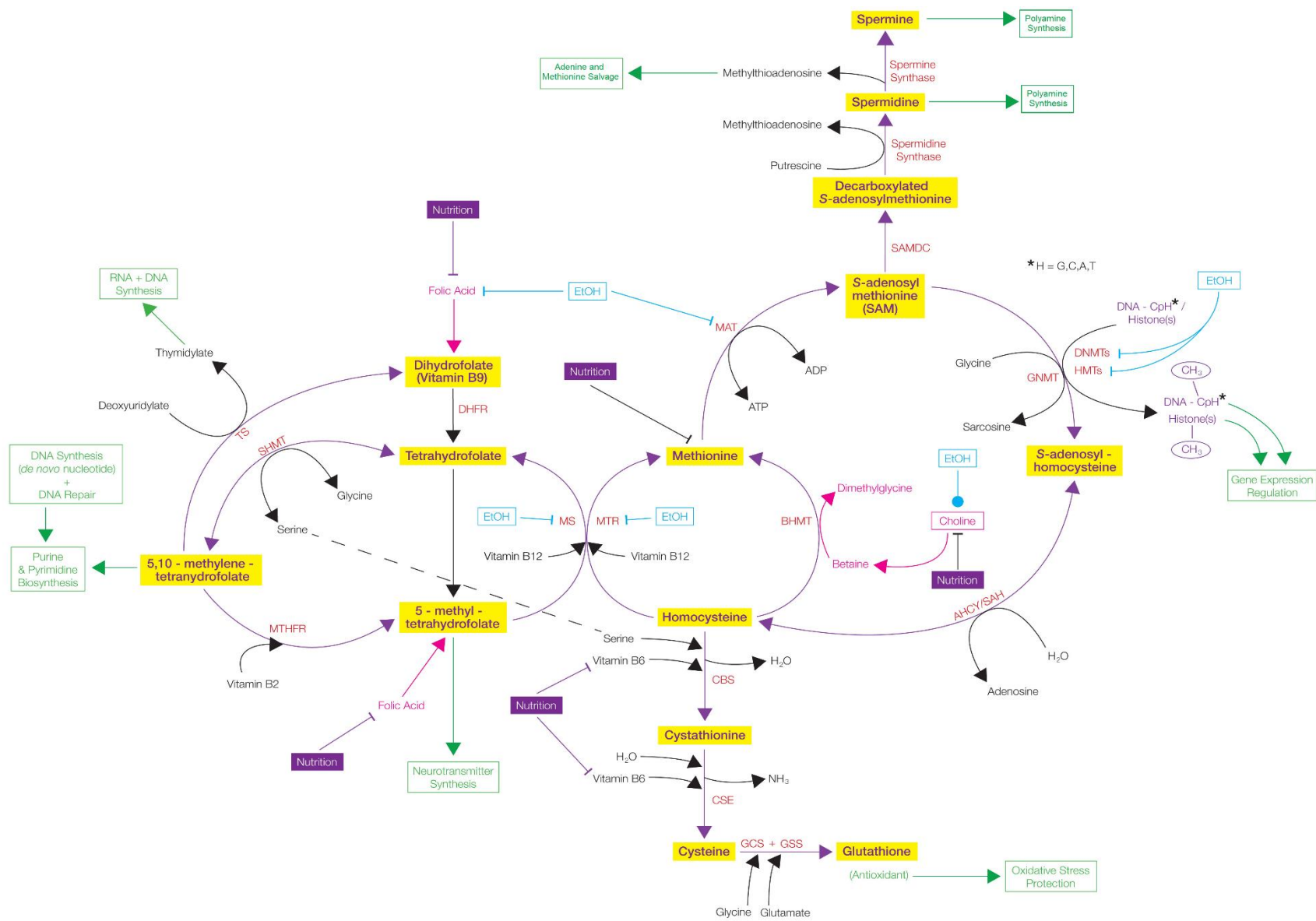
Behavioural Effects of Alcohol Consumption

Small amounts of alcohol are stimulating causing happiness, relaxation, reduced anxiety, positive social experiences and a decreased risk of cardiovascular disease. Moderate to large amounts of alcohol depresses the CNS due to its toxicity. Alcohol intoxication results in speech and motor delay, stupor, blackouts, and alcohol poisoning. Drinkers who experience blackouts or alcohol poising typically drink too much and too quickly, which causes their blood alcohol levels to rise very rapidly. Intoxicated patrons will most often engage in risky behaviour such as unsafe sex resulting in sexually transmitted infections (STIs), become violent with others or themselves, have suicidal thoughts, unintentionally harm themselves, drive under the influence, and die as a result of these actions (CPHO, 2015). In 2012, the top 5 causes of alcohol-attributable deaths were: infectious disease (34%), unintentional injury (17%), gastrointestinal disease (16%), cancers (13%), and intentional injuries (9%) (World Health Organization, 2014). Alcohol use has also been proposed to affect digestion, the immune system, fertility, and hormones (↑estrogen) (Ratna, & Mandrekar, 2017; Van Heertum, & Rossi, 2017).

Reasons for Drinking

Many people drink alcohol in social settings. Some consume alcohol as a coping mechanism to reduce stress and anxiety, increase sociability, cope with trauma, abuse or post-traumatic stress disorder (PTSD), or simply because its readily available. Sociodemographic characteristics such as sex / gender, age, race, ethnicity, culture, religious affiliation, as well as socioeconomic status (SES; income / economic factors, educational level, employment status, and housing status) affect one's decision to drink. There is a strong relationship between employment and housing with increased drinking and an elevated risk for alcohol use disorders

(AUD) (Collins, 2016). Childhood traumas such as physical and sexual abuse, and maltreatment has been consistently found to be associated with an increased risk for alcohol and drug use disorders in adulthood (Brady, & Back, 2012).

Long-Term Effects of Alcohol Consumption and Associated Disorders

The long-term effects of alcohol consumption cause a variety of diseases, primarily affecting the liver and the brain. The liver is the primary site of alcohol metabolism and is therefore the most affected by the long-term effects of alcohol consumption. Heavy ethanol consumption produces a wide spectrum of hepatic lesions: fatty liver (steatosis), hepatitis, and fibrosis / cirrhosis. Steatosis is characterized by the deposition of fat in hepatocytes, which is reversible if drinking ceases. However, chronic steatosis can progress to fibrotic liver disease. Liver hepatitis is an inflammatory type of liver injury characterized by swollen and dying hepatocytes, Kupffer cell (resident macrophages in liver) activation, neutrophilic infiltration, and Mallory bodies (collections of cytoskeletal proteins) within hepatocytes. Liver fibrosis / cirrhosis results in the deposition of abnormal amounts of extracellular matrix proteins in the hepatic parenchyma by hepatic stellate cells. This in turn activates leukocytes which attack and destroy hepatocytes, reduces blood flow through the liver and reduces the ability of the liver to regenerate (as a result of scar tissue formation) (Osna, Donohue, & Kharbanda, 2017). In 2013, the Canadian mortality rate of chronic liver disease and cirrhosis was 6.2 per 100,000 people (Statistics Canada, 2017). Long-term / chronic alcohol use has also been associated with the development of certain cancers (e.g. liver, mouth, throat, esophagus, stomach, colon and breast) since ethanol and acetaldehyde are both listed as carcinogens (Ratna, & Mandrekar, 2017; Van Heertum, & Rossi, 2017). However, the mechanisms underlying alcohol-associated cancers are

still not well understood and is mainly postulated to be the result of ethanol's interference with metabolism, ROS production, and effects on the immune system (Ratna, & Mandrekar, 2017).

Post-mortem studies of alcoholic brains have shown significant brain damage and neurodegeneration. Binge drinking animal models has been shown to cause progressive cognitive dysfunction and loss of neural plasticity due to reduced GABAergic inhibition and increased glutamatergic excitation. White matter degeneration is also frequently seen particularly in the cerebrum and the cerebellum. Acute alcohol poisoning most often causes brain hemorrhage and cerebral edema. It is also postulated that alcohol-mediated brain injury is caused consequentially by alcohol-mediated liver injury (De La Monte, & Kril, 2014). Long-term alcohol use also results in a variety of disorders such as Wernicke encephalopathy / Korsakoff syndrome or alcoholic neuropathy (De La Monte, & Kril, 2014; Simon, Jolley, & Molina, 2017; Zindel, & Kranzler, 2014). It can also lead to alcohol abuse, alcohol dependence and alcoholism. For a complete list of alcohol-related syndromes and disorders as well as a list of treatments, please see **Table 1.3**. Taken together, alcohol depletes vitamin B1, B2, B6 and B12 levels, and cause demyelination of axons as well as brain lesions.

Table 1.3: Resulting syndromes and disorders from repetitive and long-term alcohol use. (De La Monte, & Kril, 2014; Simon, Jolley, & Molina, 2017; Zindel, & Kranzler, 2014)

Alcohol related syndromes and disorders		Treatment
Alcohol abuse	Recurring harmful use of alcohol despite its negative consequences	Alcohol abstinence
Alcohol use disorder (AUD) (Alcoholism)	Compulsive alcohol use, loss of control over alcohol intake, and a negative emotional state when not drinking	Alcohol abstinence
Alcohol dependence (addiction)	An individual is physically or psychologically dependent (addicted) on alcohol where cessation causes withdrawal	Naltrexone, Nalmefene, Acamprosate, Topiramate
Wernicke Encephalopathy /Korsakoff Syndrome	Acute neuro-psychiatric condition caused by an inadequate supply of thiamine (vitamin B1) to the brain which is affected by alcohol metabolism and insufficient dietary intake and results in hemorrhagic lesions in mammillary bodies, hypothalamus, thalamus, brainstem, and cerebellum as well as neuronal loss and global atrophy	Alcohol abstinence, Parenteral thiamine
Hepatic Encephalopathy	Neuropsychiatric disorder that is clinically manifested by confusion, delirium, coma, asterixis, loss of fine motor coordination, hyper-reflexia, slowed speech and mild cognitive impairment due to severe liver dysfunction which in turn leads to a buildup of toxins in the bloodstream	No treatment
Alcoholic Neuropathy	Abnormalities in sensory, motor, autonomic and gait functions as a result of chronic alcohol consumption which in turn causes peripheral axon degeneration and demyelination. Painful sensations with or without burning quality represent the initial and major symptom	Alcohol abstinence, Gabapentin, Amitriptyline, Benfotiamine, α-lipoic acid, acetyl-L-carnitine and Methylcobalamin
Cerebellar Degeneration	Characterized by ataxia, tremor, slurred speech and nystagmus. Atrophy of the vermis as well as a loss of Purkinje and granule cells, and white matter	No treatment
Osmotic demyelination syndrome	Osmotic demyelinating disease that principally results in damage to bundles of myelinated fibers that intercalate among gray matter in pons, and other regions of brain to a lesser extent. Characterized by spastic quadriplegia, pseudobulbar palsy, dysphagia, dysarthria, and varying degrees of encephalopathy or coma.	Early - sodium and vitamins, alcohol cessation. Late - no treatment
Marchiafava-Bignami Disease	Characterized by corpus callosum lesions, demyelination and necrosis. Symptoms include seizures, ataxia, apraxia and lack of consciousness / coma.	Alcohol cessation and vitamin supplementation
Pellagra	Characterized by the clinical triad of dementia (delirium), dermatitis, and diarrhea, manifested by central chromatolysis of neurons in the brainstem	Alcohol cessation and niacin or nicotinamide supplementation
Alcoholic myopathy	A progressive disease that impairs strength due to loss of muscle mass through myofiber atrophy. Characterized by muscle weakness, spasms, cramps, stiffness and atrophy.	Alcohol cessation and vitamin supplementation and rehabilitation

The Neurobiology of Addiction

The Dopaminergic Reward System

In the brain, dopamine is a catecholamine neurotransmitter derived from tyrosine. Dopamine is primarily synthesized in the cytosol of mesencephalic neurons found in the substantia nigra (SN) and ventral tegmental area (VTA) of the brain. It is transported along axons by vesicular monoamine transporter to synaptic vesicles where it is stored. Once released from presynaptic terminals of dopaminergic neurons, dopamine binds with varying affinity to dopaminergic G-protein coupled receptors D1 to D5, which in turn inhibit protein kinase A (PKA). These dopamine receptors are expressed in many regions of the brain such as the striatum, nucleus accumbens (NAc), VTA, substantia nigra, amygdala, frontal cortex, hippocampus and hypothalamus (Beaulieu, & Gainetdinov, 2011; Purves, Augustine, Fitzpatrick, et al., 2004). Dopamine, via its dopaminergic pathways (mesolimbic, mesocortical, nigrostriatal and tuberoinfundibular), plays a critical role in the reward system of the brain, which is activated during natural activities such as feeding, socialization, and sex. Dopamine secretion makes one feel good, thereby facilitating the memory of circumstances needed to replicate the activity. This in turn promotes rapid firing of dopamine producing (dopaminergic) neurons, which only account for <1% of the total neuron population of the brain. Therefore, the dopaminergic reward system is critical and essential for feeding, sleeping, attention, motivation, memory, learning, voluntary movement and behaviour (Arias-Carrión, Stamelou, Murillo-Rodríguez, et al., 2010; Beaulieu, & Gainetdinov, 2011; Purves, Augustine, Fitzpatrick, et al., 2004).

Inhibitory and Excitatory Neurons: GABAergic and Glutamatergic

The dopaminergic reward system is a neuronal circuit primarily involving dopaminergic, GABAergic (inhibitory) and glutamatergic (excitatory) neurons (**Figure 1.9**). GABAergic neurons contain the neurotransmitter Ɣ-aminobutyric acid (GABA) and glutamatergic neurons contain the neurotransmitter glutamic acid (glutamate). The primary inhibition of dopaminergic neurons is effectuated by GABAergic interneurons in the VTA as well as in medium spiny GABAergic neurons in the NAc (Enoch, 2008; Purves, Augustine, Fitzpatrick, et al., 2004; Vlachou, & Markou, 2010). GABA is derived from glucose and binds to its receptors $GABA_A$ and $GABA_C$ (Cl^- / K^+ / Ca^{2+} ion channels), as well as $GABA_B$ (G-protein coupled receptor). Glutamate binds to its metabotropic (mGluRs; G-protein coupled receptor) and ionotropic (Cl^- / K^+ / Ca^{2+} ion channels, N-methyl-D-aspartate (NMDA), 2α-amino-3-hydroxy-5-methyl-4-isoxazolepropionic acid (AMPA) and kainate) receptors. $GABA_A$ and $GABA_C$ ion channel receptors are variably located across the brain, at synapses on axons, dendrites and neurons. They are regulated by various signaling proteins such as protein kinase C (PKC) and A (PKA) (Clapp, Bhave, & Hoffman, 2008; Enoch, 2008; Meldrum, 2000; Niciu, Kelmendi, & Sanacora, 2012; Purves, Augustine, Fitzpatrick, et al., 2004). $GABA_B$ receptors are found at synapses in almost all glial and neuronal cells. Their inhibitory mechanisms are primarily the inhibition of voltage-gated Ca^{2+} channels (VGCC) and adenylyl cyclase. Inhibition of VGCC stops calcium influx, and inhibition of adenylyl cyclase decreases adenosine monophosphate (cAMP), which in turn prevents vesicle fusion and neurotransmitter release. $GABA_B$ receptors are regulated by NMDAR-mediated Ca2+ / calmodulin-dependent protein kinase II (CaMKII) (Gassmann, & Bettler, 2012; Purves, Augustine, Fitzpatrick, et al., 2004). Glutamate is essential to the brain and is locally synthesized in the cytoplasm of neurons (by enzymatic conversion of glutamine

released by glial cells) and is packaged in synaptic vesicles by vesicular glutamate transporters (VGLUT). Glutamate receptors included NMDA, AMPA and kainate (named after their agonists) (Niciu, Kelmendi, & Sanacora, 2012; Purves, Augustine, Fitzpatrick, et al., 2004).

Figure 1.9: The dopaminergic reward system. The mesolimbic pathway (green) starts in the ventral tegmental area (VTA) and projects to the nucleus accumbens (ventral striatum). The mesocortical pathway (blue) connects the VTA with the prefrontal cortex, also spanning the caudate nucleus, hypothalamus, bed nucleus of the stria terminalis (BNST), hippocampus, amygdala, and olfactory bulbs. The nigrostriatal pathway (red) connects the substantia nigra (SNc) with the striatum. The tuberoinfundibular pathway (black) begins in the hypothalamus and primarily connects with the pituitary gland and median eminence. The VTA contains dopaminergic, GABAergic and glutamatergic neurons, and it communicates with the nucleus accumbens (NAc). The NAc contains medium spiny neurons which release GABA onto the globus pallidus (basal ganglia) which plays a role in voluntary movement. The NAc receives input from dopaminergic neurons of the VTA as well as input from glutamatergic neurons of the hippocampus, amygdala and prefrontal cortex. (Arias-Carrión, Stamelou, Murillo-Rodríguez, et al., 2010; Beaulieu, & Gainetdinov, 2011).
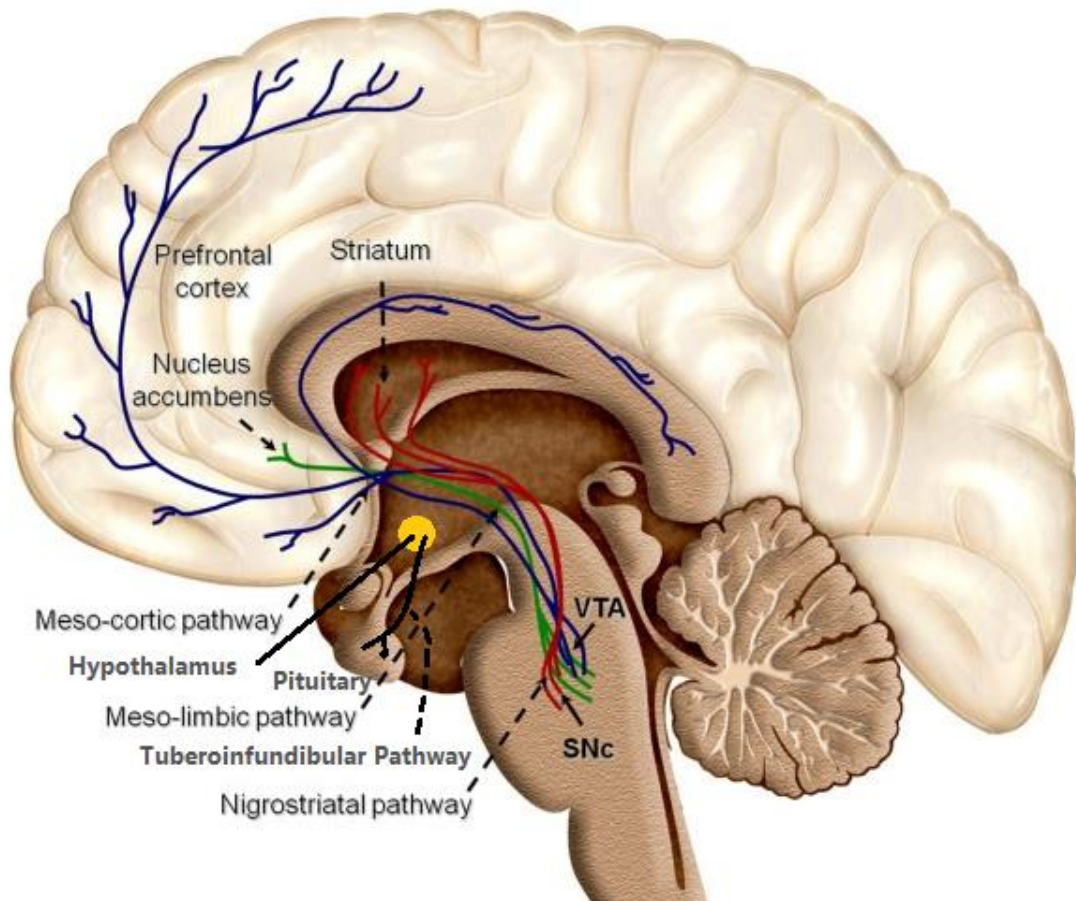
Image taken and modified from Arias-Carrion, O. *et al*. (2010). *BMC international Archives of Medicine*. 2010; (3)24, under the Creative Commons Attribution License [CC BY 3.0 (https://creativecommons.org/licenses/by/3.0], via Wikimedia Commons

The Effects of Alcohol on Dopaminergic, GABAergic and Glutamatergic Neurons

Ethanol readily binds GABA and glutamate receptors, promotes the synaptic release of dopamine primarily in the NAc, and has been shown to disrupt the expression and function of dopaminergic, GABAergic and glutamatergic receptors, which is dependent on their subunit composition (Alfonso-Loeches, & Guerri, 2011; Bernier, Whitaker, & Morikawa, 2011; Proctor, Diao, Freund, et al., 2006). Dopaminergic VTA projections to the NAc are the primary mediators

of the rewarding effects of ethanol. In different mammalian brain regions, long-term alcohol use has been shown to alter the expression of GABA$_A$ receptor subunits, cause changes to the subunit composition, and increase the overall concentration of GABA$_A$ receptors (Niladri Banerjee, 2014; Biggio, Concas, Follesa, et al., 2007; Enoch, 2008; Purves, Augustine, Fitzpatrick, et al., 2004). In an adult human post-mortem brain study, the hippocampus of known alcoholics (N=8) was subjected to gene expression analysis, where mRNA transcripts were quantified. When compared to controls, GABA$_B$ receptor subunit GABBR1 (Ɣ-aminobutyric acid type B receptor subunit 1) as well as GABA$_A$ receptor subunit GABRG2 (Ɣ-aminobutyric acid (GABA) A receptor Ɣ-2) were both down-regulated in the alcoholic hippocampus, which could potentially explain ethanol tolerance (Enoch, Zhou, Kimura, et al., 2012). GABA$_A$ receptors primarily play a role in ethanol tolerance, dependence and withdrawal, while GABA$_B$ receptors play a role in alcohol-seeking behaviour (Enoch, Zhou, Kimura, et al., 2012; Vlachou, & Markou, 2010).

In the brain, ethanol inhibits glutamate activity in the NAc and amygdala (Niladri Banerjee, 2014). Glutamate transmission is affected by acute and chronic alcohol exposure, possibly due to the differential expression of mGluR2 and mGluR7 receptors (Gyetvai, Simonyi, Oros, et al., 2011; Zhifeng Zhou, Enoch, & Goldman, 2014). Glutamate receptor NMDA has also been demonstrated to be a target in the effects of alcohol dependence, tolerance and withdrawal (Alfonso-Loeches, & Guerri, 2011). Other neurotransmitter receptors also play a role in AUD, such as μ- and δ-opioid receptors, nicotinic acetylcholine receptors (nAChRs), glycine receptors (GlyRs), serotonin receptors, and cannabinoid CB1 receptor (Feduccia, Chatterjee, & Bartlett, 2012; Pava, & Woodward, 2012; Söderpalm, & Ericson, 2013; Trigo, Martin-García, Berrendero, et al., 2010).

Alcohol Use Disorder (AUD) and the Role of Stress: Withdrawal and Abstinence

Following prolonged exposure, ethanol can cause widespread adaptations in the brain which can lead to ethanol tolerance / dependence and the development of Alcohol use disorder (AUD). In 2010, the prevalence of alcohol use disorders or dependence was 6.8% among Canadians aged 15 and older, compared to the global prevalence of 4.1% (people aged 15 and older) (World Health Organization, 2014). Sudden discontinuation of chronic alcohol use can lead to withdrawal syndrome, which is characterized by anxiety, relapse and strong alcohol-seeking behaviour (Niladri Banerjee, 2014). Both acute and chronic ethanol administration can also alter synaptic plasticity, by having an effect on long-term potentiation and long-term depression in various parts of the brain such as the hippocampus and NAc (Wills, & Winder, 2013). Stress and anxiety play a major role in AUD, particularly during withdrawal and abstinence (Moonat, Starkman, Sakharkar, et al., 2010). Research targeting ethanol withdrawal syndrome and ethanol abstinence primarily study the bed nucleus of the stria terminalis (BNST) in the extended amygdala as well as the hypothalamic-pituitary-adrenal (HPA) stress axis. The BNST is known to play a role in stress and anxiety responses by regulating HPA stress axis (**Figure 1.10**). The HPA stress axis becomes dysregulated during the transition from controlled social ethanol consumption to ethanol dependence (Avery, Clauss, Winder, et al., 2014; Bernier, Whitaker, & Morikawa, 2011; Lu, & Richardson, 2014; Stephens, & Wand, 2012; Wills, & Winder, 2013). Therefore, ethanol in low moderate doses acts as a stimulant, and at some point, at high doses or in a binge-like manner, becomes a depressant (Lu, & Richardson, 2014). Eventually, heavy chronic ethanol consumption desensitizes the neuroendocrine stress system.

Figure 1.10: The major components of the hypothalamic pituitary adrenal (HPA) axis. Both alcohol and stress can cause neurons in the paraventricular nucleus (PVN) of the hypothalamus

to release corticotropin-releasing factor (CRF) and the pituitary gland to release

adrenocorticotropic hormone (ACTH) into the general circulation. This in turn causes the release

of corticosteroids (cortisol) which follows a negative feedback loop. CRF also stimulates the

production of proopiomelanocortin (POMC) protein, which is the source of many other stress-

related hormones: ACTH, β-lipotropin (β-LPH), and β-endorphin (Lu, & Richardson, 2014;

Stephens, & Wand, 2012).
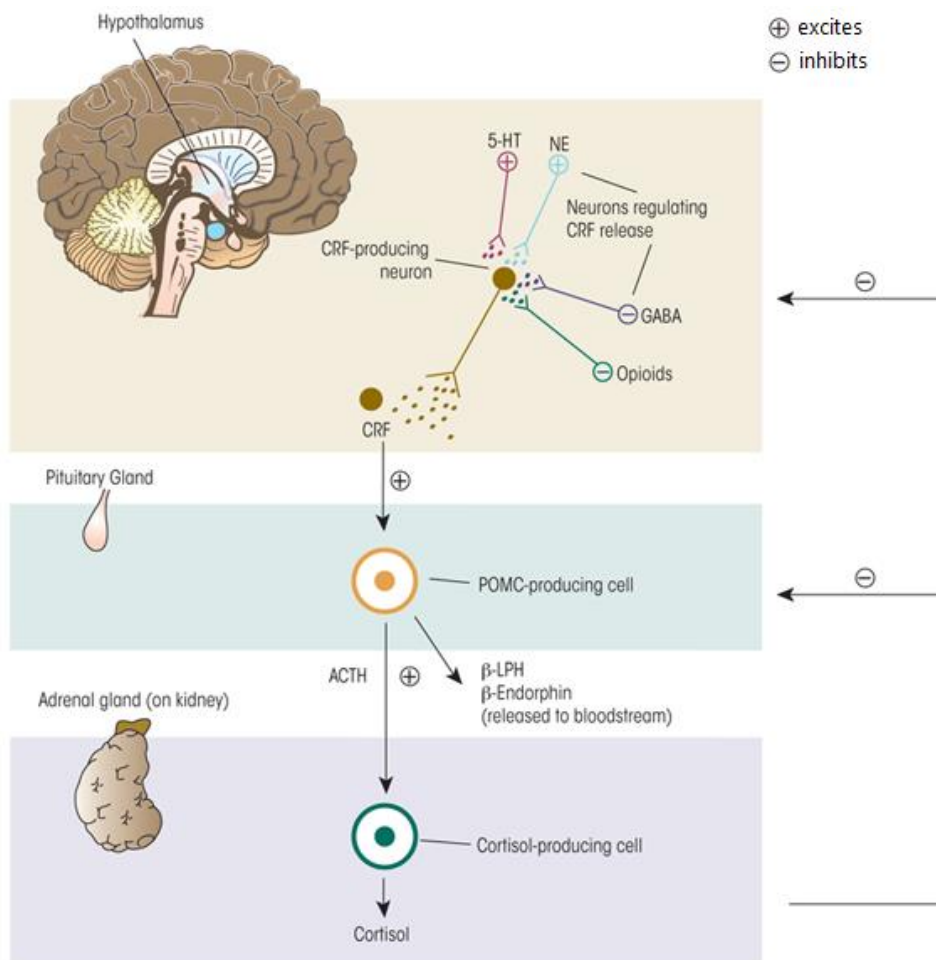
Taken from Stephens, M.A., and Wand, G. (2012). *Alcohol Research: Current Reviews*, *34*(4),

468-483. Copyright permission obtained on April 2, 2018.

Teratogenic Effects of Alcohol

Despite the known negative effects on the developing fetus, as well as public health prevention efforts, many women continue to consume alcohol during their pregnancies (McDonald, Hicks, Rasmussen, et al., 2014). In 2006-2007, approximately 10% of Canadian women who knew they were pregnant reported drinking during their pregnancy (Carson, Cox, Crane, et al., 2010), and in other countries, the rate of alcohol use during pregnancy is even higher (14.2% in South Africa) (O'Keeffe, Kearney, McCarthy, et al., 2015; Popova, Lange, Probst, et al., 2016). This in part may be due to the changes in women's drinking habits. In North America, the rate of alcohol use among women is rising as well as their rate of binge drinking, which can lead to alcohol abuse (Dawson, Goldstein, Saha, et al., 2015; Grucza, Norberg, & Bierut, 2009; Walker, Fisher, Sherman, et al., 2005; Wilsnack, Wilsnack, Kantor, et al., 2013; World Health Organization, 2014). A recent meta-analysis study found that approximately 10% of pregnant women in Canada drink alcohol, where ~3% engage in binge drinking (Popova, Lange, Probst, et al., 2017). Alcohol is a teratogen, a compound capable of causing birth defects. *In utero* alcohol exposure is associated with many adverse health consequences, including spontaneous abortion, stillbirth, preterm birth, NTDs, birth defects, sudden unexplained death of an infant (SUDI), and Fetal Alcohol Spectrum Disorder (FASD) (see **Table 1.4**) (Bailey, & Sokol, 2011; Chih-Ping Chen, 2008; Senturias, 2014).

Table 1.4: Risk factors in the mother and associated outcomes of prenatal alcohol exposure

(PNAE) on the developing fetus as well as resulting cognitive outcomes.

Fetal	Reference

• Growth retardation (small for gestational age, low birth weight) and deficits
 • Micrencephaly, reduced head circumference
 • Congenital anomalies and malformations:
   o Facial abnormalities: short palpebral fissures, smooth lip philtrum, thin upper lip, low set ears, wide spaced eyes, epicanthal folds, oral cleft lip / palate, short averted nose, flat nasal bridge, midface hypoplasia
   o Abnormal (transverse / simian) palmar creases
   o Neural tube defects
   o Skeletal anomalies: rib or vertebral, dactyly, pectus excavatum, carinatum, scoliosis
   o Renal anomalies
   o Heart defects: Atrial septal defects, Ventricular septal defects, Aberrant great vessels, Tetralogy of Fallot, conotruncal defects, coarctation and hypoplastic aortic arch
   o Ocular abnormalities: ptosis, blindness, optic nerve hypoplasia, strabismus
   o Hydrocephaly
   o Lissencephaly
   o Brain heterotopias
   o Corpus callosum abnormalities: complete or partial agenesis
 • Epilepsy or seizures
 • Neurocognitive and behavioural deficits:
   o motor deficits
   o problems with balance
   o decreased visual-spatial processing
   o compromised executive function, planning and emotion regulation
   o problems with learning, memory and attention
   o decreased academic achievement / low IQ
	(Cook, Green, Lilley, et al., 2016; Del Campo, & Jones, 2017; Kilgour, & Chudley, 2012; Senturias, 2014)

Maternal	**Reference**
• Spontaneous abortion • Stillbirth / fetal death • Preterm birth	(Bailey, & Sokol, 2011; Burd, & Wilson, 2004)
Placental	**Reference**
• decrease in size • impaired blood flow, oxygen transport and nutrient transportation • endocrine changes • abruption	(Bailey, & Sokol, 2011; Burd, Roberts, Olson, et al., 2007; Tai, Piskorski, Kao, et al., 2017; Viteri, Soto, Bahado-Singh, et al., 2015)

Effects of Alcohol on the Placenta

     It is important to discuss the placenta with regard to FASD. The placenta is an organ that produces hormones to support the pregnancy and growth, as well as provides oxygen and nutrients to the fetus, and removes waste from the fetus. This is achieved through an interface of maternal and fetal blood. The placenta has two major components, the fetal side which develops from the chorionic sac (villous chorion / chorionic plate) and the maternal side that develops from the endometrium (decidua basalis / basal plate). The placenta invaginates the uterine wall (endometrium) and remains attached until parturition (birth). It is connected to the fetus through the umbilical cord which develops at the same time as the placenta. Placental development is of fetal origin and occurs before neurulation (neural tube formation) but vascularization of the embryo and placenta coincides with neurulation (Gude, Roberts, Kalionis, et al., 2004). At days 6-7 post conception, the blastocyst attaches to the uterine epithelium by polar trophoblasts signaling the start of placental development (Myren, Mose, Mathiesen, et al., 2007). The functional unit of the placenta is the trophoblast cell. By the end of the third week of gestation, the placenta and umbilical cord are formed and by the eighth week, chorionic villi are present. At the start of the ninth to tenth week, maternal blood flow into the placenta will commence due to the start of angiogenesis. Thus, up until this point, the fetus obtains all nutrients through passive diffusion (Myren, Mose, Mathiesen, et al., 2007). The placenta grows and branching of chorionic villi occurs until 20-23 weeks gestation where it is fully developed (and when angiogenesis peaks) (Huppertz, 2008; Pereira, De Long, Wang, et al., 2015). During the third trimester, the placenta continues to grow and mature in order to keep up with the metabolic demand of the growing fetus. The maternal-fetal blood exchange occurs at the cellular level of the villi in the intervillous space which is lined with syncytiotrophoblasts and filled with spiral blood vessels.

Villi look like trees with multiple free-floating branches which are anchored in cotyledons and are in direct contact with blood. In other words, fetal blood vessels are the branches and the villi cells coat them. The fetal blood is separated from maternal blood by a combined layer of syncytiotrophoblasts, villus connective tissue and endothelial cells (Gude, Roberts, Kalionis, et al., 2004; Huppertz, 2008; Moore, Persaud, & Torchia, 2015; Pereira, De Long, Wang, et al., 2015).

Alcohol Delivery to the Fetus

Ethanol readily crosses the placenta, where maternal and fetal BAC levels are equal within an hour (Burd, Roberts, Olson, et al., 2007). Therefore high concentrations of ethanol can be found in fetal blood and in the amniotic fluid (Behnke, & Smith, 2013; Carter, Wainwright, Molteno, et al., 2016). The ability of the placenta to metabolize alcohol and subsequent metabolites is modest. Alcohol dehydrogenase (ADH) enzymes 1 through 3 and CYP2E1 is present in the human placenta (Gemma, Vichi, & Testai, 2007). However, the substrate binding affinity of placental alcohol dehydrogenase is very low (about 50,000 times less than levels in adult liver). The metabolism of acetaldehyde is 100 times lower than that of the liver, and the toxic effects of acetaldehyde accumulation can damage the placenta and subsequently harm the fetus as it remains present in the fetus for longer periods of time than in the mother. This in turn increases the duration of fetal exposure (Burd, Roberts, Olson, et al., 2007).

The direct effects of alcohol have been studied in experimental animal models, and in very few human studies. In a recent rhesus macaque study, first trimester (1-7 weeks gestation) binging resulted in decreased placental blood flow and decreased fetal brain size (measured at 15 weeks gestation) (Lo, Schabel, Roberts, et al., 2017). In a recent human placental study, 103 (66

alcohol-exposed, 37 control) placentas were examined histologically and the findings were correlated with 6 alcohol use measures. Alcohol use at the time of conception was strongly associated with smaller placental weight. Multivariable analysis showed that alcohol consumption was negatively correlated with meconium stained amnion, and positively correlated with placental hemorrhage and accelerated villous maturation (Carter, Wainwright, Molteno, et al., 2016). Another human placental study found no significant association between maternal alcohol consumption during pregnancy and placental weight or birth weight (Wang, Tikellis, Sun, et al., 2014). Salihu *et al.* studied the association between maternal alcohol consumption and placental-associated problems like abruption, placenta previa and, preeclampsia as well as preterm birth or stillbirth in a cohort of 1,315,505 births. Compared to non-drinkers, drinkers had an increased risk of placental-associated problems including preterm birth and stillbirth. Low-risk drinkers had a slight increased risk while high-risk drinkers had a twofold increased risk (Salihu, Kornosky, Lynch, et al., 2011). Taken together, alcohol directly effects the placenta by affecting growth and blood flow (details in **Table 1.4**).

Fetal Metabolism of Alcohol

The fetal liver is formed by the end of the first trimester, but is immature with regard to function (Gordillo, Evans, & Gouon-Evans, 2015; Ring, Ghabrial, Ching, et al., 1999). The umbilical vein (coming from the umbilical cord) delivers 70% of total hepatic blood flow and the portal vein only 20% (compared to 75% in adults) (Ring, Ghabrial, Ching, et al., 1999). Between gestational weeks 8 and 30, hepatocytes differentiate, followed by maturation well into term and after birth, where maturation coincides with function (Gordillo, Evans, & Gouon-Evans, 2015; Ring, Ghabrial, Ching, et al., 1999). In terms of metabolic capacity, one study reported the

presence of ADH enzymes 1 through 3 and CYP2E1 in fetal brain, fetal liver and in the neonate. Fetal brain had CYP2E1 but none of the ADH enzymes. During the first trimester, only ADH1 was present in fetal liver. By the second trimester, ADH2 was present, and during the third trimester, all three ADH enzymes were present, indicating a gradual developmental acquirement (Gemma, Vichi, & Testai, 2007). Another human fetal study looked at cytochrome P450 enzymes. In the fetal liver, CYP2E1 and CYP3A4 are not expressed (or expressed at low levels) until the second or third trimester (Hines, 2007). CYP2E1 levels, which correspond to ~20% of adult levels, are detected as early as 16 weeks gestation (Gemma, Vichi, & Testai, 2007). This indicates that the fetus is particularly vulnerable during the first trimester with regard to alcohol metabolism and may possibly reduce PNAE effects by its acquired (immature) metabolic function during the second and third trimester. In addition, CYP2E1 in fetal brain produces ROS when metabolizing alcohol, which in turn may explain the cognitive deficits in FASD.

Fetal Alcohol Spectrum Disorder (FASD)

History

Humans have been fermenting alcohol for consumption for at least 10,000 years (**Figure 1.11**). Paintings and literature throughout the 15th to 19th centuries are proposed to "hint" at the negative effects of alcohol on offspring, but nothing official was ever documented. It wasn't until the 19th century that the religious, social, criminal, and economical problems of alcohol consumption became apparent, and the Temperance Movement began. In the early 1900s, the era of prohibition commenced in select countries in Europe (1916-1932) and in North America (1920-1933) (Hanson, 2013; Sanders, 2009). Between 1895-1899, Charles Féré published three articles describing the effects of ethyl alcohol in chick embryos (Féré, 1895, 1898, 1899). In

1899, William Sullivan conducted a study regarding incarcerated women in a Liverpool (United Kingdom) jail. He found increased infant mortality rates among alcoholic women and noted healthier babies being born to incarcerated women, perhaps because there was little to no access to alcohol in jail. In 1904, Ballantyne wrote an Antenatal Pathology and Hygiene manual, where he described the adverse effects of alcohol during pregnancy, including spontaneous abortion and premature labor (Warren, 2015). In 1968, Lemoine published an article describing the effects of alcohol on 127 offspring, followed by two articles published in 1973 by Jones *et al.* describing autopsy findings of prenatal alcohol exposed case reports, leading to the development of the term "Fetal Alcohol Syndrome" (FAS) (Jones, Smith, Ulleland, et al., 1973; Jones, & Smith, 1973; Koren, 2012; Lemoine, Harousseau, Borteyru, et al., 2003).

Figure 1.11: A historical timeline of alcohol's presence among humans, major historical events involving alcohol and humans, and the discovery of Fetal Alcohol Spectrum Disorder (FASD) (Hanson, 2013; Sanders, 2009; Warren, 2015).
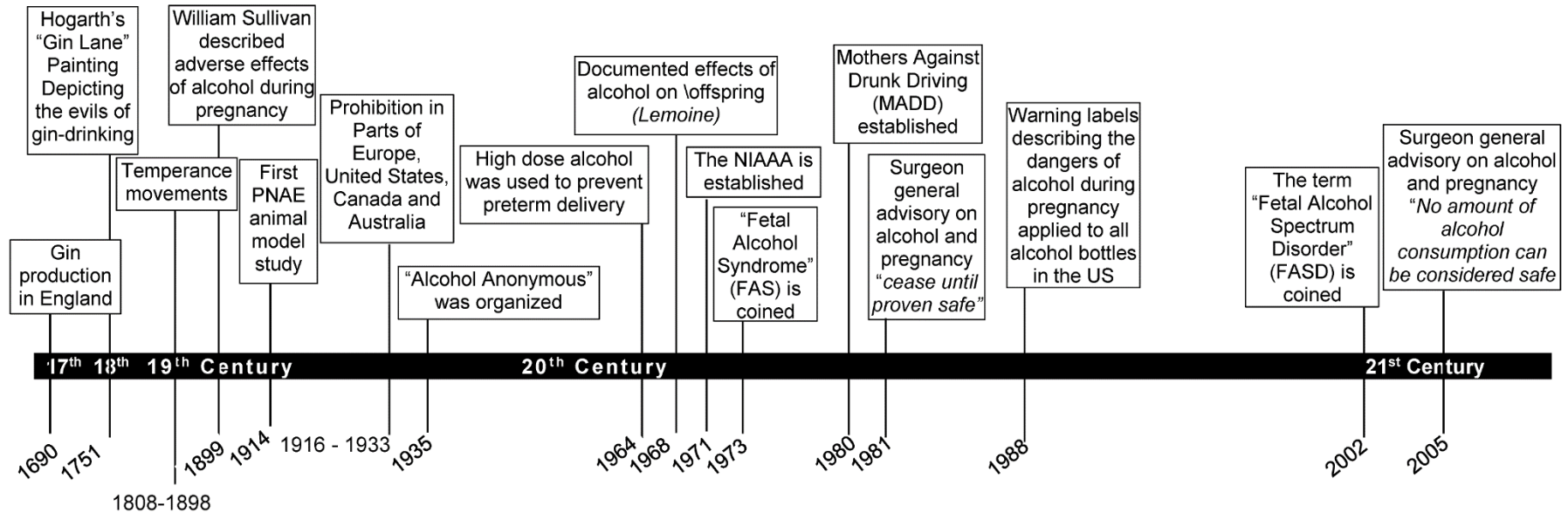
Definition, Prevalence and Societal Cost

In 2002, the term FASD was developed, which is an umbrella term covering Fetal Alcohol Syndrome (FAS), partial FAS (pFAS), Alcohol-Related Neurodevelopmental Disorder (ARND) and Alcohol-Related Birth Defects (ARBD). It is a group of disorders representing a constellation of minor to severe (1) cranio-facial dysmorphology, (2) central nervous system (CNS) dysfunction, (3) major organ malformations and (4) skeletal abnormalities (see **Table 1.4** for a complete list). The variability depends on the quantity, frequency (moderate vs. binge) and timing of alcohol exposure as well as on maternal nutrition, metabolism, genetics, and other health factors, which may be reflected generally in socioeconomic status (Coriale, Fiorentino, Di Lauro, et al., 2013; Dorrie, Focker, Freunscht, et al., 2014; Popova, Lange, Chudley, et al., 2018; Senturias, 2014; Warren, 2015). Children with FASD display and experience varying degrees of growth restriction (both body and brain) - developmental delay - attention, learning and memory deficits - delays in sensory processing - and social & behavioural problems (see **Table 1.4**). As adults, they may have mental health and substance abuse problems as well as criminal behaviour (Behnke, & Smith, 2013; Famy, Streissguth, & Unis, 1998; Merrick, Merrick, Morad, et al., 2006; Eileen M. Moore, Migliorini, Infante, et al., 2014; Pei, Denys, Hughes, et al., 2011).

The prevalence of FASD has been difficult to determine, due to under-reporting of maternal alcohol use, the difficulty of diagnosing, and the differences in diagnostic criteria among countries (Chudley, 2018; Cook, Green, Lilley, et al., 2016; Farag, 2014; Lange, Shield, Koren, et al., 2014; May, Gossage, Kalberg, et al., 2009; Ospina, & Dennett, 2013). In 2003, the Public Health Agency of Canada reported an FASD prevalence of 9 per 1,000 babies born in Canada (Public Health Agency of Canada, 2005). Among aboriginal populations in Manitoba Canada, the prevalence of FAS was reported to be 7.2 per 1,000 births in 1999. In one high-risk rural First Nations community the prevalence was estimated 31 – 62 per 1,000 births in 1997

(Kowlessar, 1997; Pacey, 2009). A more recent meta-analysis study found a pooled FASD prevalence of 5 per 1,000 among the general population in Canada, where the prevalence among Aboriginal populations was estimated to be 16 times higher (Popova, Lange, Probst, et al., 2017). This points to a bias in prevalence rates among Aboriginal people. However, a recent report assessed school children in the Greater Toronto Area (Ontario, CA) and reported a prevalence rate of 21 per 1,000 students, where >90% were not aboriginal and had high socioeconomic status (Popova, Lange, Chudley, et al., 2018).

In 2013, Ospina and Dennett conducted a systematic review of FASD prevalence, which was estimated to be 98 - 233 per 1,000 in Canadian prisons and correctional facilities (Ospina, & Dennett, 2013).

In Canada, diagnosing FASD could cost up to 7.3 million a year, based on 2011 data (Popova, Lange, Burd, et al., 2013). In 2013, the economic burden of FASD was estimated to be 1.8 billion dollars (Popova, Lange, Burd, et al., 2016). In 2014, FASD total health care costs were estimated at 2 billion, while costs to the correctional system were 3.9 billion (Thanh, & Jonsson, 2015).

Taken together, despite being 100% preventable, FASD continues to be prevalent, and a major health care burden in Canada.

Diagnosis of Fetal Alcohol Spectrum Disorder (FASD)

Diagnostic criteria and terminology have been changing since FAS was first described. With regard to FASD, there are 5 major components to the diagnosis: A. maternal alcohol consumption, B. dysmorphic facial features, C. growth impairment, D. CNS neurodevelopmental abnormalities, and E. behavioural or cognitive abnormalities. In Canada, suggested diagnostic

guidelines for FASD were published in 2005 (Chudley, Conry, Cook, et al., 2005). FASD covered fetal alcohol syndrome (FAS; A-D present), pFAS (A with either C, D or E), and ARND (A with D, E or both). ARBD was also a possible diagnosis where A is present along with a combination of a variety of congenital anomalies, malformations and dysplasias. Each of these diagnostic components all have a code (ranking of 4-1) which represents the risk of exposure (component A), degree of severity (with regard to B and C) and observed dysfunction (D). In 2016, the diagnostic terminology changed. Cook *et al.* recommended that FASD be a diagnostic term as opposed to falling under the "Neurodevelopmental Disorders" category of the Diagnostic and Statistical Manual of Mental Disorders (DSM-5). The authors also suggested that FASD be split into two diagnostic categories: FASD with or without sentinel facial findings (facial dysmorphology), subsequently eliminating FAS, pFAS and ARND (Chudley, 2018; Cook, Green, Lilley, et al., 2016). This was suggested to better represent what is currently being seen in the population as PNAE children tend to show few to no dysmorphic facial features but have varying degrees of neurodevelopmental delay and other congenital anomalies (Popova, Lange, Probst, et al., 2017). In 2014, Neurobehavioural Disorder associated with Prenatal Alcohol Exposure (ND-PAE) was also suggested as a possible diagnostic term in the DSM-5 manual to replace ARND, which is found under "Conditions for Further Study". In order to receive a ND-PAE diagnosis, a confirmed history of no more that 2 drinks on any one occasion or >13 drinks per month during pregnancy was required (Kable, & Mukherjee, 2017). This was considered controversial due to the establishment of an exposure level threshold (a rather daunting task), and somewhat implied a safe level of alcohol consumption during pregnancy (Kable, & Mukherjee, 2017).

FASD is often misdiagnosed. All over Canada, FASD centres and clinics with multidisciplinary diagnostic teams (e.g. pediatrician, psychologist, neurologist, occupational therapist, etc.) have been established. In general, diagnosis typically occurs at school age, however an individual can be diagnosed at any time (Chudley, Conry, Cook, et al., 2005). Children in foster care (or with child and family services), adolescents, and adults are difficult to diagnose because confirmed maternal alcohol consumption is difficult to establish in these individuals. In addition, changing facial features with age as well as personal drug use, substance abuse or addictions, and a history of head injury all contribute to the difficulties of diagnosing FASD in adolescents and adults (Bakhireva, Garrison, Shrestha, et al., 2018; Chudley, Kilgour, Cranston, et al., 2007). This is because the patients presenting symptoms or brain abnormalities (through brain imaging) may be as a result of the latter, therefore masking the FASD phenotype. To complicate matters, there are a variety of other disorders and syndromes that overlap with the clinical features of FASD such as Aarskog, Cornelia deLange, Dubowitz and Noonan syndrome, plus a variety of others (Chudley, Conry, Cook, et al., 2005; Leibson, Neuman, Chudley, et al., 2014). Therefore, it is also important to have suspected FASD patients undergo genetic testing to rule out chromosomal abnormalities or genetic disorders which mimic the physical, developmental and behavioural manifestations of FASD (Chudley, 2018; Leibson, Neuman, Chudley, et al., 2014).

Biomarkers of PNAE / FASD

A biomarker can be an attribute, imaging feature, or a biochemical compound that serves as an indicator of an observed medical state, and which can be accurately measured and reproduced in an affected patient (Chabenne, Moon, Ojo, et al., 2014). An ideal biomarker for

PNAE is one that can be easily measured, is non-invasive, is sensitive to potentially hazardous alcohol exposure, and has a low rate of false positive results (Chabenne, Moon, Ojo, et al., 2014). Direct biomarkers of PNAE include: fatty acid ethyl esters (FAEE; all 7 compounds), ethyl glucuronide (EtG), ethyl sulfate (EtS) and phosphatidyl ethanol (PEth) (Bager, Christensen, Husby, et al., 2017; Chabenne, Moon, Ojo, et al., 2014; Joya, Friguls, Ortigosa, et al., 2012). However, these biomarkers have different windows of detection, and are generally measured at birth in cord blood, fetal blood, meconium and in hair samples (Bager, Christensen, Husby, et al., 2017; Chabenne, Moon, Ojo, et al., 2014; Joya, Friguls, Ortigosa, et al., 2012). At birth, ethanol, its immediate metabolites (e.g. acetaldehyde), and liver enzymes (gamma glutamyltransferase, aspartate aminotransferase, alanine aminotransferase) can be measured in the mothers' blood or urine to identify PNAE. A few days after birth, EtG can be measured in urine. Within a few months after birth, long-term alcohol exposure can be determined by measuring FAEE and EtG in hair and meconium (Chabenne, Moon, Ojo, et al., 2014; Joya, Friguls, Ortigosa, et al., 2012). However, most of these direct biomarkers are as a result of ethanol metabolism. As described above, ethanol metabolism varies among individuals (due to genetics); therefore, the amount of these biomarkers would vary greatly among individuals as well. Ideally, a good biomarker would be detected at any point in the child's life, especially if there is no documented clinical history of PNAE (which is necessary for FASD diagnosis). Today, FAEE testing remains the most used tool (measured by chromatography coupled with mass spectrometry) (Joya, Friguls, Ortigosa, et al., 2012).

Placental biomarkers which predict neurodevelopmental outcome in children have also been suggested. This is determined by placental histopathology and follow-up of the liveborn child (Hodyl, Aboustate, Bianco-Miotto, et al., 2017). Although no specific biomarkers have

been suggested for human PNAE / FASD, a recent study analyzed placental growth factor (PLGF) in human fetal autopsy cases (both PNAE and control) in both the brain and placenta. They found PLGF immunoreactivity decreased in human PNAE placenta. This correlated with angiogenesis defects in both the placenta and in the human PNAE fetal brain (Lecuyer, Laquerrière, Bekri, et al., 2017). A few recent rodent studies assessing the placenta of alcohol treated dams have also identified various proteins that were dysregulated as a result of PNAE (Davis-Anderson, Berger, Lunde-Young, et al., 2017; Shukla, Sittig, Ullmann, et al., 2011).

Current research into identifying possible biomarkers has turned to epigenetics. Early evidence in DNA methylation studies using saliva (buccal epithelial cells) from FASD patients has pointed to the possibility of a pattern among differentially methylated CpGs (cytosine-phosphate-guanine) among specific genes (Laufer, Chater-Diehl, Kapalanga, et al., 2017; Lussier, Morin, MacIsaac, et al., 2018; Portales-Casamar, Lussier, Jones, et al., 2016). More research, a larger cohort, and more validation studies in different populations needs to be done before this can become a true possibility (Chudley, 2018).

Human FASD Autopsy Cases

Despite the high prevalence, autopsy brain tissue examination is described in <130 PNAE / FASD human cases and the majority of these are superficially described fetal cases (Jarmasz, Basalah, Chudley, et al., 2017; Lecuyer, Laquerrière, Bekri, et al., 2017). Reported abnormalities include: micrencephaly, disorganized brain regions, improper cortical lamination, glial or meningeal heterotopias, hydrocephalus, incomplete closure of the neural tube, partial or complete agenesis of the corpus callosum or anterior commissure, agenesis of the olfactory bulbs or nerves, cerebellar anomalies (small cerebellum, cerebellar dysgenesis, and hypoplasia of the

cerebellar vermis), brainstem dysgenesis (I. Ferrer, & Galofré, 1987; Jarmasz, Basalah, Chudley, et al., 2017; H. V Konovalov, Kovetsky, Bobryshev, et al., 1997; Roebuck, Mattson, & Riley, 1998; Tangsermkijsakul, 2016), and more recently, disorganized cortical vasculature (Jégou, El Ghazi, de Lendeu, et al., 2012; Lecuyer, Laquerrière, Bekri, et al., 2017; Solonskii, Logvinov, & Kutepova, 2008). At a cellular level abnormalities include: abnormal neural and glial migration, presence of ectopic neurons in white matter, reductions of neuronal cell populations in white and gray matter, a decrease in the number of dendritic spines of nerve cells in the cortex, and disorganization and decrease in the number of Purkinje cells in the cerebellum (Chen, Maier, Parnell, et al., 2003; Ferrer, & Galofré, 1987; Roebuck, Mattson, & Riley, 1998; Stoos, Nelsen, Schissler, et al., 2015).

Human FASD Neuroimaging Studies

Quantitative neuroimaging studies on live individuals have revealed micrencephaly, abnormal gyral patterns, asymmetry, reduced volume of brain regions (primarily basal ganglia, diencephalon and cerebellum), agenesis of the corpus callosum, and increases or decreases in cortical thickness (depending on the brain region) (Chen, Maier, Parnell, et al., 2003; McGee, & Riley, 2006; Moore, Migliorini, Infante, et al., 2014; Norman, Crocker, Mattson, et al., 2009; Nuñez, Roussotte, & Sowell, 2011; Roebuck, Mattson, & Riley, 1998; Spadoni, Mcgee, Fryer, et al., 2007). Changes in cortical thickness have been seen primarily in the perisylvian cortices of the temporal and parietal brain regions, likely as a result of a disproportionate decrease or increase in white and grey matter volumes (McGee, & Riley, 2006; Norman, Crocker, Mattson, et al., 2009). Magnetic resonance spectroscopy has revealed altered brain metabolism, changes in cerebral blood flow, lower concentrations of choline and altered levels of neurotransmitters in

various brain regions in individuals with FASD (du Plessis, Jacobson, Jacobson, et al., 2014; Crocker, Mattson, et al., 2009; Nuñez, Roussotte, & Sowell, 2011).

In Utero Alcohol Exposed Animal Models (Rodent and Non-Human Primate)

Much of what we know about FASD has been because of animal model experiments. Many FASD, PNAE and alcohol addiction animal experiments have been developed over the years. These experiments identified different strains of rodents or types of primates that are susceptible to the various routes of alcohol administration (e.g. oral or gastric gavage, IV injection, etc.) or ability to self-administer alcohol (Kelly, Goodlett, & Hannigan, 2009; Spanagel, 2003; Sprow, & Thiele, 2012). In general, FASD or PNAE animal experiments have been successful in terms of replicating the cranio-facial abnormalities, and some of the structural brain abnormalities typically found in human FASD including micrencephaly and agenesis of the corpus callosum. The majority of these studies try to determine the timing, frequency, and amount of alcohol that it takes to obtain these phenotypes (Lipinski, Hammond, O'Leary-Moore, et al., 2012; Maier, Chen, Miller, et al., 1997; Schneider, Moore, & Adkins, 2011).

Historically, animal experiments of PNAE confirmed that alcohol was indeed a teratogen. The earliest alcohol exposed animal model described in the literature dates back to 1914 (Stockard, 1914; Warren, 2015). Charles Stockard conducted many pre- and post-natal alcohol exposed studies with guinea pigs. He discovered that repeated alcohol intoxication generated malformations among offspring and that these malformations were passed down to two or more generations (Stockard, 1914). A 1977 PNAE mouse study using two different strains demonstrated a dose-effect as well as a strain effect. Their findings in gestational day (G) 18 offspring included intrauterine death, low birth weight and various malformations, including

brain anomalies (low dose alcohol), as well as cardiac and eye-lid dysmorphology (high dose alcohol), all of which varied among the two strains (Chernoff, 1977). In a 1979 study, the effect of acetaldehyde on the developing fetus was reported. Pregnant mice were injected once a day with 2% or 1% acetaldehyde on G7, 8 and 9 (first trimester human equivalency) and sacrificed on G10 or 19. The fetuses were examined and the abnormalities at G10 were primarily neural tube defects, while G19 fetuses demonstrated no abnormalities. Fetal loss (resorption) was also seen in both G10 and G19, with the highest loss being 46.3% of embryos at G10 (2% acetaldehyde) (O'Shea, & Kaufman, 1979).

Clarren, Bowden and Astley spent close to 20 years developing and studying a monkey FASD model (Schneider, Moore, & Adkins, 2011). Utilizing pigtailed Macaques, pregnant females received weekly doses of 0.3, 0.6, 1.2, 1.8 g/kg bodyweight of ethanol (nasogastrically) within the first 10 days of gestation and 2.5, 3.3, and 4.1 g/kg bodyweight of ethanol between 33 and 46 days gestation (human equivalent of 1, 2, 4, 6 and 8, 13, 16 standard alcoholic beverages). Approximately one third of pregnancies spontaneously aborted or ended in stillbirth. The remaining infants were examined postnatally up to ~6 months of age. None of the animals demonstrated all of the human FAS characteristics. Those infants who were exposed to alcohol within the first week of gestation (early exposure) were found to be developmentally delayed. Those infants who were exposed to higher doses of alcohol at week five of gestation (delayed exposure) demonstrated less developmental delay and better cognitive stability. Only one animal demonstrated characteristic FAS facial anomalies at maternal alcohol consumption of 1.8g of ethanol per kg body weight (early exposure). The animal exposed to the highest dose (4.1g/kg, delayed exposure) demonstrated significant growth deficiency, micrencephaly, strabismus, delayed motor skills and delayed facial expressions (Clarren, Astley, & Bowden, 1988; Clarren,

& Bowden, 1982, 1984; Clarren, Bowden, & Astley, 1987; Inouye, Kokich, Clarren, et al., 1985; Sheller, Clarren, Astley, et al., 1988).

Many PNAE animal experiments in brain demonstrated cell loss, delayed migration and maturation, fewer dendritic spines, as well as structural abnormalities in the brain (Chen, Maier, Parnell, et al., 2003; Guerri, & Renau-piqueras, 1997; Kotch, & Sulik, 1992; Livy, Miller, Maier, et al., 2003; West, Goodlett, Bonthius, et al., 1990). Many experiments evaluated the behavioural outcomes of PNAE (Alfonso-Loeches, & Guerri, 2011; Marquardt, & Brigman, 2016; Schneider, Moore, & Adkins, 2011). A substantial number of mouse experiments have demonstrated altered maternal care (e.g. maternal-pup interactions, nursing), conflicting results with regard to aggressiveness (due to sex differences), sexual dimorphic effects on behaviour, decreases in fear conditioning (Pavlovian measures), increases in anxiety-like behaviour (measured by elevated plus maze and in illuminated open field), and impairments in spatial learning and memory (measured by Morris water maze), which ameliorates with age. Study design appears to the be the confounding factor in the majority of animal studies due to the different strains, different types of alcohol delivery methods (injection, oral gavage, liquid diets, voluntary drinking, alcohol inhalation, etc.), single, multiple or continuous exposure, and exposure windows (prenatal vs. postnatal). The majority of mouse experiments only report results for males. Sex differences are, however, important, due to sexually dimorphic effects on behaviour (Marquardt, & Brigman, 2016).

Experimental Treatments & Preventative Measures: Retinoic Acid

More recent PNAE animal experiments are looking towards possible treatments or preventative measures to reduce or abolish the physical, genetic and biochemical effects of

alcohol *in utero*. Most studies involve nutritional supplementation (e.g. choline, folic acid,

retinoic acid (or vitamin A), zinc) (Ballard, Sun, & Ko, 2012; Bekdash, Zhang, & Sarkar, 2013;

Serrano, Han, Brinez, et al., 2010; Summers, Rofe, & Coyle, 2009). Retinoic acid has been of

particular interest due to its significant role in gastrulation and embryogenesis by mediating

patterning and growth during early forebrain, eye and face development (Feltes, de Faria Poloni,

Nunes, et al., 2014; Kot-Leibovich, & Fainsod, 2009). This has been mostly shown in zebrafish,

xenopus (frogs) and in very few mouse models (Petrelli, Weinberg, & Hicks, 2018; Shabtai, &

Fainsod, 2018). Retinoic acid is a lipophilic molecule that is derived from Vitamin A (Retinol).

Retinol metabolism / retinoic acid biosynthesis is tightly regulated and involves many enzymes

which are expressed in certain tissues at specific developmental time points (Duester, 2008).

Ethanol and its metabolite acetaldehyde compete with both vitamin A metabolism and retinoic

acid biosynthesis (**Figure 1.12**), making ethanol an inhibitor of retinoic acid production (Shabtai,

& Fainsod, 2018). Retinoic acid is a ligand for the RA receptors (RARα, RARβ, and RARγ) and

the retinoid X receptors (RXRα, RXRβ, and RXRγ). These nuclear receptors bind DNA and

directly regulate transcription and subsequent protein expression of various genes such as *Hox*

(hindbrain patterning) and *Fgf8* (somite & limb formation, heart patterning) (Duester, 2008).

Figure 1.12: Vitamin A metabolism / retinoic acid biosynthesis pathway. Ethanol breakdown by alcohol dehydrogenase (ADH) and the resulting compound acetaldehyde compete with vitamin A metabolism. This in turn can affect retinoic acid homeostasis during embryonic development through biosynthesis, catabolism and storage interference, which ultimately results in changes in transcriptional regulation. Abbreviations – AKR: Aldo-keto reductase family, BCO: beta-carotene oxygenase, CRABP: Cellular retinoic acid-binding protein, CYP26: Cytochrome P450 26A protein, DGAT: Diacylglycerol O-acyltransferase, LRAT: Lecithin retinol acyltransferase, RALDH: Retinaldehyde dehydrogenase, RAR: Retinoic acid receptor, RDH: Retinol dehydrogenase, RXR: Retinoid X receptor.
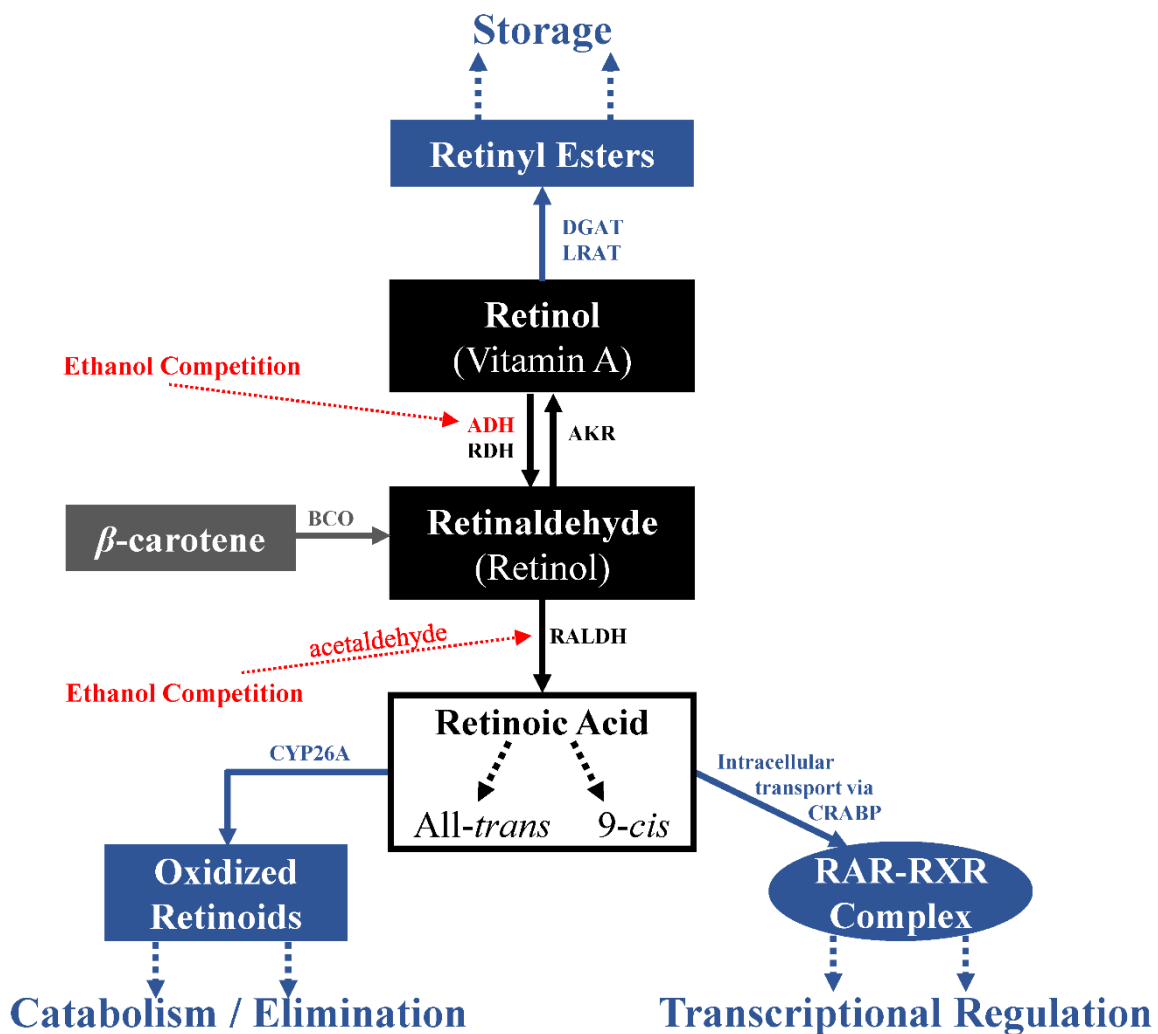
Pregnancy supplementation with vitamin A, retinoic acid or retinaldehyde has been shown to rescue these effects, but retinoic acid levels need to be carefully maintained due to its toxicity (Ferdous, Mukherjee, Ahmed, et al., 2017; Liyanage, Curtis, Zachariah, et al., 2017; Shabtai, & Fainsod, 2018). Hypervitaminosis A during pregnancy can lead to malformations of the fetal CNS (e.g. micrencephaly) (Dibley, & Jeacocke, 2001; Stånge, Carlström, & Eriksson, 1978). This makes it a dangerous possible treatment, since it is dependent on the enzymatic genetic makeup of the mother, placenta and fetus, and would also need to be introduced very early in the pregnancy, as well as throughout. Retinoic acid delivery to the fetus is solely dependant on the mother and the placenta, where the human placenta has been shown to express all enzymes responsible for vitamin A metabolism as well as retinoic acid transport, storage and catabolism and ultimately maintains retinoic acid homeostasis (Marceau, Gallot, Lemery, et al., 2007; Spiegler, Kim, Wassef, et al., 2012). The placenta is also suggested to serve as the primary site of vitamin A reserves until the fetal liver becomes functional and is proposed to release retinoic acid if maternal levels deplete (Spiegler, Kim, Wassef, et al., 2012). As described earlier (page 43 & 44), the fetus's metabolic capabilities are limited and studies that measured the levels of enzymes responsible for vitamin A metabolism in the fetal brain (compared to adult) demonstrated varied expression (Xi, & Yang, 2008). Therefore, ethanol interference of vitamin A homeostasis increases the vulnerability of the fetus to its teratogenic effects.

Apart from vitamin supplementation, a few animal experiments have also demonstrated the beneficial effects of treatment with neuroprotective peptides (e.g. Gypenosides and vasoactive intestinal peptide (VIP)-related peptides, NAPVSIPQ and SALLRSIPA (Dong, Yang, Fu, et al., 2014; Incerti, Vink, Roberson, et al., 2010).

FASD Genetic Effects

       Unlike autosomal dominant or recessive genetic disorders, FASD has not been linked to a specific genetic polymorphism. Many studies have investigated gene polymorphisms of enzymes that metabolize alcohol (described above) but this mainly pertains to the risk of FASD and not a phenotypic cause (Mead, & Sarkar, 2014). It is clear that ethanol interacts with genes (Eberhart, & Parnell, 2016) where the likely mechanism is through epigenetic changes by modifying gene expression. Since alcohol is an environmental factor, epigenetics makes a plausible area of research for FASD and will be discussed next.

Epigenetics

Homo sapiens are 99.9% genetically identical, yet, the genome is capable of producing multiple phenotypes. Several cellular mechanisms explain this – epigenetics being one of those mechanisms. The term was coined in 1942 by Conrad Waddington, who defined it as "*causal interactions between genes and their products which bring the phenotype into being*" (Waddington, 1942, 2012). In 1958, David Nanney formulated another definition where cellular heredity was a potential (but not defining) property of epigenetic systems, indicating that although our environment can influence our epigenetics, there is still some level of stability which enable proper cellular differentiation (Haig, 2012; Nanney, 1958). Today, epigenetics represents the many inheritable chemical "marks" found on and surrounding (e.g. histone proteins) the genome that influence gene expression in a controlled and selective manner, without directly changing the DNA nucleotide sequence (i.e. traditional mendelian genetic inheritance) (Gräff, Dohoon, Dobbin, et al., 2011; Gräff, & Mansuy, 2008; Hsieh, & Gage, 2004; Shukla, Velazquez, French, et al., 2008). Epigenetic changes play major roles in biological processes such as DNA replication and transcription, differentiation, protein synthesis and expression, and apoptosis. Epigenetic processes include chromatin remodeling (via chromatin modifiers and complexes (e.g. SWI / SNF)), RNA interference (micro RNAs), and reversible chemical modifications to DNA (DNA cytosine modifications) or to histones (post-translational modifications - PTMs). The "epigenome" represents all of the chemical modifications made to chromatin as well as all the key players such as chromatin-modifying complexes, enzymes and cofactors that help maintain and interpret it. Environmental factors such as chemicals and toxins, drugs of abuse including alcohol, poor nutrition and stress have been shown to modify the epigenome (Basavarajappa, & Subbanna, 2016; Davie, Drobic, Perez-Cadahia, et al., 2010; Gräff, & Mansuy, 2008; Hsieh, & Gage, 2004; Shukla, Velazquez, French, et al., 2008; Taniura, Sng, &

Yoneda, 2007). Alterations or aberrations to the epigenome as well as their respective machinery (e.g. enzymes, binding proteins), can lead to disease such as cancer, fragile-X syndrome, and Beckwith–Wiedemann syndrome (Haluskova, 2010; Moosavi, & Ardekani, 2016; Zoghbi, & Beaudet, 2016).

Chromatin

Our chromosomes are made up of chromatin, which is comprised of nucleosomes (represented by double stranded DNA wrapped tightly around a highly conserved core histone octamer) linked together by histone H1 (**Figure 1.13**). The histone core is made up of two H2A-H2B protein dimers and an H3-H4 tetramer. These histone proteins have a protruding N-terminus tail that ranges in length (16 – 44 amino acids) (**Figure 1.14**) (Davie, Drobic, Perez-Cadahia, et al., 2010; Gräff, & Mansuy, 2008; Hsieh, & Gage, 2004; Taniura, Sng, & Yoneda, 2007). Both DNA and histone N-terminal tails are epigenetically modified (discussed below) and contribute to the regulation of chromatin architecture. Chromatin structure in itself, is an epigenetic phenomenon. In comparison to compact / closed chromatin (e.g. hetero, facultative and constitutive chromatin), loose / open chromatin architecture (e.g. euchromatin) allows accessibility of transcription factors, RNA polymerase II (RNA Pol II) and chromatin remodelling complexes that in turn regulate gene expression. There are several histone protein variants (e.g. H2A.X, H2BE, H3.1, H3.X, etc.) which replace the usual histone core members, each playing different roles within the cell nucleus at different times. These histone variants can be classified into 3 groups which reflects cell cycle expression: replication-dependent and replication-independent (somatic cells) and testis-specific (spermatocytes). For example, histone variants macroH2A (replication-independent), H2A.X (replication-independent) and H3.3 all play a role in sex chromosome inactivation while H3.3 (replication-independent and -dependent)

specifically plays a major role in the formation of the paternal nucleus, which is important for the

establishment of normal heterochromatin (Davie, Drobic, Perez-Cadahia, et al., 2010; Gräff,

Dohoon, Dobbin, et al., 2011; Maze, Noh, Soshnev, et al., 2014).

Figure 1.13: Open (active) versus closed (silent) organization of nucleosomes into chromatin.
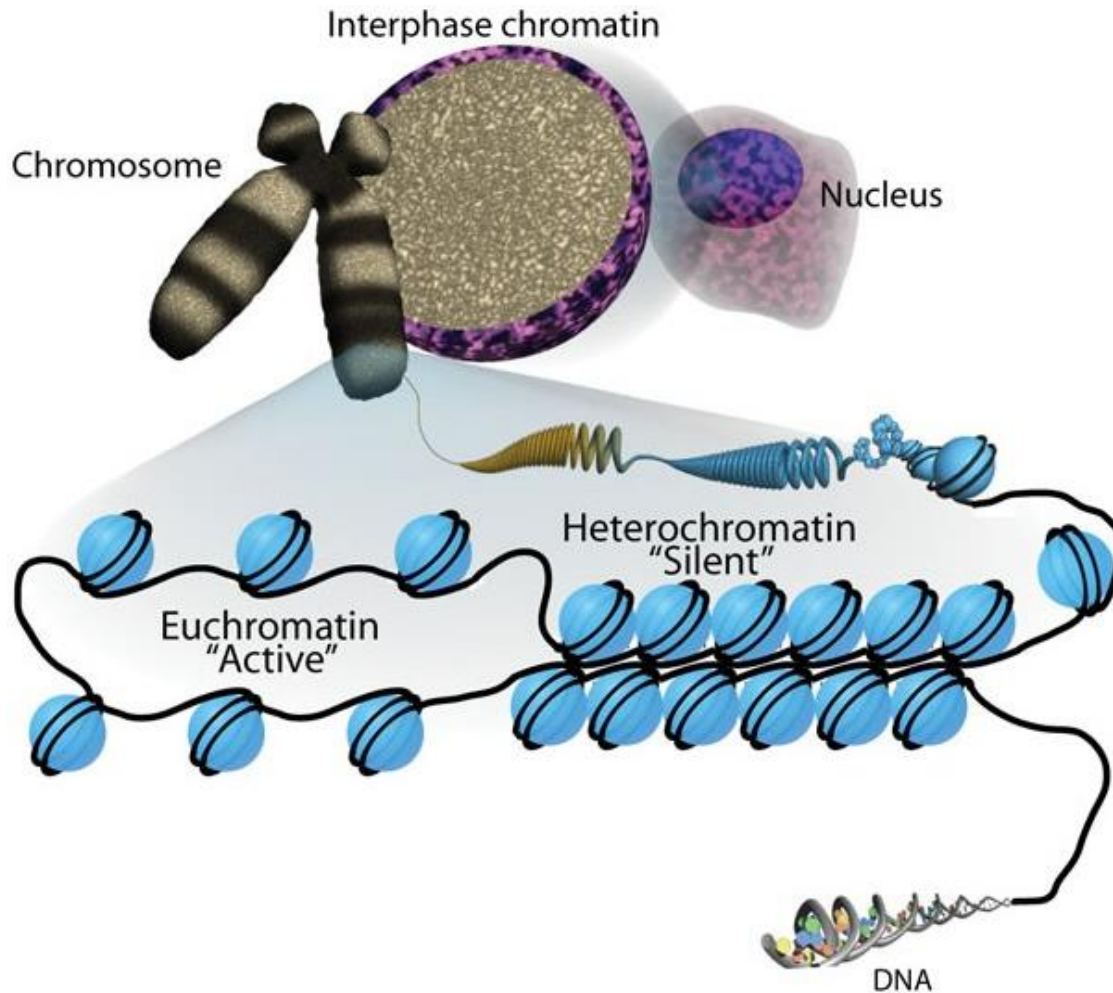
Taken from: Sha, K. and Boyer, L. A. The chromatin signature of pluripotent cells (May 31,

2009), StemBook, ed. The Stem Cell Research Community, StemBook,

doi/10.3824/stembook.1.45.1. http://www.stembook.org/node/585. This is an open-access article

distributed under the terms of the Creative Commons Attribution License (CC By 3.0),

https://creativecommons.org/licenses/by/3.0/.

Figure 1.14: The histone core represented by two H2A-H2B dimers and a H3-H4 tetramer. Each N-terminal tail varies in length and amino acid composition where each amino acid residue is subjected to various covalent modifications (e.g. methylation (me), acetylation (ac), etc.)
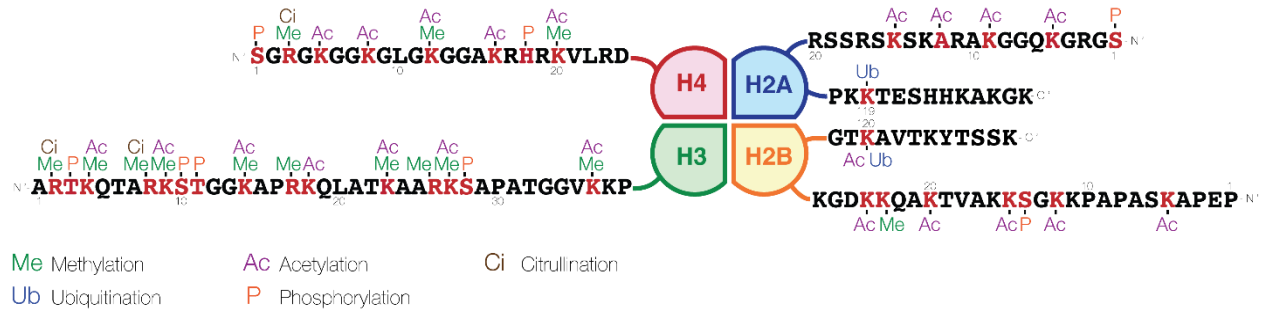
By Mariuswalter [CC BY-SA 4.0 (https://creativecommons.org/licenses/by-sa/4.0)], from Wikimedia Commons

Figure 1.15: DNA cytosine modifications generated by DNA methyltransferases (DNMTs) or Ten-Eleven Translocation enzymes (TETs).
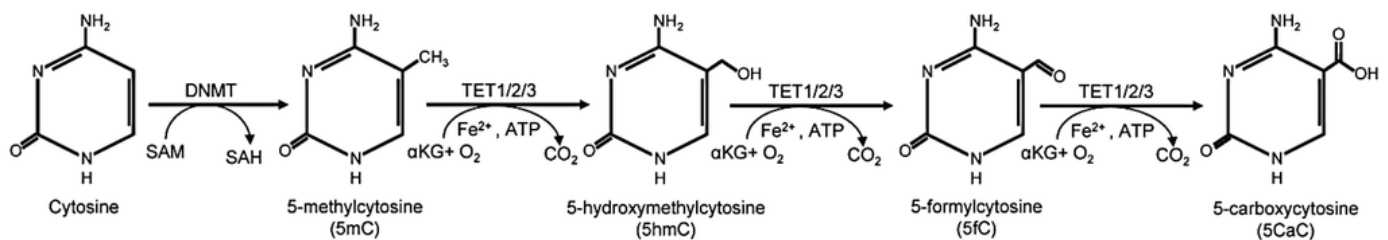
Taken from Liyanage & Jarmasz, *et al. Biology* 2014, *3*(4), 670-723. Used under Creative Commons Attribution 4.0 International (CC BY 4.0).

DNA Cytosine Modifications

5-methylcytosine (5mC)

The first epigenetic modification on DNA to be identified was 5-methylcytosine (5mC) (Hotchkiss, 1948; Wyatt, 1950). In 1977, the distribution of 5mC in the chicken genome was shown

and in 1981 its possible roles and function in the genome was proposed (Pollack, Stein, Razin, et al., 1980; Razin, & Cedar, 1977). 5mC occurs when a methyl group, donated by S-adenosylmethionine (SAM), is added to the fifth carbon of a cytosine residue, effectuated by a DNA methyltransferase (DNMT) (**Figure 1.15**). This primarily occurs at cytosine-phosphate-guanine (CpG) dinucleotides where methylation in promoters is correlated with transcriptional repression and methylation in gene bodies is correlated with activation (Christopher, Kyle, & Katz, 2017). Clusters of CpG dinucleotides (called CpG islands), which are often located near transcription start (TS) sites, in enhancer regions, and in gene promoters, are generally not methylated (Kinde, Gabel, Gilbert, et al., 2015; Ndlovu, Denis, & Fuks, 2011). Exceptions include CpG islands in somatic cells, which are methylated during X chromosome inactivation and during imprinting (discussed below) (Auclair, & Weber, 2012). There are five mammalian DNMTs. DNMT1 is found primarily in differentiated cells and is responsible for the maintenance of DNA methylation patterns (Auclair, & Weber, 2012; Ehrlich, & Lacey, 2013; Lyko, 2018). It preferentially binds palindromic hemi-methylated DNA during S phase replication and copies the existing methylation pattern on the parental DNA strand to the new daughter strand. DNMT3A and DNMT3B are considered to be *de novo* methyltransferases, which methylate DNA during early (DNMT3B) and late (DNMT3A) embryogenesis. They are both primarily found in differentiated cells. DNMT2 and DNMT3L (DNA methyltransferase-like protein) are considered cofactors because they lack certain domains. DNMT2 has a catalytic domain but no N-terminal regulatory domain. At first, it was suspected to methylate DNA but is actually responsible for the methylation of tRNA (discussed below). DNMT3L is only expressed during late embryogenesis and lacks a catalytic domain. It is proposed to induce the *de novo* methylation function of DNMT3A and DNMT3B (Auclair, & Weber, 2012; Basavarajappa, & Subbanna, 2016; Christopher, Kyle, & Katz, 2017; Sharma, De Carvalho, Jeong, et al., 2011). A sixth DNA methyltransferase has been recently

identified in mouse which plays a role in male mouse fertility (Barau, Teissandier, Zamudio, et al., 2016). DNMT3C is a *de novo* methyltransferase that silences transposons in male germline cells (Barau, Teissandier, Zamudio, et al., 2016). DNMTs are also highly regulated within the cell. DNMT activity can be aided in its function through molecular interactions (e.g. DNMT3L and E3 ubiquitin-protein ligase (UHRF1)), regulated by post-translational modifications by histone modifying enzymes (e.g. lysine demethylase LSD1, lysine methyltransferase SET7, serine / threonine kinase AKT1), and regulated by alternative splicing and through gene loss or duplication (Lyko, 2018). DNMTs also have specific domains that recognize methylated (e.g. the Pro-Trp-Trp-Pro (PWWP) domain) or unmethylated (ATRX-DNMT3-DNMT3L (ADD) domain) histones, suggesting that DNA methylation is also regulated through histone methylation (Lyko, 2018; Rose, & Klose, 2014).

5-hydroxymethylcytosine (5hmC)

The methyl group on 5mC can be oxidized by the ten-eleven translocation protein (TET) enzymes into a hydroxymethyl, formyl, or carboxyl group, which produces 5-hydroxymethylcytosine (5hmC), 5-formylcytosine (5fC), and 5-carboxylcytosine (5caC) respectively (**Figure 1.15**) (Gräff, Dohoon, Dobbin, et al., 2011; Liyanage, Jarmasz, Murugeshan, et al., 2014). 5hmC can also be deaminated into 5-hydroxymethyluracil (5hmU). These DNA cytosine modifications are targets in the "active demethylation" pathway, which represents the enzymatic removal or modification of 5mC. Therefore, 5hmC (along with 5fC, 5caC and 5hmU) are considered to be active transcriptional marks. First identified in bacteria, 5hmC was only recently found in mammalian tissues, and shown to be more abundant in brain than in other tissues (Kriaucionis, & Heintz, 2009). Mature neurons have higher levels of 5hmC than neural progenitors while oligodendrocytes progressively lose 5hmC as they mature (Jang, Shin, Lee, et al., 2017). 5hmC is primarily found in gene bodies, promoter regions and

transcription start sites, which suggests a role in activation and not in silencing (Lister, Mukamel, Nery, et al., 2013; Liyanage, Jarmasz, Murugeshan, et al., 2014; Wen, & Tang, 2014). 5fC and 5caC were discovered in 2011 and are present in low levels in genomic DNA as well as in mouse brain (Ito, Shen, Dai, et al., 2011; Wagner, Steinbacher, Kraus, et al., 2015). 5fC is enriched at poised enhancers and other regulatory elements. In both yeast and mammals, 5fC and 5caC have been shown to delay RNA Pol II elongation within gene bodies through pausing, therefore having a possible regulatory role in DNA transcription. In addition, 5fC and 5caC are postulated to be signals for the recruitment of the base excision repair system (BER) and DNA glycosylase (TDG) through active demethylation (Kellinger, Song, Chong, et al., 2012).

Active demethylation represents the enzymatic removal of 5mC by oxidation (by TET enzymes) into 5hmU, 5fC and 5caC. These modifications can then be further converted into apurine / apyramidine sites (AP sites) by TDG. This is turn activates the BER, which replaces the toxic AP site with a non-modified cytosine residue. AP endonuclease 1 (APEX1) will cleave the AP site and allow DNA polymerase to re-insert the appropriate base. "Passive" demethylation is when cytosine does not get methylated, possibly because SAM is not available or because DNMTs are inhibited, down-regulated or are not recruited to DNA (Guo, Su, Zhong, et al., 2011a, 2011b; Zampieri, Ciccarone, Calabrese, et al., 2015). This typically occurs during replication, when the methylation pattern does not get copied onto hemi-methylated DNA. Therefore, the methylation pattern is lost through generations of cellular division.

TET enzymes 1, 2, and 3 require Fe^{2+} and α-ketoglutaric acid (2-oxoglutarate (2-OG)) to bind CpGs via their CXXC (Cys-X-X-Cys chromatin-associated binding) domains (Kinde, Gabel, Gilbert, et al., 2015; Kriaucionis, & Heintz, 2009; Li, Wu, & Lu, 2015; Lister, Mukamel, Nery, et al., 2013; Liyanage, Jarmasz, Murugeshan, et al., 2014). All TET enzymes are expressed in the brain, and

are particularly enriched at CpG-rich gene promoters (Melamed, Yosefzon, David, et al., 2018). TET1 activity is high in embryonic stem cells (ESCs) and begins to decrease during differentiation. TET2 activity is also high in ESCs and is said to play a role in lineage specification. TET3 has been shown to play a role in paternal pronucleus formation directly after fertilization, is not expressed in ESCs, and plays a role in neuronal differentiation (Melamed, Yosefzon, David, et al., 2018). Vitamin C is postulated to be an additional co-factor for TET, possibly playing a role as a regulator and enhancer of TET activity. In the presence of vitamin C, TET primarily increases global oxidization of 5mC and promotes active demethylation (Blaschke, Ebata, Karimi, et al., 2013; Moore, Toomire, & Strauss, 2013). TET enzymes are regulated by miRNAs (e.g. TET1 is targeted by miR29 while TET2 is targeted by miR22). TET activity is also regulated through its various isoforms – meaning each TET isoform has their own degree of substrate affinity and reaction rate which regulates their activity (Melamed, Yosefzon, David, et al., 2018).

Non - Cytosine - Phosphate- Guanine (Non-CpG) Methylation

Non-CpG methylation (when cytosine is paired with adenine (A), cytosine (C) or thymine (T)) appears to be abundant in mouse and human ESCs, human skeletal muscle, as well as in the adult mouse and human brain (particularly in neurons). Methylation is effectuated by the *de novo* DNMTs (3A and 3B) and CpA methylation appears to be the most prevalent type of non-CpG methylation in the brain (Jang, Shin, Lee, et al., 2017). Non-CpG methylation may add another level of gene regulation during early brain development (Guo, Su, Shin, et al., 2013; Kinde, Gabel, Gilbert, et al., 2015; Lister, Mukamel, Nery, et al., 2013; Lister, Pelizzola, Dowen, et al., 2009; Pinney, 2014). In human and rodent adult brain, non-CpG methylation is much higher in neurons than in glial cells (Jang, Shin, Lee, et al., 2017; Lister, Mukamel, Nery, et al., 2013). In human fetal frontal cortex, non-CpG

methylation is low and dramatically increases in relation to synaptic development whereas CpG methylation is steady throughout development (Jang, Shin, Lee, et al., 2017; Lister, Mukamel, Nery, et al., 2013).

RNA Methylation (N6-methyl-adenosine (m6A))

In 1968, methylated RNA was discovered (Li, & Mason, 2014). The sixth nitrogen of adenosine in RNA receives a methyl group from SAM via m6A methyltransferase complex (methyltransferase like 3 and 4 (METTL3, METTL4), and Pre-mRNA-splicing regulator (WTAP)) (Yue, Liu, & He, 2015). Messenger RNA (mRNA) is the primary type of methylated RNA (estimated >15000 human genes), however ssRNA, lncRNA, tRNA, snRNA, etc. are also methylated (Li, & Mason, 2014; Yue, Liu, & He, 2015). RNA methylation is particularly enriched near stop codons, in the 3'UTR (untranslated region), and within exons (Yue, Liu, & He, 2015). Specific alpha-ketoglutarate dependent demethylase enzymes (e.g. FTO, ALKBH5) remove the methyl group (Li, & Mason, 2014; Yue, Liu, & He, 2015). Much like 5mC and TET enzymes, FTO can oxidize m6A into hydroxy and formyl intermediates (N6-hydroxymethyladenosine and N6-formyladenosine). ALKBH5 directly reverts m6a to adenosine without intermediate steps. RNA methylation is said to play a role in embryogenesis, cellular differentiation, and in circadian rhythm (Li, & Mason, 2014; Yue, Liu, & He, 2015).

Mitochondrial DNA Methylation

Mitochondria are the energy producing organelles of eukaryotic cells and possess several copies of their own DNA. Mitochondrial DNA (mtDNA) is double-stranded, circular, and contains ~17,000 base pairs and codes for ~37 genes. The structure and gene organization of

69

mtDNA is highly conserved in mammals. mtDNA is primarily inherited through the maternal side because there are more copies of mtDNA in oocytes (~10^5) than in sperm (<100) (Taanman, 1999). It was recently shown that mtDNA can also be methylated (St John, Facucho-Oliveira, Jiang, et al., 2010; van der Wijst, van Tilburg, Ruiters, et al., 2017). Bisulfite pyrosequencing of human mtDNA taken from blood and saliva identified 83 CpG sites covering nine genomic regions. The average methylation levels of all nine regions was low (~2%) (St John, Facucho-Oliveira, Jiang, et al., 2010). There is also evidence of non-CpG methylation in mtDNA. The enzyme responsible for methylating mtDNA is a mitochondria-localized DNA methyltransferase 1 transcript variant (mtDNMT1). As in nuclear DNA, the function of methylated mtDNA is regulation of gene expression, either directly or indirectly (modulation of mtDNA replication) (van der Wijst, van Tilburg, Ruiters, et al., 2017).

Histone Post-Translational Modifications (PTMs)

Histones are an ample part of the nucleosome. Chromosomal proteins represent almost 48% of total nuclear proteins, where the ratio of histone to non-histones to DNA is 1 / 1.3 / 1 respectively (Baserga, 1974). Histones undergo multiple dynamic and reversible chemical modifications at their protruding N-terminal tails, primarily at lysine, arginine and serine amino acid residues. These include enzymatic methylation, acetylation, phosphorylation, ubiquitination, sumoylation, propionylation, butyrylation, malonylation, formylation, etc. (Basavarajappa, & Subbanna, 2016; Choudhary, Weinert, Nishida, et al., 2014; Huang, Sabari, Garcia, et al., 2014). Most amino acids can undergo a single PTM, however some can undergo several different PTMs (e.g. Lysine 27 of Histone H3 – H3K27ac, K27me, K27me2, K27me3), although not simultaneously. Given that there are many different histone

modifications on many different amino acid residues to consider, I will describe the two most common forms, acetylation and methylation on the lysine residue.

Histone acetylation represents the addition of an acetyl group (donated by acetyl-CoA) on the amine group of an amino acid (typically lysine), performed by the histone acetyltransferase (KAT; "writer") family. There are five major KAT families: KAT1, GCN5 / PCAF, MYST, p300 / CBP and RTT109 (Marmorstein, & Zhou, 2014). Removal is performed by histone deacetylases ("erasers"), of which there are two families, HDACs and SIRTs (sirtuins) (Barth, & Imhof, 2010; Marmorstein, & Zhou, 2014). KATs are relatively specific in the sense that they will acetylate certain (and not all) lysine residues. For example, histone acetyltransferase GCN5 can acetylate lysine 9 and lysine 14 on histone H3, TIP60 will acetylate histone H4 at lysine 5 and 12, and p300 can acetylate multiple histones (e.g. H3K9, H3K27, H4K5, H4K12, H4K16) (Barth, & Imhof, 2010; Hou, Gong, Bi, et al., 2014; Marmorstein, & Zhou, 2014; Yun, Wu, Workman, et al., 2011). HDACs are not specific and can deacetylate virtually any acetylated histone while sirtuins tend to be more specific with regard to their substrate preference (Tanabe, Liu, Kato, et al., 2018). Histone acetylation in mammals has been shown to be sequential. On histone H3, lysine 14 is acetylated before lysine 23, 18, and 9. On histone H4, lysine 16 is acetylated before 8, 12, and 5 (Turner, 1991). KATs such as p300 are recruited to gene promotors to acetylate lysine residues (Venters, & Pugh, 2009). The acetyl group reduces the positive charge of histones which in turn weakens the interaction with DNA, subsequently relaxing chromatin structure and permitting transcription by allowing the assembly of the preinitiation complex (PIC) (Yun, Wu, Workman, et al., 2011). Histone acetylation marks are "read" by proteins containing the bromodomain (BrDs) or tandem PHD (plant homeodomain) domain typical of chromatin regulators (Marmorstein, & Zhou, 2014). Histone acetylation simultaneously takes place at multiple lysines and is

effectuated by many different writers and erasers. This suggests that acetylation activates gene transcription through cumulative effects (Yun, Wu, Workman, et al., 2011).

Lysine methylation is one of the most stable histone marks. It is present in four forms: unmethylated (me0), mono- (me1), di- (me2) and tri- (me3). Methyl groups (donated by SAM) are put on by histone methyltransferases (HMTs; "writers") (Black, Van Rechem, & Whetstine, 2012; Yun, Wu, Workman, et al., 2011). Almost all HMTs contain a SET (Su[var]3–9, Enhancer of Zeste, Trithorax) domain, which catalyzes the reaction. Histone demethylases (HDMs; "erasers") remove the mono-, di- or tri-methyl groups. Both HMTs and HDMs are specific with regard to their substrate. For example, histone methyltransferase SETD1B can tri-methylate histone H3 lysine 4 and lysine 9, but PRDM9 can only tri-methylate H3K4me3. Histone demethylases JMJD3 and UTX can remove di- and tri-methylated H3K27 but PHF8 can only remove di-methylated H3K27 (Barth, & Imhof, 2010; Black, Van Rechem, & Whetstine, 2012; Yun, Wu, Workman, et al., 2011). Many protein domains recognize methylated (and non-methylated) lysine: PHD, chromo, tudor, WD40, PWWP and more. These domains are typically found in many different proteins that regulate histone acetylation, DNA methylation, DNA damage and repair, and chromatin structure (Yun, Wu, Workman, et al., 2011).

The combination of many histone PTMs at certain genomic loci determines the activity of that particular gene, and is proposed to be the "histone code". The code recruits nearby proteins and binding molecules, which then act upon chromatin for various functions. These combinations of PTMs can silence or activate genes, change the high-order organization of chromatin, or drive a cell to death (Barth, & Imhof, 2010; Davie, Drobic, Perez-Cadahia, et al., 2010). Histone PTMs also "crosstalk" with each other, with DNA cytosine modifications, with nearby nucleosomes, and with chromatin modifying complexes. For example, DNMT3A contains an ADD domain that recognizes unmethylated H3K4 (Du, Johnson, Jacobsen, et al., 2015). Trimethylated H3K4me3

is associated with active transcription, therefore unmethylated H3K4 signals repression and brings in DNMT3A (Du, Johnson, Jacobsen, et al., 2015). A histone tail can also possess two specific histone PTMs which colocalize – termed bivalent. H3K4me3 and H3K27me3 are known bivalent marks, where K4me3 signals activation and K27me3 repression. If colocalized on a gene promotor (termed bivalent gene), the promotor is "poised" and can be readily activated or silenced via this bivalency (Harikumar, & Meshorer, 2015; Voigt, Tee, & Reinberg, 2013). This concept is typically applied to developmental genes (e.g. Oligodendrocyte Transcription Factor 1 (OLIG1)), allowing repression (or activation) in the absence (or presence) of differentiation signals (Voigt, Tee, & Reinberg, 2013). These examples represent a minority among the vast and complex histone communication network.

Micro RNAs (miRNA)

Another epigenetic regulator of gene expression are micro RNAs (miRNAs) (Chen, & Qin, 2015; Sun, & Shi, 2015; Xu, Karayiorgou, & Gogos, 2010). MicroRNAs are single small (short or long) non-coding RNA transcripts that are transcribed by RNA PolII, processed by DGCR8 (Drosha and DiGeorge syndrome critical region gene 8), and then cleaved by DICER. The resulting miRNA (through the RISC complex) then binds the 3'-UTR of a target mRNA, which in turn, blocks protein translation or marks the mRNA for degradation (Xu, Karayiorgou, & Gogos, 2010). One single miRNA can bind several different mRNA targets. MiRNAs have been heavily studied in brain development, because the brain has the highest miRNA content in comparison to other tissues (Chen, & Qin, 2015). Many miRNAs are brain specific where they play roles in neuronal proliferation, migration, and differentiation (e.g. miR-9, miR-124, miR-137, miR-219) (Chen, & Qin, 2015; Sun, & Shi, 2015; Xu, Karayiorgou, & Gogos, 2010).

Dysfunction in some miRNAs may be associated with neurodevelopmental (Fragile-X and Rett Syndrome) and neuropsychiatric diseases (e.g Schizophrenia and Bipolar disorder (Ardekani, & Naeini, 2010; Sun, & Shi, 2015).

Examples of Epigenetic Events in Early Development.

Many epigenetic events orchestrate human embryology and development. I will describe a few events that involve both DNA methylation and histone PTMs.

DNA Methylation Program (DMP)

The orderly changes in DNA methylation during mammalian development is termed the DNA methylation program (DMP) (Chen, Damayanti, Irudayaraj, et al., 2014; Chen, Ozturk, & Zhou, 2013; Zhou, 2012). During neurulation, both 5mC and 5hmC are collaboratively present in the neural tube and neural crest, and as brain development progresses with subsequent DMP cycles. In the neuroepithelium, 5mC appears first, followed by 5hmC and other active demethylation marks (5fC, 5caC), which subsequently leads migration and differentiation of the neuronal cell populations in order to form the regions of the brain. 5mC, methyl-CpG binding domain protein 1 (MBD1) and DNMT1 appear in a high to low concentration gradient from ventral to dorsal, which coincides with the start of differentiation and maturation of neurons as well as neural crest cells. Similarly, a high to low concentration gradient of DNA methylation marks is seen in the midbrain and hindbrain, followed by its progression and neuronal maturation bidirectionally (toward the forebrain and spinal cord), indicating that the brainstem is the first to differentiate. The DMP continues postnatally in the brain, with levels of DNA methylation marks staying close to those present during neurulation in the cortex, striatum and hippocampus, with

variations in 5mC / 5hmC ratios within each region (Chen, Damayanti, Irudayaraj, et al., 2014; Zhou, 2012).

Imprinting

DNA methylation is an essential process in genomic imprinting (Bartolomei, & Ferguson-Smith, 2011; Yamaguchi, Hong, Liu, et al., 2013). Genomic imprinting is maintained in somatic cells, is inheritable and involves the silencing of alleles which is dependent on the parent-of-origin. Meaning, each allele (one coming from paternal side, one from maternal) cannot be expressed at the same time (monoallelic expression). Only one allele can be, while the other is selectively methylated in the imprint control region (ICR) of that gene. This in turn turns off the gene by physically blocking ICR's binding site potential and downstream-enhancer mechanisms. As described above, CpG-islands are usually unmethylated and are associated with promotor regions of genes that are rarely repressed (i.e. housekeeping genes). CpG-islands are also located within promotors of imprinted genes and are subsequently differentially methylated (DMRs), where the repressed allele is methylated and the active allele unmethylated. These DMRs are therefore inherited and each paternal and maternal allele contains different DMRs. Maternal DMRs are generally in the promotor region while paternal DMRs are intergenic (Bartolomei, & Ferguson-Smith, 2011). Taken together, this is how transcriptional machinery is able to distinguish between parent-of-origin alleles within imprinted genes and only express the correct one. The majority of the imprinted genes are clustered in imprinted domains and these genes harbour DMRs, which are characterized by the parent-of-origin-specific DNA methylation profiles (Bartolomei, & Ferguson-Smith, 2011; Hackett, Sengupta, Zylicz, et al., 2013). Changes to imprinted gene DMR methylation patterns causes imprinting disorders such as Prader-Willi,

Angelman, Beckwith-Wiedemann, and Silver-Russell syndromes (Bartolomei, & Ferguson-Smith, 2011; Kernohan, & Bérubé, 2010). The phenotype of these syndromes are dependent on which imprinted gene is affected. There are approximately 100 human imprinted genes. These genes are highly (and widely) expressed during fetal development and are predominantly down-regulated after birth (Bartolomei, & Ferguson-Smith, 2011). *H19, IGF2, ASCL2, DLK1, UPD6* are just a few examples of imprinted genes. The *IGF2-H19* imprinted gene locus is heavily researched. *IGF2* codes for Insulin-like growth factor 2 and H19 codes for a long noncoding RNA. *IGF2* (Insulin-like growth factor 2) is paternally expressed and is located 90kb away from *H19* which is maternally expressed. The ICR is located upstream of the transcription start site of *H19* and contains a binding site for 11-zinc finger protein / CCCTC-binding factor (CTCF) which in turn, physically blocks the binding of enhancers on *IGF2* on the maternal chromosome, rendering it inactive. On the paternal chromosome, this ICR would be methylated, which in turn represses *H19* and allows *Igf2* to be expressed (Bartolomei, & Ferguson-Smith, 2011). All imprinted genes are methylated by *de novo* DNA methyltransferases.

After proper imprinting has occurred, these imprints need to be maintained. During DNA methylation reprogramming, imprinted genes need to survive this genome wide eraser of DNA methylation and chromatin modifications and be propagated throughout mitosis. There are multiple *cis-* and *trans*-acting factors that ensure this. Once example is a KRAB zinc finger protein (ZFP57) which is a repressive transcription factor. ZFP57 recruits DNMT1 and assures the methylation of DMRs and ICRs of the imprinted genes (Bartolomei, & Ferguson-Smith, 2011). ZFP57 also interacts with cofactors which in turn function as a scaffold and bind modified histones through various domains (PHD and BRM). This in turn recruits chromatin modifying

enzymes like lysine methyltransferases (SETB1) and ubiquitinases (UHRF1) (Quenneville, Verde, Corsinotti, et al., 2011; Rose, & Klose, 2014; Zuo, Sheng, Lau, et al., 2012).

Histone PTM Maintenance During Replication

During the G1 phase of the cell cycle, nucleosomes are disrupted, parental histone proteins are removed and DNA is prepared for synthesis. During the S phase of the cell cycle, double stranded DNA is unwound and subsequently copied, and histone proteins are synthesized. New and largely unmodified histones are then deposited by chaperones in order to form the nucleosome (Budhavarapu, Chavez, & Tyler, 2013). We know that the newly synthesized DNA strand will be unmethylated, and the methylation pattern on the parental strand will be quickly and readily copied onto the daughter strand by DNMT1 (Auclair, & Weber, 2012). The mechanism behind histone PTM maintenance during the cell cycle is still being investigated. The proposed mechanism is similar to the maintenance of DNA methylation patterns. The histone tetramers (H2A-H2B dimers; H3-H4 heterodimers) are proposed to split – each H2A-H2B and H3-H4 dimers are incorporated into the two daughter DNA duplexes along with newly synthesized H2A-H2B and H3-H4 dimers brought in by histone chaperones (e.g. Chromatin Assembly Factor 1 (CAF-1)) in a highly orchestrated manner, in order to form the complete nucleosome particle (Alabert, Barth, Reverón-Gómez, et al., 2015; Budhavarapu, Chavez, & Tyler, 2013). Histone PTMs are then modified and / or acquired by two proposed mechanisms. The first is through an accumulation of histone PTMs just before the start of the cell cycle, which are then transiently reduced or diluted during DNA replication (Alabert, Barth, Reverón-Gómez, et al., 2015; Budhavarapu, Chavez, & Tyler, 2013). The second is by a quick and / or gradual acquisition of the existing PTMs in combination with newly acquired PTMs during G2 and M

phases since histone modifying enzymes are differentially expressed during all phases of the cell cycle (Alabert, Barth, Reverón-Gómez, et al., 2015; Budhavarapu, Chavez, & Tyler, 2013). For example, H3K27me3 levels accumulate prior to S phase and is subsequently diluted through replication, while H3K9 methylation patterns are transiently reduced during S phase and are gradually re-acquired before the next S phase. The histone methylase responsible for H4K20 dimethylation is only expressed during G2-G1 phase, and so H4K20me2 progressively accumulates during the cell cycle (Budhavarapu, Chavez, & Tyler, 2013).

Epigenetic Effects of *In Utero* Alcohol Exposure

It has been well established that ethanol can affect epigenetic modifications and mechanisms (Basavarajappa, & Subbanna, 2016; Chater-Diehl, Laufer, & Singh, 2017; Lussier, Weinberg, & Kobor, 2017; Resendiz, Mason, Lo, et al., 2014). At the time of writing, at least 58 published articles report the epigenetic effects of alcohol in various cultured cells and tissues, in a wide range of animals, as well as in humans. Only a few will be mentioned here. These studies have revealed that ethanol can directly modify DNA cytosine modifications or histone PTMs, affect the "writers", "readers" and "erasers" of epigenetic modifications, and interfere with the biochemical compounds / metabolites that act as donors or co-factors. This in turn causes changes in gene expression at any developmental time point, at any given gene, and at any given gene promotor.

The first DNA methylation study that demonstrated the *in utero* effects of alcohol was done by Garro *et al.* in 1991. Pregnant Swiss-Webster mice were given 3g/kg body weight of ethanol by gavage twice a day on G9 and G10, and once on G11 (Garro, McBeth, Lima, et al., 1991). Animals were euthanized 5 hours after the last ethanol exposure and fetuses were removed. Hypomethylation of whole fetal PNAE DNA was found as well as a decrease in nuclear DNA methylase activity (Garro, McBeth, Lima, et al., 1991). The first study to demonstrate DNA methylation changes caused by PNAE in brain was done by Vallés *et al.* in 1997, followed by a second study by Maier *et al.* in 1999. Vallés *et al.* utilized female Wistar rats who received a liquid diet of 5% ethanol for 30 days before mating and throughout gestation (Vallés, Pitarch, Renau-Piqueras, et al., 1997). The pregnant dams were allowed to give birth and pups were sacrificed at P4, 7, 14 and 21. *In vitro* astrocyte cell culture showed a decrease in the number of astrocytes in PNAE offspring. Western blots of protein extracted from whole brains in

PNAE offspring at all ages verified this; levels of astroglial protein GFAP decreased. DNA

methylation results (methylation-sensitive restriction enzyme digestion, and Southern blotting

analysis) in P21 brains demonstrated an increase in methylation in GFAP labelled DNA (Vallés,

Pitarch, Renau-Piqueras, et al., 1997). Maier *et al.* utilized pregnant Sprague-Dawley rats who

were given 6.0g/kg alcohol daily by intragastric intubation throughout the entire pregnancy (G1-

G20) (Maier, Cramer, West, et al., 1999). On G21, a subset of dams were euthanized to remove

fetuses and extract the olfactory bulbs as well as the whole brain. The remaining dams were

allowed to give birth and pups were euthanized between P10 and P12 (depending on day of

birth), and were labelled as G33. The olfactory bulbs and entire brains were also removed. There

was an observed decrease in olfactory bulb volume, granule cell density and number in both

PNAE ages. A decrease was also seen in the expression of brain derived neurotropic factor

(BDNF) mRNA (measure by RT-PCR) in both PNAE ages, where the decrease was greater in

G33 than in G21. BDNF DNA methylation was measured by *HpaII* digestion in PNAE G33 pups

where an increase in methylation was noted (Maier, Cramer, West, et al., 1999).

The first study to look at the effects of ethanol on histone PTMs was done by Park *et al.*

in 2003. Cultured rat hepatocytes were incubated with various doses (5-200mM) of ethanol for

24 hours where ethanol treatment increased H3K9ac levels, and H3K14ac was unaffected (Park,

Miller, & Shukla, 2003). A similar study utilizing cultured hepatic stellate cells found the same

result, and expanded the histone PTMs investigated to include more acetylated marks and one

methylation mark (Kim, & Shukla, 2005). H3K9ac increased in a dose-dependent manner in all

ethanol treatments and durations. At the highest dose of ethanol treatment (200mM; 72 hour

duration) H3K23ac increased, and no effect was seen in H3K14ac, H3K18ac and methylated

H3K9 (Kim, & Shukla, 2005). The first study to look at the effects of alcohol treatment on

histone PTMs in whole brain was done by Kim *et al.* in 2006. The authors took 8-week-old

Sprague Daley rats and gave them a single binge-like amount of ethanol through oral injection

before sacrificing them at 3 different times (1, 3 and 12 hours after injection). Fifteen different

types of tissues were extracted for western blotting. The liver and testicles demonstrated a time

dependent increase in H3K9ac but the brain (as well as various other tissues like the heart)

showed no change in H3K9ac. H3K9 methylation showed little to no effect in all tissues (Kim, &

Shukla, 2006).

During the early 21st century, nutritional supplementation with choline at the time of *in*

utero and / or postnatal alcohol exposure, attenuated cognitive and behavioural deficits in rodents

(Otero, Thomas, Saski, et al., 2012; Ryan, Williams, & Thomas, 2008; Thomas, Biane, O'Bryan,

et al., 2007). A few neural cell culture studies further demonstrated the epigenetic effects of

ethanol (D'Addario, Johansson, Candeletti, et al., 2011; Hicks, Middleton, & Miller, 2010; Zhou,

Balaraman, Teng, et al., 2011). A few studies demonstrated imprinted gene specific epigenetic

effects of PNAE (Downing, Johnson, Larson, et al., 2011; Haycock, & Ramsay, 2009; Liu,

Balaraman, Wang, et al., 2009). A rat postnatal ethanol treatment study revealed changes to

histone acetylation in the cerebellum. Guo *et al.* exposed mothers and their newborn pups to

ethanol vapors for 4hrs/day between P2-12. Offspring were euthanized and the cerebellum was

removed. CREB binding protein (CBP; a histone lysine acetyltransferase) levels decreased in

alcohol treated offspring along with histone H3 and H4 acetylation levels in the cerebellum

(Weixiang Guo, Crossey, Zhang, et al., 2011).

The first study to look at the epigenetic effects of PNAE in the brain was done by

Govorko *et al.* in 2012. Pregnant Sprague-Dawley rats were given a liquid ethanol diet to

consume ad libitum on G7 through G21 (Govorko, Bekdash, Zhang, et al., 2012). The dams gave

birth and the pups were sacrificed between 60 and 80 days after birth. Blood and the arcuate

nucleus (ARC) or paraventricular nucleus (PVN) of the hypothalamus were sampled. The

authors were interested in the neurons that contained proopiomelanocortin (POMC) peptide,

which plays a role in stress, metabolism and immunity. POMC mRNA levels were lower in

PNAE animals ARC (no effect in blood) when compared to pair-fed controls. β-endorphine

levels decreased in PNAE offspring, which regulates the stress response by decreasing the

release of stress hormones (corticosterone and corticotropin (ACTH)). The levels of these

hormones were higher in PNAE offspring hypothalamus. *HpaII* digestion of *Pomc* gene and

Dnmt3a gene revealed an increase in methylation in *Pomc* but no effect in *Dnmt3a*. RT-PCR

analysis demonstrated the increase in methylation was at the *Pomc* promotor. The authors then

evaluated the possible alterations of histone PTMs in β-endorphine positive POMC neurons of

the ARC. H3K9ac and H3K4me2/me3 decreased while H3K9me2 increased. The enzymes

responsible for these histone modifications were also analyzed (via mRNA levels). *G9a* and

Setdb1 (both methylate H3K9) mRNA levels increased and *Set7/9* (methylate's H3K4)

decreased. mRNA levels of *Dnmt1* as well as the protein level of 5hmC were also measured in β-

endorphine positive POMC neurons of the ARC. *Dnmt1* and 5hmC increased in PNAE offspring

when compared to controls. A subset of animals were treated with a Dnmt1 inhibitor (AZA) and

a HDAC inhibitor (TSA) on days 1, 3 and 5 after birth. Inhibitor treatment rescued the *Dnmt1*

and 5hmC increases in PNAE offspring. This study was also the first to demonstrate

transgenerational inheritance of epigenetic modifications induced by PNAE (Govorko, Bekdash,

Zhang, et al., 2012), which is discussed below.

After this study, Subbanna and colleagues conducted a series of postnatal alcohol

exposure epigenetic studies in rodent brain to assess neuronal cell death. They primarily looked

at histone methylation and treatment effects with histone demethylase inhibitors. This first study demonstrated a significant neuronal cell loss after one binge-like ethanol treatment at P7 in mouse brain. G9a activity increased which in turn increased H3K9me2 and H3K27me2 methylation. This increase in methylation targets Caspase-3 driven proteolytic degradation and treatment with a G9a inhibitor (BIX) prior to ethanol treatment rescued these effects (Subbanna, Shivakumar, Umapathy, et al., 2013). The studies that followed confirmed the neuroprotective effects of G9a inhibitor BIX treatment (Subbanna, Nagre, Shivakumar, et al., 2014) as well as G9a capabilities of associating with DNMT3A and MeCP2, therefore affecting DNA methylation (Subbanna, & Basavarajappa, 2014). In 2015, Subbanna and colleagues took a different direction, demonstrating that the same P7 binge-like ethanol treatment in mouse affected the acetylation of cannabinoid type 1 (CB1R) receptor which in turn upregulates CB1R function and causes neurobehavioural deficits in adults (Subbanna, Nagre, Umapathy, et al., 2015).

Recently, research on *in utero* alcohol effects on epigenetics has moved towards whole genome methylome studies, as well as specific gene expression studies. First, looking at specific DNA methylation changes at gene promotors in PNAE mouse models, particularly in the brain (Chater-Diehl, Laufer, Castellani, et al., 2016; Laufer, Mantha, Kleiber, et al., 2013; Marjonen, Sierra, Nyman, et al., 2015; Veazey, Parnell, Miranda, et al., 2015; Zhang, Ho, Vega, et al., 2015). Then, moving onto human studies where human ESCs are treated with ethanol (Khalid, Kim, Kim, et al., 2014). Now, living human FASD patients through buccal saliva (Laufer, Kapalanga, Castellani, et al., 2015; Lussier, Morin, MacIsaac, et al., 2018; Portales-Casamar, Lussier, Jones, et al., 2016). Therefore, the current literature lacks specific histone PTM changes in humans, which is what I set out to do by analyzing PNAE human autopsy brain tissue.

Paternal Aspect

Although maternal alcohol consumption is the primary cause of FASD in offspring, paternal alcohol consumption is a contributing factor to FASD phenotype and is fairly well documented. Particularly with epigenetics, paternal alcohol consumption (with no maternal PNAE) has been associated with increased risk for spontaneous abortion, low birth weight, congenital defects, and cognitive and behavioural changes (including hyperactivity) in offspring (Abel, & Bilitzke, 1990; Abel, 2004; Finegersh, Rompala, Martin, et al., 2015; Liang, Diao, Liu, et al., 2014). Paternal alcohol consumption has also been associated with affected sperm and reduced fertility (Stuppia, Franzago, Ballerini, et al., 2015). One study analyzed imprinted gene CpG methylation in sperm from human volunteers (median age 25) who drank alcohol. DNA methylation was negatively correlated with alcohol consumption in DMRs of imprinted genes *IG* (*DLK1* and *GTL2*) and *H19* (*H19* and *IGF2*). Meaning, a decrease in methylation was seen at these reciprocally expressed imprinted genes which worsened with higher alcohol consumption (Ouko, Shantikumar, Knezovich, et al., 2009). Because almost all histones are replaced by protamines during spermatogenesis (histone variants H3.2 and H3.3 tend to remain while H3.1 and H3.5 are replaced) (Shiraishi, Shindo, Harada, et al., 2018), there is no known paternal alcohol study that has demonstrated altered histone PTMs in sperm.

Transgenerational Epigenetic Effects

The term transgenerational implies that a specific trait is inherited across multiple generations. However, in the context of PNAE, the more appropriate term is intergenerational. This is because the mother (F0) consumes the alcohol and if carrying a female (F1) can therefore affect her offspring directly, resulting in FASD, and potentially affect the future offspring (F2)

since their germ cells are present. A trait becomes transgenerational if offspring of F2 (F3) also has the trait in question. Among males, transgenerational inheritance would be in F2 offspring, since F0 would be carrying F1 male offspring (which carries F2) and if the trait is present in F2, then it has been transgenerationally transmitted. In the context of FASD, intergenerational (two generations) and transgenerational (three generations) inheritance is difficult to believe because of the lack of genetic link to FASD (alcohol being an environmental factor) as well as the multiple mechanisms in place that protect future offspring from parental experiences such as the DNA methylation reprogramming events that take place not only in the F1 offspring, but in F2, through reprogramming of primordial germ cells (PGCs) (Finegersh, Rompala, Martin, et al., 2015; Reik W, Dean W, 2001).

A few animal models have looked into the transgenerational epigenetic effects of PNAE with varying success (Finegersh, Rompala, Martin, et al., 2015; Finegersh, & Homanics, 2014; Knezovich, & Ramsay, 2012; Sarkar, 2016; Yohn, Bartolomei, & Blendy, 2015). One example that has extensively been studied is the effects of PNAE on the *POMC* gene promotor methylation (full study was described above). Govorko *et al.* demonstrated the hypermethylation of several CpG dinucleotides in the *POMC* promotor region of FASD rat offspring (F1) (Govorko, Bekdash, Zhang, et al., 2012). These offspring were allowed to mate with non-affected rats of the opposite sex and subsequently produced F2 (male and female) and F3 (male and female) generations. In the second generation, the same decrease in *POMC* gene expression was seen in male progeny only, produced by both female and male F1. In the third generation, only male F2 produced F3 males that had the same result (Govorko, Bekdash, Zhang, et al., 2012). Therefore, there were intergenerational as well as transgenerational epigenetic effects. In addition, the authors measured *POMC* gene methylation in sperm of all three generations and

observed the same decrease (Govorko, Bekdash, Zhang, et al., 2012; Sarkar, 2016). Another recent study also demonstrated specific gene methylation effects that were transgenerationally inherited (Abbott, Rohac, Bottom, et al., 2017). P90 mice (F0) were bred and self-ingested a solution of 25% ethanol throughout the entire pregnancy. F2 and F3 generations were produced by cross-fostering PNAE males from F1 and F2 with control females. The animals were sacrificed at birth and the neocortex was isolated for gene expression, DNA methylation and DNMT expression studies. A variety of genes demonstrated differential expression between PNAE and control. *Id2* and *Rzrβ* demonstrated decreases in promotor methylation resulting in increased transcription in all three generations of mice. Global 5mC and 5hmC results demonstrated a decrease in 5mC and an increase in 5hmC in F1 offspring. These results were not seen in the second and third generations. DNMT1, 3A and 3B expression in the neocortex also decreased (Abbott, Rohac, Bottom, et al., 2017).

Complexity of Alcohol Exposure: Tobacco and Other Drugs

Women who abuse alcohol during pregnancy also abuse other drugs, mainly tobacco / cigarette smoking, marijuana, cocaine, opioids, and methamphetamines (Jarmasz, Basalah, Chudley, et al., 2017; Muckle, Laflamme, Gagnon, et al., 2011). These licit and illicit drugs all readily cross the placenta and all act primarily on the brain, which in turn lead to various behavioural and cognitive deficits (Behnke, & Smith, 2013; Irner, 2012; Kohlmeier, 2014; Szutorisz, & Hurd, 2016; Yohn, Bartolomei, & Blendy, 2015). They have been associated with negative fetal outcomes such as reduced growth, congenital anomalies and increased risk for preterm birth, miscarriage, stillbirth and withdrawal (see **Table 1.5** for complete details).

A limited number of studies have been conducted to investigate the epigenetic effects of these drugs *in utero*. Pregnant mice were exposed to drinking water containing nicotine (200µg/ml) or saccharin from conception up until P21. At three months of age, the brains of exposed offspring had increased density and complexity in dendritic spines of cortical neurons. ChIP-PCR revealed increases in H3K4me3 levels associated with the *Mef2C* locus (Myocyte Enhancer Factor 2C) in the cortex (Jung, Hsieh, Lee, et al., 2016). Fetuses (G20) of pregnant rats exposed to 2.0mg/kg of nicotine from G9 to G20 had decreased promotor methylation of *Gad67* (Glutamate decarboxylase), decreased *Dnmt1* expression, and increased GABA content in the hippocampus (He, Lu, Dong, et al., 2017). Human fetuses exposed to maternal smoking and subjected to elective abortion during the second trimester had alterations in DNA methylation patterning in promotor regions of *GNA15* and *SDHAP3* (Chatterton, Hartley, Seok, et al., 2017). A few other human studies of maternal smoking showed CpG methylation in human placentas (Maccani, Koestler, Houseman, et al., 2013), newborn infants (Joubert, Håberg, Nilsen, et al., 2012), and in children (Breton, Byun, Wenten, et al., 2009).

Only one study of *in utero* exposure to cannabis has been conducted in the context of epigenetics. Pregnant rats received IV injections of 9-tetrahydrocannabinol (9-THC) (150ug/kg) from G5-P2. In P2 and P62 THC exposed offspring, mRNA expression of Dopamine Receptor D2 (*Drd2*) was downregulated in the nucleus accumbens (NAc). ChIP analysis revealed a decrease in H3K9me2 and an increase in H3K4me3 levels near the transcription start site of *Drd2* (Dinieri, Wang, Szutorisz, et al., 2011).

A few *in utero* cocaine exposure epigenetic studies have also revealed changes in gene expression (Kabir, Kennedy, Katzman, et al., 2014; McCarthy, Mueller, Cannon, et al., 2017; Novikova, He, Bai, et al., 2008). Paternal cocaine use has also been shown to affect offspring

and these effects can be intergenerationally inherited (Finegersh, Rompala, Martin, et al., 2015; Vassoler, White, Schmidt, et al., 2013).

There is only one *in utero* methamphetamine epigenetic study. Before mating, male and female C57Bl/6J mice were injected every-other day with methamphetamine (or saline) from adolescence (P46–51) into adulthood (P87–94). The amount of methamphetamine increased weekly between P33 up to P60. Once pregnant, female mice continued methamphetamine use (fixed dose) up until G17. Cross-fostering assessed the effect of maternal care of drug and saline exposed offspring. P40–P45 offspring were sacrificed for DNA methylation analysis utilizing MeDIP-ChIP in the hippocampus. The authors found differentially methylated regions as a result of both *in utero* methamphetamine exposure and maternal care (Itzhak, Ergui, & Young, 2015). To our knowledge, no one has looked at *in utero* opioid exposure and analyzed epigenetics in offspring.

Ideally, combinational drug exposure studies would better represent the human condition and there is a paucity of mixed toxicity animal model studies (Bhattacharya, Majrashi, Ramesh, et al., 2018; Church, Holmes, Overbeck, et al., 1991; Martin, Martin, Chao, et al., 1982; Mitchell, Keller, & Snyder-Keller, 2002; Morris, Dinieri, Szutorisz, et al., 2011; Wells, Bhatia, Drake, et al., 2016).

Table 1.5: Licit and illicit drugs as well as their effect on the mother, fetus and the placenta.
(Behnke, & Smith, 2013; Howard S. Smith, 2009; Tai, Piskorski, Kao, et al., 2017; Viteri, Soto, Bahado-Singh, et al., 2015; Whiteman, Salemi, Mogos, et al., 2014; Yohn, Bartolomei, & Blendy, 2015)

Drug Details		Maternal & Fetal Effects	Placental Effects
Tobacco smoking	**Active component:** Nicotine	↑ hypoxia ↓ birth weight Growth restriction Preterm birth Stillbirth Congenital anomalies ↑ Premature Mortality & SUDI Hypertonia Withdrawal / neonatal abstinence syndrome	↓ uterine blood flow to placenta ↓ blood flow in placenta ↑ hypoxia Abruption, previa Affected nutrient transport
	Acts on: Nicotinic acetylcholine receptors (nAChRs)		
Marijuana	**Active component:** 9-tetrahydrocannabinol (9-THC)	↑ or ↓ birth weight ↑ Neonatal morbidity Preterm birth	↑ weight
	Acts on: Gi-coupled cannabinoid type 1 and 2 (CB1R and CB2R) receptors		
Methamphetamine	**Active component:** Amphetamine	↑ risk of intrauterine death smaller placenta-to-birth weight ratio Withdrawal / neonatal abstinence syndrome	↑ weight Abruption Affected nutrient transport
	Acts on: Trace amine-associated receptor 1 (TAAR1), a G protein-coupled receptor (GPCR)		
Cocaine	**Active component:** Cocaine	Miscarriage ↓ birth weight Growth restriction Withdrawal	↓ blood flow Abruption, previa, infarction, preeclampsia Affected nutrient transport
	Acts on: Binds to the serotonin, norepinephrine transporter, dopamine transporter, and sodium channels		
Opioids: Morphine Codeine Oxycodone Fentanyl Methadone Heroin, etc.	**Active component:** Hydromorphone, morphine, and dihydromorphine	Growth restriction ↑ risk of stillbirth Severe withdrawal / neonatal abstinence syndrome	**unknown**
	Acts on: Opioid G-protein coupled receptors; mu-, kappa- and delta		

Human Autopsy Material

Human autopsy material, brain banks and other tissue banks (e.g. cancer) are mainly based on tissue obtained from living patients (through biopsy) or after death (through autopsy). Outside of brain tumors and epilepsy, the opportunity to obtain "fresh" tissue is rare, forcing one to rely on brain banked tissue samples or autopsy material (Stan, Ghose, Gao, et al., 2006). Such samples inherently have several limitations. These include: variation in the circumstances before death (agonal state), variation in the circumstances after death, variation in the time between death and autopsy (post-mortem delay - PMD), post-mortem artefacts, tissue pH, differences in preservation and storage, differences in tissue acquisition and processing. Even after considering all these logistic and technical variables, there are considerable relative differences in the vulnerability of DNA, RNA, proteins and metabolites.

Trauma, seizures, prolonged hypoxia, use of anesthetic, infection, fever and acidosis can all have an effect on the brain tissue sample, particularly at a molecular level (Ferrer, Martinez, Boluda, et al., 2008; Srinivasan, Sedmak, & Jewell, 2002). Brain tissue pH does not appear to be a good "quality indicator", as pH is rather stable in all regions of the brain; however, it can be a useful screening tool in the selection of research samples (e.g Control vs. ischemic) (Monoranu, Apfelbacher, Grünblatt, et al., 2009; Stan, Ghose, Gao, et al., 2006). Brain tissue pH is dependent on the circumstances before death (prolonged versus rapid death; ischemia) to a greater extent than the PMD (Li, Vawter, Walsh, et al., 2004; Monoranu, Apfelbacher, Grünblatt, et al., 2009).

Considerable changes can occur in the antemortem period. It has been reported that individuals who suffered ischemic brain injury leading to death have lower levels of histone acetylation, thereby inhibiting the transcription of many genes (Faraco, Pancani, Formentini, et

al., 2006). In rodent models, long and repeated (e.g. 2 hours daily) or single and short (e.g. 20 minutes) exposure to anesthesia has been shown to up-regulate the expression of certain genes in the hippocampus (Ju, Jia, Sun, et al., 2016; Pekny, Andersson, Wilhelmsson, et al., 2014). Two-hour long exposure to sevoflurane in P7 mice affected the phosphorylation of epigenetic protein MeCP2 in the hippocampus (Han, Li, Zhang, et al., 2014). Changes in histone acetylation proximal to certain gene promoters is also affected by the anesthesia sevoflurane (Mori, Iijima, Higo, et al., 2014).

Taken together, the uncontrollable variability of autopsy or tissue bank studies could compromise our ability to interpret molecular findings.

Tissue Fixation, Preservation and Storage

German physician Ferdinand Blum in 1893 accidentally discovered that formaldehyde (discovered in 1859) can preserve ("fix") tissue (Donczo, & Guttman, 2018; Fox, Johnson, Whiting, et al., 1985; Frankel, 2012). Formaldehyde is a naturally occurring organic compound that is a simple chemical modification of methanol. Today, formaldehyde is used as an industrial disinfectant, for preservation of tissues for medical and research purposes, for embalming, and can be found in medicines and cosmetics (Fox, Johnson, Whiting, et al., 1985). The most widely used tissue fixative is 10% buffered formalin which is a 4% formaldehyde solution with ~1.2% methanol, and ~1% sodium phosphate in water (Donczo, & Guttman, 2018; Fox, Johnson, Whiting, et al., 1985; Srinivasan, Sedmak, & Jewell, 2002). However, it is easily oxidized by atmospheric oxygen to produce formic acid. Therefore, the phosphate salt is added to neutralize the pH and formulate a working solution. Formaldehyde crosslinks proteins and nucleic acids through the formation of methylene bridges, thereby conserving the architecture and structure of

cells, making it the most popular fixative (Donczo, & Guttman, 2018). The tissue penetration by diffusion and covalent reaction is slow. Solid tissues are fixed at approximately 1mm per hour at room temperature. An excess of formalin is also required (approximately 10-20 times more volume) in order to properly fix the tissue (Srinivasan, Sedmak, & Jewell, 2002). Formaldehyde is extremely toxic and carcinogenic. Therefore, alternatives are often sought out. Many do not achieve the same level of morphological preservation, which is ideal for histology. Other fixatives include glutaraldehyde (stronger cross linking, slower diffusion rate), ethanol or methanol (often combined with acetic acid or chloroform; risk of tissue shrinkage), and honey (a safer alternative) (Donczo, & Guttman, 2018; Lalwani, Surekha, Vanishree, et al., 2015; Srinivasan, Sedmak, & Jewell, 2002). Once fixed, the tissue is then dehydrated through a series of graded alcohols and xylene, then embedded in wax (paraffin). This allows for the tissue to be cut and mounted onto slides for staining or immunohistochemistry (Donczo, & Guttman, 2018; Srinivasan, Sedmak, & Jewell, 2002). The formalin-fixed paraffin-embedded (FFPE) blocks can be stored are room temperature for many years, however, some suggest a "shelf-life" ($\leq$10 years) for FFPE blocks when it comes to their use in proteomic or genomic studies (Donczo, & Guttman, 2018). Pre-cut tissue slides are more vulnerable to oxidation and other chemical changes, therefore it is preferable to avoid exposing slides to air, by sealing them in vacuum bags and storing at a freezing temperature (Andeen, Bowman, Baullinger, et al., 2017).

The other option is to freeze tissue samples as-is (ideal for biochemical analysis) at -80°C (Donczo, & Guttman, 2018). Small pieces of tissue can be placed in a cryoprotective solution such as OCT (Optimal cutting temperature compound), quickly frozen, and then sectioned on a cryostat. The sections are then fixed for a short period of time (seconds) in acetone, ethanol or a

combination of both (Shabihkhani, Lucey, Wei, et al., 2014). The disadvantage to freezing samples is the cost of storage, both short and long-term (Shabihkhani, Lucey, Wei, et al., 2014).

Post-Mortem Changes in DNA

Very soon after death, DNA is well preserved and of high quality when frozen at -80°C or formalin-fixed and paraffin-embedded. A post-mortem delay of up to 48 hours at 4°C, followed by freezing at -80°C or FFPE also produces high quality extracted DNA. Extremely prolonged fixation (10 to 20 years) in non-buffered formalin produces low quality extracted DNA (Ferrer, Armstrong, Capellari, et al., 2007). If carrying out genetic studies (e.g. point mutation or polymorphism studies) certain preservation and fixing parameters need to be respected. Sample(s) must be stored at -80°C (≤35 years) or fixed in buffered-formalin for (≤4 weeks) prior to paraffin embedding. One study demonstrated that FFPE block storage for 4-6 years was associated with a decrease in yield compared to recent embedded tissue (Guyard, Boyez, Pujals, et al., 2017). Preservation in buffered- or non-buffered-formalin for greater than 6 months with no paraffin embedding is not ideal (Ferrer, Armstrong, Capellari, et al., 2007). It is also recommended to use commercial kits for DNA extraction (e.g. Qiagen), particularly for frozen tissue or recent (<1 year) FFPE tissue as opposed to salting out or phenol–chloroform methods (Funabashi, Barcelos, Visoná, et al., 2012). With regard to genomics, DNA extracted from FFPE tissue blocks is feasible (Donczo, & Guttman, 2018; Frankel, 2012).

Post-Mortem Changes in RNA

RNA preservation and integrity appear to depend on post-mortem delay, the storage temperature (ideally -80°C or lower), and on thawing time (the shorter the better). In general,

RNA integrity decreases with increasing PMD (Ferrer, Martinez, Boluda, et al., 2008; Srinivasan, Sedmak, & Jewell, 2002; Stan, Ghose, Gao, et al., 2006). Depending on the RNA of interest, the half-life of that RNA may be long, therefore being unaffected by longer PMDs (Buesa, Maes, Subirada, et al., 2004; Ferrer, Martinez, Boluda, et al., 2008). In the brain, studies have shown that PMD was not a predictor of RNA integrity, nor was assessing the pH post-mortem (Stan, Ghose, Gao, et al., 2006). Other studies indicate that the brain pH is a good indicator of RNA quality (Chevyreva, Faull, Green, et al., 2008; Durrenberger, Fernando, Kashefi, et al., 2010). When sampling or preserving tissue for RNA analysis, it is recommended that an RNase inhibitor be added (Buesa, Maes, Subirada, et al., 2004) to reduce the risk of degradation. With regard to genomics, RNA extracted from FFPE tissue blocks is also feasible through specific tailored extraction methods (Donczo, & Guttman, 2018; Frankel, 2012).

Post-Mortem Changes in Proteins

Protein preservation depends on the protein itself, the PMD and storage temperature (4°C being ideal, room temperature detrimental) (Crecelius, Götz, Arzberger, et al., 2008; Ferrer, Santpere, Arzberger, et al., 2007). Some proteins begin to degrade within minutes or with increasing PMD (Hunsucker, Solomon, Gawryluk, et al., 2008), while others appear to increase (Hilbig, Bidmon, Till Oppermann, et al., 2004). Some studies suggest structural and metabolic proteins tend to degrade first (Crecelius, Götz, Arzberger, et al., 2008; Ferrer, Santpere, Arzberger, et al., 2007); synaptic proteins vary, and synaptophysins appear resistant (Chandana, Mythri, Mahadevan, et al., 2009; Ferrer, Santpere, Arzberger, et al., 2007; Monoranu, Apfelbacher, Grünblatt, et al., 2009; Siew, Love, Dawbarn, et al., 2004). In addition, protein receptors appear to be resistant to degradation, however, certain receptor subunits are susceptible

(González-Maeso, Torre, Rodríguez-Puertas, et al., 2002; Mato, & Pazos, 2004; Wang, TesFaye, Yasuda, et al., 2000). As mentioned above, pre-cut slides exposed to air (ranging from 0, 1 and 6 weeks to 24 and 52 weeks) can have reduced immunoreactivity. This has been shown with antibodies targeting various proteins such as p53, Ki-67, and synaptophysin, where Ki-67 was less stable than p53 and synaptophysin with increasing air exposure duration (Andeen, Bowman, Baullinger, et al., 2017). The reason why some proteins are more resistant to degradation than others is unclear. What is clear is the caution one must take when undertaking and interpreting proteomics in human post-mortem brain tissue.

Post-Mortem Changes in Epigenetic Modifications

Compared to DNA and RNA, less is known about the maintenance of epigenetic modifications following death. Two studies found nucleosomes to be stable after death; DNA remains attached to histones for at least 30 hours post-mortem (Huang, Matevossian, Jiang, et al., 2006; Stadler, Kolb, Rubusch, et al., 2005). Histone tail PTMs have been investigated, but not extensively. Utilizing immunohistochemistry, one study showed that histone methylation (H3K4me2, H3K4me3, H3K27me3, H4K20me3) at glutamate receptor gene promoters is maintained in brain tissue for at least 11 hours post-mortem (Stadler, Kolb, Rubusch, et al., 2005). Utilizing chromatin immunoprecipitation (ChIP), Huang *et al* reported histone PTMs H3K4me3 and H3K27me3 to be stable up to 30 hours post-mortem at various gene promoters (Huang, Matevossian, Jiang, et al., 2006). Barrachina *et al*. reported that histone acetylation (H3K9ac and H3K27ac) is not well-maintained post-mortem. In a small cohort of heterogeneous control and Alzheimer's samples, native chromatin immunoprecipitation (NaChIP) revealed histone acetylation variability within the first 48 hours after death (Barrachina, Moreno, Villar-

Menéndez, et al., 2012). However, the authors did not attempt any statistical analysis, which means their results may be inconclusive. A study of FFPE brain samples from two adults verified integrity of DNA and DNA methylation using a variety of molecular techniques. The authors concluded that global DNA methylation along with gene-specific DNA methylation appear preserved (Bak, Staunstrup, Starnawska, et al., 2018). Methylation patterns were successfully analyzed using bisulphite conversion of DNA extracted from human brains with Alzheimer's disease and a PMD of ~48 hours (Barrachina, & Ferrer, 2009). Enzyme activities (methyltransferase and acetyltransferase) responsible for epigenetic modifications were measured in 12 human brain cases with PMD ranging from 5 to 100 hours; the activities showed a tendency to decline but the change was not statistically significant (Monoranu, Apfelbacher, Grünblatt, et al., 2009).

Preserved Tissue Use in Future Research

An abundance of FFPE tissue samples are stored in pathology departments worldwide. These could be of great use to study human neurological diseases. Various biochemical methods have been optimized to overcome the crosslinking effects of formaldehyde preservation in FFPE tissue samples (Donczo, & Guttman, 2018; Frankel, 2012). DNA, RNA (mRNA and miRNA) and protein extracted from FFPE tissues has been considered unfit for high-throughput biochemical analysis, where high quality and yield of nuclear extracts is necessary. Studies utilizing human extracted bisulfite converted DNA from living patients followed by pyrosequencing to examine DNA methylation patterns at CpG sites are increasingly frequent. Their patterns in specific neurological diseases have the potential to be diagnostic biomarkers (Hyerim Kim, Wang, & Jin, 2018; Levenson, 2010). This points to the need for protocols that are

capable of extracting high quality DNA, RNA and protein in FFPE tissue. Recent studies do

demonstrate the abilities of extracting DNA from FFPE blocks and its use for methylation

profiling microarrays (Haile, Pandoh, McDonald, et al., 2017; Thirlwell, Eymard, Feber, et al.,

2010; Yakovleva, Plieskatt, Jensen, et al., 2017). Therefore, the future potential of FFPE tissue

samples is increasing.

CHAPTER 2: HYPOTHESIS AND RESEARCH AIMS

The overarching research questions are whether epigenetic changes occur *in utero* as a consequence of prenatal alcohol exposure (PNAE) and if they in turn lead to the brain abnormalities seen in fetal alcohol spectrum disorder (FASD).

Main Hypothesis

Following PNAE, abnormal epigenetic modifications occur in human brain tissue.

Research Aims

1. Retrospectively review autopsy records to identify individuals with a history of PNAE or diagnosis of FASD and to describe the epidemiologic and neuropathologic features of the cases. This database and tissue source will be used to test the main hypothesis.

2. Determine the stability of histone post-translational modifications (PTMs) and DNA cytosine modifications in rodent, porcine, and non-PNAE / non-FASD human brain after death using immunohistochemistry and select biochemical methods. This will ensure that findings in the main experiment are not artifacts of post-mortem delay (PMD) that are misinterpreted as PNAE-associated changes.

3. A) Perform immunohistochemical labeling and semi-quantitative analyses to identify histone PTMs and DNA cytosine modifications in temporal lobe specimens (including hippocampus) of stillborn fetuses and infants with PNAE. Comparisons to age-, sex-, and PMD-matched controls will allow us to identify the neuronal and glial cell populations abnormally affected.

B) Using the same methods as aim A), histone PTMs and DNA cytosine modifications will be examined in brain samples of a non-human primate (*Macaca nemestrina*) model of binge-PNAE. The fact that the amount and timing of alcohol has been controlled will increase our confidence in conclusions reached in the human tissue study.

CHAPTER 3: MANUSCRIPT 1 - HUMAN BRAIN ABNORMALITIES ASSOCIATED WITH PRENATAL ALCOHOL EXPOSURE AND FETAL ALCOHOL SPECTRUM DISORDER

Authors: Jessica S. Jarmasz, Duaa A. Basalah, Albert E. Chudley, and Marc R. Del Bigio

Published in: Journal of Neuropathology and Experimental Neurology. 2017 Sep 1;76(9):813-833.

Preface

This publication was the result of the first research aim.

Author contributions:

I (the first author) assembled the clinical database, put together 80% of the results and wrote the manuscript. The last author (Del Bigio) planned the project, conducted the search of the autopsy database to identify the possible PNAE / FASD autopsy cases, reviewed all of the neuropathology report findings for each case in the final cohort, prepared the figures and finalized the manuscript. The second author (Basalah) helped with the review of the neuropathology by documenting the notes and comments. The third author (Chudley) is a clinical geneticist; provided access to clinical - diagnostic databases and provided context to the clinical syndrome of FASD.

ABSTRACT

Fetal alcohol spectrum disorder (FASD) is a common neurodevelopmental problem, but neuropathologic descriptions are rare and focused on the extreme abnormalities. We conducted a retrospective survey (1980 – 2016) of autopsies on 174 individuals with prenatal alcohol exposure or an FASD diagnosis. Epidemiologic details and neuropathologic findings were categorized into 5 age groups. Alcohol exposure was difficult to quantify. When documented, almost all mothers smoked tobacco, many abused other substances, and prenatal care was poor or non-existent. Placental abnormalities were common (68%) in fetal cases. We identified micrencephaly (brain weight $<5^{th}$ percentile) in 31, neural tube defects in 5, isolated hydrocephalus in 6, corpus callosum defects in 5 (including some with complex anomalies), probable prenatal ischemic lesions in 5 (excluding complications of prematurity), minor subarachnoid heterotopias in 4, holoprosencephaly in 1, lissencephaly in 1, and cardiac anomalies in 26 cases. The brain abnormalities associated with prenatal alcohol exposure are varied; cause-effect relationships cannot be determined. FASD is likely not a monotoxic disorder. The animal experimental literature, which emphasizes controlled exposure to ethanol alone, is therefore inadequate. Prevention must be the main societal goal however, a clear understanding of the neuropathology is necessary for provision of care to individuals already affected.

INTRODUCTION

The potential for adverse effects of alcohol (ethanol) on the developing fetus has been recognized for centuries (Sanders, 2009). The modern era of medical study began after the publications by Lemoine and coworkers in 1968 and by Jones and coworkers in 1973 (Jones, Smith, Ulleland, et al., 1973; Lemoine, Harousseau, Borteyru, et al., 2003). They identified

101

stillbirths, prematurity, growth retardation, cognitive delay, face and limb anomalies, microcephaly, and cardiac defects. The first autopsy description of presumed alcohol-related teratogenic effects documented microphthalmia, partially fused cerebral hemispheres with leptomeningeal hamartomas, simplified gyral pattern, large lateral ventricles, and agenesis of the corpus callosum (Jones, & Smith, 1973). Images from this extreme case have been widely reproduced in publications and on the Internet. This was originally termed Fetal Alcohol Syndrome (FAS). The more recent designation, Fetal Alcohol Spectrum Disorder (FASD), encompasses cases with functional abnormalities but not necessarily overt physical anomalies (Senturias, 2014). However, the clinical diagnostic criteria (which include historical evidence of *in utero* alcohol exposure, facial anomalies, growth rate, head size, and neurodevelopmental features) are not unanimously agreed upon, with several different methods in use (Coles, Gailey, Mulle, et al., 2016; Cook, Green, Lilley, et al., 2016; Hoyme, Kalberg, Elliott, et al., 2016; Kable, & Mukherjee, 2017).

The prevalence of FASD has been difficult to determine, due to under-reporting of maternal alcohol use and differences in diagnostic criteria. In the broad population up to 0.5% might be affected, while in certain geographic groups >20% might be affected (Ospina, & Dennett, 2013). FASD is among the most common neurodevelopmental disorders (Bishop, 2010; Roozen, Peters, Kok, et al., 2016) and is associated with substantial costs to society because of lost productivity due to premature mortality and morbidity (Popova, Lange, Burd, et al., 2016).

Despite the apparently high prevalence of FASD, neuropathological findings have been described in only 33 autopsy cases of suspected FASD (Clarren, Alvord, Sumi, et al., 1978; Clarren, 1977; Peiffer, Majewski, Fischbach, et al., 1979; Roebuck, Mattson, & Riley, 1998; Wisniewski, 1983). Reported abnormalities include micrencephaly, regional cortical dysgenesis,

leptomeningeal heterotopias, hydrocephalus, holoprosencephaly, neural tube closure defects, partial or complete agenesis of the corpus callosum, cerebellum and brainstem dysgenesis. In addition, approximately 80 fetuses with a history of prenatal alcohol exposure (PNAE) have been described; the most convincing features are subtle abnormalities of the cortical vasculature (Jégou, El Ghazi, de Lendeu, et al., 2012; Konovalov, Kovetsky, Bobryshev, et al., 1997; Solonskii, Logvinov, & Kutepova, 2008) (see details of all known prior autopsy reports in **Table 3.1**). Quantitative neuroimaging studies on people with FASD highlight the micrencephaly, abnormal gyral patterns, reductions in regional brain volume (primarily basal ganglia, diencephalon, and cerebellum), and abnormalities of the corpus callosum (Hendrickson, Mueller, Sowell, et al., 2017; Moore, Migliorini, Infante, et al., 2014; Nardelli, Lebel, Rasmussen, et al., 2011; Norman, Crocker, Mattson, et al., 2009).

The reported autopsy material tends to document extreme abnormalities that are less frequently reported in the imaging literature. Therefore, our goals were: 1) to assemble a community-based autopsy database of cases with reported PNAE and / or FASD diagnosis; 2) to document the epidemiological and neuropathological features of those cases; and 3) to assemble a collection of tissues to be used for future studies capable of validating pathogenetic hypotheses that have arisen from animal experimentation (Muralidharan, Sarmah, Zhou, et al., 2013), including the potential association between PNAE and epigenetic modifications (Lussier, Weinberg, & Kobor, 2017).

METHODS

Identification of Cases

Ethics approval was obtained from the Health Research Ethics Board of the University of Manitoba (approval #HS13161 – H2011:213). We conducted a retrospective survey of autopsies performed at the Health Sciences Centre (HSC) in Winnipeg, Canada from 1980 – 2016. HSC serves a population of about 1.3 million people. Manitoba has a relatively high prevalence of FASD (Popova, Lange, Probst, et al., 2017) and has had a centralized diagnostic center for two decades (Singal, Brownell, Hanlon-Dearman, et al., 2016). One of the co-authors (Chuldey) has been a leader in developing diagnostic criteria for FASD (Chudley, Conry, Cook, et al., 2005; Cook, Green, Lilley, et al., 2016). Approximately 1,100 autopsies are performed annually, among which ~80% are medico-legal. The total includes 100-200 fetal / pediatric cases and ~350 complete brain examinations per year. All pediatric autopsies since 1980 and all adult autopsies since 1996 (both medico-legal and family permission) are amenable to full-text search using DocFetcher software (SourceForge.net; open source software license from Eclipse Public License).

The senior author (Del Bigio) identified candidate cases by whole text search using a wide range of key words related to alcohol consumption during pregnancy or a clinical diagnosis of FASD; e.g. EtOH, alcohol, ethanol, booze, fetal alcohol, FASD, FAS, pFAS, FAE, ARND, ARBD, binge, drink, drank, drunk, liquor, beer, wine, vodka, whisky, home brew, substance abuse, etc. The clinical details of approximately 500 reports were screened; approximately 200 cases with probable PNAE or FASD were identified. Files predating 1994 had been scanned into searchable PDF format from microfilms, which at times did not allow for perfect text recognition. Candidate reports were thoroughly reviewed and summarized by the first author

(Jarmasz). Cases with a diagnosis or "suspected" FASD diagnosis were further investigated by

review of records in the Program in Genetics and Metabolism database, the Manitoba FASD

Centre (formerly the Clinic for Alcohol & Drug Exposed Children; established in 1999), or by

hospital chart review. Cases that were not confirmed remained "suspected", as a physician might

have made the diagnosis without referral to the Manitoba FASD Centre, where a

multidisciplinary team assessment is standard. The inclusion criteria were met by 174 cases.

Age Groupings and Descriptive Epidemiology

Cases were divided into five age groups: fetuses (stillborn / intrauterine death; n=52),

infants (1 day old to 12 months of age, including premature births; n=65), children (13 months to

12 years; n=32), teens (13 to 19 years; n=14), and adults (20 to 65 years; n=11). Details extracted

from the reports included: age, sex, birth characteristics (gestation, weight, method of birth,

stillborn / liveborn), and maternal health and substance abuse during pregnancy (e.g. disease,

infections, estimated alcohol use, tobacco use, other drug use, age at birth, prior abortions, parity

and gravida, level of prenatal care, etc.). The maternal details were seldom available for children,

teens, and adults. Additional information in these age groups included the history of FASD

diagnosis, history of foster care or contact with Child & Family Services (CFS), history of

epilepsy, and the individuals' own substance abuse. Autopsy details included: cause of death,

brain weight, FASD facial anomalies (short palpebral fissures, smooth philtrum, thin upper lip),

other facial anomalies, abnormal palmar creases, and congenital abnormalities affecting other

body regions (heart, kidneys, skeletal). Brain weight percentiles were classified as $<5^{th}$, $>5^{th}$ –

$\leq 50^{th}$, $>50^{th}$ - $\leq 95^{th}$ and $>95^{th}$ percentile according to published autopsy databases (Dekaban,

1978; Fracasso, Vennemann, Pfeiffer, et al., 2009; Maroun, & Graem, 2005; Phillips, Billson, &

Forbes, 2009). A brain weight <5th percentile was classified as micrencephalic. Microcephaly is usually defined as a head circumference of ≤3rd percentile, but it may not be a sensitive marker of PNAE (Treit, Zhou, Chudley, et al., 2016). Because this is a retrospective analysis, almost all cases were missing some information. Percentage values only represent cases for which information was reported; they are not based on the totals.

Maternal alcohol ingestion was difficult to estimate because descriptors concerning amount, timing, and duration of alcohol exposure were varied. We broadly categorized alcohol ingestion as minimal / moderate use ("one episode of drinking", "occasional alcohol", "in the first trimester only", etc.) or heavy / chronic use ("binge drinking", "drinking heavily throughout pregnancy", "arrived in hospital intoxicated and in labor", etc.). Descriptors such as "drank during pregnancy", "mother abuses alcohol", or "mother has a history of alcohol abuse" were harder to classify. In rare cases, other children in the family had been diagnosed with FASD, but the mother denied current alcohol use.

Neuropathologic Examinations

Photographs of the brain were retrieved to verify gross abnormalities. Complete neuropathological assessment was conducted in 135 cases. Nine stillborn infants had autolytic liquefaction of the brain, which was not examined by microscopy. Among the teen and adult cases, the forensic pathologist cut 6 brains fresh with only 1 or 2 tissue samples saved for histology, and in 8 cases the brain was not examined. In general, brain samples had been fixed in 10% buffered formalin for 1-2 weeks, and then select regions were embedded in paraffin. Cases with a complete examination by a neuropathologist had, at a minimum, samples taken of: parasagittal frontal lobe (level of caudate nucleus head), basal nuclei, hippocampus / medial

106

temporal lobe, thalamus, midbrain, pons, and posterior cerebellum. In all cases, the glass slides (or recut slides) were reviewed by the senior author (Del Bigio), an experienced neuropathologist. The minimum histologic evaluation included hematoxylin and eosin (H&E) staining of 5µm thick paraffin sections mounted on glass slides.

RESULTS

Complete epidemiological details of the 174 cases are presented in **Table 3.2-3.4.** Details of the neuropathologic abnormalities are presented in **Table 3.5** and are briefly summarized below.

Stillbirth and Intrapartum Deaths

In the stillborn / intrapartum death cohort we had 52 fetuses (20 to 41 weeks gestation, median 32 weeks gestation), with an almost equal ratio of male to females (25:27). Three pregnancies were electively terminated for malformation (neural tube defects for 2, kidney and bladder defects for 1), 5 cases were live born premature infants who died <1 day, and the remaining 44 were stillborn fetuses. Most (38/52) were premature (<37 weeks). Birth weight was below the 10th percentile (definition of small for gestational age) in 22 cases (11 of which were below the 5th percentile). The maternal age ranged from 15-39 years (median 25 years). Nine mothers had a vaginal or sexually transmitted infection at the time of birth and 5 had diabetes (Type I or II, 4 cases; gestational diabetes, 1 case). When indicated, >75% reported poor or no prenatal care during their pregnancy. Twelve cases had exclusively early / first trimester alcohol exposure (3 "minimal", 4 "heavy"), 21 cases had the vague description of minimal use during pregnancy or history of alcohol use, and 19 had descriptors suggesting more substantial use into the second trimester or throughout pregnancy. In addition to alcohol ingestion, 86% of mothers smoked tobacco during the pregnancy and 77% abused other illicit drugs (when reported).

Anomalies were identified in the heart (n= 5), kidneys (n= 3), and skeletal system (n= 10). Diagnostic FASD facial anomalies were identified in 3 cases and other facial anomalies were identified in 10 cases. Placentas were examined in 50/52 cases; 16 were normal, 14 had

chorioamnionitis, 10 had hemorrhage or focal infarction, 4 had features of placental abruption

and the remaining 6 had other findings.

Brain weight was < 5th percentile in 11 cases. Congenital neuropathological findings

included: 4 cases with neural tube defects (2 lumbosacral, 1 exencephaly, (**Figure 3.1A, B**) 1

anencephaly); 1 case with a complex brain malformation (moderately severe hydrocephalus due

to aqueduct stenosis, partial agenesis of the posterior corpus callosum) (**Figure 3.1C-H**); and 1

case with alobar holoprosencephaly. Multiple congenital anomalies were found in two cases.

Acquired neuropathological findings included 12 cases with widespread hypoxic neuronal

damage (typically apoptotic neurons in the hippocampus and pons), 2 cases with small

periventricular hemorrhages, and 1 case with small foci of white matter necrosis (periventricular

leukomalacia). Among the cases with placental anomalies, 12 brains had hypoxic neuron

damage, 5 brains were not examined due to severe autolysis, 2 brains were not examined (for

unknown reasons), 1 case had a neural tube defect, and 1 case had periventricular leukomalacia.

Infants

In the infant cohort, 65 individuals died between the ages of ≥1 day and 12 months

(median 5 weeks). Male sex predominated (65%), 24 (39%) were premature, and 4 had a birth

weight <5th percentile. Mother's age at birth ranged from 15-40 years of age (median 24 years).

Eighteen reported poor or no prenatal care (no information was available for the remainder). At

the time of birth, 5 mothers had a vaginal / sexually transmitted infection (or had been treated for

one during the pregnancy). Two had diabetes (one type II and one gestational), 1 had

tuberculosis, 1 had hypertension, and 1 had Grave's disease. In terms of PNAE, 17 (26%) cases

had a maternal history of alcohol use / abuse, 19 (29%) reportedly drank alcohol during /

throughout the pregnancy, 9 had minimal or occasional alcohol during pregnancy, 11 had documented drinking during a specific trimester (first - 6 cases, second - 4 cases, third - 1 case) with the amount unspecified, and 7 had heavy / chronic use of alcohol during pregnancy (2 during the first trimester exclusively). Seven infants had a history of seizures / epilepsy; among these 3/7 had been born prematurely, and 2/7 had multiple congenital anomalies. The top four causes of death were: sudden unexplained death in an infant (SUDI) (28%), complications due to malformations (23%), infection / sepsis (bacterial or viral) (19%), and unsafe sleeping environment (17%).

Fourteen cases had heart defects, 6 had kidney defects, and 4 had skeletal system defects. Twelve cases had typical FASD facial anomalies and 12 had other facial anomalies. Only 6 cases had placental examination; 3 had chorioamnionitis (no brain abnormalities), 1 had abruption (rare heterotopia in frontal leptomeninges), and 2 were normal.

Eight cases (13%) had a brain weight below the 5th percentile (i.e. micrencephaly). One case had lumbosacral myelomeningocele with Chiari type 2 malformation (NTD), 1 case had lumbar diplomyelia (NTD) (**Figure 3.3A, B**), 4 cases had hydrocephalus (2 mild, 2 with agenesis of posterior corpus callosum) (**Figure 3.2A-F and G-J**), and 1 cases had partial agenesis of the corpus callosum and micrencephaly (**Figure 3.2K**). Four cases had only minor leptomeningeal heterotopias (**Figure 3.3C-G**). Non-malformative neuropathologic findings included 10 cases with hypoxic-ischemic neuronal changes or resolving brain hemorrhage (complications of premature birth), 1 case with periventricular leukomalacia (infant had been born at term), and 5 cases with bacterial meningitis. Among the 7 infants with a history of seizures or epilepsy (the hippocampi were normal).

Children

In the child cohort, 32 individuals died between 13 months and 12 years of age (median 3.5 years). Most were female (59%). A minority of autopsy reports documented maternal factors (18%) or details of the child's birth (28%); this is likely because the details were less relevant to the child's cause of death. Four cases had a confirmed FASD diagnosis, while 12 had a suspected FASD diagnosis. Seven cases had a seizure disorder or epilepsy. A bacterial or viral infection was the cause of death in 50%, followed by drowning or other environmental cause in 19%.

Six cases had a heart defect, 3 had kidney defects and 10 had skeletal anomalies. Seven cases had FASD facial anomalies, and 4 cases had other facial anomalies.

Six cases (21%) had a brain weight <5th percentile; 3 of these had ischemic brain lesions acquired in the perinatal period (**Figure 3.5A-G**). One case, with a brain weight <10th percentile, had mild delay in cerebral myelination and mildly enlarged cerebral ventricles. Three cases had moderate to severe hydrocephalus (**Figure 3.4A-H**), 1 had Miller-Dieker type lissencephaly (**Figure 3.4I**), and 1 had small subarachnoid heterotopia. Non-malformative neuropathologic findings include 4 cases with residual damage due to hypoxic and hemorrhagic complications of premature birth, 1 with an old occipital lobe hemorrhagic infarct (**Figure 3.5H**), 1 with severe acute brain trauma, 1 with acute meningitis, and 1 with chronic damage related to perinatal meningitis. Among the 7 cases with seizure disorder / epilepsy, 3 had hippocampi with neuron loss and reactive glial changes ("mesial temporal sclerosis").

Teens

In the teen cohort 14 individuals died between 13 and 19 years (median 15.5 years). Ten were male and 4 were female. Eight had a confirmed FASD diagnosis, while 4 had a suspected

FASD diagnosis. Four cases had history of personal substance abuse problems, and 3 cases had a seizure disorder / epilepsy. The causes / manners of death were: suicide by hanging (n=6), accident (n=3), homicide (n=3), and complications of a chronic neurological disorder (n=2).

FASD facial anomalies were generally not described in these autopsy reports. No major somatic malformations were identified; 1 case had a minor cardiac defect.

No major brain malformations were identified. One case had a brain weight <5th percentile. Two cases had acute brain trauma, and 1 case had old damage related to hypoxic and hemorrhagic complications of premature birth at 29 weeks gestation. Among the 3 cases with a seizure disorder, the hippocampi were normal in all.

Adults

Eleven individuals died between 20 and 65 years (median 25 years); 10 were male. Two had a confirmed FASD diagnosis, while 9 had a suspected FASD diagnosis. Five cases had personal substance abuse problems. Five had psychiatric problems: 1 with multiple threats to commit suicide, 1 with depression, 1 with paranoid schizophrenia, 1 "heard voices", and 1 had a criminal history of repeated car theft. Two cases had a seizure disorder / epilepsy. The causes / manners of death were: no anatomical cause (n=3), trauma due to homicide (n=3), cardiac (n=2), multi-drug toxicity (n=2), and suicide (n=1).

As in the teenage group, facial features were not well described. No major somatic malformations were identified; 1 had mild thoracic scoliosis. Six cases (55%) were micrencephalic, and 1 had mild hydrocephalus due to aqueduct stenosis (**Figure 3.6A-C**). Other neuropathologic findings included acute brain trauma (n=1) and old brain trauma (n=1).

DISCUSSION

Mortality and PNAE / FASD

The risk of spontaneous abortion and stillbirth increases with the quantity of alcohol consumed during pregnancy (Bailey, & Sokol, 2011; O'Leary, Jacoby, D'Antoine, et al., 2012; Salihu, Kornosky, Lynch, et al., 2011). *In utero* PNAE deaths have been linked to placental insufficiency, which can result in hypoxia, and intrauterine growth restriction (Tai, Piskorski, Kao, et al., 2017). In humans, alcohol consumption was positively correlated with placental hemorrhage and accelerated villous maturation (Carter, Wainwright, Molteno, et al., 2016). Administration of ethanol to Rhesus macaque monkeys daily for the first 60 days of gestation is associated with decreased placental blood flow and reduced fetal brain size at 110 days gestation (Lo, Schabel, Roberts, et al., 2017). In the present study, placental abnormalities (including abruption) were documented in at least 68% of the fetal (and some infant) cases. Half of those cases were born prematurely and had a birth weight below the 50th percentile. Cigarette smoking, which is common among women who drink during pregnancy, is also a contributing factor to fetal hypoxia due to vasoconstrictor effects on the placental and umbilical cord vessels (Behnke, & Smith, 2013).

PNAE is also associated with increased risk of infant and child mortality (Burd, Klug, Bueling, et al., 2008). Among our infant and child cohorts, 32% had a documented history of premature birth, which increases the risk for adverse neurological outcome or early death (Committee on Understanding Premature Birth and Assuring Healthy Outcomes, & Board on Health Sciences Policy, 2007). A search of the medical literature for information concerning mortality and FASD identified only 57 individuals, majority of whom died within the first year of life (54%) (Thompson, Hackman, & Burd, 2014). Contributors to death were heart

malformations (76%), brain malformations (51%), sepsis (14%), kidney malformations (14%), and cancer (8%). In our infant and child cohorts, 19% had infections and 23% had severe malformations that contributed to death. In the remainder, the cause of death was not obvious. Sudden unexplained death in infancy (SUDI) is defined as the death between the ages 1 day and 12 months that remains unexplained by autopsy (Byard, 2009). Risk factors for SUDI include premature birth, household tobacco smoke exposure, and unsafe sleep conditions (e.g. bed sharing with an adult; 17% in our infant cohort). Maternal alcohol use during pregnancy may be associated with continued use during the postnatal period and a risk for child neglect (Burd, & Wilson, 2004). In our PNAE / FASD cohorts, 19% of infants and 44% of children were either in foster care at the time of death or involved with child and family services (Brownell, Chartier, Au, et al., 2015).

Teens and young adults with FASD have disabilities such as mental illness, reckless and criminal behaviour, and substance abuse problems (Senturias, 2014), which put them at risk for suicide (7/25 in our combined teen and adult cohorts), homicide (6/25), and accidental traumatic or drug-related deaths (5/25).

Brain Abnormalities in PNAE and FASD

PNAE is postulated to interfere with normal neurological development through a range of mechanisms including: alteration of gene expression through epigenetic modifications (Liyanage, Curtis, Zachariah, et al., 2017), interference with neural crest cell migration (Susan M. Smith, Garic, Flentke, et al., 2014), cell toxicity through reactive oxygen species (Brocardo, Gil-Mohapel, & Christie, 2011), apoptosis of neurons (Creeley, & Olney, 2013), damage to radial glia and astrocytes (Wilhelm, & Guizzetti, 2016), and inappropriate activation of microglia

(Drew, & Kane, 2014). In our cohorts collectively, the observed brain malformations were micrencephaly (32 cases), neural tube defects (6 cases), dysgenesis of the posterior corpus callosum combined with hydrocephalus (3 cases), isolated hydrocephalus of varied etiology and severity (5 cases), dysgenesis of the posterior corpus callosum combined with other minor anomalies, isolated minor leptomeningeal heterotopias (4 cases), and ischemic / vascular brain lesions not attributable to a complication of birth or prematurity (6 cases) (see **Table 3.6** for summary). The three youngest age groups had the most severe brain abnormalities. At least two factors might explain this: 1) the most severe malformations often involve multiple organ systems and are therefore likely to cause early death; or 2) among people who survived to adulthood, the ascertainment of FASD in the death investigation might be less reliable. In a meta-analysis of 127 clinical studies in which imaging was used to identify brain anomalies, 428 comorbid conditions were identified in individuals with FASD. These included microcephaly (62%), congenital hydrocephalus (58%), malformations of the corpus callosum (31%), epilepsy (21%), and spina bifida (<3%) (Popova, Lange, Shield, et al., 2016). In a recent magnetic resonance (MR) imaging study of 62 children and teens with FASD, thin (hypoplastic) corpus callosum was found in 24, partial agenesis was found in 2, and cerebellar vermis hypoplasia in 11 (Boronat, Sanchez-Montanez, Gomez-Barros, et al., 2017). Also using MR imaging, small corpus callosum was identified in newborns with PNAE even after adjusting for brain volume (Jacobson, Jacobson, Molteno, et al., 2017; Yang, Phillips, Kan, et al., 2012). In the absence of reliable normative data and photographs of mid-sagittal brain slices, subtle hypoplasia of the corpus callosum might be underreported in autopsy material. We identified a history of epilepsy or seizures in 19 / 122 (16%) cases (excluding stillbirths); among them 5 had micrencephaly, 4 had hydrocephalus, 3 had mesial temporal sclerosis, 3 had multiple congenital anomalies, and 2

115

had a history of meningitis. In the absence of an overt brain abnormality, epilepsy suggests that there may be subtle neuronal abnormalities in PNAE brains. Three-dimensional analysis of brain surface contours on MR images indicates that children and adolescents with FASD have significantly smoother cortices than controls (Hendrickson, Mueller, Sowell, et al., 2017). One MR imaging study showed reduced thickness of neocortex (males only), reduced regional brain volumes, and altered fractional anisotropy ("microstructure") in white matter tracts of FASD children (Treit, Chen, Zhou, et al., 2017). However, another study showed increased cortical thickness in FASD subjects (Yang, Roussotte, Kan, et al., 2012). Unfortunately, in the absence of post-mortem imaging, it is difficult to mirror these quantitative parameters using conventional histopathological methods and, further, the structural correlate of fractional anisotropy changes is unclear.

The possible contributions of PNAE to nervous system malformations must be considered in the context of developmental timing. Neural tube defects typically occur during weeks 3-4 of human gestation, although cranial defects due to amniotic band adhesions could develop later. Among our 6 cases with neural tube defects, drinking exclusively in the first trimester was reported in 1 case and drinking throughout pregnancy was reported in the others. Ethanol administered to pregnant rats on gestational days 6 to 12 is associated with delayed closure of the caudal neural tube (Ross, & Persaud, 1989), although the adverse effect of alcohol on neural tube closure in mice seems to be strain specific (Becker, Diaz-Granados, & Randall, 1996). In humans, pioneer axons of the corpus callosum genu appear during gestational weeks 11-12, with the posterior aspect (splenium) developing during weeks 16-18 (Rakic, & Yakovlev, 1968). We identified 5 cases with corpus callosum dysgenesis (3 combined with hydrocephalus). The historical information was suggestive of high levels of PNAE (one heavy drinking, three

drinking throughout the pregnancy, and one binges in the first trimester). Corpus callosum anomalies in animal PNAE experiments are generally subtle. Sheep fetuses exposed to alcohol from gestational day 30 to 60 had activated microglia in the corpus callosum (Watari, Born, & Gleason, 2006). Three-day-old male, but not female, rats exposed to alcohol from gestational day 6 to birth had a ~20% reduction in corpus callosum area, however this was associated with overall reduction in brain volume (Zimmerberg, & Scalzi, 1989). In contrast to humans, 3 to 5-year-old macaque monkeys with PNAE had enlarged corpus callosa (Miller, Astley, & Clarren, 1999). Neocortical leptomeningeal heterotopias, which reflect migration through the damaged glia limitans / pia mater, are postulated to occur in midgestation (Iida, Hirano, Takashima, et al., 1994). Periventricular heterotopias reflect failed migration of germinal cells away from the ventricle wall. Although this is location dependent, heterotopia along the roof of the ventricle likely indicate an insult before 20 weeks gestation (Del Bigio, 2011). The timing of an insult that causes isolated hydrocephalus is difficult to determine; the cerebral aqueduct can be secondarily obstructed at any time during development (Del Bigio, 2010). Among our 9 cases with hydrocephalus, 6 had aqueduct stenosis with some disorganization and chronic reactive astroglial changes, 1 had a venous anomaly compressing the aqueduct, and 2 had no obvious site of cerebrospinal fluid obstruction. Historical information did not identify a particular period of alcohol exposure. In a rat model of PNAE, a small proportion of offspring developed severe hydrocephalus with periventricular heterotopia; the site of cerebrospinal fluid obstruction was not identified (Sakata-Haga, Sawada, Ohnishi, et al., 2004).

The most common brain abnormality, micrencephaly (31 cases), cannot be attributed to a specifically timed insult. Hypotrophy of the brain could be caused by interference with progenitor cell proliferation, or through toxin-induced death of cells. Long projection neurons are

generated in the first half of gestation, but interneuron and glial progenitors are generated well into the third trimester (Arshad, Vose, Vinukonda, et al., 2016). Alternately, neurons of normal quantity could be small because they fail to mature properly (Ernst, 2016). We found no evidence for an obvious defect in myelination.

Hypoxic-ischemic lesions were very common. In the stillborn population, scattered dead neurons are likely due to hypoxia immediately preceding death and 7 cases had lesions that could be attributed to complications of premature birth. Six cases had discrete regions of infarction that appeared to represent pre- or perinatal insults. Three were arterial zone (one with cardiac anomaly) and one was deep periventricular. Compared to controls, alcohol-exposed human fetuses from 31 to 38 weeks gestation showed disorganized radial organization and angular branching of the cortical microvessels, which were immunolabeled with antibody to GluN1 (Jégou, El Ghazi, de Lendeu, et al., 2012). However, the pathogenesis of these large lesions, which correspond to the clinical entity known as perinatal arterial ischemic stroke, is difficult to explain on the basis of alcohol exposure alone. Other prenatal risk factors include prolonged rupture of amniotic membranes, preeclampsia, maternal smoking, infection, thrombophilia, and congenital heart disease (Lehman, & Rivkin, 2014).

PNAE and FASD are not Monofactorial Exposure Problems

In our PNAE cases with maternal information available, a large majority of mothers smoked tobacco (89%) or abused other drugs (83%) during their pregnancies. Furthermore, many had other diseases that can be associated with adverse pregnancy outcomes, including diabetes (8 cases), hypertension (1 case), obesity (1 case), and sexually transmitted infections (14 cases) (Ornoy, Reece, Pavlinkova, et al., 2015). When reported, 88% of mothers had poor or no

prenatal care. Poor nutrition is known to increase the risk of FASD (Young, Giesbrecht, Eskin, et al., 2014). There is good evidence that harmful effects of toxins on the fetus may be either additive or synergistic, which confounds any attempt to attribute a causal effect to PNAE alone (Chen, & Maier, 2011; Viteri, Soto, Bahado-Singh, et al., 2015). For example, administration of ethanol alone to pregnant rats on gestational day 9-12 had no adverse effects on the embryos, while the combination of ethanol and nicotine significantly retarded embryonic development (Woo, & Persaud, 1988). Nicotine has a constricting effect on the uterine arteries, which in turn reduces the amount of oxygenated blood the fetus receives (Scott-Goodwin, Puerto, & Moreno, 2016). Maternal cigarette smoking causes episodic carbon monoxide and cyanide elevations in blood, which is associated with reduced head growth (Phelan, 2014). MR imaging of female (but not male) adolescents showed that maternal cigarette smoking was associated with reduced size of posterior corpus callosum (Paus, Nawazkhan, Leonard, et al., 2008).

Limitations of the Study

As with any retrospective human autopsy study, this report has limitations. Maternal histories and details of PNAE were inconsistently reported and self reported levels of consumption are frequently lower than reality (Bager, Christensen, Husby, et al., 2017). Therefore, our estimate of alcohol consumption is crude. There remains uncertainty whether low doses of alcohol have any adverse effect in pregnant humans (Charness, Riley, & Sowell, 2016). Because these autopsy cases were acquired over several decades, the FASD diagnostic criteria were not applied uniformly and the information collected at autopsy differed. Brain sampling also varied because several different neuropathologists did the examinations. Hopefully the prospective study being conducted by the Prenatal Alcohol in SIDS and Stillbirth Network will

overcome some of these problems (Dukes, Burd, Elliott, et al., 2014). There was likely a referral

and ascertainment bias, particularly among the teenage and adult death groups. Only one of the

teenage FASD brains available for study had micrencephaly, which is reportedly the most

common abnormality. However, the circumstances of death were often associated with brain

swelling; therefore, reliance on the brain weight could mask the presence of pre-existing

micrencephaly. The two cases with anomalies typically ascribed to genetic mutations

(holoprosencephaly and Miller-Dieker lissencephaly) did not undergo genetic testing. Overall,

we can only report on the associations between PNAE / FASD and human brain abnormalities;

we cannot ascribe a cause-effect relationship.

Summary and Conclusions

This is the largest study of human PNAE and FASD autopsy brains reported. The

information elicited is important, despite the deficiencies. There is no characteristic

neuropathologic pattern associated with PNAE or FASD. Malformations must be distinguished

from *in utero* vascular insults and complications of prematurity, which can contribute to the

neurological phenotype but might be only indirectly related to PNAE. The almost ubiquitous

concurrent use of tobacco is a critical point because of its direct association with placental

dysfunction. Some of the brain features of PNAE / FASD might be teratogenic in the sense of a

direct adverse effect of ethanol on brain development. However, we also provide indirect

evidence that some of the brain damage might be caused by hypoxic / ischemic events. Although

animal studies are necessary to understand the human abnormalities related to PNAE, the animal

research community might be doing a disservice by focusing too much on fine details of ethanol-

alone teratogenicity. Increased attention should be paid to combined toxicities, in particular

120

ethanol plus nicotine or other vasoactive agents in tobacco. With respect to the clinical diagnosis

of FASD, information more specific than "structural brain anomalies" should be provided,

considering the diverse pathogenesis of these anomalies. Prevention through avoidance of

alcohol, tobacco, and other substance abuse during pregnancy must be the main societal goal

(Jonsson, Salmon, & Warren, 2014). Nevertheless, tissues accrued in the current study will be

used to validate hypotheses about the pathogenesis of FASD that have been developed in animal

experimentation.

Table 3.1: Studies in which brain pathology has been reported following autopsy of humans with documented prenatal alcohol exposure or clinical diagnosis of FASD (in chronological order).

Primary ref	# of Cases	Age at death	Sex	Major neuropathologic findings	Additional case details and comments
(Jones, & Smith, 1973)	1	32 weeks gestation birth + 5 days	Female	Microencephaly (140g); lissencephaly; extensive leptomeningeal heterotopia on dorsal cerebrum (bridging midline); absent corpus callosum; periventricular heterotopia; dysplastic inferior olivary nuclei	Case 2 in the publication. Well-documented maternal alcohol intake. Face, limb, and heart anomalies. Gross photos of this case were not originally shown, but later appeared in several versions (Jones, 1975; Volpe, 2000). In disparity with other descriptions of this case, in one publication, the child was reported to have died at 6 weeks of age (Clarren, Alvord, Sumi, et al., 1978). A figure from Clarren comparing this brain to a normal brain (Clarren, 1986) appears on many internet sites, where it is professed to be the typical FAS brain. It is, in fact, an extreme example.
(Clarren, 1977)	1	Born at Term + 10 weeks	Male	Brain normal weight (660g); hydrocephalus (moderate) caused by leptomeningeal heterotopia around brainstem; absent brainstem nuclei; hypoplastic cerebellum and pons	Case 1 in this document is the same case published by Jones (Jones, & Smith, 1973). The new case in this publication is also described elsewhere (Clarren, Alvord, Sumi, et al., 1978). Hypoplastic pons and cerebellum were reported in a neonate with FAS using MR imaging (Yigazu, Kalra, & Altinok, 2014).
(Peiffer, Majewski, Fischbach, et al., 1979)	6	17 weeks gestation	Not indicated	Microdysplasia of brainstem nuclei; leptomeningeal lipoma adjacent to medulla oblongata; cardiac anomaly	The same cases are described in less detail in two other publications (Majewski, 1981; Majewski, Fischbach, Peiffer, et al., 1978).
		18 weeks gestation	Not indicated	Microdysplasia of dentate nuclei and inferior olivary nuclei	Well-documented alcohol intake.
		20 weeks gestation stillbirth	Not indicated	Hydranencephaly	Well-documented alcohol intake plus clomethiazole, a suspected teratogen (Heberlein, Leggio, Stichtenoth, et al., 2012).
		6 months postnatal	Male	Mild microencephaly (640g); mild hydrocephalus; "retarded maturation" of white matter; heterotopic cerebellar gyri	Well-documented drinking during pregnancy. Multiple congenital anomalies including heart defect

Primary ref	# of Cases	Age at death	Sex	Major neuropathologic findings	Additional case details and comments
				near the tonsils; lumbar spina bifida occulta	
		9 months	Female	Microencephaly (840g); polymicrogyria, absent olfactory bulbs; severe hydrocephalus with rupture of occipital lobes; agenesis of corpus callosum; occipital meningocele with associated cerebellar abnormalities; hydromyelia / syringomyelia	Polymicrogyria is not illustrated; note that severe hydrocephalus can be associated with the appearance of polygyria. From the published photographs it appears that the corpus callosum might have been destroyed by the severe ventriculomegaly (i.e. not agenesis)
		4 ½ years	Male	Normal size brain (1280g); many ectopic neurons in white matter; partial fusion of thalami	Congenital heart defect
(Clarren, Alvord, Sumi, et al., 1978)	2	29 weeks gestation stillbirth	Male	Mild hydrocephalus with "rudimentary brainstem and cerebellum"	Cases #1 and #2 in this publication were previously described (Clarren, 1977; Jones, & Smith, 1973). Weekly binge drinking in this case. Facial and cardiac anomalies
		30 weeks gestation + 3 days	Not indicated	Brain weight normal (210g); 5mm neuroglial heterotopia on cerebellar folium	Well-documented maternal alcohol intake - multiple binges per week.
(Kinney, Faix, & Brazy, 1980)	1	35 weeks gestation premature birth + 3 months	Male	Microencephaly (300g); partial agenesis of corpus callosum.	Well-documented maternal drinking. Multiple anomalies including diaphragmatic hernia. Paravertebral neuroblastoma (1.5cm).
(Clarren, 1981)	1	4-year-old	Female	"brain showed small size (weight not reported), marked reduction in cerebral white matter, and neuronal heterotopias along the lateral ventricular surfaces"	Child with clinical diagnosis of FAS died in traumatic accident. Illustration shows hydrocephalus, not "greatly reduced white matter" as claimed.
(Majewski, 1981)	1	between 17 and 20 weeks gestation	Not indicated	Normal	Seven cases are briefly described, the 6 abnormal ones were previously described in greater detail (Peiffer, Majewski, Fischbach, et al., 1979).
(van Rensburg, 1981)	1	Term + 1 day	Female	Probable microencephaly (head 28cm; <3rd percentile); "brain was histologically normal"	Well-documented heavy maternal drinking. Severe phocomelia of all limbs, facial anomalies.

Primary ref	# of Cases	Age at death	Sex	Major neuropathologic findings	Additional case details and comments
(Wisniewski, 1983)	5	8 months	Female	Severe microencephaly (450g); absent corpus callosum; underdeveloped cerebellar vermis; heterotopic glial clusters in the meninges	Maternal history of heavy drinking is well documented in all cases. Except for the 29-week case, all had cardiac anomalies. This case is also described elsewhere (Dambska, Wisniewski, & Sher, 1986).
		32 weeks gestation + 4 months	Male	Microencephaly (395g); shallow sulci with heterotopic glial clusters in leptomeninges causing gyral fusion	In another publication, the brain weight is reported as 359g (Dambska, Wisniewski, & Sher, 1986).
		Full term birth + 2 days	Male	Microencephaly (263g); small meningeal glial heterotopic protrusions forming bridges between adjacent gyri	
		35 weeks gestation + 17 days	Male	"Heavy but small" brain (405g); single "small glio-neuronal meningeal heterotopia"	Ischemic changes (white matter necrosis) and edema following 3 days survival after cardiac resuscitation.
		29 weeks gestation + 4 days	Male	Small brain (124g); single heterotopia in temporal lobe white matter	
	6	stillbirths	Not indicated	Authors wrote, "Six products of miscarriage of drinking mothers which we had examined previously (Byrne *et al.* in preparation) did not display gross brain malformations."	We could not find evidence that this had ever been published.
(Pratt, & Doshi, 1984)	1	21 months	Female	Severe microencephaly (684g); heterotopic neurons and microcalcification in white matter	It is not clear what this case represents; authors wrote, "possible case of FAS", "enquiries failed to elicit a history of maternal drinking"
(Ferrer, & Galofré, 1987)	1	4 months	Male	Microencephaly (440g); small frontal lobes with exposed insula; irregular gyri; "discrete enlargement of the lateral ventricles"; Golgi staining showed simplified dendrites of cortex layer 5 neurons	Well documented heavy maternal drinking. Facial and cardiac anomalies. It is not clear if "discrete" means mild. The published image shows a distinct vertical groove extending upward from the Sylvian fissure; it is not clear if this is an abnormal sulcus of a schizencephalic cleft.
(Bönnemann, & Meinecke, 1990)	1	31 weeks gestation stillbirth	Male	Holoprosencephaly with cyclopia and agnathia	Normal male karyotype.

Primary ref	# of Cases	Age at death	Sex	Major neuropathologic findings	Additional case details and comments
(Ronen, & Andrews, 1991)	1	28 weeks gestation premature birth + 8 days	Not indicated	Holoprosencephaly (alobar)	Mother was heavy drinker, smoker, and took chlordiazepoxide and imipramine during pregnancy. Authors also reported 2 other cases of semilobar holoprosencephaly without autopsy.
(Coulter, Leech, Schaefer, et al., 1993)	1	37 weeks gestation + 2.5 months	Female	"incomplete" (i.e. semilobar) holoprosencephaly with microencephaly (293g); diffuse and patchy loss of Purkinje neurons	Maternal binge drinking during first trimester. Very detailed description.
(Norman, McGillivray, Kalousek, et al., 1995)	3	Not specified	Not indicated	Microencephaly without other malformations	All had clinical diagnosis of FAS - no details published. The authors noted, "it is apparent that the large majority of surviving children with FAS do not have gross morphologic abnormalities".
		Not specified	Not indicated	Normal	"few small calcifications in centrum semiovale" is nonspecific
		Not specified	Not indicated	Complex malformation with: abnormal lamination of cerebral cortex; heterotopic gray matter at the ventricle surface; Dandy-Walker malformation; calcification of the brainstem	
(Konovalov, Kovetsky, Bobryshev, et al., 1997)	47	5–12 weeks gestation embryos and early fetuses (n=44); 14-15 weeks gestation fetuses (n=3); terminated pregnancies from alcoholic women (+ 16 cases from non-alcoholic mothers)	Not indicated	Abnormalities in 74% of cases (allegedly dose dependent); 25 cases with abnormal "folding" and invagination of the neuroepithelium which might be precursors of microgyria or heterotopia; 2 cases agenesis of olfactory bulbs; 2 cases agenesis of epiphysis; 1 case agenesis of optic chiasm and visual tracts; 6 cases "dysraphia" at midbrain level; 1 case cerebellum agenesis; 7 cases cerebellum dysplasia	The same cases are described in a series of publications in Russian (Konovalov, Kovetskiĭ, Solonskiĭ, et al., 1988; Kovetskiĭ, 1989a, 1989b, 1991; Kovetskiĭ, Konovalov, Orlovskaia, et al., 1991; Kovetskiĭ, Solonskiĭ, & Moiseeva, 1995). Inspection of the published micrographs suggests that some of these alleged abnormalities might be artifactual. Convoluted cortical surfaces (Konovalov, Kovetskiĭ, Solonskiĭ, et al., 1988; Konovalov, Kovetsky, Bobryshev, et al., 1997) might be due to autolysis. The cerebral distortions in many cases (Kovetskiĭ, 1989b) appear to be folding artifacts. Many of the examples of midbrain dysraphia (Kovetskiĭ, 1991) appear to be cracks or folds in the tissue. Other reported abnormalities are not illustrated. Therefore, this set of publications likely

Primary ref	# of Cases	Age at death	Sex	Major neuropathologic findings	Additional case details and comments
					exaggerates the abnormalities possible in the embryo and early fetus.
(Solonskii, Logvinov, & Kutepova, 2008)	23	10 – 12 weeks gestation fetuses; terminated pregnancies from alcoholic women (+ additional controls)	Not indicated	Light and electron microscopic analysis of neocortical blood vessels showed increased density of abnormally small blood vessels at 10-12 weeks compared to controls. Authors speculate that abnormal vasculogenesis might be a response to hypoxia, secondary to placental dysfunction.	Macroscopic abnormalities (if any) were not described. Samples of unspecified brain parts fixed in glutaraldehyde. Illustrations are sparse, so out confidence in these data is not high. The same cases are described in a series of publications in Russian (Solonskiĭ, Kovetskiĭ, & Iarygina, 1991; Solonskiĭ, Logvinov, & Ketepova, 2007). Ultrastructural features of abnormal mitochondria were claimed; however, there are no illustrations so we cannot determine the veracity (Solonskiĭ, & Kovetskiĭ, 1989)
(Jégou, El Ghazi, de Lendeu, et al., 2012)	11	20 to 38 weeks gestation	Not indicated	Microscopic analysis of neocortical blood vessels showed disorganization of branching (but no difference in density) in fetuses >30 weeks compared to controls	In Table 2, summary information shows no malformations in nine cases; three cases with brain weight at or below 5th percentile (including the 38 week case described below); one 33 week case with "Diffuse astrogliosis, Decreased cellular density into [sic] ganglionic eminences"; and one 38 week case with "White matter heterotopic neurons, Microcephaly, Inferior olivary complex pachyria [sic]".
(Stoos, Nelsen, Schissler, et al., 2015)	1	34-year-old	Female	Brain weight at low end of normal range (1150g). Focal dysgenesis with enlarged right superior temporal gyrus; focal abnormal neuron columnar organization	Clinical diagnosis of FAS with facial anomalies and chronic cognitive impairment. Died from pulmonary embolus.
(Sarnat, Philippart, Flores-Sarnat, et al., 2015)	1	Term birth + 1 day	Male	Bilateral areas of cortical pachygyria and polymicrogyria; synaptophysin immunoreactivity in frontal cortex comparable to 33 weeks gestation	Microcephaly (head size not specified) and "typical facies". Possible delayed synaptogenesis.
(Tangsermkijs akul, 2016)	1	6 months	Male	Microencephaly (400g); agenesis of corpus callosum	Died from aspiration pneumonia. Abnormal facial features, head 36cm ($<10^{th}$ percentile).

In addition to the primary sources of information listed above, many of which review earlier papers, collations of the published

autopsy reports appear in several other secondary references (Clarren, 1986; Roebuck, Mattson, & Riley, 1998).

Table 3.2: Major malformative neuropathologic features in cases with documented prenatal alcohol exposure (PNAE) or clinical diagnosis of fetal alcohol spectrum disorder (FASD). Tabular summary in each case shows age, clinical history and non-neurological anomalies (absent (-) or present (+)) possibly attributable to PNAE, estimated magnitude and duration of alcohol exposure *in utero* (+ = rare / minimal; ++ = occasional; +++ = regular / heavy, and uncertain), and other *in utero* substance exposures (admitted use (+), denied use (-), unknown (?). PNAE exposure amount is estimated from available history, which is imprecise and possibly an underestimate.

Age Group	Case	Age at Death	Clinical History	PNAE estimated amount	PNAE estimated duration	Tobacco	Other Drugs	Neuropathologic Findings	Facial anomalies	Cardiac anomalies	Organ / Skeletal anomalies
1	Case 4	20 weeks gestation male	Mother 17 years, hypothyroid (treated with levothyroxine), drank monthly, used cannabis daily, and smoked approximately 10 cigarettes per day during pregnancy. Pregnancy terminated.	+++	Entire	+	marijuana	Exencephaly with focal defect in calvarium, destruction of cerebrum, and secondary destructive changes in diencephalon and hindbrain; asymmetry of eyes and cleft palate are suggestive of amniotic band adhesion.	+	-	-
1	Case 13	24 weeks gestation female	Mother 30 years, occasional alcohol and cigarettes during pregnancy. Stillborn.	++	Entire	+	-	Anencephaly, vertebral and rib anomalies, absent kidneys, absent left lung, ambiguous female genitalia.	-	-	+
1	Case 14	23 weeks gestation male	Mother 37 years, drank during pregnancy. Pregnancy terminated.	uncertain	Entire	?	-	Brain 122g (≥50th percentile). Lumbosacral myelomeningocele and Chiari type 2 malformation with distorted cerebellum.	-	-	-

1	Case 21	29 weeks gestation male	Mother 19 years, history of physical abuse during pregnancy. Liveborn by emergency caesarean section - died immediately	++	Entire	+	-	Brain 710g (≥95th %ile). Moderately severe hydrocephalus due to aqueduct stenosis, partial agenesis of the posterior corpus callosum, misshapen midbrain with rudimentary cerebral peduncles, microscopic subventricular zone heterotopia on surface of lateral ventricle temporal horn, microscopic glial heterotopia in meninges ventral to thalamus and posterior to midbrain, asymmetric cerebellum, microphthalmia.	-	-	-
1	Case 27	33 weeks gestation male	Mother 30 years, type 2 diabetes, drank during pregnancy and smoked ~4 cigarettes per day. Stillborn.	uncertain	Entire	+	-	Brain 133g (<5th percentile). Fused eyes, superior proboscis, alobar holoprosencephaly, horseshoe kidney with two ureters, arachnodactyly. Genetic analysis was not done.	+	-	+
1	Case 45	38 weeks gestation male	Mother (age not documented), drank and abused other drugs during pregnancy. Stillborn.	uncertain	Entire	-	+ (not specified)	Brain 233g (<5th percentile). Sacral spina bifida with dermal sinus and filum terminale lipoma.	+	-	+
2	Case 60	3 days (32 weeks gestation) male	Mother 34 years, chronic alcohol abuser and smoked tobacco (1 package cigarettes per day).	+++	?	+	-	Brain 247g (>50th %ile). Lumbosacral myelomeningocele with Chiari type 2 malformation, bilateral cystic kidneys.	-	-	+
2	Case 64	17 days (33 weeks gestation) male	Mother 21 years, drank heavily during first trimester (binged 3 times) and smoked tobacco (5-10 cigarettes per day). Died from complications of prematurity.	+++	First trimester	+	-	Chromosomes normal. Abnormal face with micrognathia, small palpebral fissures, flat philtrum, tethered tongue. Brain 267g (10th %ile). Absent posterior corpus callosum and slightly enlarged lateral ventricles, stenotic cerebral aqueduct and distorted pons, small cerebellum with deficiency of the inferior vermis, periventricular heterotopia on lateral ventricle walls (associated with no hemosiderin, no astroglial scar, and no buried ependymal cells), extensive leptomeningeal	+	-	-

								heterotopia erupting from posterior surface of midbrain			
2	Case 71	17 days female	Mother 18 years, drank alcohol and sniffed solvents during pregnancy. Born at term, non-dysmorphic, died from congenital Langerhans histiocytosis.	uncertain	Entire	?	solvent (toluene) inhalation	Brain 436g (20th %ile), grossly normal; multiple small subarachnoid heterotopia on temporal lobe.	-	-	-
2	Case 72	13 days female	Born at 41 weeks. Hydrocephalus demonstrated by MR imaging at 4 days. Sudden death in bed.	uncertain	Entire	+	-	Low set ears, small muscular ventricle septal defect in heart and polydactyly on one hand. Brain 540g (>50th %ile). Moderately severe hydrocephalus, agenesis of posterior corpus callosum (likely not attributable to ventriculomegaly), and aqueduct stenosis	+	+	-
2	Case 76	22 days male	Mother 28 years, born at term, seizures. Died from complications due to congenital anomalies.	++	First trimester	-	-	Multiple anomalies: Bilateral cleft lip and palate, tetralogy of Fallot, single cystic kidney, bifid scrotum / hypospadias / cryptorchidism, upslanted eyes. Brain 387g (<5th %ile). Small cysts with hemosiderin near interventricular foramen (probable *in utero* hemorrhage), small neuroglial heterotopia on ventricle wall near hippocampus, multiple small glial heterotopia in leptomeninges around midbrain	+	+	+

2	Case 79	28 days female	Mother (age not documented) drank heavily during pregnancy, possible viral illness ~16th week. Baby born at term. Died from congenital cardiac malformation.	+++	Entire	?	-	Multiple anomalies; growth retarded, microcephaly, complex cardiac defect (aortic isthmus hypoplasia, atrial and ventricular septal defects, large foramen ovale), thin lips, abnormal T7 vertebra, abnormal ovaries. Brain 276g (<5th %ile), asymmetric temporal lobe gyri, agenesis posterior corpus callosum.	-	+	+
2	Case 83	1 month male	Mother 28 years, drank and smoked during pregnancy. Mother was drinking before going to bed with her infant (born at term). Died in bed with parent.	uncertain	Entire	+	-	Nondysmorphic. The left hand showed a single transverse palmar crease. Brain 600g (>50th %ile). Diplomyelia with splitting of central canal at mid lumbar level and duplication of sacral spinal cord (no external signs).	-	-	-
2	Case 85	5 weeks male	Born at term. Failure to thrive and dehydration. Multiple congenital anomalies. Died in bed.	Clinical diagnosis FAS	(denies use)	?	-	Multiple anomalies: typical facial dysmorphism (low set ears, short palpebral fissures, poorly formed philtrum, thin upper lip, anteriorly tethered tongue), complex cardiac anomalies (subaortic VSD, partially closed by tricuspid valve tissue, ostium secundum ASD), dysplastic right kidney. Brain 421g (10th %ile), grossly normal, rare heterotopia in frontal leptomeninges.	+	+	+
2	Case 91	7 weeks male	Mother had Grave's disease (on propylthiouracil), Group B Streptococcus positive, poor prenatal care. Smoked during pregnancy and had alcohol early on. Born at term; died in bed with parent.	uncertain	Early	+	-	Nondysmorphic. Brain 558g (>50th %ile), grossly normal. Small glial heterotopia in leptomeninges around midbrain.	-	+	-

2	Case 109	4.5 months female	Born at term, infantile epilepsy treated with phenobarbital. MR imaging showed mild ventriculomegaly. Sudden unexplained death in bed.	uncertain	Early	?	marijuana	Brain 888g (95th %ile). Mild hydrocephalus with no obvious histologic abnormalities. Site of CSF obstruction not identified.	-	-	-
2	Case 114	7 month male	Born at term. Mother smoked and consumed large amounts of alcohol during pregnancy. Sudden unexplained death in bed.	+++	Early	+	-	Dolichocephalic skull (long head), wide spaced eyes, low set posteriorly rotated ears, high arched palate, abnormal right kidney and arachnodactyly. MR of brain showed mild ventriculomegaly. Brain 1221g (95th %ile), slightly abnormal gyri and mild hydrocephalus (photographs were not available for review), no microscopic abnormalities. Site of CSF obstruction not identified.	+	-	+
3	Case 118	12.5 month male	Mother has history of drug and alcohol abuse. Born at term, nondysmorphic, Sudden unexplained death in bed.	uncertain	Unknown	-	+ (not specified)	Brain 930g (<50th %ile), mid corpus callosum narrow (2mm vs. 4mm on microscopy; no photographs available for review), old occipital lobe infarct (1 cm maximum dimension cavity with hemosiderin in wall), mild enlargement of lumbar central canal (hydromyelia).	-	-	+
3	Case 127	2 years female	No maternal details available. Severe neurological handicap, suspected fetal alcohol syndrome. Died from adenovirus pneumonia.	Clinical diagnosis FAS	Unknown	?	?	Dysmorphic face (microcephaly, smooth upper lip, epicanthic folds). Heart - ventricular septal defect, posterior overriding aorta. Brain weight not recorded, lissencephaly with abnormally thick neocortex, calretinin immunostain does not define lamination, poor distinction with underlying white matter. Miller-Dieker phenotype but no chromosomal or genetic analysis.	+	+	+
3	Case 132	3.5 years female	Mother sniffed gasoline regularly during pregnancy; full birth details not available (child in	Clinical diagnosis FAS	Unknown	?	gasoline inhalation	Scoliosis, congenital dysplasia of the left hip. Brain 420g (<5th %ile), frontal ulegyria, occipital microgyria with laminar necrosis, cavitated infarct in thalamus, unilateral ventricular	-	-	+

131

	Case	Age/Sex	History	Diagnosis			Substance	Neuropathology			
			foster care). Severe cognitive delay. Died from pneumonia.					enlargement, hippocampal atrophy, severe Purkinje neuron loss. The pattern of destruction is suggestive of a prenatal insult.			
3	Case 139	5.5 years male	Mother abused a variety of substances including alcohol. Born at term. Hydrocephalus. Unexplained episodic bradycardia. Died of sudden respiratory arrest.	uncertain	Entire	?	solvent (toluene) inhalation	Nondysmorphic. Brain weight not recorded. Moderately severe chronic hydrocephalus caused by midbrain venous malformation that compressed cerebral aqueduct. Secondary axon damage in periventricular white matter indicates acute exacerbation. No other malformations.	-	-	-
3	Case 141	5.5 years female	Mother 21 years, smoked and drank during pregnancy; birth at 29 weeks gestation. Multiple congenital anomalies and multiple corrective surgeries. Died from complications of severe hydrocephalus.	uncertain	Entire	+	-	Multiple congenital anomalies including: hydrocephalus, vertebral defects, partial sacral agenesis, imperforate anus, cloacal outlet obstruction (VATER-H complex). Brain 1450g (>95th %ile); very severe hydrocephalus due to aqueduct stenosis with secondary destructive changes in periventricular structures.	+	+	+
3	Case 143	7 years female	Maternal & birth details not available. Cerebral palsy, seizures, mild scoliosis. Died from pneumonia.	Clinical diagnosis FAS	?	?	?	Microcephaly and hypertelorism. Brain 750g (<5th %ile), atrophy and discoloration bilateral cerebral white matter with cystic destruction in left frontal lobe, hydrocephalus (predominantly ex vacuo), and severe neuron loss from hippocampi (mesial temporal sclerosis). The pattern of damage is suggestive of premature birth complications.	-	-	+
3	Case 146	9.5 years female	Mother abused various substances during pregnancy. Born at term, severe cognitive delay and	Clinical diagnosis FAS	?	?	+ (not specified)	Abnormal head shape and scoliosis. Brain 1380g (>95th %ile), moderately severe ventriculomegaly due to aqueduct stenosis and destructive changes in white matter secondary to the ventricular	-	-	+

			epilepsy, severe hydrocephalus, died from pneumonia.					enlargement, and mesial temporal sclerosis.			
3	Case 147	11 years	Birth age not available. Female with severe cerebral palsy, spastic quadriparesis, severe developmental delay, and epilepsy. Died from pneumonia.	uncertain	First trimester	+	-	Brain 385g (<5th %ile). Bilateral symmetric destruction (likely ischemic) of cerebral hemispheres in distribution of middle cerebral arteries. Hippocampi were normal. The pattern of damage is suggestive of a midgestation *in utero* insult.	-	-	-
3	Case 157	15.5 years female	Female born at 29 weeks gestation. Mother smoked and drank alcohol during the pregnancy. In foster care. Small ventricular septal defect, atrial septal defect, and patent ductus arteriosus surgically repaired. Spastic quadriparesis (right > left), hearing and vision impaired, seizures treated with carbamazepine, and autistic-like features. Died from acute gastric volvulus.	uncertain; clinical diagnosis FAE	entire	+	-	Brain 1180g (<50th %ile). The main neuropathological abnormality was an old infarct in the middle cerebral artery distribution involving the left temporal and parietal lobes. The lesion is more typical of an arterial ischemic lesion related to the cardiac anomaly, rather than a direct complication of premature birth.	-	+	-
5	Case 174	60 years male	Cognitive delay, epilepsy. Cause of death was atherosclerotic coronary artery disease	Clinical diagnosis FAS	?	?		Dysmorphic face (flat philtrum, wide spaced eyes), brain 1270g (<5th percentile), mild ventriculomegaly, aqueduct stenosis at level of lower midbrain	+	-	-

133

Table 3.3. Epidemiologic details of autopsy Group 1 Stillborn / Intrapartum Death (20-41 weeks gestation).

	Group 1 Counts
Total number of autopsies in group [a]	52
Sex (male; female)	25; 27
Mother's age at birth (years)	
≤ 18	7
19-24	12
25-30	9
31-35	11
36+	4
Not indicated in autopsy report	9
Maternal disease (indicated in autopsy report)	
Vaginal / sexually transmitted infections [b]	9
Diabetes [c]	5
Respiratory illness (asthma)	2
Obesity	1
Mental illness (schizophrenia)	1
Prenatal Care	
Yes (level unknown)	3
Poor	9
Regular	2
None	7
Not indicated in autopsy report	31
Gravida	
Primigravida	8
2-4	17
5-7	18
8+	9
Not indicated in autopsy report	0
Parity	
None	11
1-2	18
3-4	11
5+	10
Not indicated in autopsy report	2
Previous Abortions	
Previous spontaneous abortion	9

Previous elective abortion	3
Previous abortion not otherwise specified	2
None	25
Not indicated in autopsy report	13
In Utero Alcohol Exposure	
Drank early in the pregnancy	5
Minimal / occasional use of alcohol - first trimester	3
Heavy / chronic use of alcohol - first trimester	4
Heavy / chronic use of alcohol - second trimester	2
Heavy / chronic use of alcohol - third trimester	4
Drank alcohol during / throughout pregnancy	9
Minimal / occasional use of alcohol during pregnancy	8
Heavy / chronic use of alcohol during pregnancy	4
Mother has a history of alcohol use or abuse	13
Mother smoked tobacco during pregnancy	
Yes	24
No	4
Not indicated in autopsy report	24
Mother abused other drugs during pregnancy	
Yes	20
multiple [d]; cocaine; marijuana; other [e]; not specified	*4;4;6;3;3*
No	6
Not Indicated in Autopsy Report	26
Gestation at Birth [f]	
≤ 27 weeks (extremely premature)	18
28-31 weeks (very premature)	6
32-36 weeks (premature)	14
37-41 weeks (term)	14
≥ 42 weeks (late term)	0
Not indicated in autopsy report	0
Method of birth	
Vaginal delivery	39
Breech (complicated vaginal birth)	5
Caesarean section	3
Not indicated in autopsy report	5
Birth Weight [g]	
<5th percentile	11
≥5th to <50th percentile	20
≥50th to <95th percentile	11
≥95th percentile	0

Not indicated in autopsy report	10
Cause of death / birth status	
Stillborn [h,i]	44
Induced (elective termination) for malformation(s)	3
Prematurity with survival ≤24 hours	5
Brain weight [j]	
<5th percentile [k]	10
≥5th to <50th percentile	11
≥50th to <95th percentile	13
≥95th percentile	2
Not indicated in autopsy report	16
Brain malformation(s)	
Neural tube defect	4
Complex malformations [l]	1
Holoprosencephaly	1
Microencephaly	10
Other neuropathologic findings [m]	
Widespread hypoxic neuronal damage [n]	12
Focal brain hemorrhage (periventricular)	2
Periventricular leukomalacia	1
Placental findings	
Abruption	4
Hemorrhage or infarction	10
Chorioamnionitis [o]	14
Villis inflammation	2
Other [p]	4
Normal	16
Not submitted	2
Heart Anomalies	
Major [q]	3
Minor [r]	2
None	38
Not identified (due to advanced autolysis / maceration)	9
Kidney anomalies	3
Skeletal anomalies [s]	10
FASD facial anomalies [t]	3
Other associated facial anomalies [U]	10

Abnormal (transverse / simian) palmar creases	5

[a] Total cohort N = 174

[b] Chlamydia (n=3), syphilis (n=1), trichomoniasis (n=1), sexually transmitted infection not otherwise specified (n=1), Group B streptococcus + (n=2), candidiasis (n=1)

[c] Type II (n=1), gestational (n=1), not otherwise specified (n=2)

[d] Combinations of: pentazocine, methylphenidate, marijuana, heroin, lysergic acid diethylamide, cocaine, acetaminophen with codeine, diazepam

[e] Opioids and solvents (glue)

[f] Source of terminology: http://www.who.int/mediacentre/factsheets/fs363/en/ accessed June 2015

[g] Source of percentile classification: http://www.phac-aspc.gc.ca/rhs-ssg/bwga-pnag/pdf/bwga-pnag_e.pdf accessed June 2015

[h] Undetermined (n=22), with bacterial / viral infection (n=4), with placental problems (n=12), with malformation(s) (n=6)

[i] Often designated as sudden infant death syndrome (SIDS) in autopsy reports conducted prior to 2008

[j] According to Phillips JB et al., Pathology. 2009, 41(6);515–526 and Maroun LL and Graem N., Pediatric and Developmental Pathology. 2005, 8;204–217

[k] Although 10 cases had brain weights ≤5th percentile, there may be underestimation of exact brain weight due to early stages of autolysis or maceration

[l] With: moderately severe hydrocephalus due to aqueduct stenosis, partial agenesis of the posterior corpus callosum, misshapen midbrain with rudimentary cerebral peduncles, microscopic subventricular zone heterotopia on surface of lateral ventricle temporal horn, microscopic glial heterotopia in meninges ventral to thalamus and posterior to midbrain, asymmetric cerebellum, microphthalmia

[m] Minor acute hypoxic-ischemic changes were also identified but were related to death and subsequently not listed

[n] Born premature (n=5)

[o] One case with abruption, one case with focal infarction

[p] Adhesion to head (n=1), atrophic left umbilical artery (n=1), hypovascular (n=1), tight umbilical cord around neck and adhesion of cord to amnion (n=1)

[q] Ventricular septal defect (VSD), VSD (with atrial septal defect)

[r] Displaced coronary ostium

[s] Rib or vertebral (n=6), dactyly (n=3), scoliosis (n=1)

[t] The 3 characteristic facial features are short palpebral fissures, smooth philtrum and thin upper lip; based on diagnostic criteria listed in Chudley AE et al., CMAJ 2005, 172(5 suppl);S1-21

[U] Other FASD associated anomalies include: low set ears (n=6), high arched or grooved palate (n=2), cleft palate (n=2)

Table 3.4. Epidemiologic details of autopsy Group 2 Infants (1 day old - 12 months) and autopsy Group 3 Children (13 months - 12 years).

	Group 2 Counts	Group 3 Counts
Total number of autopsies in group [a]	65	32
Sex (male; female)	42; 23	13; 19
Mother's age at birth (years)		
≤ 18	4	0
19-24	15	3
25-30	8	2
31-35	9	0
36+	2	0
Not indicated in autopsy report	27	27
Maternal disease (only when indicated in autopsy report)		
Vaginal / sexually transmitted infections [b]	5	---
Respiratory illness [c]	2	---
Diabetes [d]	2	1
Hypertension	1	---
Mental illness (panic disorder) [e]	1	---
Graves disease	1	---
Prenatal care		
Yes (level unknown)	0	0
Poor	9	1
Regular	0	0
None	9	2
Not indicated in autopsy report	47	29
Gravida		
Primigravida	8	1
2-4	23	2
5-7	19	3
8+	5	0
Not indicated in autopsy report	10	26
Parity		
None	8	1
1-2	19	3
3-4	20	2

5+	8	1
Not indicated in autopsy report	10	25
Previous abortions		
Spontaneous abortion	4	2
Elective abortion	2	0
Abortion not otherwise specified	3	0
None	36	3
Not indicated in autopsy report	20	27
In utero alcohol exposure / FASD diagnosis		
Drank during the first trimester / early in the pregnancy	6	3
Minimal / occasional alcohol during the first trimester	1	---
Heavy / chronic use of alcohol during first trimester	2	---
Drank during the second trimester	4	---
Drank during the third trimester	1	---
Drank alcohol during / throughout pregnancy	19	11
Minimal / occasional alcohol use during pregnancy	8	---
Heavy / chronic use of alcohol during pregnancy	5	---
Mother has a history of alcohol or use / abuse	17	2
Confirmed FASD diagnosis [f]	---	4
Suspected FASD [g]	2	12
Mother smoked tobacco during pregnancy		
Yes	33	2
No	2	0
Not indicated in autopsy report	30	30
Mother abused other drugs during pregnancy		
Yes	23	10
multiple [h]; cocaine; marijuana; other [i]; not specified	*2; 4; 8; 3; 6*	*1; 0; 1; 5; 3*
No	4	1
Not indicated in autopsy report	38	21
Gestation at birth [j]		
≤ 27 weeks (extremely premature)	4	1
28-31 weeks (very premature)	5	2
32-36 weeks (premature)	15	4
37-41 weeks (term)	37	5
≥ 42 weeks (late term)	0	1
Not indicated in autopsy report	4	19
Method of birth		

Vaginal delivery	28	4
Breech (complicated vaginal birth)	2	1
Caesarean section	12	2
Not indicated in autopsy report	23	25
Birth status		
Premature with survival ≤24 hours	5	---
Premature with survival >24 hours	19	---
Term with survival ≤24 hours	1	---
Term with survival >24 hours	36	---
Late term with survival >24 hours	0	---
Not indicated in autopsy report	4	---
Birth Weight [k]		
<5th percentile	4	1
≥5th to <50th percentile	15	3
≥50th to <95th percentile	16	3
≥95th percentile	3	0
Not indicated in autopsy report	26	25
In foster care / contact with child and family services (CFS)	12	14
Seizure disorder / epilepsy	7	7
Cause of death		
Sudden unexplained death [l]	18	2
Sudden unexplained death with unsafe sleeping environment	11	---
Drowning and other environmental [m]	---	6
Bacterial / viral infection	12	16
Complications of premature birth	9	1
Malformation(s)	15	3
Trauma (suspected homicide)	---	2
Suicide by hanging	---	2
Brain weight [n]		
<5th percentile	8	6
≥5th to <50th percentile	23	5
≥50th to <95th percentile	24	9
≥95th percentile	8	9
Not indicated in autopsy file	2	3
Brain malformation(s)		
Lumbosacral myelomeningocele with Chiari type 2 malformation	1	---

Deficient posterior corpus callosum, hydrocephalus, stenotic cerebral aqueduct, distorted pons, small cerebellum with deficiency of inferior vermis, periventricular and leptomeningeal heterotopias	1	---
Microencephaly, asymmetric temporal lobe gyri, agenesis of the posterior corpus callosum	1	---
Miller-Dieker type lissencephaly (genetic status not determined)	---	1
Mild hydrocephalus [o]	2	---
Hydrocephalus due to aqueduct stenosis, and partial agenesis of corpus callosum	1	---
Severe hydrocephalus [p]	---	3
Narrow mid corpus callosum, mild enlargement of lumbar central canal, old occipital lobe infarct	---	1
Minor subarachnoid heterotopia(s) [q]	4	---
Microencephaly [r]	3	6
Microencephaly with prenatal / perinatal ischemic brain lesions	3	---
Microencephaly with mild changes likely secondary to epilepsy	---	1
Other neuropathologic findings [s]		
Complications of premature birth (hypoxia; hemorrhage)	10	4
Periventricular leukomalacia (born at term)	1	---
Meningitis	5	1
Complications of perinatal meningitis	---	1
Severe brain trauma	---	1
Placental findings		
Abruption	1	---
Chorioamnionitis	3	---
Normal	2	---
Not examined	59	---
Heart anomalies		
Major [t]	8	3
Minor [u]	6	3
None	51	26
Kidney anomalies	6	3
Skeletal anomalies [v]	7	10
FASD facial anomalies [w]	12	7
Other associated facial anomalies [x]	12	4
Abnormal (transverse / simian) palmar creases	7	3

[a] Total cohort N = 174

[b] Group 2: chlamydia (n=3), Group B Streptococcus + (n=1), hepatitis C + (n=1)

[c] Group 2: tuberculosis (n=1), asthma (n=1)

[d] Group 2: Type II diabetes (n=1), gestational diabetes (n=1); Group 3: gestational diabetes (n=1)

[e] Group 2: panic disorder (n=1)

[f] Group 3: with heavy gasoline and solvent exposure (n=1)

[g] Group 2: with lead exposure (n=1); Group 3: with gasoline/solvent exposure (n=2)

[h] Multiple - Combinations of: opiates, crack cocaine, cocaine, and marijuana

i Other - solvents (hairspray, nail polish, glue, gasoline), diazepam, acetaminophen

[j] Source of terminology: http://www.who.int/mediacentre/factsheets/fs363/en/ accessed June 2015

[k] Source of Percentile Classification: http://www.phac-aspc.gc.ca/rhs-ssg/bwga-pnag/pdf/bwga-pnag_e.pdf accessed June 2015

[l] Often designated as sudden infant death syndrome (SIDS) in autopsy reports conducted prior to 2008

[m] Drowning (n=3), hypothermia (n=2), hyperthermia (n=1)

[n] Group 2: According to Phillips JB et al., Pathology. 2009, 41;515–526, Maroun LL and Graem N., Pediatric and Developmental Pathology. 2005, 8;204–217 and Fracasso, T., Am J Forensic Med Pathol. 2009, 30;231-34.
 Group 3: According to Dekaban AS and Sadowsky D., Ann Neurol. 1978, 4;345-56

[o] Group 2: dysmorphic brain (n=1)

[p] Group 2: secondary to aqueduct stenosis (n=1); secondary to aqueduct stenosis with partial sacral agenesis and VATER association (n=1);
 Secondary to midbrain vascular malformation (n=1)

[q] Group 2: cerebral (n=2); midbrain (n=2)

[r] Group 3: with no other overt destructive brain lesions (n=3)

[s] For both groups, minor acute hypoxic-ischemic changes were also identified but were related to death and subsequently not listed

[t] Ventricular septal defect (VSD) (small; subaortic), VSD (with atrial septal defect (ASD), patent ductus arteriosus (PDA), double outlet right ventricle (DORV), or fenestrated valve of foramen ovale), tetralogy of Fallot (with VSD, ASD), Ebstein's anomaly of the tricuspid valve (with bicuspid aortic valve, hypoplastic distal transverse aortic arch)

[u] Atrial septal defect (ASD) (with fenestrated valve of foramen ovale), patent ductus arteriosus (PDA) (with patent foramen ovale), PDA and ASD, displaced coronary ostium, superior versa cava draining into coronary sinus

[v] Group 2: rib or vertebral (n=3), dactyly (n=3), scoliosis (n=1); Group 3: rib or vertebral (n=5), scoliosis (n=5)

[w] The 3 characteristic facial features are short palpebral fissures, smooth philtrum and thin upper lip; based on diagnostic criteria listed in Chudley AE et al., CMAJ 2005, 172(5 suppl);S1-21

[x] Other FASD associated anomalies include (Group 2; Group 3): low set ears (n=9;2), wide spaced eyes (n=5;3), high arched or grooved palate (n=1;0), epicanthic folds (n=0;4), short upturned nose (n=1;0), micrognathia (n=1;0), cleft palate (n=2;1)

Table 3.5: Epidemiologic details of autopsy Group 4 Teens (13-19 years) and autopsy Group 5

Adults (20+ years).

	Group 4 Counts	Group 5 Counts
Total number of autopsies in group [a]	14	11
Sex (male; female)	10; 4	10; 1
In utero alcohol exposure / FASD diagnosis		
Drank during / throughout pregnancy	1	---
Mother has a history of alcohol use / abuse	1	---
Confirmed FASD diagnosis	8	2
Suspected FASD diagnosis	4	9
Personal substance abuse problems	4	5
In foster care / with child and family services (CFS)	7	2
Seizure disorder / epilepsy	3	2
Cause of death		
Accidental / environmental	3	---
Trauma (homicide)	3	3
Cardiac [b]	---	2
Complications of chronic neurological disorder	2	---
Multi-drug toxicity	---	2
Suicide by hanging	6	1
No anatomical cause of death	---	3
Brain Weight [c]		
<5th percentile	1	6
$\geq$5th to <50th percentile	2	0
$\geq$50th to <95th percentile	4	1
$\geq$95th percentile	6	2
Not indicated in autopsy file	1	2
Brain malformations		
Microencephaly	1	5
Mild hydrocephalus due to aqueduct stenosis with microencephaly	---	1
Other neuropathologic findings [d]		
Complications of premature birth (hypoxia, hemorrhage)	1	---
Acute brain trauma	2	2
Old brain trauma	---	2

Heart anomalies		
Minor [e]	1	0
None	10	10
Not indicated in autopsy file	3	1
Kidney anomalies	0	0
Skeletal anomalies [f]	0	1
FASD facial anomalies [g]	*Not well documented*	
Other associated facial anomalies	0	0
Abnormal (transverse / simian) palmar creases	1	0

[a] Total cohort N = 174

[b] Atherosclerotic coronary artery disease (n=1), cardiomyopathy (n=1)

[c] According to Dekaban AS and Sadowsky D., Ann Neurol. 1978, 4;345-56

[d] For both groups, minor acute hypoxic-ischemic changes were also identified but were related to death and subsequently not listed

[e] Atrial septal defect (ASD) and patent ductus arteriosus (PDA), which was surgically closed at birth

[f] Group 5: scoliosis (n=1)

[g] Based on diagnostic criteria listed in Chudley, AE et al., CMAJ. 2005, 172(5 suppl);S1-21

Figure 3.1. Neuropathologic features in fetal cases (see Table 3.3 for details). A and B - Case 4. Photographs show face and vertex view of craniofacial defects associated with amniotic band. C to H - Case 21. C- Coronal slice showing moderately severe hydrocephalus. D - Coronal section through the mid cingulate gyrus shows a thin corpus callosum, which was absent more posteriorly (12.5x original magnification). E - Misshapen midbrain with rudimentary cerebral peduncles and a narrow cerebral aqueduct (12.5x original magnification). F - Microscopic subventricular zone heterotopia are present on surface of lateral ventricle temporal horn (400x original magnification). G - Microscopic glial heterotopia are present in meninges ventral to thalamus and (H) posterior to midbrain (both 400x original magnification). All hematoxylin & eosin stain.
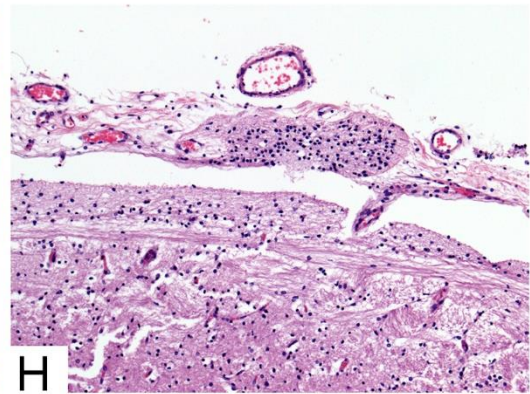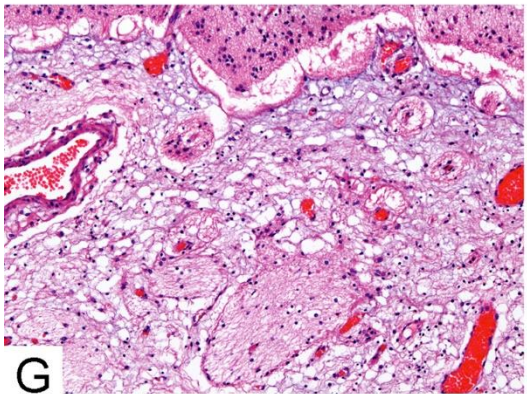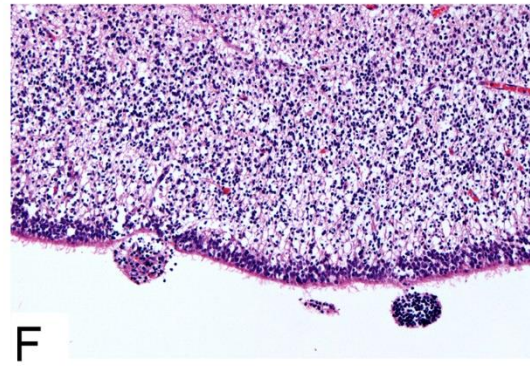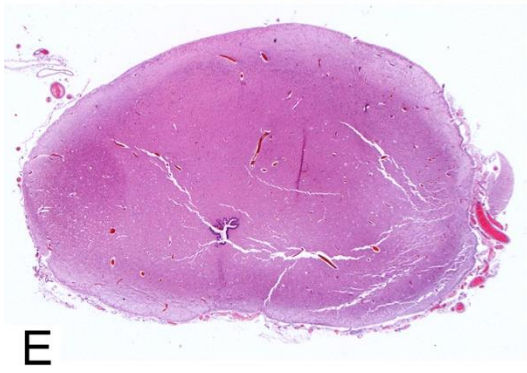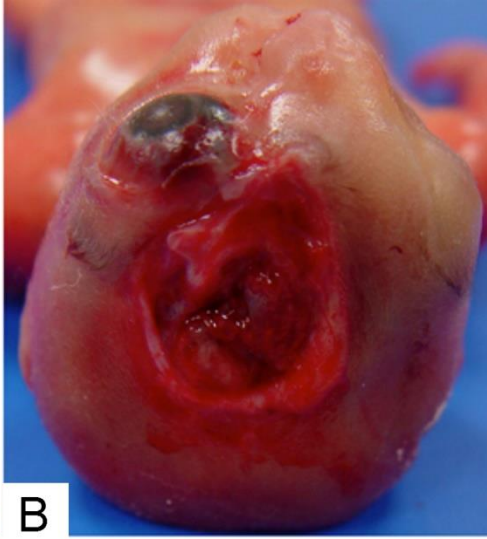
Figure 3.2. Neuropathologic features in infant cases with complex anomalies including corpus callosum defects (see Table 3.4 for details). A to F - Case 64. A - Coronal slice through posterior frontal level shows absent posterior corpus callosum and slightly enlarged lateral ventricles. B - Horizontal slices through upper brainstem showing stenotic cerebral aqueduct and distorted pons. C - Horizontal slices showing small cerebellum with deficient inferior vermis. D - Periventricular heterotopia on lateral ventricle walls (12.5x original magnification). Heterotopias were not associated with hemosiderin, astroglial scar, or buried ependymal cells. E - Extensive leptomeningeal heterotopias cover the posterior surface of midbrain (12.5x) through interruptions in the pial surface (F, 400x; arrows). G to J - Case 72. G - Magnetic resonance image (T2 weighted) at 4 days age shows hydrocephalus and absence of posterior corpus callosum. H - Coronal slice through frontal lobes shows moderately severe hydrocephalus and thin corpus callosum. I - Coronal slice of brain showing agenesis of posterior corpus callosum. J - Horizontal slice through midbrain showing aqueduct stenosis. K - Case 79. Coronal slice through posterior frontal level of a 28-day-old infant with no history of seizures shows asymmetric temporal lobes with incomplete rotation of the hippocampi (normal microscopic features) and agenesis of posterior corpus callosum.
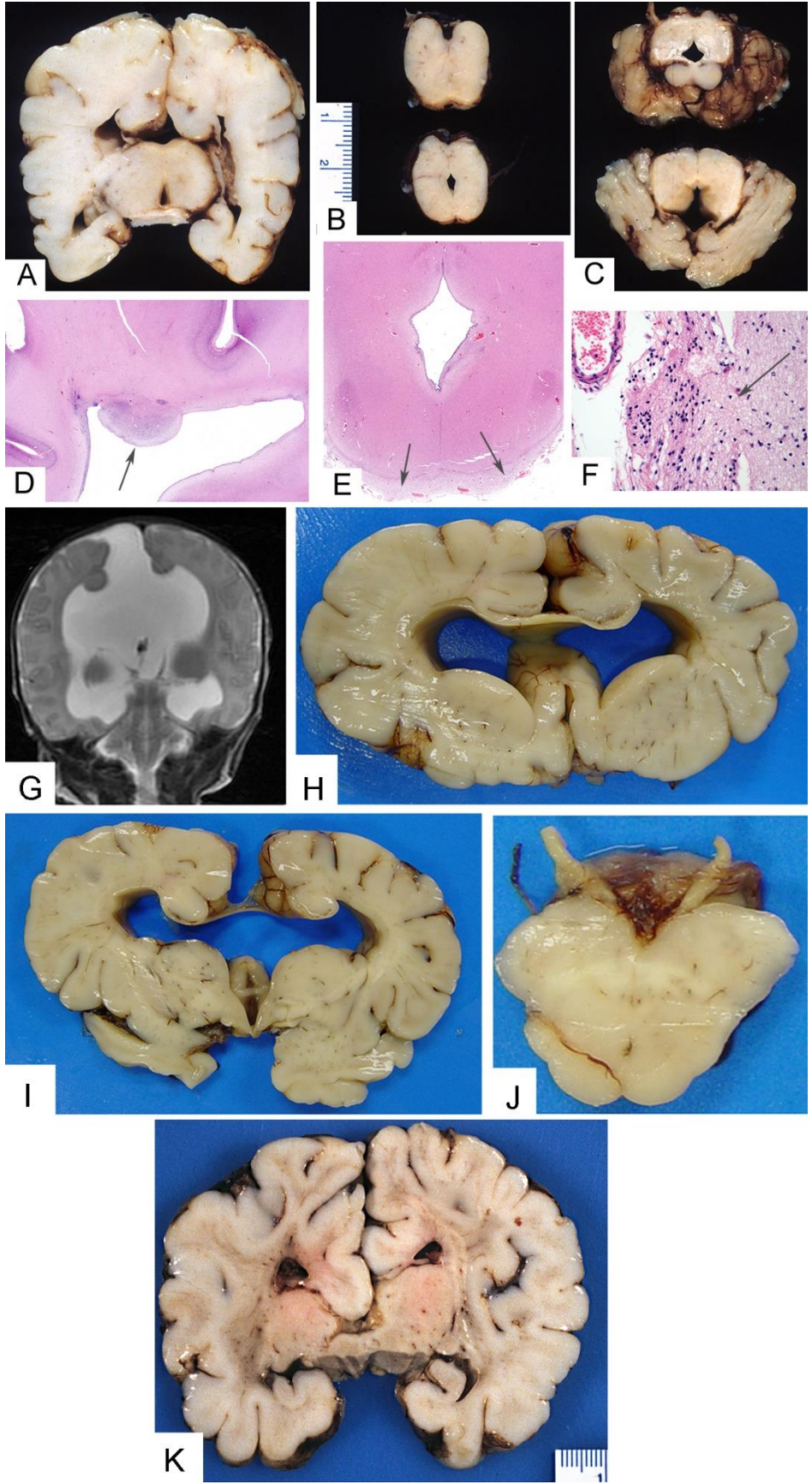
Figure 3.3. Neuropathologic features in infant cases with other less severe anomalies (see Table 3.4 for details). A and B - Case 83. Photomicrographs (solochrome cyanin stain; 12.5x original magnification) showing diplomyelia with splitting of central canal at mid lumbar level (arrows) and duplication of sacral spinal cord. There were no external abnormalities. C to E - Case 76. C - Small cysts (arrow) with hemosiderin, likely caused by *in utero* hemorrhage, near the interventricular foramen (12.5x, hematoxylin & eosin stain). D - Small neuroglial heterotopia on ventricle wall near hippocampus (100x). E - Multiple small glial heterotopia in leptomeninges around midbrain (40x). F - Case 71. Multiple tiny subarachnoid heterotopias (arrow) in leptomeninges over lateral temporal lobe. Some of these surround small blood vessels (400x). G- Case 85. Rare small heterotopias (arrow) in frontal lobe sulcus (100x).

150
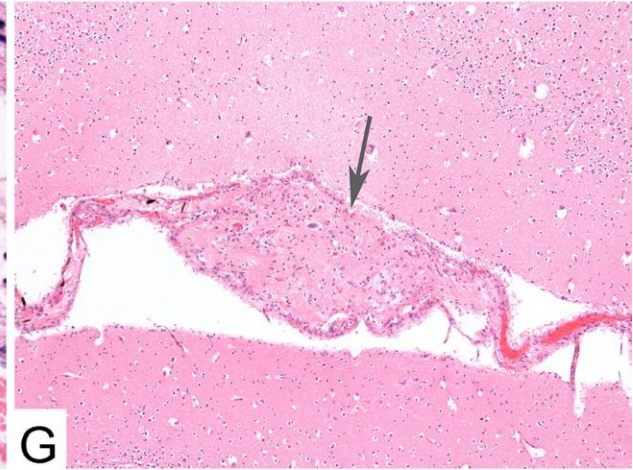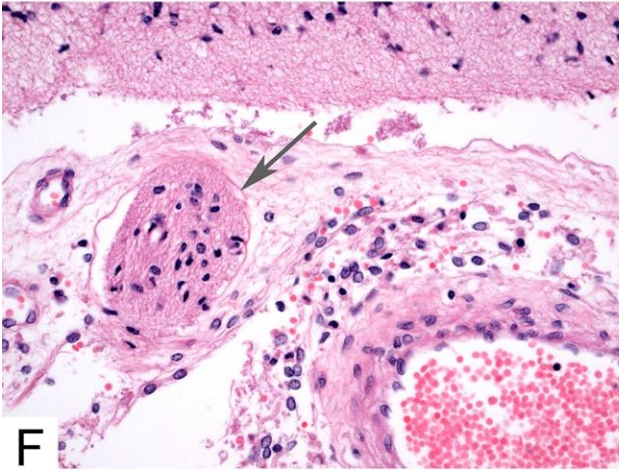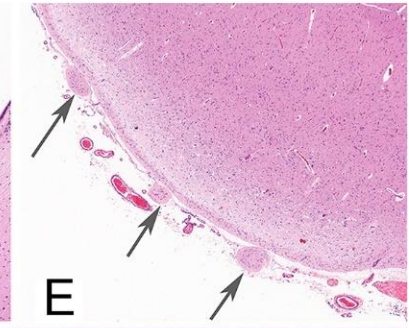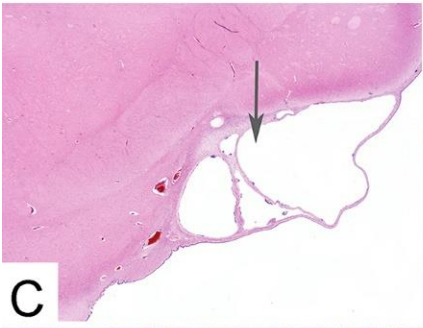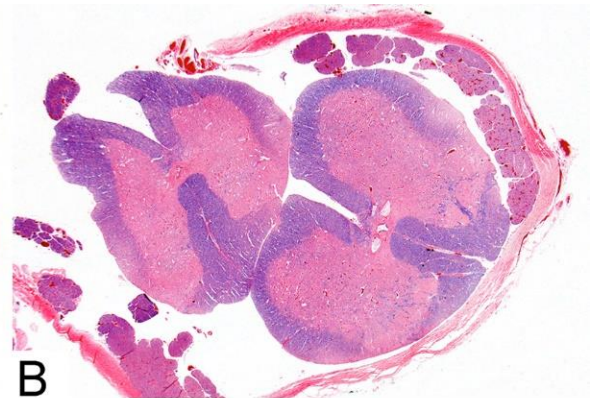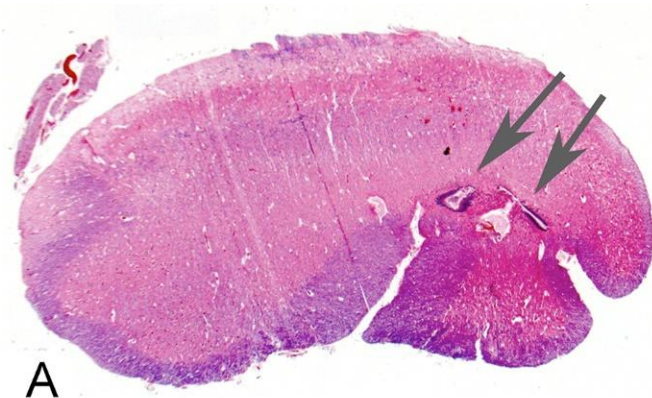
Figure 3.4. Neuropathologic features in childhood cases with hydrocephalus and other anomalies due to malformations (see Table 3.4 for details). A to C - Case 139 A - Coronal slice showing moderately severe chronic hydrocephalus with disruption of the septum pellucidum. B - The midbrain had a narrow cerebral aqueduct that was compressed by a venous malformation (C; 40x original magnification; hematoxylin and eosin). Immunostain for amyloid precursor protein demonstrated damaged axons in the periventricular white matter (not shown), which is indicative of acute exacerbation of the ventriculomegaly. D to F - Case 146. D - CT scan of brain at 6 years age showed severe hydrocephalus. E - Coronal slice showing moderately severe chronic hydrocephalus with disruption of the septum pellucidum. F - Midbrain slice shows aqueduct stenosis. G and H - Case 141. G - CT scan at 5 years age showing extreme hydrocephalus in a child with vertebral defects, partial sacral agenesis, imperforate anus, and cloacal outlet obstruction (VATER-H complex). H - Midbrain had aqueduct stenosis (12.5x). I - Case 127. Photograph of the brain of a 2-year-old with severe lissencephaly; on morphologic grounds this was Miller-Dieker phenotype (poorly defined cortical lamination, no heterotopic overgrowth). No chromosomal or genetic analysis had been performed.
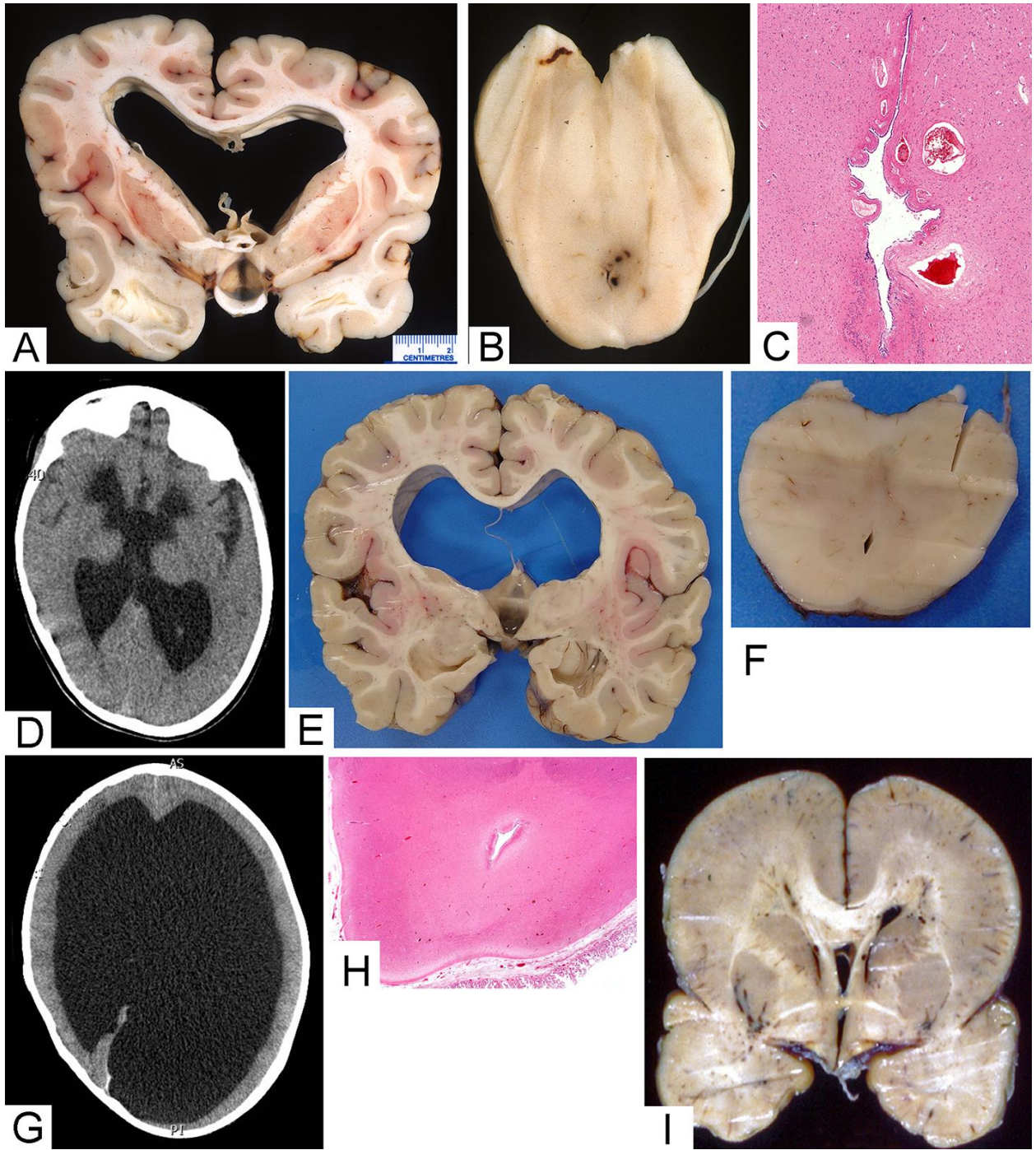
Figure 3.5. Neuropathologic features in childhood cases with anomalies likely due to prenatal or perinatal ischemic brain insults (see Table 3.4 for details). A and B - Case 132. Lateral view of the brain shows frontal ulegyria (red arrowhead) and occipital microgyria with laminar necrosis (yellow arrowhead). Coronal slice of the brain shows a cavitated infarct in the thalamus (red arrowhead) and unilateral ventricular enlargement. In addition, there was hippocampal atrophy and severe Purkinje neuron loss (not shown). The pattern of destruction is suggestive of a prenatal insult. C and D - Case 143. Coronal slices through the brain show atrophy and discoloration bilateral cerebral white matter with cystic degeneration in left frontal lobe, and compensatory ventricular enlargement. In addition, there was >90% neuron loss from the hippocampi, especially the CA1 sectors (mesial temporal sclerosis). The pattern of damage is suggestive of premature birth complications. E and F - Case 147. CT scan at 8 years age showed bilateral cerebral destruction. At autopsy, the brain exhibited bilateral symmetric loss of tissue in the distribution of the middle cerebral arteries. Hippocampi were preserved. The pattern of damage is suggestive of a midgestation *in utero* ischemic damage. G - Case 157. Photograph showing an old ischemic infarct in the middle cerebral artery distribution involving the left temporal and parietal lobes; this is possibly related to the cardiac anomaly. H - Case 118. Photomicrograph showing hemosiderin (blue) along the wall of a cavity extending from the surface of the occipital lobe to the ventricle wall (Perls' Prussian blue stain; 12.5x original magnification). This appears to be an old hemorrhagic infarct near the middle-posterior cerebral artery interface.

154
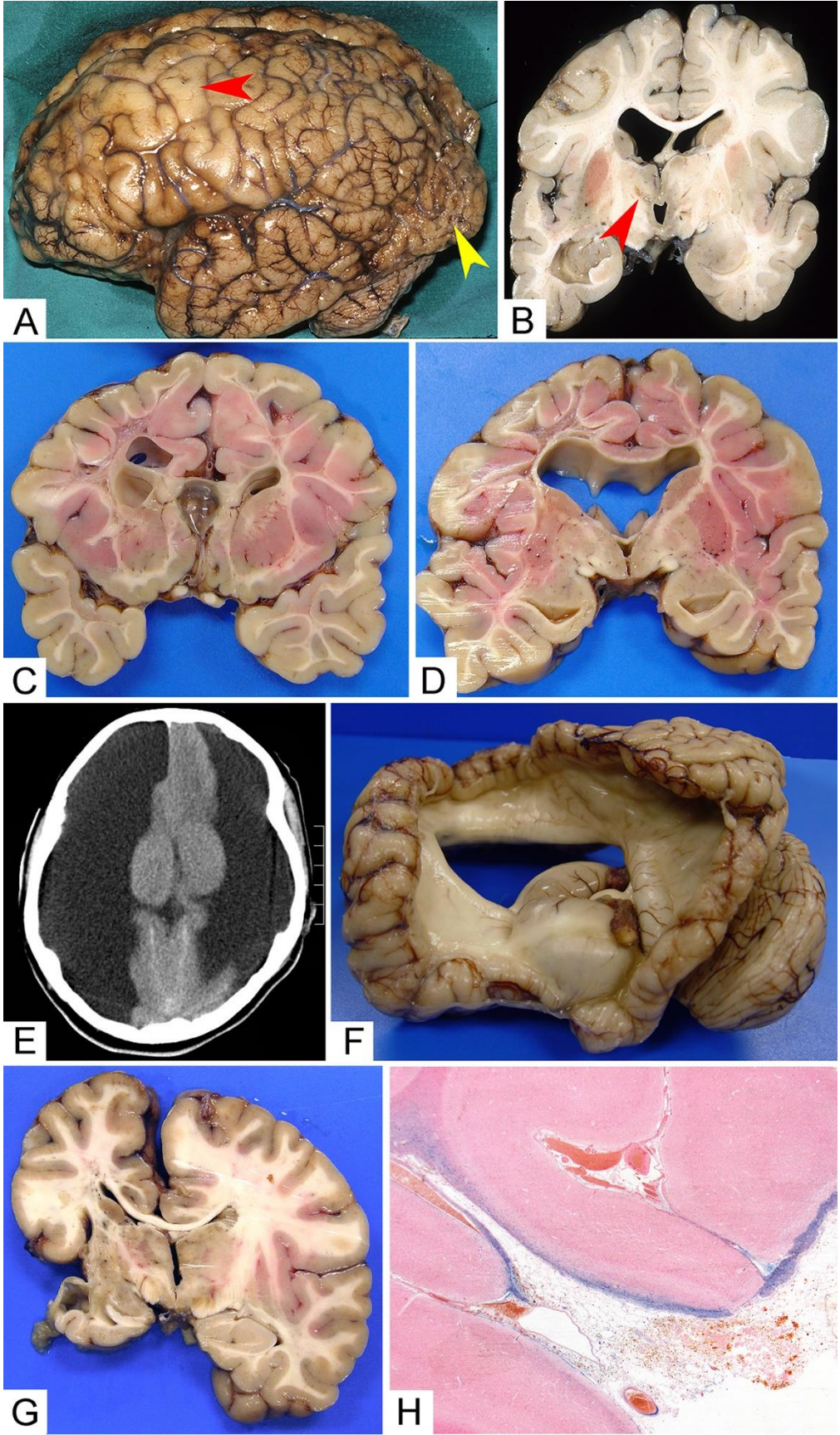
Figure 3.6. Case 174. 60-year-old male with cognitive delay and clinical diagnosis of fetal alcohol syndrome spectrum disorder (see Table 3.5 for details). A - Coronal slice of brain shows mild ventriculomegaly. B - Lower midbrain had a very narrow cerebral aqueduct. C - Microscopic examination of the aqueduct showed a narrow, irregular channel lined by ependymal cells (40x; hematoxylin and eosin).
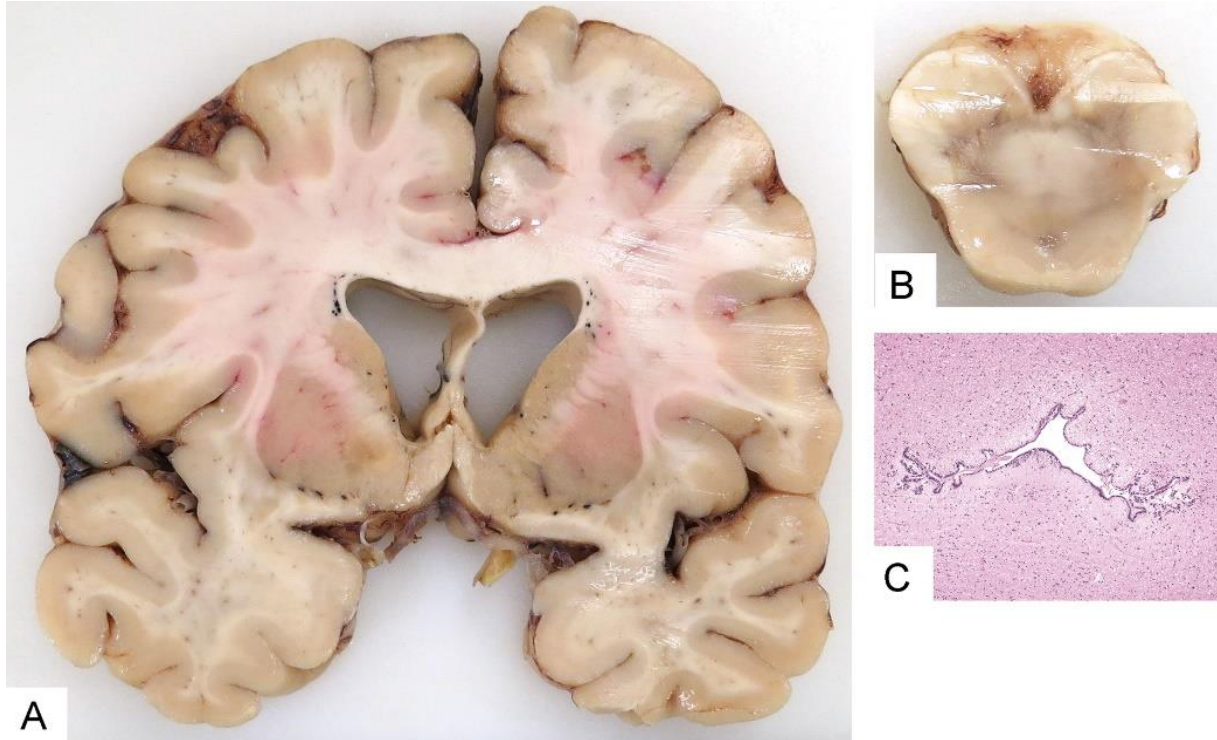
Table 3.6: Summary of brain abnormalities in autopsy cases with prenatal alcohol exposure or clinical diagnosis of fetal alcohol spectrum disorder.

	Stillbirths	Infants	Children	Teenage	Adults
Total # of cases	52	65	32	14	11
Total brains examined*	34	65	31	12	7
Micrencephaly	10	8	6	1	6
Neural tube defects	4	1	-	-	-
Corpus callosum dysgenesis + hydrocephalus	1	2	-	-	-
Corpus callosum dysgenesis + other minor anomaly	-	1	1	-	-
Hydrocephalus	-	2	3	-	1
Minor heterotopias	-	4	-	-	-
Regional hypoxic-ischemic or hemorrhagic lesions unrelated to prematurity	1	1	4	-	-
Brain lesions related to prematurity	-	2	4	1	-
Probable genetic brain malformation	1	-	1	-	-
Mesial temporal sclerosis	-	-	3	-	-

*Number of cases with brain pathological examination

CHAPTER 4: MANUSCRIPT 2 - DNA METHYLATION AND HISTONE POST-TRANSLATIONAL MODIFICATION STABILITY IN POST-MORTEM BRAIN TISSUE

Authors: Jessica S. Jarmasz, Hannah Stirton, James R. Davie, and Marc R. Del Bigio

Preface

This publication was the result of the second research aim.

Author contributions:

I (the first author) conducted almost all the research, put all the results together, and wrote the manuscript. The last author (De Bigio) planned the project and finalized the manuscript. The second author (Stirton) performed the DNA post-mortem stability analysis as a summer project. The third author (Davie) contributed to planning the experiment and editing the manuscript.

ABSTRACT

Background: Epigenetic (including DNA and histone) modifications occur in a variety of neurological disorders. If epigenetic features of brain autopsy material are to be studied, it is critical to understand the post-mortem stability of the modifications.

Methods: Pig and mouse brain tissue were formalin-fixed and paraffin-embedded or frozen after post-mortem delays of 0, 24, 48 and 72 hours. Epigenetic modifications frequently reported in the literature were studied by DNA agarose gel electrophoresis, DNA methylation enzyme-linked immunosorbent assays, Western blotting, and immunohistochemistry. We constructed a tissue microarray of human neocortex samples with devitalization or death to fixation times ranging from <60 minutes to 5 days.

Results: In pig and mouse brain tissue, we found that DNA cytosine modifications (5mC, 5hmC, 5fC and 5caC) were stable for ≥72 hours post mortem. Histone methylation was generally stable for ≥48 hours (H3K9me2/K9me3, H3K27me2, H3K36me3) or ≥72 hours post mortem (H3K4me3, H3K27me3). Histone acetylation was generally less stable. The levels of H3K9ac, H3K27ac, H4K5ac, H4K12ac, and H4K16ac declined as early as ≤24 hours post-mortem, while the levels of H3K14ac did not change at ≥48 hours. Immunohistochemistry showed that histone acetylation loss occurred primarily in the nuclei of large neurons, while immunoreactivity in glial cell nuclei was relatively unchanged. In the human brain tissue array, immunoreactivity for DNA cytosine modifications and histone methylation was stable, while subtle changes were apparent in histone acetylation at 4 to 5 days post-mortem.

Conclusion: We conclude that epigenetic studies on human post-mortem brain tissue are feasible, but great caution is needed for selection of post-mortem delay matched controls if histone acetylation is of interest.

BACKGROUND

Epigenetics represents the modification of gene expression by changes in the chemical makeup of nucleotides or the associated histone proteins, rather than alteration of the genetic code itself. Various DNA methylation changes, covalent histone tail modifications, and modulation of the enzymes responsible for epigenetic modifications are critical in neural development, aging, and neurological disease (Jakovcevski, & Akbarian, 2012; Weng, An, Shin, et al., 2013). Animal models have provided valuable insights into epigenetic events (Babenko, Kovalchuk, & Metz, 2015; Mychasiuk, & Metz, 2016; Rosenfeld, 2010). However, direct study of human brain tissue is necessary for understanding the human condition (Farré, Jones, Meaney, et al., 2015). Despite this necessity, use of human autopsy material has several inherent limitations. Variation in the circumstances before death (agonal state) including brain trauma, hypoxia, and seizures, can alter the molecular constituents of tissue (Ferrer, Martinez, Boluda, et al., 2008; Srinivasan, Sedmak, & Jewell, 2002; Stan, Ghose, Gao, et al., 2006). For example, human brains with ischemic injury had lower levels of histone acetylation, possibly associated with inhibited transcription of many genes (Schweizer, Meisel, & Märschenz, 2013). Post-mortem variables include: the environment after death (especially temperature), the time between death and autopsy (post-mortem delay - PMD), post-mortem artefacts such as putrefaction, method of preservation (chemical fixation or freezing), and storage temperature (room vs. refrigerated). In general, the differential vulnerability of DNA, RNA, proteins, and metabolites to PMD is well recognized. However, it is equally important to understand the post-mortem changes in epigenetic modifications.

DNA is well preserved when quickly extracted and frozen at -80°C, or fixed in buffered formalin for a short period (≤1 month) prior to paraffin-embedding (Ferrer, Armstrong,

Capellari, et al., 2007). Less is known about the maintenance of epigenetic modifications following death. Two chromatin immunoprecipitation (ChIP) studies of human post-mortem brains showed that DNA remained attached to histones for at least 30 hours after death (Sung Huang, Matevossian, Jiang, et al., 2006; Stadler, Kolb, Rubusch, et al., 2005). In samples of brain from deceased adult humans that had been infused with "formalin within the first hours post-mortem" and embedded in paraffin after up to 2 months in fixative, global DNA methylation is generally preserved although gene-specific DNA methylation studies can be compromised if the tissue has been stored for decades (Bak, Staunstrup, Starnawska, et al., 2018). Methylation patterns were successfully analyzed using bisulphite conversion of DNA extracted from human brains with Alzheimer disease and a PMD of ~48 hours (Barrachina, & Ferrer, 2009). In an extreme example, methylation patterns in DNA extracted from >10,000-year-old bone was successfully analyzed by bisulphite allelic sequencing (Llamas, Holland, Chen, et al., 2012). Using immunohistochemistry (IHC), histone methylation (H3K4me2, H3K4me3, H3K27me3, H4K20me3) appears to be maintained in human cerebellum for at least 11 hours post-mortem (Stadler, Kolb, Rubusch, et al., 2005). Utilizing ChIP, histone H3 trimethylated at lysine 4 (H3K4me3) and H3K27me3 were stable at various gene promotors up to 30 hours post-mortem (Huang, Matevossian, Jiang, et al., 2006). Barrachina *et al.* reported that histone acetylation (H3K9ac and H3K27ac) post-translational modifications (PTMs) at certain gene promotors varied substantially between 0 and 50 hours post-mortem (Barrachina, Moreno, Villar-Menéndez, et al., 2012). Lysine methyltransferase and acetyltransferase enzyme activities, which generate histone PTMs, were measured in 12 human post-mortem brain samples. Both enzyme activities tended to decline with increasing PMD from 5 to 100 hours, although the changes were not statistically significant (possibly due to small sample size)

(Monoranu, Grünblatt, Bartl, et al., 2011). To our knowledge, histone deacetylase (HDAC) and histone demethylase (HDM) enzymes have not been studied in the context of PMD nor have the enzymes responsible for DNA cytosine modifications (DNA methyl transferases (DNMTs), ten-eleven translocation (TETs), etc.).

We hypothesize that the delay between death and tissue preservation will affect epigenetic modifications in brain tissue. We addressed this by determining the stability of histone PTMs and DNA cytosine modifications in murine, porcine, and human brain samples after death using immunohistochemistry and biochemical methods.

METHODS

Porcine Brain

Pig brains (*Sus domesticus*) (4 normoxic, 3 hypoxic; N=7) were donated by investigators studying the effects of hypoxia on immature lung (Sikarwar, Hinton, Santhosh, et al., 2014). Ethics approval was obtained through the University of Manitoba Animal Care Committee (Protocol # 14-008/1). Briefly, female newborn (8-24 hours old) piglets were obtained from a local pathogen-free supplier. Six of the seven piglets were raised to 3 days of age before sacrifice. Piglets were bottle fed with swine milk replacer and housed in temperature-controlled isolettes. They were raised in normobaric hypoxia (10% oxygen) or in normoxia (21% oxygen) for 72 hours. The hypoxic piglets were smaller (body weight mean $\pm$ SEM: normoxic 1.71 ± 0.14 kg; hypoxic 1.53 ± 0.07 kg). Animals were euthanized with an intraperitoneal injection of pentobarbital followed by exsanguination. The time between injection and pedal reflex test was approximately 5-10 minutes. The scalp was stripped, and the skull was opened with scissors. The medulla - spinal cord junction was transected, then the brain was removed, weighed, and immediately placed into a humid container. Concordant with body weights, brains from the hypoxic piglets were smaller (normoxic 35.11 ± 0.40 g; hypoxic 31.15 ± 0.26 g). The cerebellum and brainstem were frozen separately and used for assay optimization. The cerebral hemispheres were split in the midline, then sliced into 8 or 14 pieces of neocortex, which were each assigned a PMD time point of 0, 24, 48 or 72 hours (**Figure 4.1**). Therefore, each pig brain yielded all four PMD time points. The delays were designed to mimic human post-mortem and autopsy conditions, where some bodies are cooled immediately after death (e.g. death in hospital) while others are subject to a room temperature delay (e.g. found dead in home). The 0 hour specimens were formalin-fixed or frozen immediately, while the other brain pieces remained in humidified

163

Petri dishes at 4°C until the designated time (24, 48, or 72 hours; **Figure 4.2**). Some pieces remained at room temperature for 6-8 hours before being transferred to 4˚C. One sample from each pair was immersion fixed in 10% buffered formalin (Fisher Scientific #23-245-685) and the other sample was frozen and stored at -70°C for biochemical assays. After fixation for no more than 1 week, the samples were painted with various colors (to designate the PMD identity) before being placed in 3x2 cm tissue cassettes for embedding in single blocks of paraffin (**Table 4.1; Figure 4.3**). This ensured that all immunostaining conditions were identical for comparison of the different time points. To test for adverse effects of over fixation, brain samples from the 24-hour post-mortem time point remained in formalin for 2.5, 5, 6, 8, 9, 10 and 12 weeks followed by sample coloring and embedding in a single block of paraffin. For all pig details, please see **Table 4.2**.

Murine Brain

Ethics approval was obtained through the University of Manitoba Animal Care Committee (Protocol # 14-012; AC10924). Outbred CD1 mice (*Mus musculus*) were locally supplied in three age groups: 0-24 hour old newborn (8 male, 8 female; body weight 1.64 ± 0.03 g), 10-day (8 male, 8 female; body weight 7.02 ± 0.23 g) and 8-10 week (8 male, 8 female; body weight 36.67 ± 1.01 g). Two male and 2 female brains from each age were processed at each PMD time point of 0, 24, 48, and 72 hours (**Figure 4.4**). Two dams (~13 weeks old; body weight 44.12 ± 2.48 g) were sacrificed for a PMD time of 96 hours. That is a total of 16 brains per age group (4 sets of PMD time points; 48 mouse brains total) + two dam brains. Newborn mice were euthanized by direct decapitation with scissors (no anesthetic). Infant and adult mice were euthanized by a 4-5% isoflurane anesthesia followed by bilateral pneumothorax or cervical

dislocation. Time between isoflurane exposure and pedal reflex test was approximately 10-20 minutes. The scalp was opened with scissors, and the brain was removed and weighed (newborns 0.085 ± 0.003 g; 10-day 0.33 ± 0.01 g; young adults 0.49 ± 0.01 g). Each mouse brain gave rise to a single PMD time point. The right hemisphere was weighed and frozen at -70°C for biochemical assays. The left hemisphere was fixed in 10% buffered formalin followed by paraffin embedding. The cerebellum and brainstem were discarded (**Figure 4.4**). Samples for the 0 hour time point were formalin-fixed or frozen immediately. For the remaining time points, brains remained at room temperature in a humidified Petri dish for 6.9 ± 0.1 hours before transfer to 4°C. Fixed brain samples were coloured and processed in the same manner as pig brains (**Figure 4.5**). For all mouse details, please see **Table 4.3**.

Human Brain

A tissue microarray consisting of anonymized brain samples was constructed under the Diagnostic Services Manitoba institutional approval for quality assurance procedures. Neuropathology records were reviewed to identify neocortical specimens with no microscopic abnormality (determined upon examination by a neuropathologist) that had been formalin-fixed after a range of devitalization or post-mortem periods. Brain samples with known hypoxic damage were also identified. Four (4) millimeter (mm) diameter samples were punched out of 14 formalin-fixed paraffin-embedded tissue blocks and assembled into a 5x3 array (**Table 4.4**). The microarray was subject to immunohistochemistry with antibodies to the following epigenetic modifications: 5mC, 5hmC, H3K4me3, H3K27me3, H3K36me3, H3panAc, H3K9ac, H3K14ac, histone H4 acetylated at lysine 5 (H4K5ac) and H4K12ac (see details below).

Histone Extraction

Histones were extracted from porcine brain using a histone extraction kit (Abcam; #113476) according to the manufacturer's protocol with minor changes. Briefly, 0.1g of tissue was put into 500µl of 1X pre-lysis buffer, homogenized, and centrifuged to obtain a pellet. Pellets were resuspended in 400-700µl of lysis buffer, mixed, and put on ice for 1 hour. The samples were centrifuged to obtain a supernatant that contained the acid extracted histones, which were then transferred into a pH neutralizing buffer solution containing dithiothreitol (DTT), followed by the addition of phenylmethylsulfonyl fluoride (PMSF) to inhibit proteases. Histone protein concentrations were measured using the Bradford method (Bio-Rad DC Protein Assay kit # 5000112). Absorbance was measured at 750nm on an Epoch Microplate Reader (Gen5 2.08 Software) and concentrations were calculated from a standard curve. The average histone concentration was 33.8µg/µl from the 0-hour sample, 26.9µg/µl from the 24-hour sample, 22.1µg/µl from the 48-hour sample, and 19.6µg/µl from the 72-hour sample.

DNA Extraction and Purification

DNA was extracted using the DNeasy Blood and Tissue DNA extraction kit (Qiagen #69505) according to the manufacturer's protocol with minor changes. Briefly, porcine brain samples (25-30mg) were thawed at room temperature, combined with primary lysis buffer and proteinase K, mixed, and incubated (with periodic stirring) in a water bath at 56°C for 3-3.5 hours. RNase A (100 mg/ml) was added to the samples, and after 2 minutes at room temperature, secondary lysis buffer and ~100% ethanol were added and mixed immediately. The mixture was pipetted onto the DNeasy Mini Spin column, centrifuged, and repeatedly washed. DNA captured in the DNeasy membrane was eluted with AE buffer twice (total eluted volume of 400µl). DNA

166

was quantified and tested for purity using spectrophotometric analysis at 260nm and 280nm (Ultrospec 3000), then stored at 4°C. The average DNA concentration was 0.023 μg/μl (12.5μg) per sample. All DNA samples were precipitated in a 1:10 volume of 3M sodium acetate at pH 5.2 followed by addition of an equal volume of ~100% ice cold ethanol, and stored at -20°C overnight. Samples were mixed then centrifuged at 9660 – 15000G for 1 hour. The DNA pellet was washed twice with ice cold 70% ethanol and centrifuged for 30 minutes. DNA pellets were air dried overnight then dissolved in Qiagen Elution Buffer (Tris-EDTA solution) to the desired volume at ~50°C for 10 minutes, mixed, and stored at 4°C. DNA was quantified using spectrophotometric analysis at 260nm (Ultrospec 3000; Pharmacia Biotech) to obtain final concentrations, and at 280nm to verify purity.

DNA Integrity

Twelve-well 0.8% agarose gels were prepared by combining 0.8 grams of agarose (Invitrogen Ultra Pure Agarose, #15510-027) in 100ml of 0.5X running buffer (1L of DNA / RNA-free water (Gibco, #10977-015) with 50mL of 10X Tris-borate-EDTA (TBE) buffer). Gel Star Nucleic Acid Gel Stain (10μl, Lonza #50535) was added before the gel was set. Cold 6X DNA loading buffer (2.5% Ficoll-400, 11mM EDTA, 3.3mM Tris-HCl, 0.017% sodium dodecyl sulfate (SDS), 0.015% bromophenol blue, pH 8.0 25°C) and DNA samples were combined in a 3:1 ratio of loading buffer to DNA, then pipetted into individual wells (20μl/well) along with a DNA ladder (Quick-Load DNA Marker, Broad Range; NEB #N0303). The gels ran at 100 volts for 1.5 hours and were imaged using a chemiluminescence imager and computer program (FluorChem HD2; ProteinSimple, San Jose, CA).

Western Blotting

Histone samples (30μg / 8μl per well; in duplicate) were prepared in a 1:1 ratio with 2X

sample buffer (1M Tris pH 6.8, 35% glycerol, 10% SDS, 0.2mg Bromophenol Blue), loaded into

a 15 lane SDS–15% polyacrylamide gel, and separated by electrophoresis (135V, 100 minutes)

with 1X running buffer at pH 8.3 (25mM Tris, 182mM Glycine, 0.1% SDS) along with protein

standard (Bio-Rad, #161-0374) and a positive control (1mg/μl of pure histone mix from calf

thymus; Roche, #10 223 565 001) (**see Figure 4.6**). Samples were transferred onto 0.2μm

polyvinylidene difluoride (PVDF) membrane (Bio-Rad, #162-0177) at a constant amperage of

400mA (70 minutes on ice) using a wet transfer system and a transfer buffer with no SDS

(25mM Tris, 192mM glycine, pH 8.3, 20% methanol). Protein transfer was verified with

Ponceau S stain. The PVDF membrane was incubated with 5% skim-milk (Carnation Fat Free

Instant Skim Milk powder) blocking solution or bovine serum albumin (BSA; Sigma, A9647;

Chem Cruz, SC-2323) in 1X TBS (depending on the antibody) for 1.5 hours at room

temperature. Membranes were cut in half; one half was incubated with primary antibodies

specific for histone PTMs and the other half with the respective "total histone" antibody (either

H3 or H4) overnight (**Table 4.5** and **Table 4.6**). Peroxidase-conjugated AffiniPure sheep anti-

mouse IgG (Jackson ImmunoResearch #515-035-062) or goat anti-rabbit IgG (Sigma, A6154)

was applied to the membrane at a concentration of 1:7000 for 2 hours at room temperature.

Chemiluminescent reagent (Clarity Western ECL Substrate, Bio-Rad #170-5060) applied to the

membrane for 3 minutes; histone bands were visualized on Classic Blue Autoradiography Film

BX (MidSci, EBNU2).

Bands were quantified using the Bio-Rad ChemiDoc TM MP System (Universal hood III

model) and ImageLab Software (Version 5.2.1). The software generated a table with: "relative

front" (position related to molecular size), the "volume" of the band (a product of the band area and the mean intensity of all pixels within the band area boundaries), and the relative quantification (in comparison to the reference band, which is the 0-hour time point). All bands underwent automatic background subtraction ("rolling ball" method; disk size 10mm). The specific histone modification "volume" was divided by the respective total histone "volume" and all results are shown as the normalized "volume" ratios.

DNA Methylation Enzyme-Linked Immunosorbent assay (ELISA)

The 5mC DNA ELISA Kit (Zymo, #D5325) kit was used to measure DNA methylation in pig brain samples using the indirect method. The manufacturer's suggested protocol was followed, except for the addition of gentle rocking / agitation during all 37°C incubation steps. Briefly, 100ng of purified DNA from each pig brain sample (N=7) was brought to a total volume of 200μl with 5mC coating buffer. Samples, along with the standards, were heated at 98°C then immediately iced to denature the DNA. Samples (100μl) were pipetted in triplicate into the 96-well 5mC coated plate and incubated at 37°C for 1 hour. Residual fluid was discarded and the wells were repeatedly washed, then 200μl of 5mC ELISA blocking buffer was added and incubated at 37°C for 30 minutes. The buffer was discarded and 100μl of anti-5-methylcytosine (1:2000) and secondary antibody (1:1000) were simultaneously added to the wells and incubated at 37°C for 1 hour. The wells were washed, then 100μl of horseradish peroxidase (HRP) developer was added and absorbance was measured every 5-10 minutes at 405nm using the Epoch Microplate Reader (Gen5 2.08 Software) to measure the color change (yellow / green to bluish/green). Absorbance values were averaged and the percentage of 5-methylcytosine was calculated ($\%5mC = e\{((absorbance - y\text{-}intercept) / slope)\}$) and multiplied by the fold

difference in CpG density of the E. coli derived standards (E. coli / pig 0.0747 / 0.0108 = 6.91). Values are reported as the percent of CpG methylation. Originally, we tried the Global DNA Methylation ELISA Kit (5'-methyl-2'-deoxycytidine Quantitation) (Cell Biolabs, #STA-380). However, our calculated sample values fell below the linear curve, which precluded proper calculation of global DNA methylation.

DNA Hydroxymethylation Enzyme-Linked Immunosorbent Assay (ELISA)

The Quest 5-hmC DNA ELISA Kit (Zymo, #D5426) kits was used to measure DNA hydroxymethylation levels in the pig brain samples using the sandwich method. The manufacturer's suggested protocol was followed, except for the addition of gentle rocking / agitation during all 37°C incubation steps. Briefly, plate wells were loaded with 1ng/µl of anti-5-hydroxymethylcytosine polyclonal antibody diluted in coating buffer and incubated at 37°C for 1 hour, then the wells were washed. Each well was filled with 200µl of 5mC ELISA buffer, then the plate was incubated at 37°C for 30 minutes. Control DNA (1ng) and purified sample DNA (1ng) in triplicate from each pig brain sample was heated at 98°C for 5 minutes, cooled on ice, then pipetted into each well and incubated at 37°C for 1 hour. The wells were washed, 100µl of anti-DNA antibody conjugated to HRP (1:100) was added and incubated at 37°C for 30 minutes, the wells were washed again, then 100µl of HRP developer was added, and absorbance was measured every 5-10 minutes at 405nm using the Epoch Microplate Reader (Gen5 2.08 Software) to monitor the color change. Absorbance values were averaged and the percentage of 5-hyroxymethylcytosine was calculated using the formula provided (%5-hmC = (absorbance – y-intercept) / slope). Values are reported as the percent of 5-hydroxymethylcytosine in reference to the control DNA (standards).

Immunohistochemistry

Paraffin-embedded brain samples from mice (anterior left hemisphere) and pigs (temporal and / or parietal cortices) were sectioned at a thickness of 5-6μm and mounted onto charged glass slides (Fisher Superfrost Plus #12-550-15, 25 X 75 X 1.0mm) then left to dry overnight. Sections were subjected to immunohistochemistry at room temperature unless otherwise stated. Optimal primary antibody concentration was determined by running a series of dilutions greater and less than the manufacturer's suggestions. See **Table 4.6** for antibody details, **Table 4.7** for specific immunostaining conditions and **Table 4.8** for recipes. Paraffin was melted at ~60°C for 25 minutes, and tissue samples were rehydrated through graded xylene and ethanol solutions. For antigen retrieval, slides were submerged in boiling buffer in a pressure cooker (Hamilton Beach, 37539C) for 20 minutes, then cooled in ddH$_2$0. Endogenous peroxidase was blocked with a 1:10 solution of 30% hydrogen peroxide (Fisher, H325-500) in methanol (Fisher, A433P-4) for 15 minutes. For the DNA cytosine modification antibodies, the tissue was incubated with 3N hydrochloric acid (HCl) (Fisher, #351278-212) for 15 minutes. The slides were then subjected to a 30-minute block with 10% goat (Jackson ImmunoResearch #005-000-121) or sheep (Jackson ImmunoResearch #013-000-121) serum (depending on the secondary antibody) in diluent (1% BSA in either 1X TBS or 1X PBS). Blocking solution was discarded and the primary antibody was applied for 2 hours, followed by washing (3X washing buffer #1, 1X buffer #2), application of the secondary antibody for 1 hour (1:300 dilution; biotin-conjugated streptavidin goat anti-rabbit, Jackson ImmunoResearch #111-065-144 or biotin-conjugated streptavidin sheep anti-mouse, Jackson ImmunoResearch #515-065-003), followed by washing, application of peroxidase-conjugated streptavidin for 45 minutes (1:300 dilution; Jackson ImmunoResearch #016-030-084), washing, and finally 1:10 dilution of 30% hydrogen

peroxide with 3,3' diaminobenzidine (DAB; Sigma, D5905) to develop the slides. The slides were counterstained with Harris hematoxylin solution, dehydrated through graded ethanol and xylene solutions, coverslipped with Permount (Fisher, SP15- 100 Toluene solution VN1294), and left to air dry overnight.

Specificity of Epigenetic Mark Antibodies

Selected anti-histone antibodies were tested for specificity using peptide interference to block all possible methyl modifications (e.g. for H3K4me3, peptides for H3K4me3, H3K4me2, H3K4me were used) and one acetyl modification (H3K27ac). Antibodies were prepared at the dilution used for immunostaining (**Table 4.7**). Peptide solution of an equal concentration (in µg/µL) was added. Because the IgG antibodies are ~150kD and the peptides are ~15kD (~100 amino acids), this allowed for a 10:1 molar concentration surplus of blocking peptide. The antibody-peptide solution was rocked gently for 30 minutes before being applied to the slides. The immunohistochemistry protocol was executed as described above.

Antibodies against H3K14ac, H3K27ac, H4K5ac, H4K12ac, H3K4me3, H3K27me3, H3K36me3, H3panAc, total histone H3, and total histone H4 were also tested via dot blot on nitrocellulose membrane (Bio-Rad #162-0146, Lot 9396). Peptides specific to the antibodies, peptides that might cross-react, as well as unmodified histone H3 and unmodified histone H4 were pipetted directly onto the nitrocellulose membrane (0.1, 0.5,1 or 2µg). The membrane was air dried for 5 minutes, then wrapped in foil and baked for 15 minutes at 50-60°C before following the same detection protocol used for Western blotting, starting at the blocking step. For the complete list of all peptides used, see **Table 4.9**.

Immunohistochemical Imaging and Semiquantitative Evaluation

Immunostained slides were imaged using a standard upright microscope (Olympus BX51TRF microscope; QImaging camera 32-0110A-568; MicroPublisher 5.0, Model LH100HG). Images were obtained at 40x, 200x, or 400x using QCapture (v2.8.1, 2001-2005, QImaging Corp.) software. Two semiquantitative scales were developed to estimate the proportion of immunoreactive nuclei (graded 4 to 0) (**Figure 4.7**) and the intensity of immunoreactivity (graded 3 to 0) (**Figure 4.8**). Morphologic features of nuclei were used as a surrogate for probable brain cell type (**Figure 4.9**). This is based upon the experience of the senior author (MRD), an experienced neuropathologist. The semiquantitative scale of proportion was validated by manual cell counting on photomicrographs produced at 200x magnification. The number of positive (any degree of brown) versus negative (blue stained) nuclei were counted in two morphologic criteria: large round nuclei (neurons) and smaller round to irregular nuclei (glial cells). The long narrow nuclei of endothelial and smooth muscle cells were excluded; we observed even at the zero time point that there was an inexplicable mix of positive and negative cells using almost all antibodies.

Quantitative analysis was applied to pig brain photomicrographs (all PMD time points) for all 6 histone acetylation marks. Nuclei with any detectable brown coloration were considered positive for determination of the proportion quantitation. Using Image J 1.52a software (National Institute of Health, USA), the perimeters of large nuclei were manually traced on photomicrographs taken at 400x magnification, and the mean intensity values were calculated. Results were graphed and compared to the semiquantitative intensity scale results. Note that the immunohistochemistry results did not have a complete 0 to 256 gray scale range because the hematoxylin has some color. Both the numeric and intensity results were found to be similar by

173

quantitative and semiquantitative analyses. The latter approach is much quicker and therefore suited for screening of major changes, but likely miss subtle differences. ImageJ intensity graph results are not shown.

Statistical Analysis

Statistical data were analyzed using JMP 13 software (SAS Institute Inc.; Cary NC) and the Data Analysis Tab in Microsoft Excel (Office Professional Plus 2016). Descriptive statistics were generated using Microsoft Excel to produce 95% confidence intervals. ELISA data, which are parametric, were subjected to a 2-sample t-test assuming unequal variance. Two-tailed p-values were reported; $p < 0.05$ was considered significant. Western blot densitometry data, and semiquantitative (proportion and intensity) immunohistochemistry rank assessments are non-parametric and therefore were subjected to a Wilcoxon / Kruskal-Wallis Rank sums test ($p < 0.05$). For mouse brain data (immunohistochemistry), all ages were pooled. Immunohistochemistry quantitative (counts) data were subjected to a 2-sample t-test assuming unequal variance; one-tailed p-values ($p < 0.05$) are reported.

RESULTS

DNA Integrity

Purified DNA from the 7 pig brains (frontal cerebrum) electrophoresed on 0.8% agarose gels showed no smearing (i.e. no fragmentation) of the >23,130 base pair bands at any of the 4 PMD time points (**Figure 4.10**). Note that 20 – 48% degradation of pig brain DNA has been previously reported after 120 hours post-mortem (Rhein, Hagemeier, Klintschar, et al., 2015).

DNA Methylation and Hydroxymethylation

ELISA results for 5-methylcytosine (5mC) and 5-hydroxymethylcytosine (5hmC) are shown in **Figure 4.11**. The percentage of 5mC in normoxic pig brain frontal cortex was approximately 8%, which coincides with previous reports of ~4% in adult mouse cerebral cortex and ~3% in newborn mouse hippocampus (Globisch, Münzel, Müller, et al., 2010; Münzel, Globisch, Brückl, et al., 2010). The percentage of 5mC was stable up to 72 hours post-mortem, with no statistically significant changes across PMD time points. This is consistent with a recent study of methylated CpGs in post-mortem pig and human brain (Rhein, Hagemeier, Klintschar, et al., 2015). The percentage of 5hmC in pig brain was approximately 0.45%, which coincides with prior reports of ~0.6% in adult mouse cortex and ~0.35% in newborn mouse hippocampus (Globisch, Münzel, Müller, et al., 2010; Münzel, Globisch, Brückl, et al., 2010). The percentage of 5hmC also remained stable for at least 72 hours PMD. Both 5mC and 5hmC levels were slightly higher in hypoxic pigs at 48 hours (5mC; $p<0.05$) and at 0 and 24 hours (5hmC; $p<0.05$) (**Figure 4.11**).

Antibody Specificity

Some histone PTM antibodies can cross react with histone PTMs other than their advertised specificity. In particular, the multiple methylation modifications on lysine residues might not be entirely distinguished. Selected antibodies were evaluated for specificity using peptide blocking immunohistochemistry and with dot blot. By immunohistochemical staining, anti-H3K27ac was appropriately blocked by its corresponding peptide (**Figure 4.12**). Of the 5 histone methylation antibodies, only anti-H3K27me3 and anti-H3K36me3 showed the expected patterns of blocking (**Table 4.10**). Both H3K4me3 antibodies were blocked by various peptides. Note that a similar lack of specificity has been previously reported for H3K4me3 (Kundakovic, Jiang, Kavanagh, et al., 2017). Anti-H3K27me2 was not blocked by its corresponding peptide.

Antibodies tested via dot blot showed similar results (**Table 4.11, Figure 4.13**). Antibodies to total histone H3, H3panAc, H3K27me3, H3K14ac, H3K27ac and H4K5ac bound only their respective peptides. Anti-H4K12ac bound its corresponding peptide strongly and H4K5ac weakly. Anti-H3K4me3 bound all peptides blotted on the membrane. Anti-H3K36me3 bound the majority of the peptides. Anti-H3K27me2 bound all but one peptide. Anti-total H4 bound none of the peptides, but it did bind calf thymus total histone mix.

Histone Integrity

In pig brain, total histone H3 and histone H4 levels were stable up to 72 hours post-mortem (**Figure 4.14** and **4.16**). H3K4me3 and H3K27me3 histone methylation modifications also remained stable up to 72 hours post-mortem, while H3K36me3 showed a decline by 48 hours (p<0.05) (**Figure 4.15** and **4.16**). Histone acetylation tended to decline by 24 hours PMD and was significantly reduced by 48 hours (**Figure 4.15** and **4.16**). The quantities of all histone

PTMs were higher in normoxic pig brain than in hypoxic pig brain except for H3K36me3, but this was not statistically significant (results not shown). For an example of full western blot images, see **Figure 4.17**.

Post-Mortem Stability of Immunoreactivity

Among both pig and mouse brain samples, DNA cytosine modifications, all histone methylation PTMs, H3K14ac, H4K5ac, and total histone H4 showed stable immunoreactivity up to 72 hours post-mortem (**Figures 4.18-4.20, and 4.22**). In pig brain (temporal and parietal cortices), H3K9ac was stable up to 48 hours post-mortem (**Figure 4.21 and 4.23**). H3K27ac, H4K12ac, H4K16ac, and total histone H3 were stable up to 24 hours post-mortem (**Figures 4.21 and 4.23**). In mouse dentate gyrus, H4K5ac showed a downward trend (not statistically significant) with increasing PMD (**Figure 4.24**). H3K9ac was stable up to 48 hours post-mortem (**Figure 4.24**). H3K27ac, H4K12ac and H4K16ac were stable only up to 24 hours post-mortem (**Figure 4.24**).

In pig brain temporal and parietal cortices, the (semiquantitative) proportion of cells labeled with antibodies to DNA cytosine modifications, all histone methylation PTMs, H3K14ac, H4K12ac, and total histone H4 appeared stable up to 72 hours post-mortem (**Table 4.12; Figures 4.18-4.22** and **4.25**). Total histone H3 declined after 48 hours post-mortem in all cell types (**Table 4.12**; **Figures 4.22** and **4.25**). H3K9ac and H3K27ac were stable up to 24 hours; thereafter loss of staining was observed in large neuronal nuclei (**Table 4.12; Figure 4.21** and **4.25**). H4K5ac and H4K16ac had already declined by 24 hours in neuronal nuclei (**Table 4.12; Figure 4.21** and **4.25**).

Where the semiquantitative evaluation indicated changes in the immunohistochemical detection of PTMs, a quantitative evaluation was used to validate the results (**Figure 4.26**). On images of pig neocortex, the intensity of nuclear immunoreactivity was measured and the proportions of immunoreactive cells were counted in two morphologic populations: large round nuclei (neurons) and smaller round to ovoid nuclei (glial cells and small interneurons; elongated nuclei of endothelial and smooth muscle cells were excluded). Because DNA cytosine modifications and histone methylation PTMs are stable up to 72 hours post-mortem, we did a quantitative validation for only 5mC and H3K27me3. With 5mC immunostaining, neither cell population exhibited differences over progressive PMD. H3K27me3 immunostaining showed a small but statistically significant decrease in neurons at 48 hours post-mortem. Among the acetyl marks H3K9ac, H3K27ac and H4K12ac, statistically significant decreases were seen in neurons, but not in glial cells. H4K5ac demonstrated decreases in both neurons and glia by 24 hours post-mortem. H3K14ac and H4K16ac were expressed at very low levels in neurons to begin with. Statistically significant post-mortem decreases of these two marks were demonstrated in glial nuclei.

Reflecting their cell maturation-dependent state, regional localization of most epigenetic marks differed between the three age groups of mice (**Figures 4.18, 4.20,** and **4.22**). However, with respect to post-mortem stability, immunostaining of mouse brains yielded essentially the same result as the pig brains. The three age groups showed similar patterns of stability and were therefore pooled for analysis. DNA cytosine modifications, histone methylation, H3K14ac and H4K12ac were stable from 0 to 72 hours post-mortem (**Figures 4.18, 4.20** and **4.27**). Total histone H3 and H4 declined after 48 hours (**Figure 4.22 and 4.27**); the loss did not appear to be cell type specific (**Table 4.13**). H3K9ac and H3K27ac were stable up to 24 hours post-mortem

178

(**Figure 4.27**); after that, loss of immunoreactivity was seen in large neurons (**Table 4.13**).

H4K5ac and H4K16ac declined by 24 hours in large neurons (**Figure 4.27** and **Table 4.13**). A

limited analysis of 96 hour PMD was conducted on two ~13-week-old mouse brains.

Immunoreactivity for 5mC, 5hmC, 5fC, 5caC, H3K4me3, H3K27me3, and H3K36me3 was

unaltered. There was a slight decrease in the intensity of H3K9me2,K9me3 and H3K27me2

immunoreactivity.

There were no differences in the pig brain samples cooled after 6-8 hours at room

temperature compared to those cooled immediately (results not shown). There were no obvious

differences between normoxic and hypoxic pig brains (results not shown). Of the 15 epigenetic

modifications assessed by immunostaining for over fixation (using the 24-hour post-mortem pig

brain samples), 8 were slightly affected by over fixation. H3K27ac and H4K5ac started to show

minor decreases in immunoreactivity if stored for 5 weeks in formalin prior to paraffin

embedding. H3K9ac and H3K14ac started to show minor decreases in immunoreactivity when

fixed for 6 weeks. 5mC, 5hmC, H3K9me2/K9me3, and H3K27me2 started to show changes

when fixed for 12 weeks. Overall, the minor decrease in immunoreactivity was primarily seen in

large neuronal nuclei.

Human Brain Tissue Microarray

The two surgical samples (temporal cortex), which were fixed <1 hour after

devitalization, exhibited strong immunoreactivity using all epigenetic modification antibodies. In

the autopsy samples (frontal cortex), almost all epigenetic modifications tested were stable up to

4 days post-mortem. Acetyl marks H3K9ac, H3K27ac, H4K5ac and H4K12ac showed

apparently greater stability in human brain than in pig and mouse brain. Sample 12 exhibited a

decline in immunoreactivity for all six acetylation marks. The body of the deceased had been at room temperature for ≤2 days before being stored at 4°C for 3 days prior to autopsy. The two samples from brains with hypoxic damage showed minor decreases in intensity and proportion of positive cells in all but four epigenetic modifications (5fC, H3K27me3, H4K5ac and H4K12ac) (**Figure 4.28** and **Table 4.14**).

DISCUSSION

A summary of the immunohistochemical labeling stability of epigenetic modifications is shown in **Table 4.15**. Overall, we conclude that DNA cytosine and histone methylation modifications are stable ≥48 hours and usually ≥72 hours post-mortem in human, pig, and mouse brain. By contrast, histone acetylation modifications are generally not stable with increasing post-mortem delay. Furthermore, immunohistochemistry seemed to be more sensitive than Western blotting for detection of H3K9ac, H3K27ac, H4K5ac and H4K12ac.

Although we found that DNA, DNA methylation, and DNA hydroxymethylation were stable ≥72 hours post-mortem, other studies have indicated that some degradation can occur earlier. In a comet assay of cells isolated from the brains of mice that were killed and stored at room temperature, DNA degradation was apparent at 6 hours and progressed to substantial levels by 72 hours (Zheng, Li, Shan, et al., 2012). In a study of pig brains that remained in the skull at room temperature until the desired PMD time points were reached, up to 48% of DNA was degraded by 120 hours post-mortem, and there was increased variance in DNA methylation (Rhein, Hagemeier, Klintschar, et al., 2015). In a study of neonatal and adult rat cerebellum left at room temperature for 0, 5, and 9 hours post-mortem, there was a significant decrease in global 5mC at 9 hours in the adult brains ($2.9 \pm 0.7\%$ vs. $3.7 \pm 0.6\%$ in control), but no change in the neonates (Sjöholm, Ransome, Ekström, et al., 2017). Not surprisingly, storage at cool temperature after death is an important factor, possibly because enzyme kinetics associated with autolysis are slowed.

We must explain the post-mortem degradation of histone acetylation modifications. The main enzymes involved in the removal of acetyl groups from lysine residues are histone deacetylases (HDAC) and sirtuins. Sirtuins are NAD+-dependent nuclear proteins, therefore

when energy production by mitochondria ceases after death, sirtuins are rendered inactive (Zakhary, Ayubcha, Dileo, et al., 2010). In mouse brain, HDAC 1 and 2 are the most prevalent, HDAC 3, 4 and 5 moderately so, and HDAC 6 is of low abundance [25]. In human frontal cortex, HDACs 1, 2, 5, and 6 are present, with HDAC2 the most highly expressed and HDAC5 the least (Anderson, Chen, Wang, et al., 2015). In rat hippocampus, during the first postnatal week HDAC2 is predominantly nuclear, and then appears in neuronal cytoplasm (Hou, Gong, Bi, et al., 2014). In young adult and 12-month-old mouse cingulate cortex and hippocampus, HDACs 1, 2 and 3 are present in neurons and astrocytes; in the aging brain, they move from being primarily cytoplasmic to nuclear (Baltan, 2012). We postulate that increased post-mortem permeability of nuclear membranes allows cytoplasmic HDACs to enter the nucleus, creating an environment for nonspecific deacetylation of histones. Another possible explanation for the post-mortem loss of immunostaining is nonspecific block of the epitope by something liberated by autolysis.

The reason why some acetylation PTMs are more stable than others is unclear. On mammalian histone H3, acetylation is sequential with lysine 14 acetylated before lysine 23, 18, and 9 (Turner, 1991). We observed that H3K14ac was most stable, particularly in glial cells. On histone H4, lysine 16 is acetylated before 8 and 12, and 5 (Turner, 1991). We observed that H4K5ac had less PMD stability than H4K12ac and H4K16ac. It is possible that post-mortem deacetylation of histone PTMs occurs in the reverse order of their post-translational addition. Loss of immunostaining was observed mainly in neurons with relative preservation of all epitopes in the nuclei of glial cells. This might be explained by the amounts of the HDACs present in the different cell types. In rat brain, HDAC 2, 3, 5, and 11 expression is high in neurons, moderate in oligodendrocytes, and low in astrocytes (Baltan, Bachleda, Morrison, et al.,

182

2011; Broide, Redwine, Aftahi, et al., 2007; MacDonald, & Roskams, 2008; Michael J. Morris, & Monteggia, 2013; Murko, Lagger, Steiner, et al., 2010).

Histone methylation was generally stable. Demethylation by histone lysine demethylases (HDM) is dependent on oxygen delivery to flavin-adenine dinucleotide and therefore unlikely to occur in dead tissue (Kong, Ouyang, Liang, et al., 2011). HDMs tend to be specific with regard to the type of histone lysine residue they will demethylate (Thinnes, England, Kawamura, et al., 2014). The selectivity of HDMs might explain the relative lack of post-mortem change.

In contrast to pig and mouse brain where H4K5ac labelling diminished after 1-day post-mortem, H4K5ac labelling persisted in the human brain samples even at 4-5 days post-mortem. This might be a chance observation in the small number of human samples. This might also reflect upon the specificity of the antibodies, which were raised against human epitopes; however, core histone proteins H3 and H4 are highly conserved in mammals. Another possibility is the different agonal states between humans (the subjects died under various circumstances) and animals (which were anesthetized very briefly for euthanasia). In rodents, single brief (e.g. 20 minutes) or long (e.g. 2 hours daily) exposures to sevoflurane or isoflurane anesthesia have been shown to promote hypermethylation of certain genes in brain; however, this is seen at the earliest 6 hours after exposure (Ju, Jia, Sun, et al., 2016; Pekny, Andersson, Wilhelmsson, et al., 2014). A 1-hour long exposure to sevoflurane decreased histone acetylation levels of the circadian rhythm gene Period2 (*Per2)* in the mouse suprachiasmatic nucleus (Mori, Iijima, Higo, et al., 2014). Artifact related to tissue oxidization cannot be excluded; the human tissue array slides were subjected to immunohistochemistry <24 hours after being prepared, whereas the pig and mouse slides were cut and stored for 1-12 weeks before use (Andeen, Bowman, Baullinger, et al., 2017). Another possible explanation is the baseline level of HDACs in developing brain

versus mature brain; we studied young pigs and mice, but the human samples were derived largely from middle age individuals (Michishita, Park, Burneskis, et al., 2005).

Although changes related to hypoxia were not a primary outcome measure in this study, the donated neonatal pig brain samples were from a well-controlled experiment, and so they deserve a brief comment. In hypoxic pig brain samples, ELISAs showed higher levels of 5mC and 5hmC and Western blots showed lower levels H4K5ac, H4K12ac, H3K4me3 and H3K27me3, and slightly higher levels of H3K36me3. The two hypoxic samples in the human brain microarray showed overall decreases in the intensity of immunoreactivity for most epigenetic marks, which likely reflects cell compromise. In general, decreases in histone H3 and H4 acetylation and increases in DNA methylation have been reported in the context of experimental cerebral ischemia (Miao, He, Xin, et al., 2015; Schweizer, Meisel, & Märschenz, 2013), global hypoxia (Biswal, Das, Barhwal, et al., 2017), and in cultured cells subjected to hypoxia (Johnson, Denko, & Barton, 2008; Mariani, Vasanthakumar, Madzo, et al., 2014; Xia, Lemieux, Li, et al., 2009).

The shortcomings to this study are primarily technical. We cannot fully explain why the post-mortem stability of histone PTMs in pig brain appears to differ between immunohistochemical detection and Western blotting methods. Formalin fixation arrests protein changes quickly and immunohistochemistry allows regional and subcellular evaluation of antibody binding patterns. Isolation of nuclei from frozen preceded Western blotting; the histone purification procedures might be associated with some artifactual changes despite the inclusion of protease inhibitors. The brain regions assessed also differed; frontal cerebrum was used for Western blot and temporal/parietal cortex was used for immunostaining. Differences in the antibody incubations likely do not explain the discrepancy. We did not test all anti-histone

antibodies with multiple peptides to fully evaluate blocking in immunohistochemistry and specificity in dot blot. Some antibodies targeting specific histone marks (e.g. H4K5ac, H3K27ac) showed more widespread immunoreactivity than the "total" histone H3 and H4 antibodies, the opposite of what one would expect. The discrepancy on immunoreactivity means that use of the "total histone" H3 or H4 antibodies to normalize Western blots might not be entirely reliable. However, despite these uncertainties about the specificity of some of the antibodies, and the differences between assay results, our general conclusions about post-mortem stability remain valid. This type of study, however, only shows where broad changes occur; gene-specific epigenetic changes are not shown and might mask the sum of increases and decreases in the broader epigenome.

In conclusion, epigenetic studies on post-mortem brain tissue are feasible, and may be helpful to understand the pathogenesis of many neurodevelopmental and neurodegenerative diseases. We recommend that the post-mortem stability of the epigenetic marks be predetermined if human autopsy brain tissue is to be studied. The apparent stability might be dependent on the method of detection, the tissue species, the brain region analyzed, the brain cell type, and the antibodies themselves. Caution is especially needed when interpreting histone acetylation results; degradation was evident in the animal tissues by <24 hours in some cases, although there appeared to be relatively greater stability in the small number of human specimens studied. Ideally, the samples of interest should have a PMD time of ≤48 hours, but in some circumstances (e.g. where tissue samples are rare), ≤72 may be reasonable. In theory, affected and control samples should be matched for age, sex, and PMD. Many anti-histone PTM antibodies remain to be validated. Comparison of developing, mature, and aged subjects, and verification of the post-mortem stability of histone PTMs using gene-specific molecular

techniques such as ChIPseq and DNA cytosine modifications via bisulfite conversion would be

valuable.

Figure 4.1: Pig brain dissection. Lines on the photograph show the dissection planes used to divide the pig brain into samples used for formalin fixation and subsequent immunohistochemical staining (white) or freezing at -70˚C and subsequent biochemical analyses (yellow).
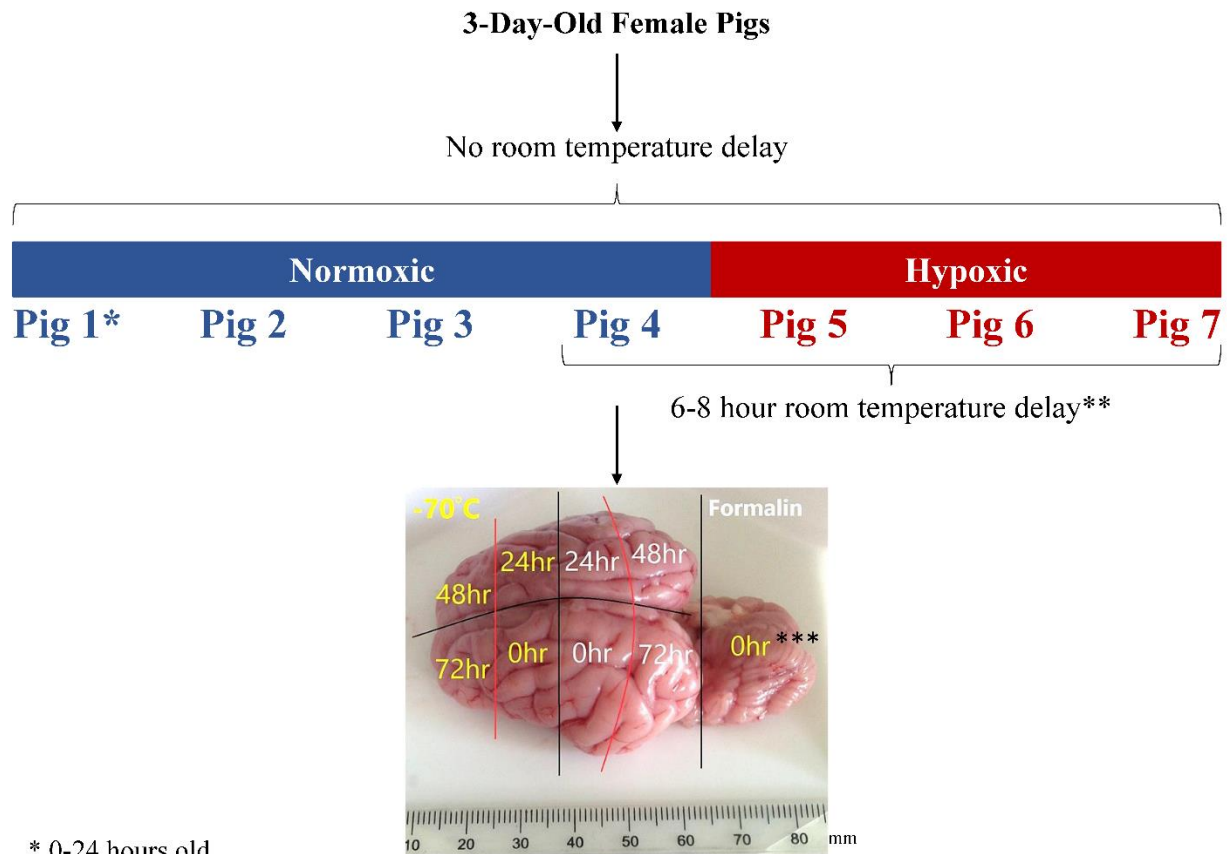
* 0-24 hours old
** each post-mortem delay brain section was further cut into 2; one section had no room temperature delay and the other had a room temperature delay
*** the cerebellum and brainstem were removed and frozen as practice tissue from assay optimization

Figure 4.2: Photograph showing pig brain sample sections that were stored at 4°C until their designated post-mortem delay time point.

Table 4.1: Paint colours used to colour the tissue before being processed and embedded in paraffin.

Colour	Product Name	Number	Porcine	Murine
Red	Koh-I-Noor	0728-4	0h	0h
Light Green	Koh-I-Noor	9065-4	24h	n/a
Orange	Koh-I-Noor	0728-6	48h	n/a
Yellow	Cancer Diagnostic CDI	0728-5	24h*	24h*
Red Violet	Koh-I-Noor	9065-4	48h*	48h*
Super Black	Speedball India Ink	3398	72h*	72h*
No colour	n/a	n/a	72h	n/a

* there was a 6-8 hour room temperature delay before being placed at 4°C

Figure 4.3: Photograph showing coloured PMD pig brain samples embedded in paraffin blocks.
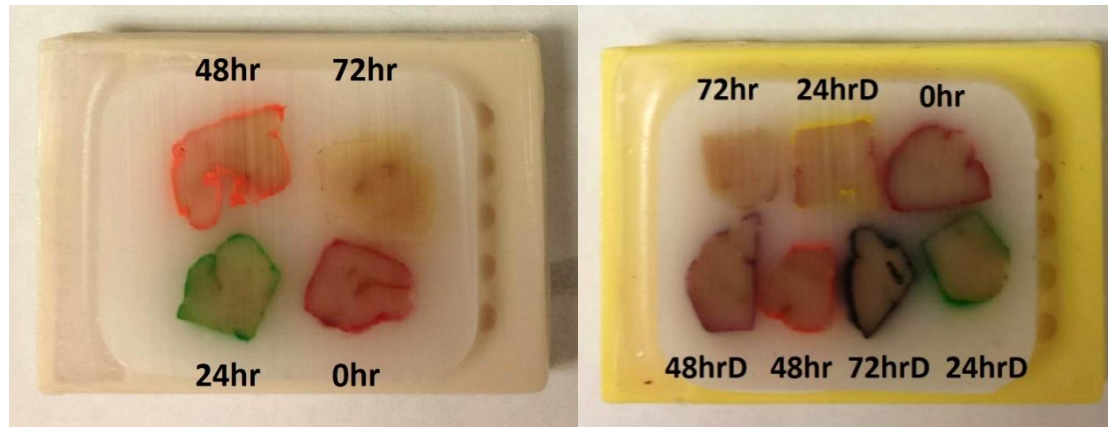
Table 4.2: Pig brain sample details.

Brain	Oxygen	Age	Sex	Body Weight	Brain Weight (g)	Time of Death	Time of Autopsy	Post-mortem delay (PMD) in hours						
								0hrs	24hrs	48hrs	72hrs	Delayed** 24hrs	Delayed** 48hrs	Delayed** 72hrs
1	Normoxic	8-24 hours	F	1.2-1.4kg	n/a	9:50am	10:15am	✓	✓	✓	✓	·	·	·
2	Normoxic	3 days	F	1.7-2kg	35.63g*	9:30am	9:40am	✓	✓	✓	✓	·	·	·
3	Normoxic	3 days	F	1.7-2kg	34.33g*	10:20am	10:30am	✓	✓	✓	✓	·	·	·
4	Normoxic	3 days	F	1.7-2kg	35.38g	10:01am	10:06am	✓	✓	✓	✓	✓	✓	✓
5	Hypoxic	3 days	F	1.6kg	30.95g	10:20am	10:25am	✓	✓	✓	✓	✓	✓	✓
6	Hypoxic	3 days	F	1.6kg	30.83g	10:21am	10:27am	✓	✓	✓	✓	✓	✓	✓
7	Hypoxic	3 days	F	1.4kg	31.66g	9:46am	9:50am	✓	✓	✓	✓	✓	✓	✓

*Brain was transported from animal care to the lab in 1X PBS before being weighed. The walk from building to building was approximately 15mins.
**brain sections received a 7hr room temperature delay before being placed at 4°C for the remainder of the PMD time point

Figure 4.4: Mouse brain dissection. The left brain hemisphere was used for formalin fixation (FFPE) and subsequent immunohistochemical staining and the right hemisphere for freezing at -70˚C.
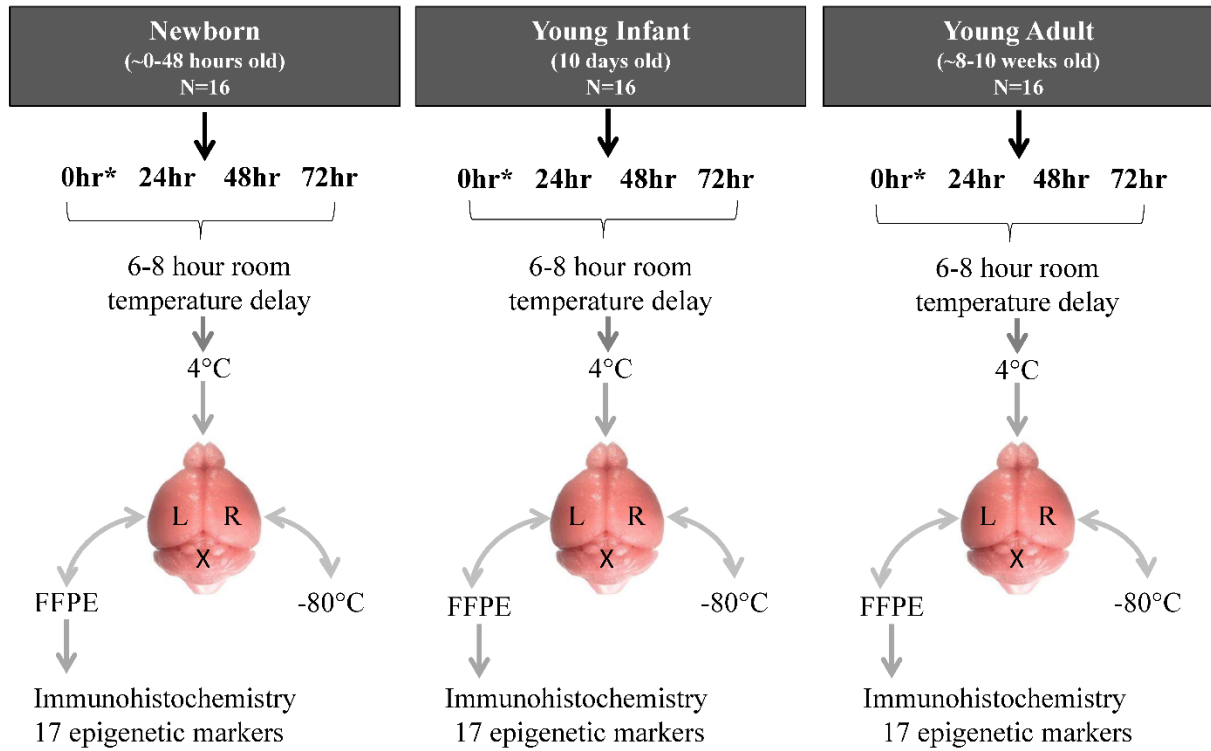
*0 hour time point was processed immediately
The cerebellum was removed and discarded which is represented by an "X"
FFPE = Formalin-fixed paraffin-embedded

Figure 4.5: Photograph showing coloured mouse brain samples embedded in paraffin blocks.
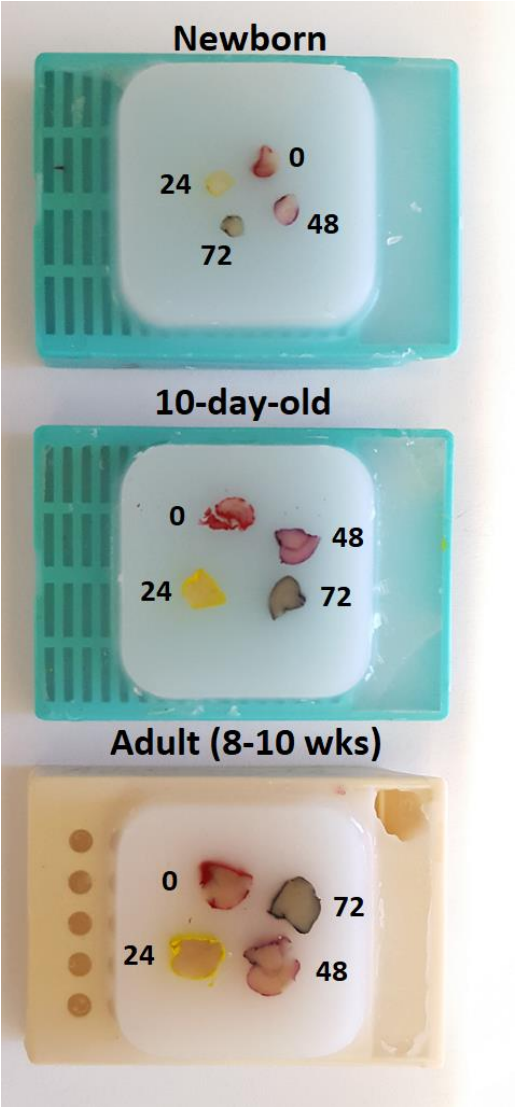
Table 4.3: Mouse brain sample related details for PMD study (N=50).

Mouse #	Age	Sex	Body weight (g)	Fresh Brain Weight (g)*	Left Hemisphere (g)	Time of Death & Autopsy	Room Temp Delay (hours)	PMD Time point (hours)
1	Adults 8-10 weeks	Male	41.0g	0.46g	0.15g	10:08am	7 hours	0hr
2		Male	35.16g	0.49g	0.18g	10:40am		24hr
3		Male	38.2g	0.47g	0.18g	11:15am		48hr
4		Male	34.7g	0.48g	0.15g	11:45am		72hr
5	Adults 8-10 weeks	Male	44.3g	0.42g	0.15g	10:20am	6.5 hours	0hr
6		Male	40.68g	0.48g	0.17g	10:35am		24hr
7		Male	36.82g	0.49g	0.19g	10:55am		48hr
8		Male	40.38g	0.55g	0.19g	11:09am		72hr
9	Adults 8-10 weeks	Female	33.98g	0.47g	0.17g	9:10am	7 hours	0hr
10		Female	32.1g	0.5g	0.18g	9:25am		24hr
11		Female	38.46g	0.44g	0.17g	9:39am		48hr
12		Female	31.6g	0.5g	0.19g	10:00am		72hr
13	Adults 8-10 weeks	Female	41.3g	0.51g	0.18g	10:20am	6 hours	0hr
14		Female	32.3g	0.5g	0.17g	10:35am		24hr
15		Female	34.6g	0.51g	0.17g	10:53am		48hr
16		Female	31.2g	0.52g	0.18g	11:12am		72hr
1	Infants 10 days	Male	8.32g	0.36g	0.14g	8:53am	8 hours	0hr
2		Male	8.47g	0.32g	0.10g	9:02am		24hr
3		Male	8.36g	0.33g	0.12g	9:16am		48hr
4		Male	8.53g	0.35g	0.11g	9:35am		72hr
1	Dam ~13 weeks	Female	41.64g	0.47g	96hr - 0.08g	9:45am	2.5 hours	96hr
					120hr - 0.08g			120hr
2	Dam ~13 weeks	Female	46.6g	0.50g	96hr - 0.06g	11:20am	6 hours	96hr
					120hr - 0.08g			120hr
5	Infants 10 days	Male	6.6g	0.34g	0.15g	9:23am	7.5 hours	0hr
6		Male	6.7g	0.33g	0.13g	9:36am		24hr
7		Male	6.8g	0.35g	0.14g	9:44am		48hr
8		Male	6.6g	0.35g	0.13g	9:54am		72hr
9	Infants 10 days	Female	6.82g	0.32g	0.12g	10:06am	7 hours	0hr
10		Female	5.94g	0.29g	0.12g	10:16am		24hr
11		Female	6.86g	0.34g	0.13g	10:24am		48hr
12		Female	6.54g	0.29g	0.12g	10:34am		72hr
13	10 days	Female	6.92g	0.33g	0.11g	10:40am	6.5 hours	0hr
14		Female	5.82g	0.33g	0.12g	10:55am		24hr
15		Female	7.09g	0.34g	0.13g	11;00am		48hr
16		Female	5.95g	0.32g	0.14g	11:11am		72hr
1	Newborns 0-24 hours	Male	1.78g	0.10g	0.03g	10:06am	7 hours	0hr
2		Male	1.57g	0.08g	0.03g	10:21am		24hr
3		Male	1.82g	0.09g	0.03g	10:34am		48hr
4		Male	1.70g	0.06g	0.03g	10:43am		72hr

Mouse #	Age	Sex	Body weight (g)	Fresh Brain Weight (g)*	Left Hemisphere (g)	Time of Death & Autopsy	Room Temp Delay (hours)	PMD Time point (hours)
5	Newborns 0-24 hours	Male	1.71g	0.09g	0.04g	10:50am	7 hours	0hr
6		Male	1.62g	0.06g	0.02g	11:00am		24hr
7		Male	1.73g	0.10g	0.02g	11:06am		48hr
8		Male	1.74g	0.08g	0.03g	11:11am		72hr
9	Newborns 0-24 hours	Female	1.54g	0.09g	0.03g	11:17am	7 hours	0hr
10		Female	1.70g	0.07g	0.02g	11:22am		24hr
11		Female	1.59g	0.08g	0.02g	11:28am		48hr
12		Female	1.48g	0.09g	0.04g	11:33am		72hr
13	Newborns 0-24 hours	Female	1.58g	0.08g	0.03g	11:39am	7 hours	0hr
14		Female	1.64g	0.10g	0.04g	11:45am		24hr
15		Female	1.56g	0.10g	0.03g	11:52am		48hr
16		Female	1.40g	0.09g	0.02g	11:57am		72hr

Table 4.4: Human brain tissue microarray - case details and construction. Sample 1 (cerebellum) is for orientation only. Samples 2 and 3 (temporal cortex) were obtained from routine neurosurgical specimens. All autopsy cases were handled in the routine manner with storage of the body at 4˚C beginning ~4-8 hours after death; case 12 is the exception with the body remaining at room temperature 1-2 days prior to cooling. During autopsy, brains were removed and placed in formalin whole within 30 minutes.

Slide Position	Brain region	Age / sex	Description (a)	Delay between tissue death & fixation	Fixation duration
1	Cerebellum	17y, male	Autopsy - normal	24 hours	4 days
2	Temporal cortex	72y, male	Normal tissue adjacent to tumor	<1 hour	1 days
3	Temporal cortex	12y, male	Normal tissue adjacent to hippocampus removed for epilepsy procedure	<1 hour	1 days
4	Frontal cortex	66y, female	Autopsy - normal	6 hours	14 days
5	Frontal Cortex	17y, male	Autopsy - normal	24 hours	4 days
6	Frontal Cortex	8m, male	Autopsy - normal (sudden infant death)	26 hours	8 days
7	Frontal Cortex	42y, male	Autopsy - severe hypoxia (cardiac arrest) + 7 day survival before death	31 hours	19 days
8	Frontal Cortex	53y, male	Autopsy - severe hypoxia + 2 day survival before death	43 hours	19 days
9	Frontal Cortex	10m, male	Autopsy - normal (sudden infant death)	52 hours	2 days
10	Frontal Cortex	15y, female	Autopsy - normal	53 hours	1 days
11	Frontal Cortex	21y, male	Autopsy - normal	3 days	17 days
12	Frontal Cortex	61y, male	Autopsy - no antemortem pathology; body partially decomposed with deep brain putrefaction	3 days +	18 days
13	Frontal Cortex	17y, male	Autopsy - acute brain trauma with immediate death - uninvolved brain	4 days	2 days
14	Frontal Cortex	76y, female	Autopsy - Alzheimer disease	5 days	55 days

Slide layout

194
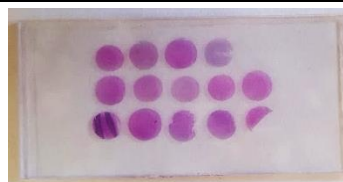
Figure 4.6: Sodium dodecyl sulfate–polyacrylamide gel electrophoresis (SDS-PAGE) stained with Coomassie after transfer of histone proteins to PVDF membrane. After transfer, the membrane was divided (represented by the dotted line); the left membrane received antibodies targeting histone PTMs while the right membrane received antibodies targeting total histone H3 or H4. "L" represents the molecular size ladder, "B" is a blank lane, 0-72 indicate the PMD time point (hours), +C represents the positive control (histone mix from calf thymus).
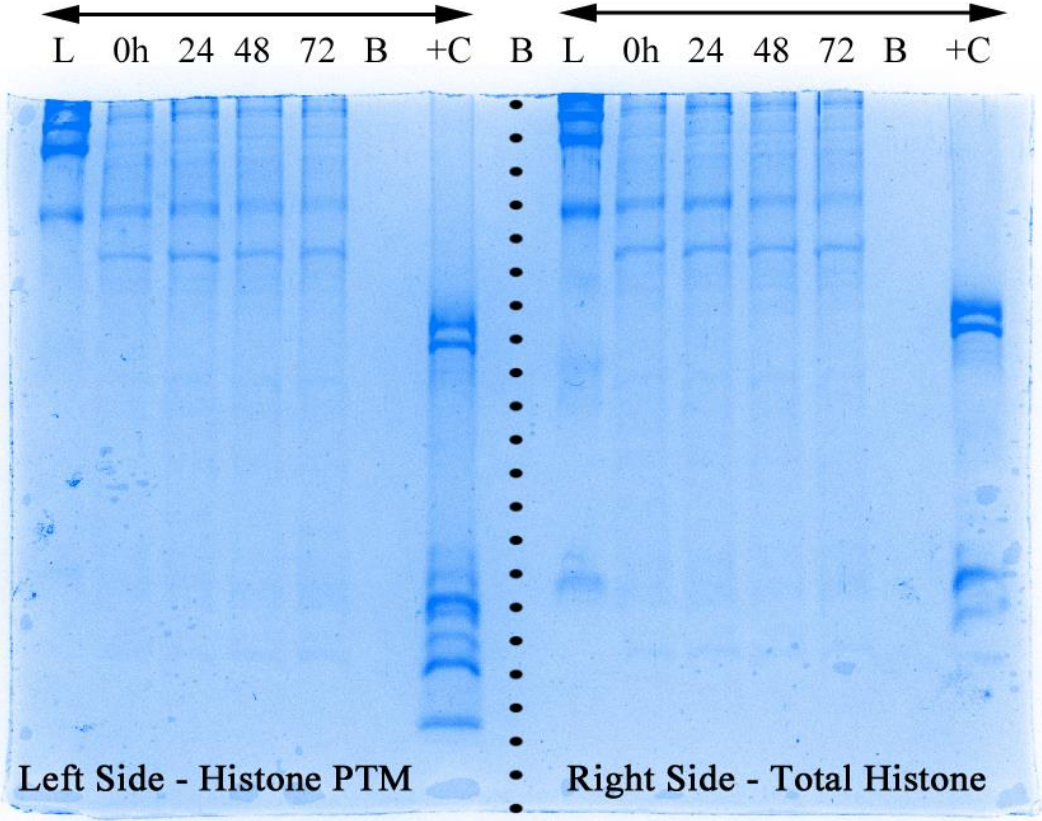
Table 4.5: Epigenetic mark antibody details and sources.

Antibody	Details	Isotype	Species	Type	Company Details	Lot #
5mC	Clone 33D3 recognizes the modified base 5-methylcytidine found in plant and vertebrate DNA.	IgG	Mouse	Monoclonal	Active Motif, #39649	8614012 24516019
5hmC	Raised against 5-hydroxymethylcytidine conjugated to KLH and recognizes 5-hydroxymethylcytosine.	Serum	Rabbit	Polyclonal	Active Motif, #39769	10210001 06116002
5fC	Raised against 5-formylcytidine conjugated to KLH and recognizes 5-formylcytosine.	Serum	Rabbit	Polyclonal	Active Motif, #61223	34711001
5caC	Raised against 5-carboxylcytidine conjugated to KLH and recognizes 5-carboxylcytosine.	Serum	Rabbit	Polyclonal	Active Motif, #61225	32115002
H3K4me3	Raised against a peptide including trimethyl-lysine 4 of histone H3.	Serum	Rabbit	Polyclonal	Active Motif, #39159	12613005
H3K4me3	Synthetic peptide within Human Histone H3 aa 1-100 (tri methyl K4) conjugated to Keyhole Limpet Haemocyanin (KLH). The exact sequence is proprietary.	IgG	Rabbit	Polyclonal	Abcam, #ab8580	GR144288-1 GR224369-1 GR240214-4
H3K9ac	Synthetic peptide corresponding to Human Histone H3 aa 1-100 (N terminal) (acetyl K9) conjugated to Keyhole Limpet Haemocyanin (KLH).	IgG	Rabbit	Polyclonal	Abcam, #ab10812	GR287797-1
H3K9me2, K9me3	Synthetic peptide within Human Histone H3 aa 1-100 (tri methyl K9). The exact sequence is proprietary.	IgG1	Mouse	Monoclonal	Abcam, #ab71604	GR117765-1
H3K14ac	Synthetic peptide within Human Histone H3 (acetyl K14). The exact sequence is proprietary.	IgG	Rabbit	Monoclonal	Abcam #ab52946	GR149741-17 GR149741-20 GR302893-8
H3K27ac	Synthetic peptide corresponding to Human Histone H3 aa 1-100 (acetyl K27) conjugated to Keyhole Limpet Haemocyanin (KLH).	IgG	Rabbit	Polyclonal	Abcam, #ab4729	GR81163-1 GR288020-1
H3K27me2	Synthetic peptide corresponding to Human Histone H3 aa 1-100 (N Terminal) (di methyl K27) conjugated to Keyhole Limpet Haemocyanin (KLH).	IgG	Rabbit	Polyclonal	Abcam, #ab24684	GR31501-6 GR31501-1

Antibody	Details	Isotype	Species	Type	Company Details	Lot #
H3K27me3	Synthetic peptide within Human Histone H3 aa 1-100 (tri methyl K27) conjugated to keyhole limpet haemocyanin (Sulfosuccinimidyl 4-N-maleimidomethyl-cyclohexane-1-carboxylate (Sulfo-SMCC)). The exact sequence is proprietary.	IgG fraction	Mouse	Monoclonal	Abcam, #ab6002	GR218433-5 GR275911-1 GR275911-2 GR275911-7
H3K36me3	Synthetic peptide within Human Histone H3 aa 1-100 (tri methyl K36) conjugated to Keyhole Limpet Haemocyanin (KLH). The exact sequence is proprietary.	IgG	Rabbit	Polyclonal	Abcam, #ab9050	GR249065-1 GR3177961-1
H4K5ac	Synthetic peptide within Human Histone H4 aa 1-100 (N terminal) (acetyl K5). The exact sequence is proprietary.	IgG	Rabbit	Monoclonal	Abcam, #ab51997	GR295999-2 GR295999-7
H4K12ac	Synthetic peptide corresponding to Human Histone H4 aa 10-15 (acetyl K12). Synthetic acetylated peptide derived from human Histone H4 around the acetylation site of lysine 12 LGK(Ac)GG	IgG	Rabbit	Polyclonal	Abcam, #ab61238	GR325039-1 GR325039-3
H4K16ac	Synthetic peptide (the amino acid sequence is considered to be commercially sensitive) corresponding to Human Histone H4 (acetyl K16).	IgG	Rabbit	Monoclonal	Abcam, #ab109463	GR53193-15 GR187780-8
H3panAc	This antibody was raised against a peptide including acetyl-lysines contained in the N-terminal tail of human Histone H3.	IgG	Rabbit	Polyclonal	Active Motif, #61637	28915002
Total H3	Raised against a peptide containing the N-terminus of histone H3.	IgG2b	Mouse	Monoclonal	Active Motif, #39763	07716018 34614001 5217020
Total H4	Raised against a synthetic peptide containing human Histone H4.	IgG2b	Mouse	Monoclonal	Active Motif, #61521	24615004 7715006

Table 4.6: Antibody dilutions and respective Western Blotting conditions.

Antibody	Manufactured Concentration	Dilution	Blocking Solution
H3K4me3	n/a	1:600	BSA
H3K27me3	1μg/μl	1:1000	BSA
H3K36me3	0.2μg/μl	1:200	BSA
H4K5ac	0.523μg/μl	1:1000	Skim Milk
H4K12ac	1μg/μl	1:1000	Skim Milk
H3panAc	1μg/μl	1:1000	Skim Milk
Total H3	0.68μg/μl	1:5000	Skim Milk or BSA
Total H4	0.52μg/μl	1:2000	Skim Milk

BSA - Bovine Serum Albumin

Table 4.7: Antibody dilutions and respective Immunohistochemistry conditions.

Antibody	Dilution	DAB Time	Antigen Retrieval	Ab Diluent	Washing Buffer #1	Washing Buffer #2
5mC	1:500	4min	Sodium Citrate pH 6.0	1% BSA in PBS	1X PBS + 0.2% Triton-X-100	1X PBS
5hmC	1:3000	5min	Tris-EDTA pH 9.0	1% BSA in TBS	1X TBS + 0.1% Tween 20	1X TBS
5fC	1:400	5min	Tris-EDTA pH 9.0	1% BSA in TBS	1X TBS + 0.1% Tween 20	1X TBS
5caC	1:250	5min	Tris-EDTA pH 9.0	1% BSA in TBS	1X TBS + 0.1% Tween 20	1X TBS
H3K4me3	1:500	5min	Sodium Citrate pH 6.0	1% BSA in PBS	1X PBS + 0.2% Triton-X-100	1X PBS
H3K9ac	1:500	5min	Tris-EDTA pH 9.0	1% BSA in TBS	1X TBS + 0.1% Tween 20	1X TBS
H3K9me2, K9me3	1:700	4min	Sodium Citrate pH 6.0	1% BSA in PBS	1X PBS + 0.2% Triton-X-100	1X PBS
H3K14ac	1:150	5min	Sodium Citrate pH 6.0	1% BSA in PBS	1X PBS + 0.2% Triton-X-100	1X PBS
H3K27ac	1:500	5min	Sodium Citrate pH 6.0	1% BSA in PBS	1X PBS + 0.2% Triton-X-100	1X PBS
H3K27me2	1:700	4min	Sodium Citrate pH 6.0	1% BSA in PBS	1X PBS + 0.2% Triton-X-100	1X PBS
H3K27me3	1:150	5min	Sodium Citrate pH 6.0	1% BSA in PBS	1X PBS + 0.2% Triton-X-100	1X PBS

Antibody	Dilution	DAB Time	Antigen Retrieval	Ab Diluent	Washing Buffer #1	Washing Buffer #2
H3K36me3	1:100	6mins	Tris-EDTA pH 9.0	1% BSA in TBS	1X TBS + 0.1% Tween 20	1X TBS
H4K5ac	1:350	5min	Tris-EDTA pH 9.0	1% BSA in TBS	1X TBS + 0.1% Tween 20	1X TBS
H4K12ac	1:300	5min	Tris-EDTA pH 9.0	1% BSA in TBS	1X TBS + 0.1% Tween 20	1X TBS
H4K16ac	1:100	6min	Sodium Citrate pH 6.0	1% BSA in PBS	1X PBS + 0.2% Triton-X-100	1X PBS
H3panAc	1.200	5min	Sodium Citrate pH 6.0	1% BSA in PBS	1X PBS + 0.2% Triton-X-100	1X PBS
Total H3	1:300	6min	Sodium Citrate pH 6.0	1% BSA in PBS	1X PBS + 0.2% Triton-X-100	1X PBS
Total H4	1:1000	5min	Tris-EDTA pH 9.0	1% BSA in TBS	1X TBS + 0.1% Tween 20	1X TBS

PBS – phosphate buffered saline

TBS – tris-buffered saline

Table 4.8: Recipes for antigen retrieval buffers, stains and 10X washing buffers specific to

immunohistochemistry.

Sodium Citrate Buffer, 0.05% Tween 20, pH 6.0	**Hematoxylin Stain**
Tri-sodium citrate (dihydrate) 2.94 g	5 g Harris Hematoxylin
ddH$_2$O 1,000 ml	50 mL 100% Ethanol
Mix to dissolve. Adjust pH to 6.0 with 5N HCl and then add 0.5 ml of Tween 20.	Dissolve (may turn slightly murky brown)
	1 L H$_2$O
Tris-EDTA Buffer, 0.05% Tween 20, pH 9.0	100 g aluminum ammonium sulfate
Tris Base 1.21 g	Heat till steaming to dissolve while stirring
EDTA 0.37 g	Add Hematoxylin in ethanol solution
ddH$_2$O 1,000 ml	Let cool for ½ hour
Mix to dissolve. Adjust pH to 9.0 with 5N HCl and then add 0.5 ml of Tween 20.	Add 0.5 g sodium iodate
	Let stir and cool further 1 hour
10X TBS, 1 Litre	Add 40 mL glacial acetic acid
ddH$_2$0 1,000ml	Filter into bottle
Tris 60.5g	
NaCl 87.6g	**Eosin Stain**
	2.25g Eosin Y
10X PBS, 1 Litre	150 mL H$_2$O
ddH$_2$0 1,000ml	750 mL 95% Ethanol
NaCl 80g	Add 1mL of glacial acetic acid per 200 mL of solution before use
Na$_2$(HPO$_4$) di basic 11.5g	
KH$_2$PO$_4$ 2g	
KCl 2g	

Table 4.9: Peptides used for antibody specificity experiments.

Peptide Name		Company	Catalogue #	Manufactured Concentration	Lot #
H3K4me	Human Histone H3 (mono methyl K4) synthetic peptide	Abcam	ab1340	1mg/ml	GR163991-1
H3K4me2	Human Histone H3 (di methyl K4) synthetic peptide	Abcam	ab7768	1mg/ml	GR261696-1
H3K4me3	Human Histone H3 (tri methyl K4) synthetic peptide	Abcam	ab1342	1mg/ml	GR110532-1
H3K9me	Human Histone H3 (mono methyl K9) synthetic peptide	Abcam	ab1771	1mg/ml	GR98366-1
H3K9me2	Human Histone H3 (di methyl K9) synthetic peptide	Abcam	ab1772	1mg/ml	GR239054-1
H3K9me3	Human Histone H3 (tri methyl K9) synthetic peptide	Abcam	ab1773	1mg/ml	GR22285-1
H3K27me	Human Histone H3 (mono methyl K27) synthetic peptide	Abcam	ab1780	1mg/ml	GR207247-1
H3K27me2	Human Histone H3 (di methyl K27) synthetic peptide	Abcam	ab1781	1mg/ml	GR214313-1
H3K27me3	Human Histone H3 (tri methyl K27) synthetic peptide	Abcam	ab1782	1mg/ml	GR99419-1
H3K36me	Human Histone H3 (mono methyl K36) synthetic peptide	Abcam	ab1783	1mg/ml	GR257939-1
H3K36me2	Human Histone H3 (di methyl K36) synthetic peptide	Abcam	ab1784	1mg/ml	GR207248-1
H3K36me3	Human Histone H3 (tri methyl K36) synthetic peptide	Abcam	ab1785	1mg/ml	GR224578-1
H3K27ac	Human Histone H3 (acetyl K27) synthetic peptide	Abcam	ab24404	1mg/ml	GR221083-1
H4K5ac	Human Histone H4 (acetyl K5) synthetic peptide	Abcam	ab154430	1mg/ml	GR243684-1
H4K12ac	Human Histone H4 (acetyl K12) synthetic peptide	Abcam	ab154463	0.5mg/ml	GR185742-1
Unmodified H3	Human Histone H3 (unmodified) synthetic peptide	Abcam	ab7228	1mg/ml	GR295574-4
Unmodified H4	Human Histone H4 synthetic peptide (unmodified)	Abcam	ab14963	1mg/ml	GR803316

Figure 4.7: Standard scale images used for grading the proportion of immunoreactive nuclei. Any degree of brown was considered positive. Photomicrographs show: 4 - ~100% positive; 3 - ~75% positive; 2 - ~50% positive; 1 <25% positive; 0 - ~0% positive. Images taken at 400x magnification. DAB detection of antibody (brown) and hematoxylin counterstain (blue).
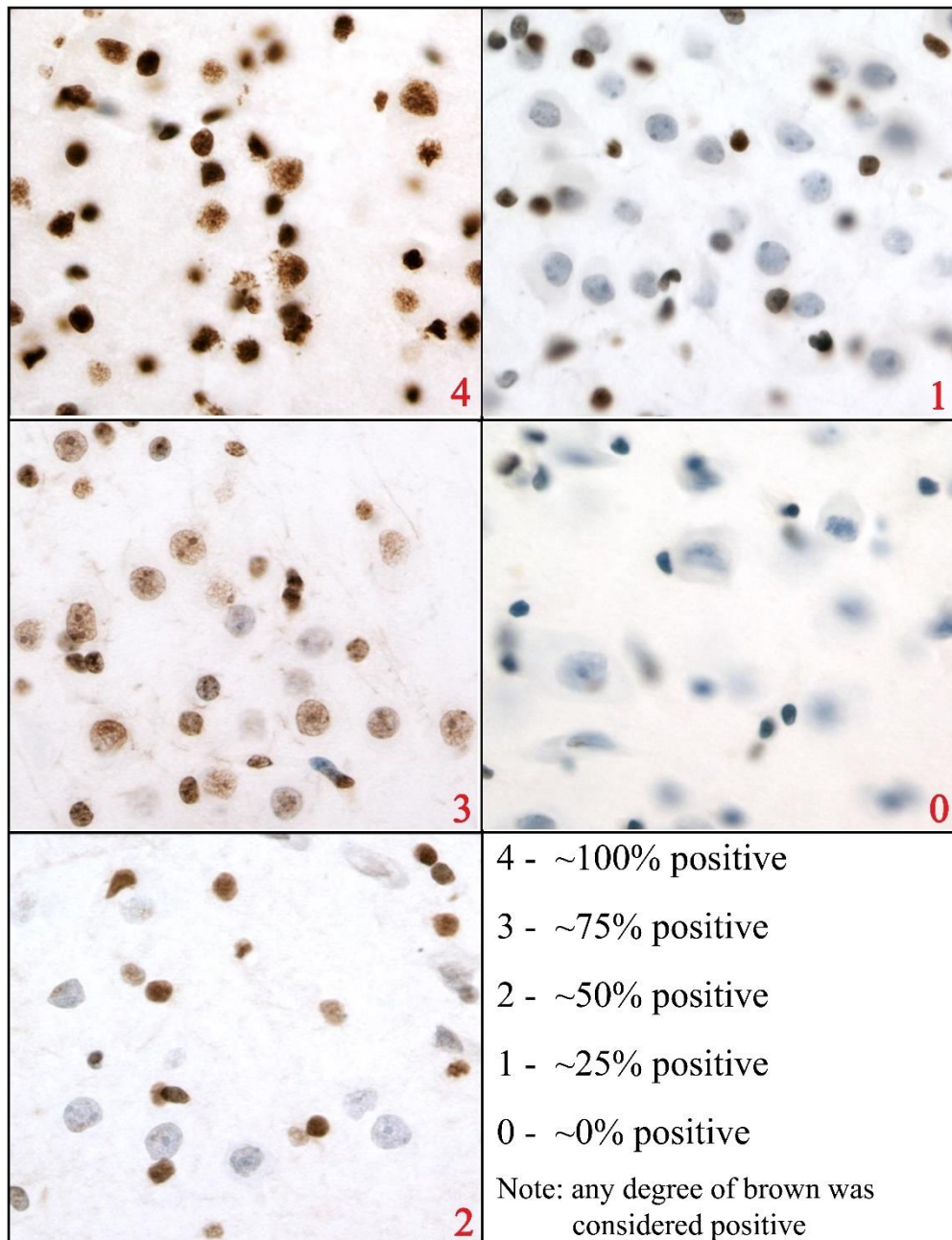
Figure 4.8: Standard scale images used for grading the intensity of immunoreactive nuclei. A score of 3 represents strong almost black labelling. A 2 represents medium intensity. A 1 demonstrated faint labeling. Half scores were also possible (2.5, 1.5 and 0.5). Images taken at 400x magnification. DAB detection of antibody (brown) and hematoxylin counterstain (blue).
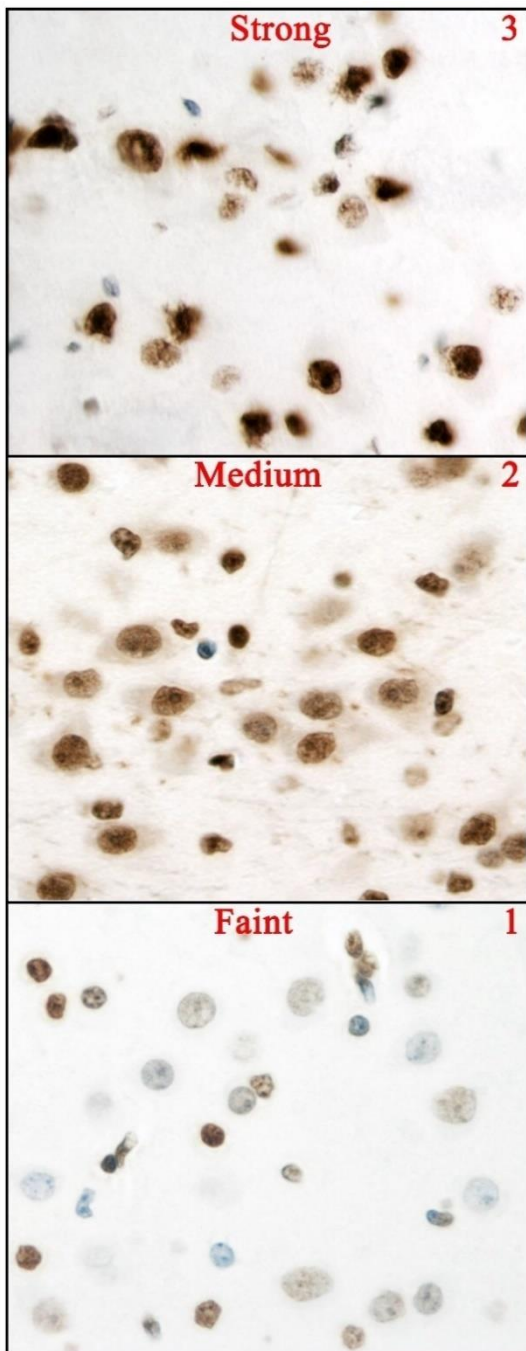
Figure 4.9: Presumed cell type based on nuclear morphology.
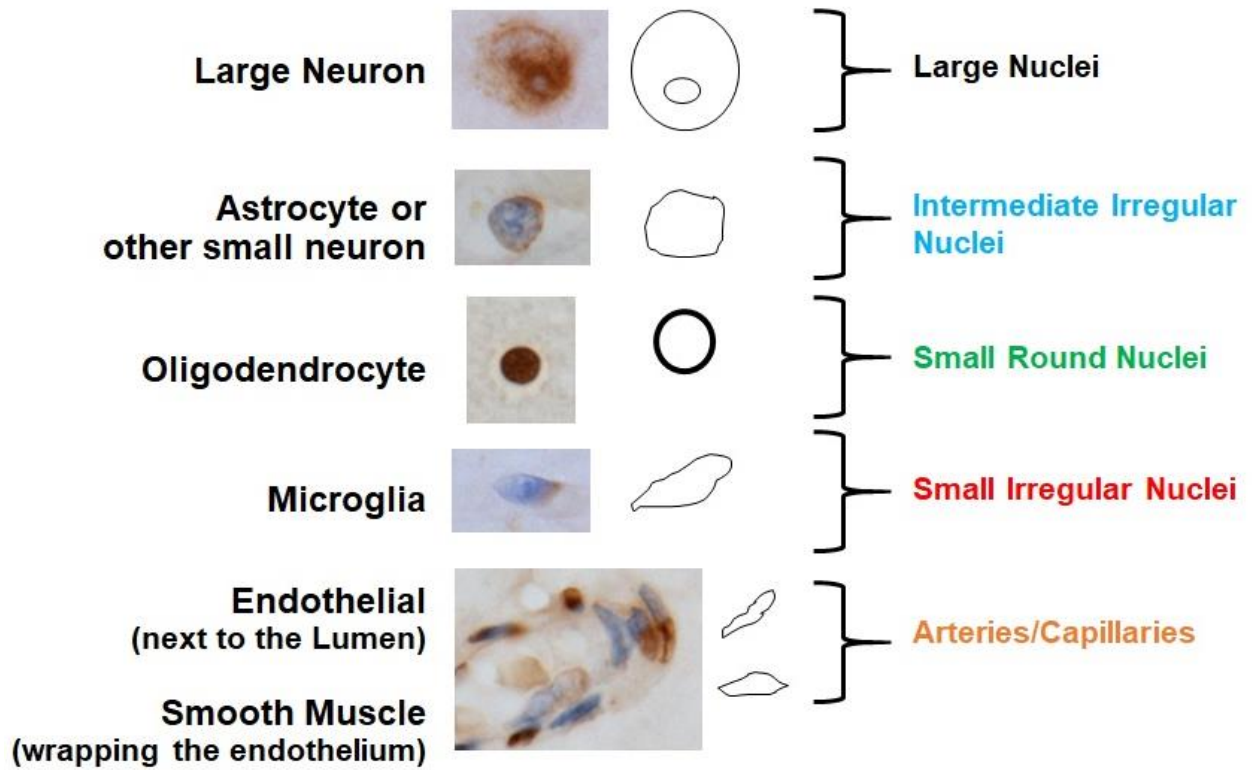
Figure 4.10: DNA integrity in neonatal pig frontal cortex after post-mortem delays to freezing. Agarose gel showing DNA extracted from all 7 pigs, at all 4 PMD time points (0 hour (hr), 24, 48 and 72). M represents the DNA size markers in base pairs (bp). Bands at all post-mortem delay time points remain intact with no obvious smearing.
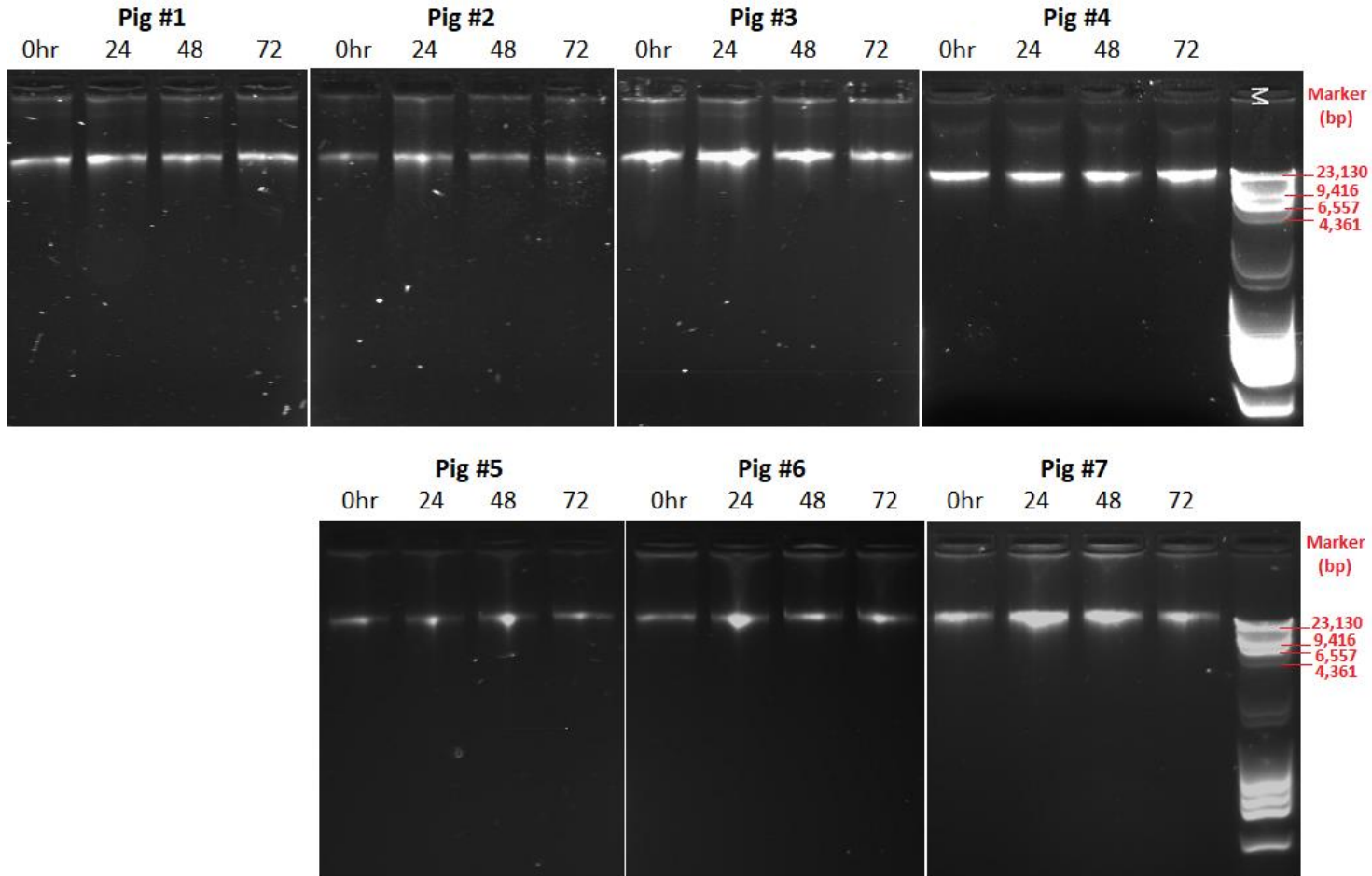
Figure 4.11: Percentage of DNA methylation (5mC; a) and hydroxymethylation (5hmC; b) in neonatal pig frontal cortex after post-mortem delays to freezing. In general, 5mC levels are higher than 5hmC levels. Temporal analysis shows no significant difference between the 0 and 72-hour time points for pigs raised in normoxic (n = 4) and hypoxic (n = 3) conditions. At three time points, there are differences between the normoxic and hypoxic pigs (p-values shown in figure).
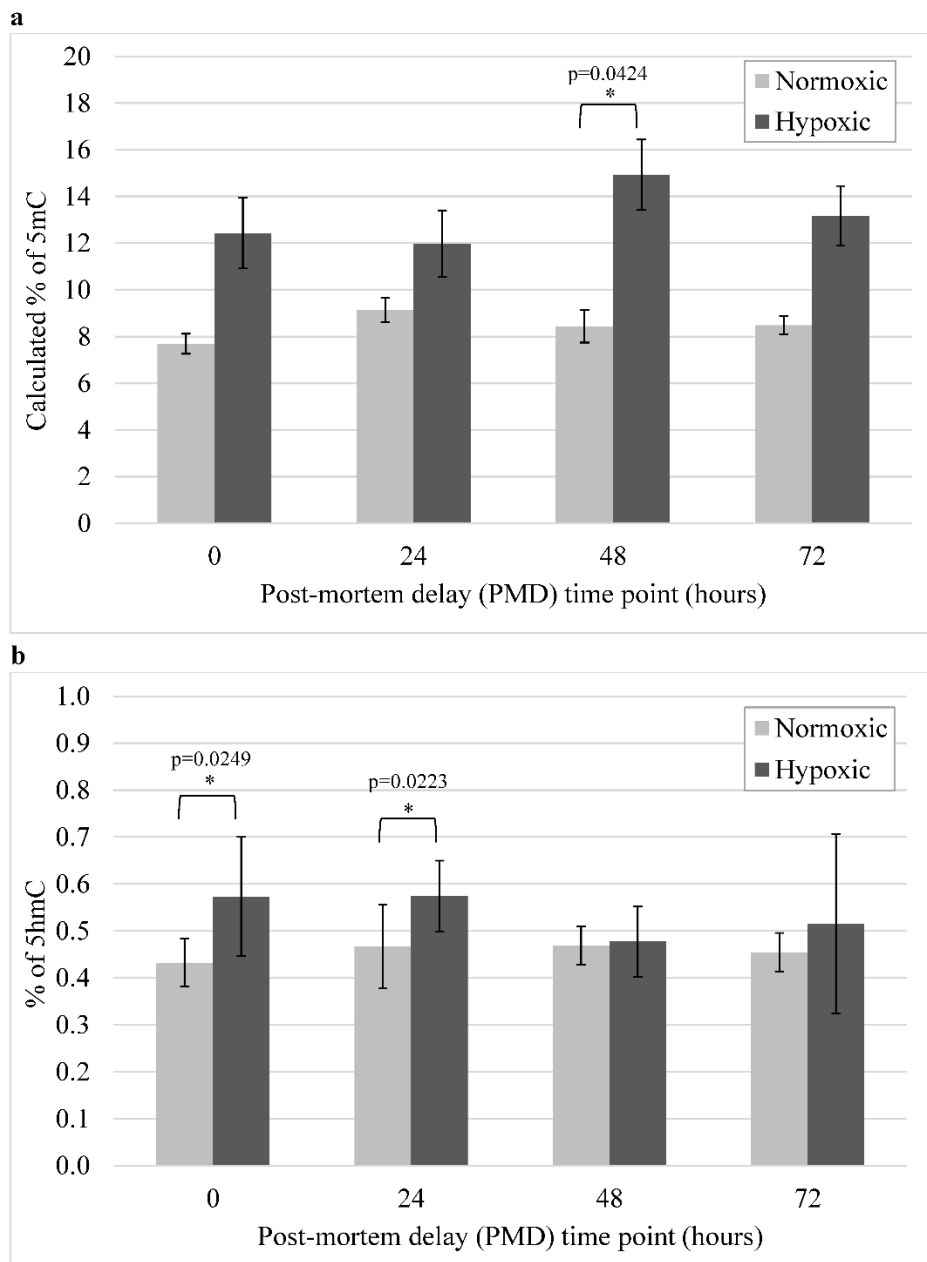
Figure 4.12: Examples of peptide blocking immunohistochemistry for histone post-translational modifications in neonatal pig neocortex. Top row photomicrographs show anti-histone H3 trimethylated at lysine 4 (H3K4me3). It was blocked by its own peptide (K4me3), but also partially blocked by other less specific peptides (K4me, K4me2, K9me3). Bottom row photomicrographs show anti-H3K27ac. It was blocked only by its own peptide (K27ac) and not by others (H4K5ac; others not shown). Images all taken at 400x magnification. DAB detection of antibody (brown) and hematoxylin counterstain (blue).
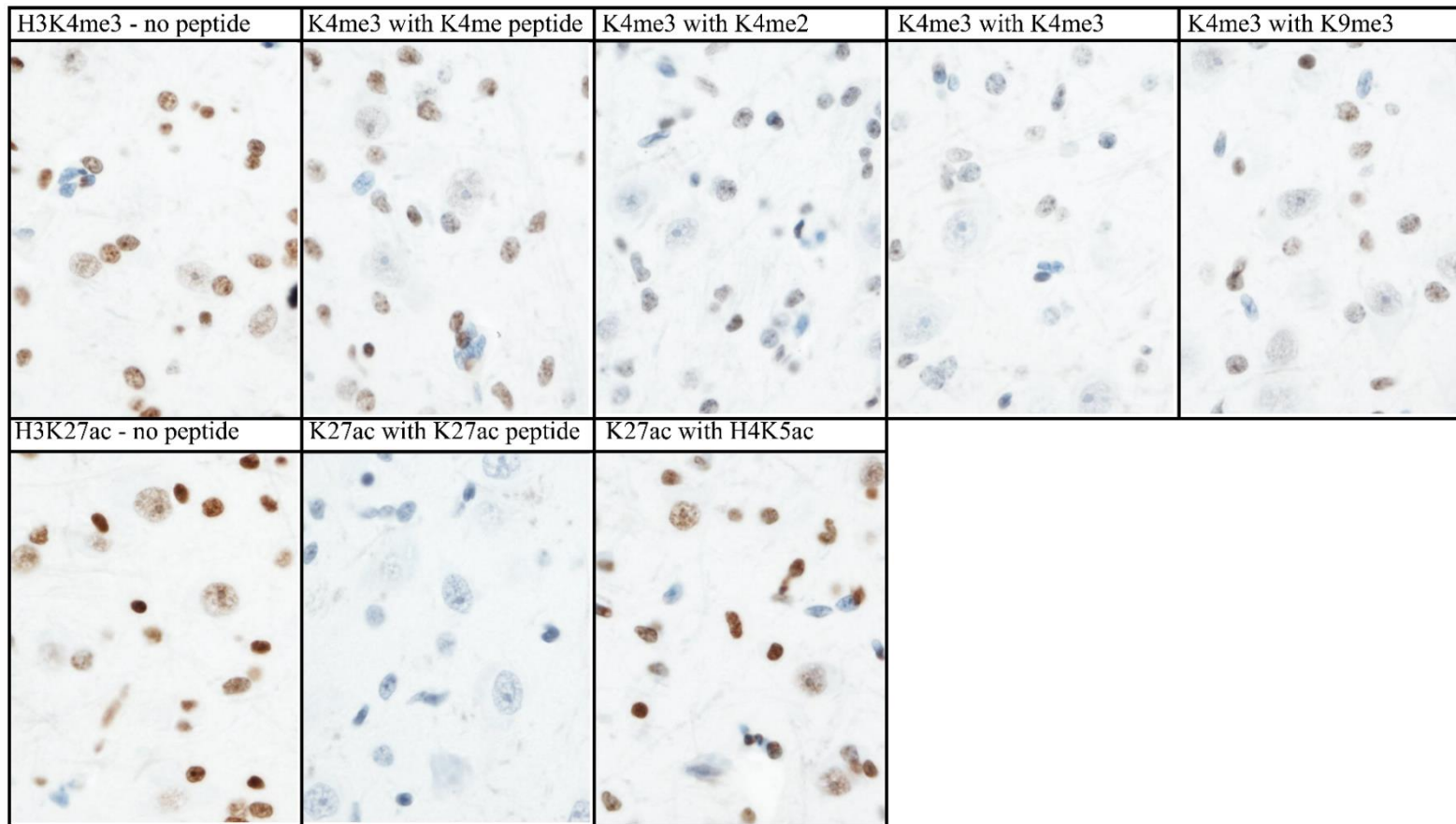
Table 4.10: Summary of immunohistochemistry peptide blocking results.

Peptide	Antibody						
	H3K4me3 (Abcam)	H3K4me3 (Active Motif)	H3K9me2, K9me3	H3K27me2	H3K27me3	H3K36me3	H3K27ac
H3K4me	[+]	[+]					
H3K4me2	[++]	[++]		--			
H3K4me3	+++	+++				--	
H3K9me			[+]				
H3K9me2				--			
H3K9me2, H3K9me3			++				
H3K9me3	[+]	[++]			--	--	
H3K27me				--	--		
H3K27me2				[--]	--		
H3K27me3	[+]	[+]		--	+++	--	
H3K36me						--	
H3K36me2				--		--	
H3K36me3					--	+++	
H3K27ac				--			+++
H4K5ac							--
Summary	Fairly specific	Fairly specific	Fairly specific	Not specific	Specific	Specific	Specific

+++ Complete block ++ Partial block + Minimal block -- No block

Square brackets [ ] represent an unexpected result.
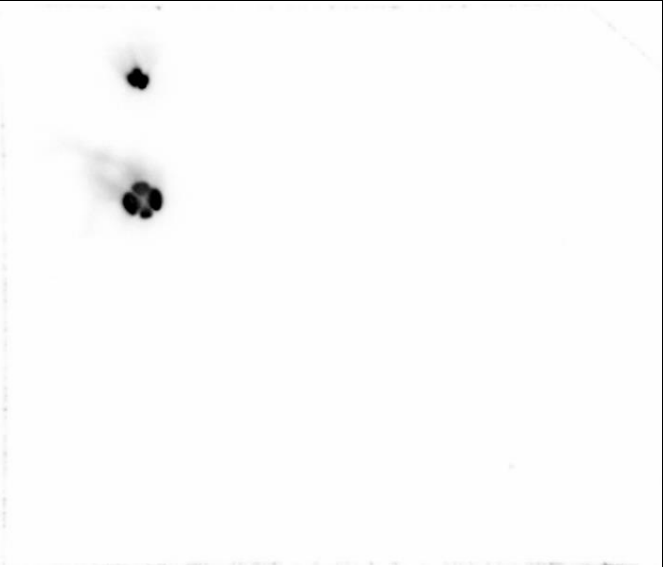
Table 4.11: Summary of dot blot evaluation of antibody specificity.

Peptide	Antibody											
	Total H3	Total H4	H3K27ac	H3K14ac	H4K5ac	H4K12ac	H3panAc	H3K4me3 (Abcam)	H3K4me3 (Active Motif)	H3K27me2	H3K27me3	H3K36me3
Histone mix		Strong										None
Unmodified H3	Strong	None	None	None			None		[Weak]		None	
Unmodified H4	None	[None]			None	None						
H3K4me								[Weak]	[Weak]			
H3K4me2								[Weak]	[Strong]	[Weak]		
H3K4me3								Strong	Strong			[Weak]
H3K9me	None											
H3K9me2		None								[Weak]		
H3K9me3								[Weak]	[Weak]		None	
H3K27me										None	None	
H3K27me2										[Weak]	None	
H3K27me3	None							[Weak]	[Strong]	Strong	Strong	[Strong]
H3K36me												None
H3K36me2										[Weak]		[Strong]
H3K36me3								[Weak]			None	Strong
H3K14ac			None	Strong	None	None	Strong					
H3K27ac	None	None	Strong	None	None	None	Weak					
H4K5ac	None	None			Strong	[Weak]	None					
H4K12ac		None	None	None	None	Strong	None					
Summary	Specific	Specific*	Specific	Specific	Specific	Fairly specific	Specific	Fairly specific	Not very specific	Fairly specific	Specific	Fairly specific

"Strong" indicates that the antibody bound to the peptide with strong affinity, "weak" indicates that the antibody bound but with weak affinity, and

"none" indicates that the antibody did not bind to the peptide. A blank cell means not applicable, and square brackets [ ] represent an unexpected result.

*A discussion with the manufacturer suggested the unmodified H4 peptide may have been a bad or incorrect batch.

Figure 4.13: Complete dot blot peptide blocking results. A small quantity of peptide was directly pipetted onto nitrocellulose membrane. The membrane was blocked and incubated with the antibody overnight

Unmodified H3 0.5μg	H3K27ac 0.5μg	H3K9me 0.5μg	Total Histone H3
Unmodified H3 2μg	H3K27ac 2μg	H3K9me 2μg	
Unmodified H4 0.5μg	H4K5ac 0.5μg	H3K27me3 0.5μg	
Unmodified H4 2μg	H4K5ac 2μg	H3K27me3 2μg	
Unmodified H4 0.5μg	H4K5ac 0.5μg	H4K12ac 0.5μg	Total Histone H4
Unmodified H4 2μg	H4K5ac 2μg	H4K12ac 2μg	
Unmodified H3 0.5μg	H3K27ac 0.5μg	H3K9me2 0.5μg	
Unmodified H3 2μg	H3K27ac 2μg	H3K9me2 2μg	

Unmodified H4 0.5μg	H3K14ac 0.5μg	H3K27ac 0.5μg		H4K5ac
Unmodified H4 2μg	H3K14ac 2μg	H3K27ac 2μg		
H4K5ac --------------------------------------> 0.1μg	0.5μg	2μg		
H4K12ac -------------------------------------> 0.1μg	0.5μg	2μg		
Unmodified H4 0.5μg	H3K14ac 0.5μg	H3K27ac 0.5μg		H4K12ac
Unmodified H4 2μg	H3K14ac 2μg	H3K27ac 2μg		
H4K5ac --> 0.1μg	0.5μg	2μg		
H4K12ac --> 0.1μg	0.5μg	2μ		
Unmodified H3 0.5μg	H4K5ac 0.5μg	H4K12ac 0.5μg		H3panAc
Unmodified H3 2μg	H4K5ac 2μg	H4K12ac 2μg		
H3K14ac -------------------------------------> 0.1μg	0.5μg	2μg		
H3K27ac -------------------------------------> 0.1μg	0.5μg	2μg		

211

H3K4me----------------------------------->
0.1μg   **0.5μg**   **2μg**   Unmodified H3
                                          0.5μg

H3K4me2----------------------------------->
0.1μg   **0.5μg**   **2μg**   Unmodified H3
                                          2μg

H3K4me3----------------------------------->
0.1μg   **0.5μg**   **2μg**   H3K27me3
                                          2μg

H3K9me3   H3K9me3   H3K27me3
0.5μg   **2μg**   **0.5μg**

H3K4me3 (Active Motif)

H3K27me----------------------------------->
0.1μg   **0.5μg**   **2μg**   Unmodified H3
                                          0.5μg

H3K27me2----------------------------------->
0.1μg   **0.5μg**   **2μg**   Unmodified H3
                                          2μg

H3K27me3----------------------------------->
0.1μg   **0.5μg**   **2μg**   H3K36me3
                                          2μg

H3K9me3   H3K9me3   H3K36me3
0.5μg   **2μg**   **0.5μg**

H3K27me3

H3K36me----------------------------------->
0.1μg   **0.5μg**   **2μg**   Unmodified H3
                                          0.5μg

H3K36me2----------------------------------->
0.1μg   **0.5μg**   **2μg**   Unmodified H3
                                          2μg

H3K36me3----------------------------------->
0.1μg   **0.5μg**   **2μg**   H3K27me3
                                          2μg

H3K4me3   H3K4me3   H3K27me3
0.5μg   **2μg**   **0.5μg**

H3K36me3

212

Histone Mix ------------------------------------>		
0.1μg	**0.5μg**	**2μg**
Unmodified H4 ------------------------------------>		
0.1μg	**0.5μg**	**2μg**
H4K5ac	H4K12ac	Unmodified H3
0.5μg	**0.5μg**	**0.5μg**
H4K5ac	H4K12ac	Unmodified H3
2μg	**2μg**	**2μg**

Total Histone H4

H3K27ac	H3K14ac
0.1μg	**0.1μg**
H3K27ac	H3K14ac
0.5μg	**0.5μg**
H3K27ac	H3K14ac
2μg	**1μg**
H4K12ac	Unmodified H3
1μg	**1μg**

H3K27ac

H3K14ac	H3K27ac
0.1μg	**0.1μg**
H3K14ac	H3K27ac
0.5μg	**0.5μg**
H3K14ac	H3K27ac
1μg	**2μg**
H4K12ac	Unmodified H3
1μg	**1μg**

H3K14ac

H3K4me---------------------------------->				
0.1μg	**0.5μg**	**2μg**	H3K36me3 **0.5μg**	
H3K4me2---------------------------------->				
0.1μg	**0.5μg**	**2μg**	H3K36me3 **2μg**	
H3K4me3---------------------------------->				
0.1μg	**0.5μg**	**2μg**	H3K27me3 **2μg**	
H3K9me3 **0.5μg**	H3K9me3 **2μg**	H3K27me3 **0.5μg**		

H3K4me3 (Abcam)

H3K27me2---------------------------------->				
0.1μg	**0.5μg**	**2μg**	H3K36me2 **0.5μg**	
H3K27me---------------------------------->				
0.1μg	**0.5μg**	**2μg**	H3K36me2 **2μg**	
H3K27me3---------------------------------->				
0.1μg	**0.5μg**	**2μg**	H3K9me2 **2μg**	
H3K4me2 **0.5μg**	H3K4me2 **2μg**	H3K9me2 **0.5μg**		

H3K27me2

214

Figure 4.14: Total histone Western blot graphical results. Raw quantity ("volume") measurements are shown for all pigs combined (n=7). Total histone H3 and H4 levels were stable across all post-mortem delay time points (not significant at p<0.05)

215
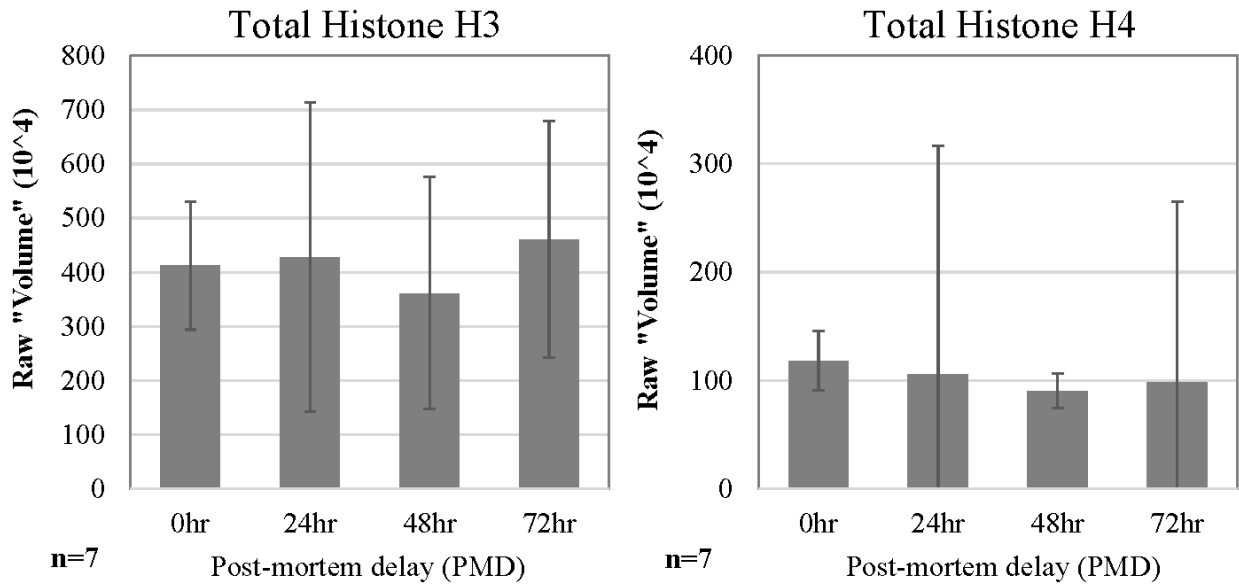
Figure 4.15: Quantitation of histone epigenetic modifications on Western blots of neonatal pig brain. There were no differences between normoxic and hypoxic samples, therefore all data were pooled (n=7) and densitometric band "quantity" displayed (mean ± 95% confidence intervals). H3K4me3 and H3K27me3 remained stable ≥72 hours post-mortem. H3K36me3 was stable for 24 hours but decreased significantly by 48 hours. H3panAc decreased at 24 hours and was negligible by 48 hours; the difference was not significant because the initial values were low with wide variation. H4K5ac and H4K12ac were significantly decreased by 48 hours. P-values shown in figure.
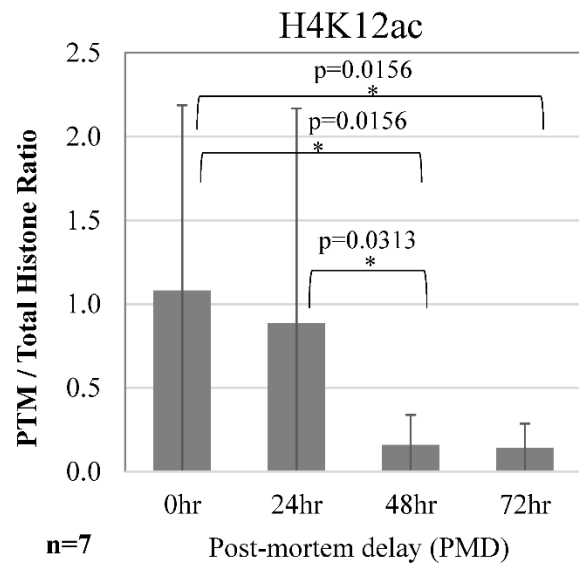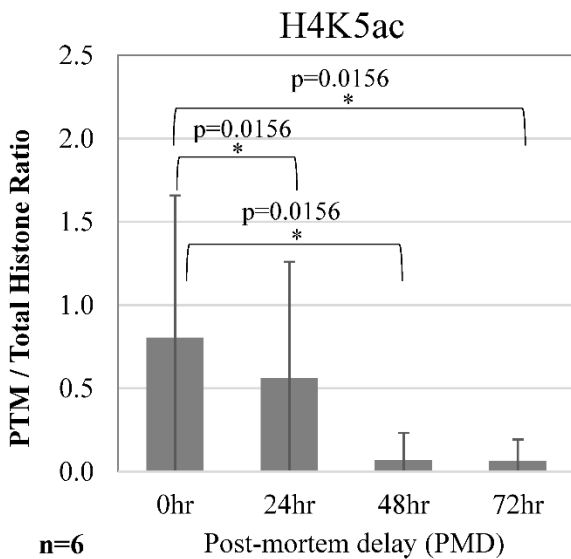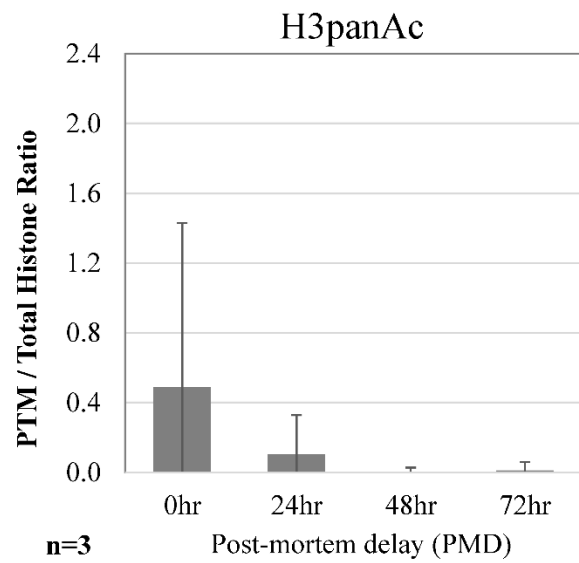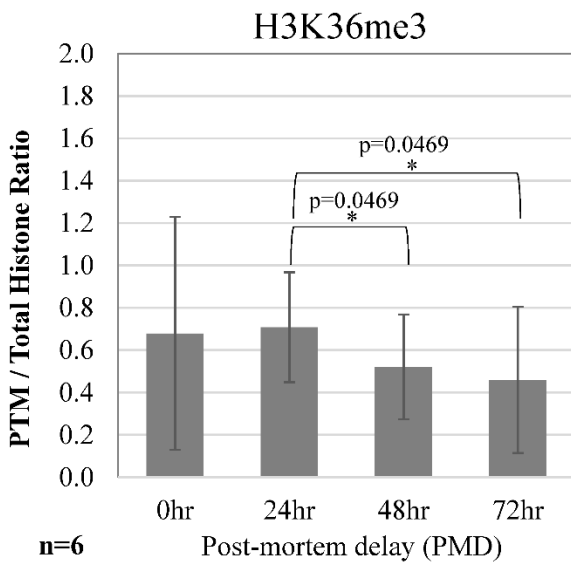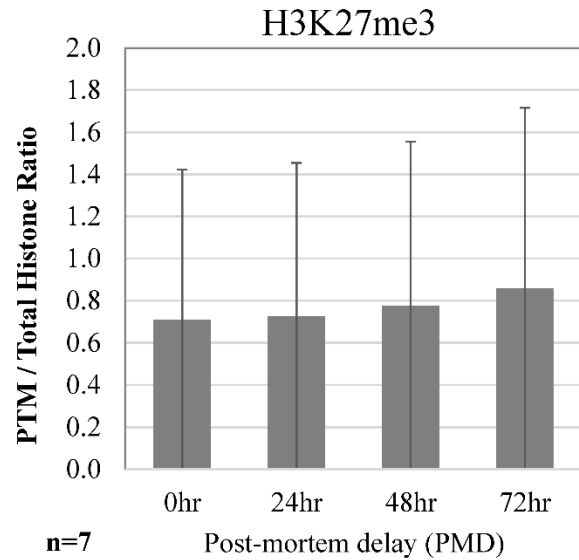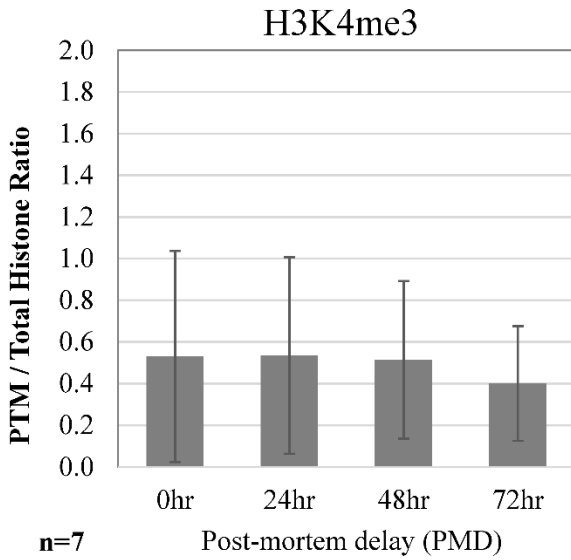
Figure 4.16: Western blots of neonatal pig brain samples for histone PTMs (left) and corresponding total histone (right).

A) On Western blots of H3K27me3, all normoxic pigs (1-4) and hypoxic pigs (5-7) show stability across all 4 post-mortem time points. "hr" = hour, B represents a blank lane, +C represents the positive control (calf thymus histone mix).
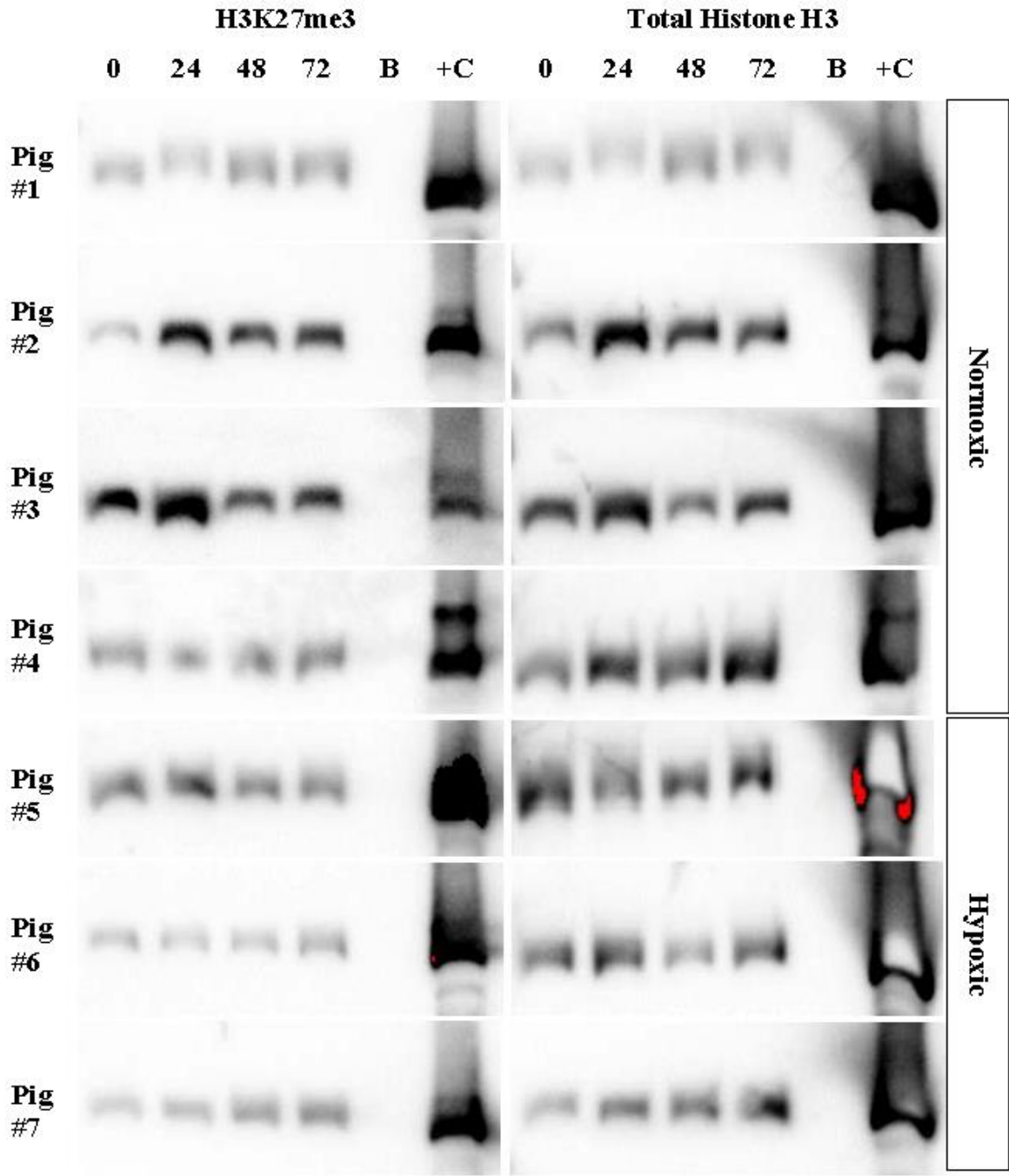
B) On Western blots of H4K12ac, all normoxic pigs (1-4) and hypoxic pigs (5-7) show declines with increasing post-mortem times. "hr" = hour, B represents a blank lane, +C represents the positive control (calf thymus histone mix).
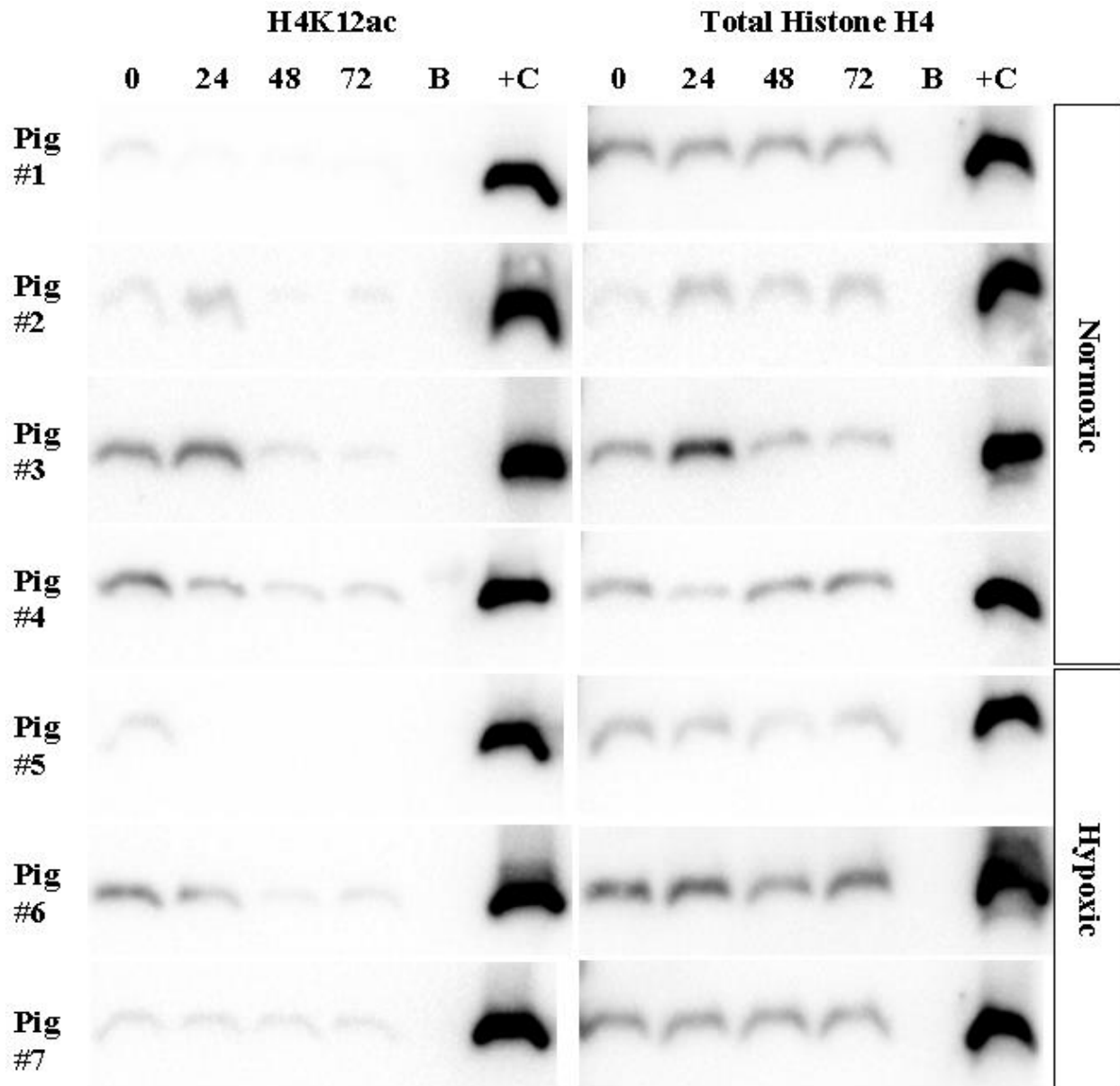
C) On Western blots of normoxic pig brain (#4), the three histone methylation PTMs are stable across all 4 post-mortem time points while the two histone acetylation PTMs decline. "hr" = hour, B represents a blank lane, +C represents the positive control (calf thymus histone mix).
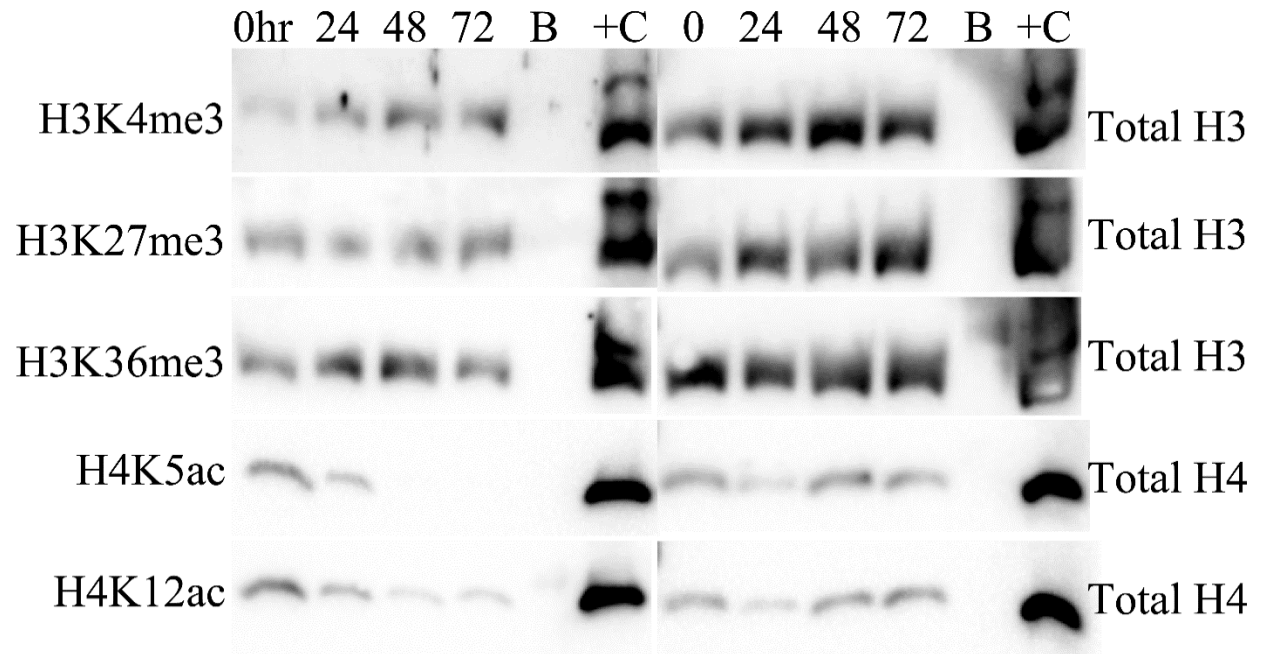
D) On Western blots of hypoxic pig brain (#7), the three histone methylation PTMs are stable across all 4 postmortem time points while the three histone acetylation PTMs decline. "hr" = hour, B represents a blank lane, +C represents the positive control (calf thymus histone mix).

Pig #7 – Hypoxic – All Histone PTMs
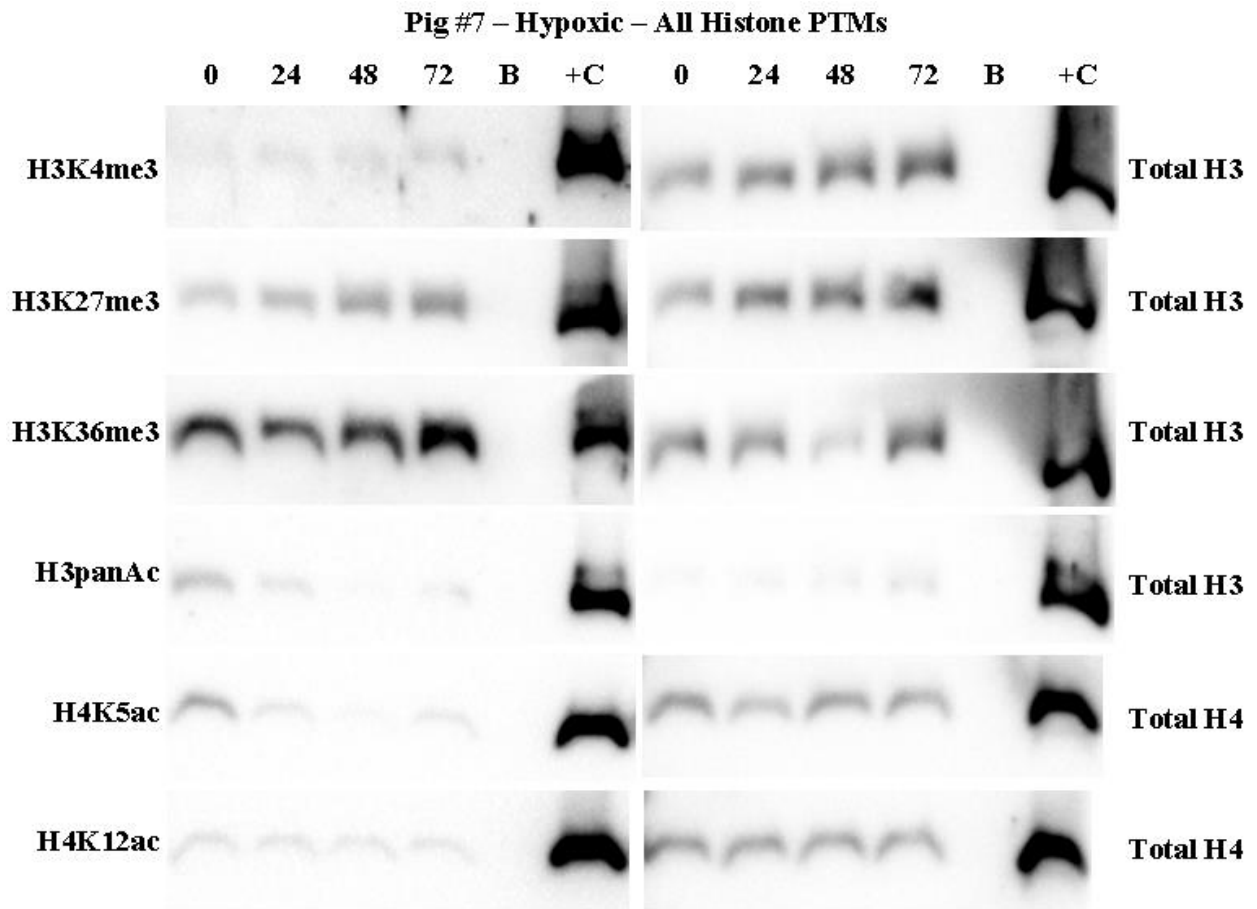
Figure 4.17: Full western blot images for H3K36me3 and H4K12ac. Histone PTM (left)

corresponding Total Histone (right). L represents the protein standard ladder (kD), B represents a

"blank" lane, +C represents the positive control (calf thymus histone mix).
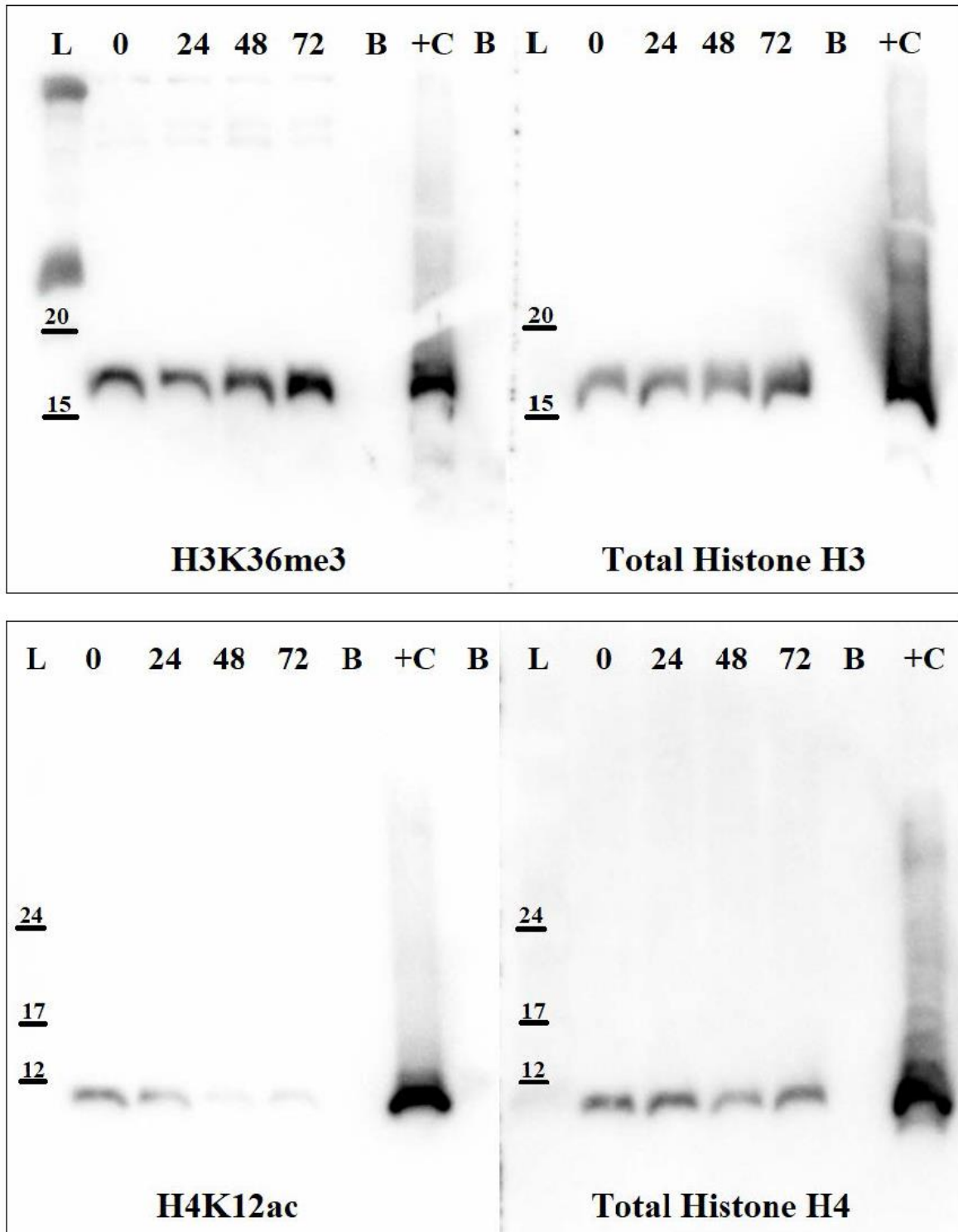
Figure 4.18: Immunohistochemical detection of 5-methylcytosine (5mC) in mouse (all ages) and neonatal pig neocortex. Labeling is strongest in the large round nuclei of neurons in mouse brain; note that immature neurons in newborn mouse are usually negative. In pig brain, smaller glial nuclei are also labeled. Elongated nuclei of endothelial cells are generally negative. There is no difference between 0 (left) and 72 (right) hours post-mortem in any of the animal groups. Images taken at 400x magnification. DAB detection of antibody (brown) and hematoxylin counterstain (blue).

0 hour PMD time point   72 hour PMD time point

8-24 hour mouse

10-day-old mouse

8-10 week mouse

3-day-old pig
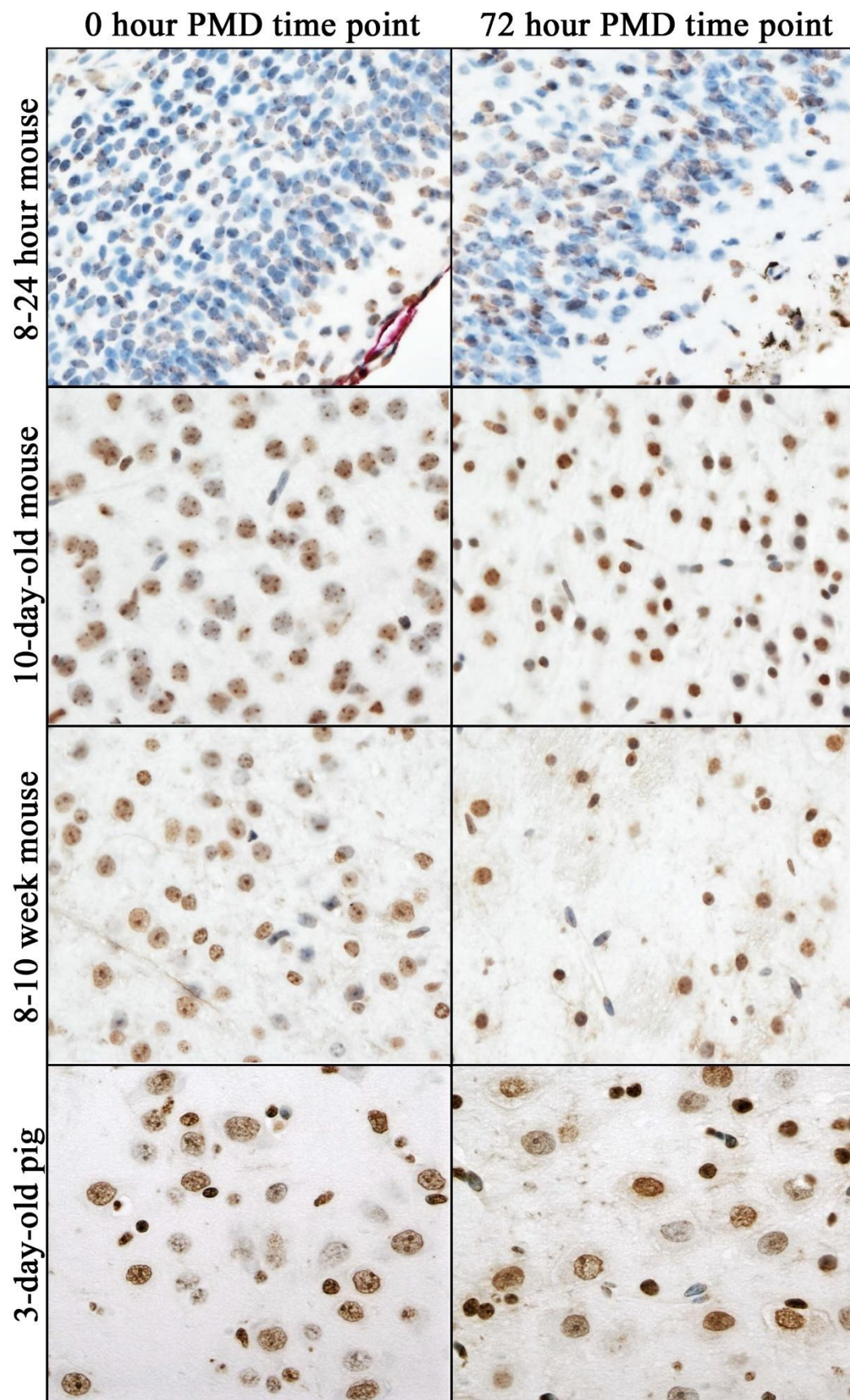
Figure 4.19: Immunohistochemical detection of histone H3 methylation (H3K4me3, H3K36me3) in neonatal pig neocortex. In control (0 hour) brain, the nuclei of almost all cell types are positive except rare endothelial cells. Photomicrographs show that some large neurons (red arrows) have a minor decrease in intensity of immunoreactivity for H3K4me3 at 72 hours. Images taken at 400x magnification. DAB detection of antibody (brown) and hematoxylin counterstain (blue).
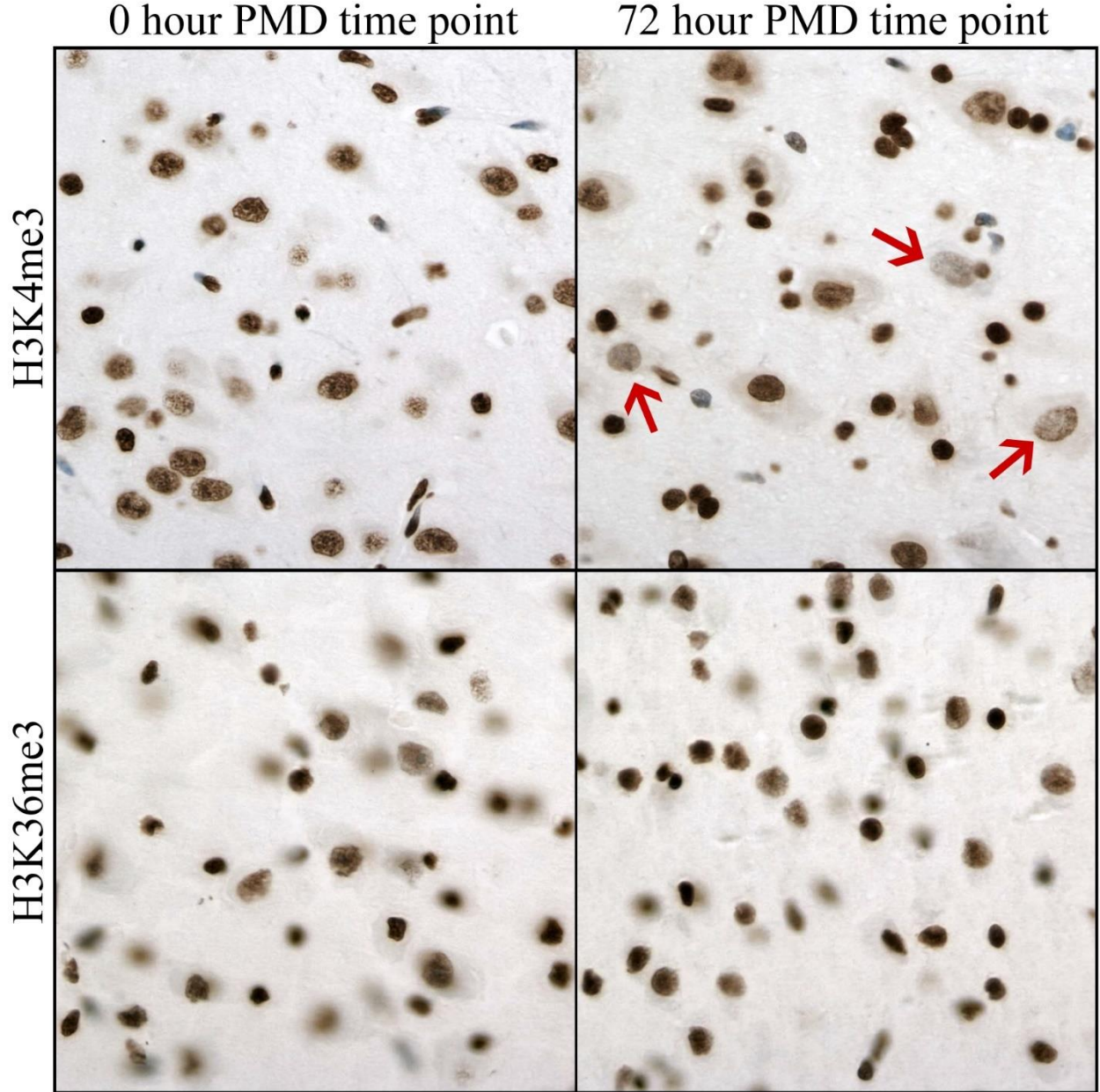
Figure 4.20: Immunohistochemical detection of H3K27me2 in 10-day-old mouse and neonatal pig neocortex. Immunohistochemical detection of H3K27me2 in 10-day mouse and neonatal pig neocortex. In control brains (0 hour), the nuclei of all cells, except for a subpopulation of endothelial cells, are positive. Photomicrographs show decreased intensity of immunoreactivity in medium-size nuclei of mouse brain at 48 and 72 hours post-mortem, and in large neuronal nuclei of pig brain by 72 hours post-mortem. Images taken at 400x magnification. DAB detection of antibody (brown) and hematoxylin counterstain (blue).
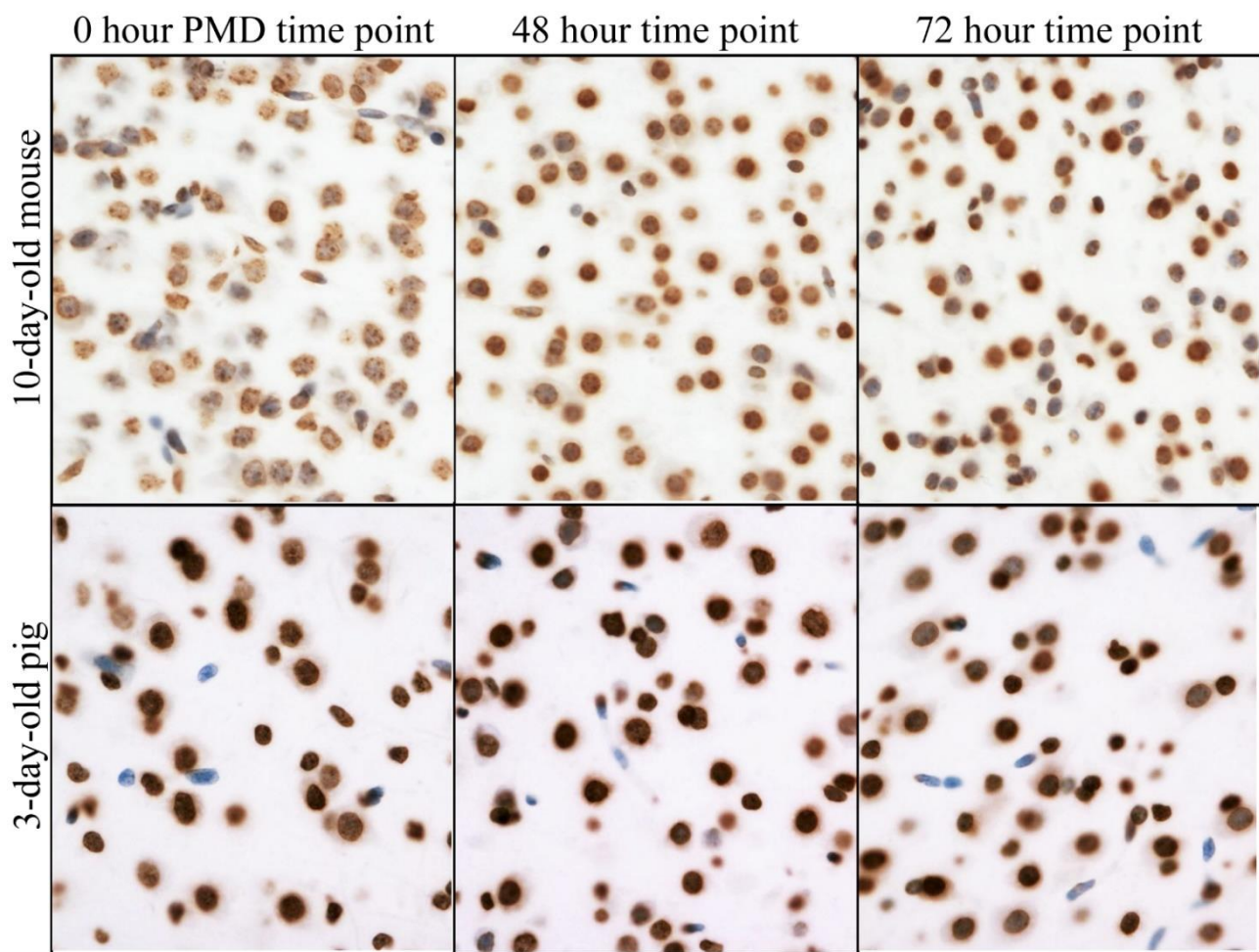
Figure 4.21: Immunohistochemical detection of histone H3 acetylation PTMs in neonatal pig brain neocortex. In control brain (0 hours) anti-H3K9ac strongly labels nuclei of large neurons (red arrows) and smaller glial cells. Anti-H3K27ac and anti-H4K5ac label smaller glial nuclei (blue arrows) more intensely than those of neurons (red arrows). Anti-H3K14ac labels only smaller glial nuclei. Photomicrographs show a loss of immunoreactivity in large neurons but not glial cells (note different time points at which change was first observed). Images taken at 400x magnification. DAB detection of antibody (brown) and hematoxylin counterstain (blue).
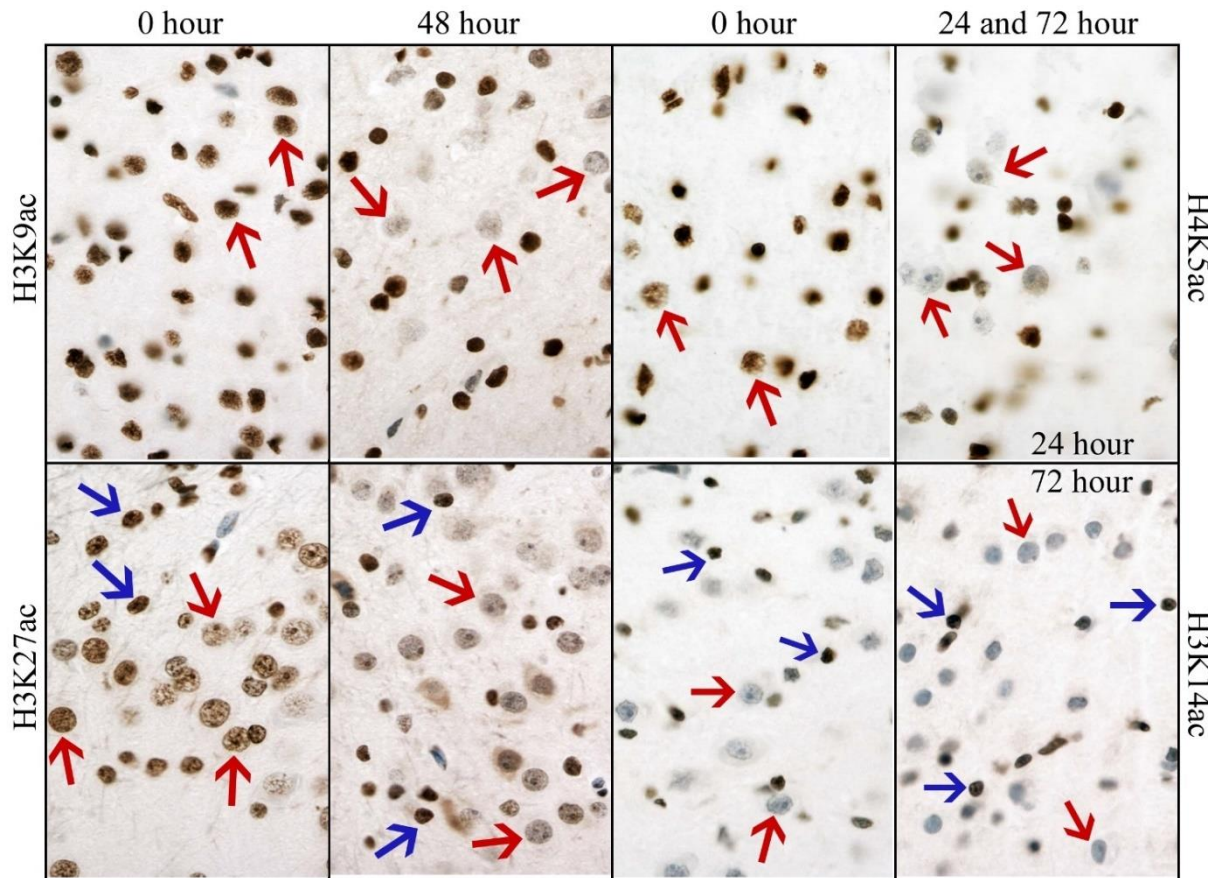
Figure 4.22: Immunohistochemical detection of "total" histone H3 and H4 in neonatal pig and mouse (all ages) neocortex. Despite the antibody being called "Anti-total histone", not all nuclei are labelled. In control (0 hour) pig brain and in both 10-day and 8-10 week mouse brains, anti-H3 and anti-H4 label nuclei in all but a subset of endothelial cells. However, in newborn mouse brain, anti-H3 does not label the most immature cells. Photomicrographs show a minor decrease in the intensity of immunostaining of large neurons in pig brain at 72 hours post-mortem. In mouse brain at all ages, loss of H3 and H4 immunoreactivity is more substantial at 72 hours post-mortem. Images taken at 400x magnification. DAB detection of antibody (brown) and hematoxylin counterstain (blue).

	0 hour H3	72 hour H3	0 hour H4	72 hour H4
3 day pig				
8-24 hour mouse				
10 day mouse				
8-10 weeks mouse				

229
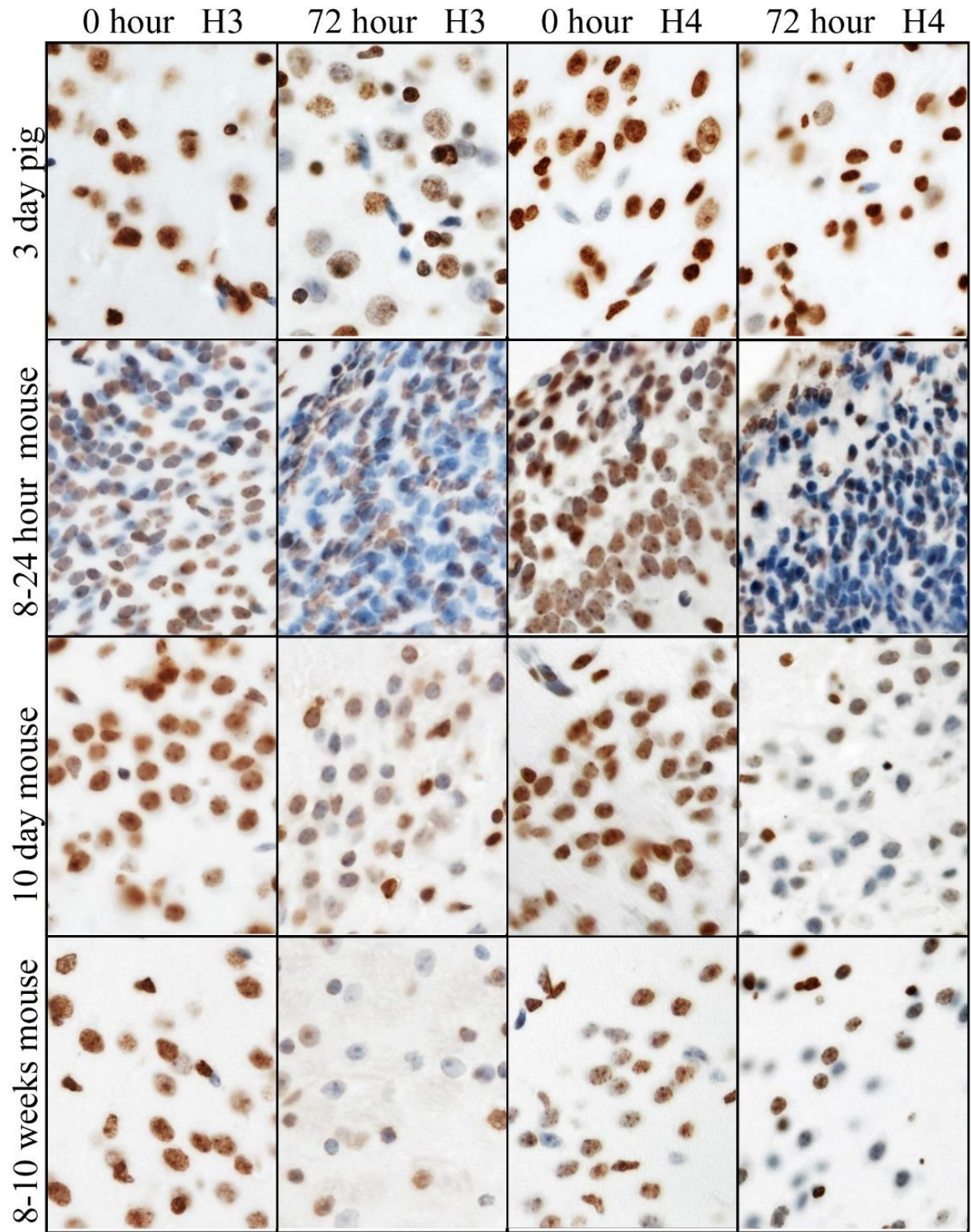
Figure 4.23: Bar graphs showing semiquantitative intensity scores (mean ± 95% confidence intervals; maximum 3) for all epigenetic modification antibodies used in neonatal pig neocortex. DNA cytosine modifications, total histone H4, all histone methylation PTMs, H3K14ac, and H4K5ac and showed stable immunoreactivity up to 72 hours post-mortem. H3K9ac was stable up to 48 hours post-mortem. Total histone H3, H4K16ac, H3K27ac, and H4K12ac all showed a significant decline by 48 hours post-mortem. P-values for all statistical comparisons are shown on the graph or at the bottom.

Legend: ■ 0 hours ■ 24 hours ■ 48 hours □ 72 hours

Top panel categories: 5mC, 5hmC, 5fC, 5caC, Total H3, Total H4

Total H3 annotations: p=0.0078 *, p=0.0156 *, p=0.0156 *

Middle panel categories: H3K4me3, H3K9me2,K9me3, H3K27me2, H3K27me3, H3K36me3

Bottom panel categories: H3K9ac, H3K14ac, H3K27ac, H4K5ac, H4K12ac, H4K16ac

P Value	0 vs. 24	0 vs. 48	0 vs. 72	24 vs. 48	24 vs. 72	48 vs. 72
H3K9ac	0.25	0.0625	**0.0156**	0.125	**0.0313**	0.125
H3K14ac	0.5	0.5	0.5	0.5	0.5	0.375
H3K27ac	0.0625	**0.0020**	**0.0020**	**0.0156**	**0.0078**	0.1094
H4K5ac	0.25	0.25	0.0625	0.5	0.25	0.25
H4K12ac	0.5	**0.0156**	**0.0313**	**0.0156**	**0.0313**	0.5
H4K16ac	0.125	**0.0078**	**0.0156**	0.0625	0.0938	0.5

231

Figure 4.24: Bar graphs showing the semiquantitative intensity scores (mean ± 95% confidence intervals; maximum 3) for all epigenetic modification antibodies used in mouse brain. There values are shown for dentate gyrus, where there were no age-related differences (all ages combined). DNA cytosine modifications, total histone H4, all histone methylation PTMs, and H3K14ac showed stable immunoreactivity up to 72 hours post-mortem. H4K5ac showed a downward trend (not statistically significant) with increasing PMD. Other acetylation marks (H3K9ac, H3K27ac, H4K12ac and H4K16ac) tended to decrease by 24 hours and were significantly decreased by 48 hours post-mortem. P-values for all statistical comparisons are shown on the graph or at the bottom.

P Value	0 vs. 24	0 vs. 48	0 vs. 72	24 vs. 48	24 vs. 72	48 vs. 72
H3K9ac	0.25	0.0625	**0.0156**	0.125	**0.0313**	0.125
H3K14ac	0.5	0.5	0.5	0.5	0.5	0.375
H3K27ac	0.0625	**0.002**	**0.002**	**0.0156**	**0.0078**	0.1094
H4K5ac	0.25	0.25	0.0625	0.5	0.25	0.25
H4K12ac	0.5	**0.0156**	**0.0313**	**0.0156**	**0.0313**	0.5
H4K16ac	0.125	**0.0078**	**0.0156**	0.0625	0.0938	0.5

233
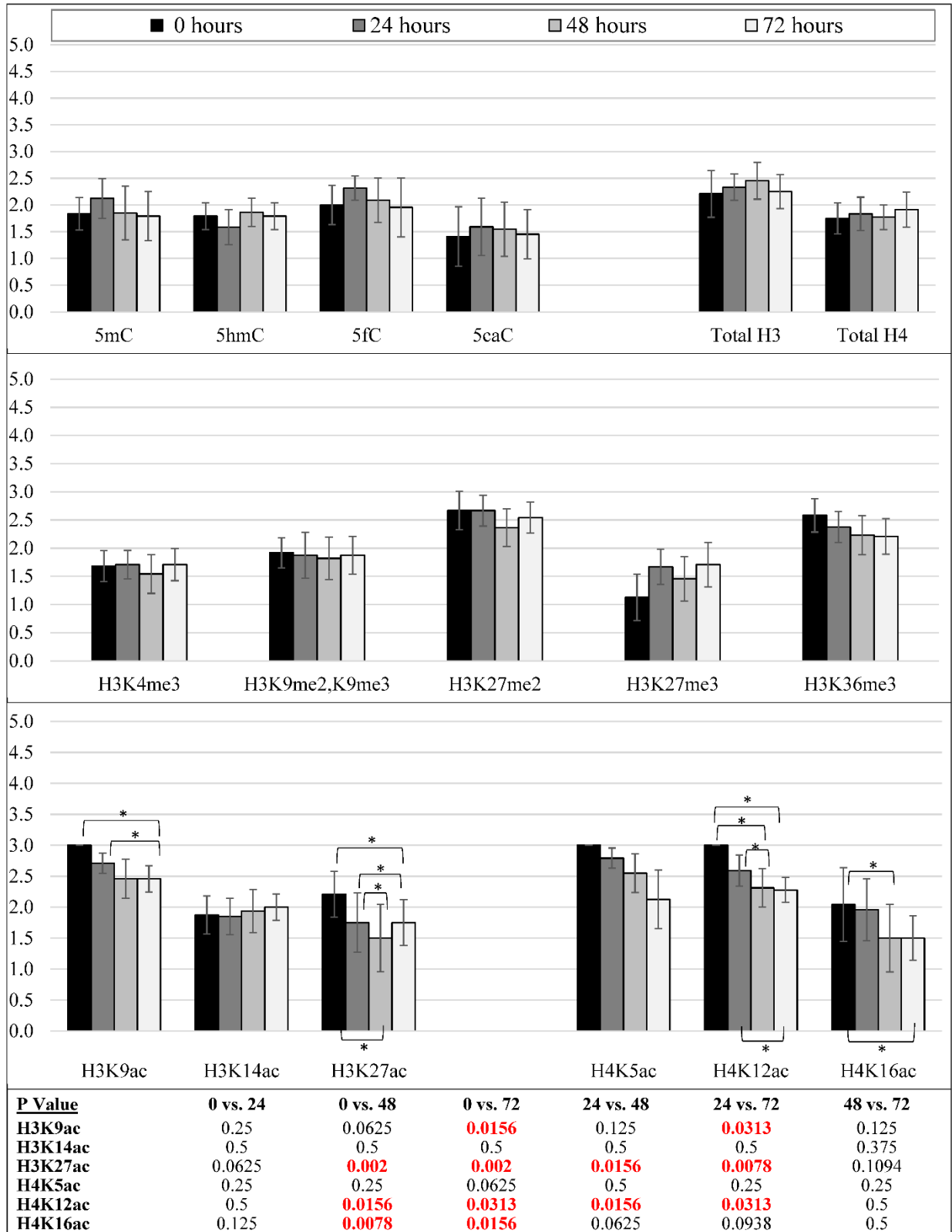
Table 4.12. Loss of epigenetic mark immunoreactivity among different cell types in neonatal pig temporal / parietal cortices.

Epigenetic Modification	Observed change (time point)	Nuclear Morphology				
		Large	Intermediate	Small round	Small irregular / longer	Endothelial / Smooth muscle
5mC	72 hour	minimal	minimal	minimal		
5hmC	72 hour			minimal		
5fC	72 hour					
5caC	72 hour	n/a				
H3K4me3	72 hour	minimal			minimal	Minimal
H3K9me2, K9me3	72 hour	minimal			minimal	
H3K27me2	72 hour	minimal				
H3K27me3	72 hour	minimal			minimal	
H3K36me3	72 hour					Minimal
H3K9ac	48 hour	moderate				
H3K14ac[A]	72 hour	n/a	minimal	minimal	minimal	
H3K27ac	72 hour	moderate	minimal	moderate		
H4K5ac	48 hour	moderate	minimal		minimal	
H4K12ac	48 hour	minimal			minimal	
H4K16ac	48 hour	minimal				
Total H3	48 hour	minimal	minimal	minimal	minimal	Minimal
Total H4	72 hour				minimal	

[A] large nuclei were not positively stained at 0 hour

A blank cell represents no change

Figure 4.25: Bar graphs showing the semiquantitative proportion scores (mean ± 95% confidence intervals; maximum 4) for all epigenetic modification antibodies used in neonatal pig neocortex. DNA cytosine modifications, total histone H4, all histone methylation PTMs, H3K14ac, and H4K12ac were stable up to 72 hours post-mortem. Total histone H3 declined after 48 hours post-mortem and was significantly decreased at 72 hours. H3K9ac was stable at 24 hours and decreased significantly thereafter. H3K27ac, H4K5ac, and H4K16ac had all declined by 24 hours and were significantly decreased by 48 hours. P-values for all statistical comparisons are shown on the graph or at the bottom.

Legend: ■ 0 hours ■ 24 hours ■ 48 hours □ 72 hours

Top panel (y-axis 0.0–5.0)
Categories: 5mC, 5hmC, 5fC, 5caC, Total H3, Total H4

Total H3 annotations:
p=0.0078 *
p=0.0156 *
*

Middle panel (y-axis 0.0–5.0)
Categories: H3K4me3, H3K9me2,K9me3, H3K27me2, H3K27me3, H3K36me3

Bottom panel (y-axis 0.0–5.0)
Categories: H3K9ac, H3K14ac, H3K27ac, H4K5ac, H4K12ac, H4K16ac
(significance markers * shown over several groups)

P Value	0 vs. 24	0 vs. 48	0 vs. 72	24 vs. 48	24 vs. 72	48 vs. 72
H3K9ac	0.5	**0.0313**	0.0625	**0.0313**	0.0625	0.5
H3K14ac	0.5	0.5	0.3125	0.5	0.25	0.375
H3K27ac	0.125	**0.0313**	**0.0313**	0.25	**0.0313**	0.0625
H4K5ac	**0.0313**	**0.001**	**0.0005**	**0.0078**	**0.0039**	**0.0078**
H4K12ac	0.5	0.5	0.5	0.5	0.5	0.5
H4K16ac	**0.0156**	**0.0039**	**0.0078**	0.125	0.1875	0.5

236

Figure 4.26: Bar graphs showing the quantitative analysis (mean ± 95% confidence intervals; maximum 100%) for nuclear immunostaining of selected epigenetic marks in neonatal pig neocortex. Data are shown separately for large round nuclei (neurons) and smaller irregular nuclei (glial cells and / or interneurons). 5mC was stable at all post-mortem times to 72 hours in both populations. H3K27me3 showed a slight decline in neurons by 48 hours. H3K9ac, H3K27ac, and H4K12ac declined in neurons, but not glial cells. H3K14ac declined in glial cells, but only rare neurons were labeled in the control state (0 hour). H4K5ac and H4K16ac were lost from both neurons and glial cells. P-values for all statistical comparisons shown at bottom.
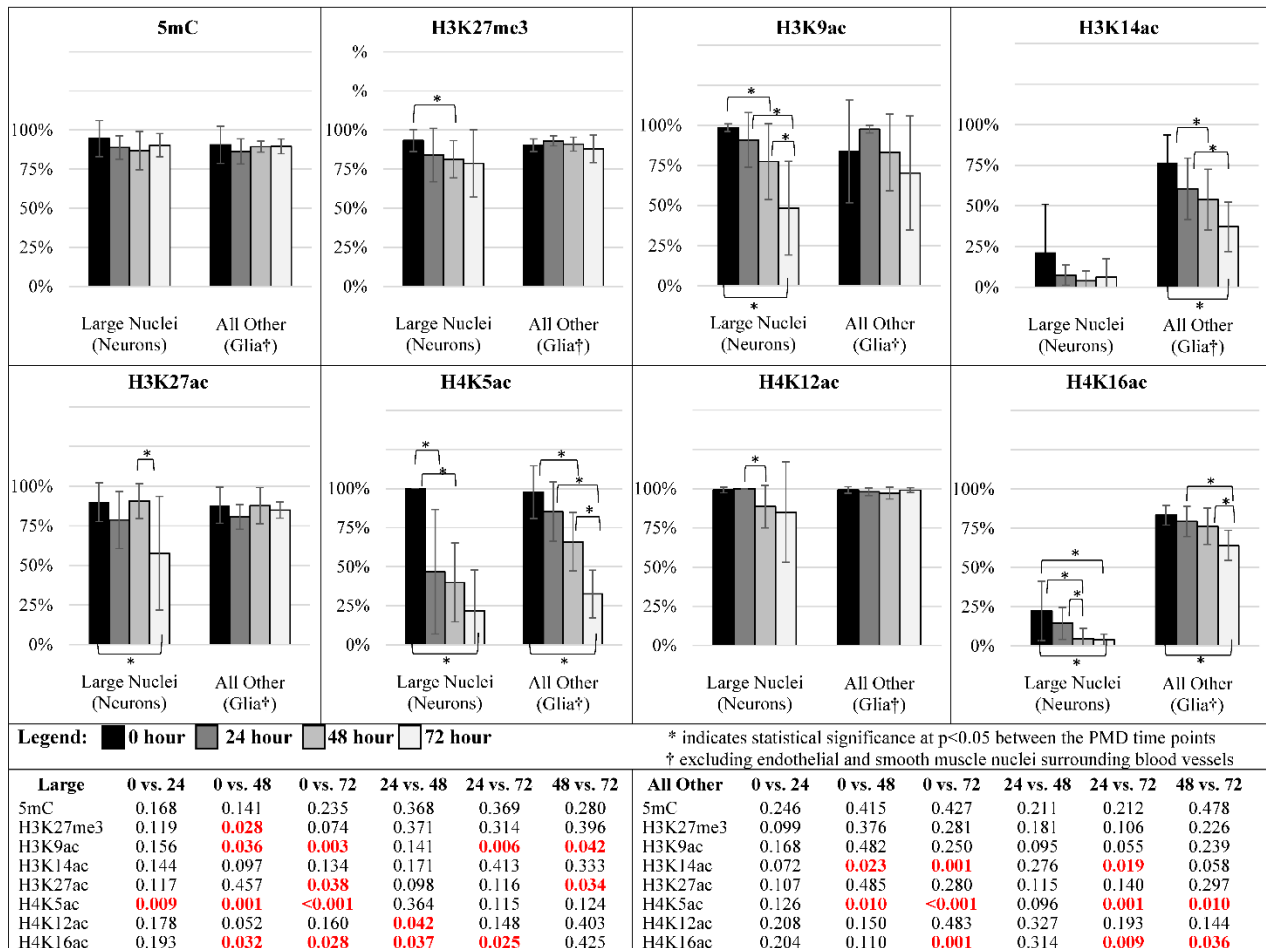
Figure 4.27: Bar graphs showing the semiquantitative proportion scores (mean ± 95% confidence intervals; maximum 4) for all epigenetic modifications in mouse brain dentate gyrus (all ages combined). DNA cytosine modifications and histone methylation were stable from 0 to 72 hours post-mortem. Total histone H3 and H4 labeling declined gradually after 48 hours. All of the acetylation modifications showed progressive declines by 24 hours, although not all of the trends were statistically significant. P values for all statistical comparisons shown at bottom. P-values for all statistical comparisons are shown on the graph or at the bottom.

P values	0 vs. 24	0 vs. 48	0 vs. 72	24 vs. 48	24 vs 72	48 vs 72
H3K9ac	0.5	**0.0313**	0.0625	**0.0313**	0.0625	0.5
H3K14ac	0.5	0.5	0.3125	0.5	0.25	0.375
H3K27ac	0.125	**0.0313**	**0.0313**	0.25	**0.0313**	0.0625
H4K5ac	**0.0313**	**0.001**	**0.0005**	**0.0078**	**0.0039**	**0.0078**
H4K12ac	0.5	0.5	0.5	0.5	0.5	0.5
H4K16ac	**0.0156**	**0.0039**	**0.0078**	0.125	0.1875	0.5

239
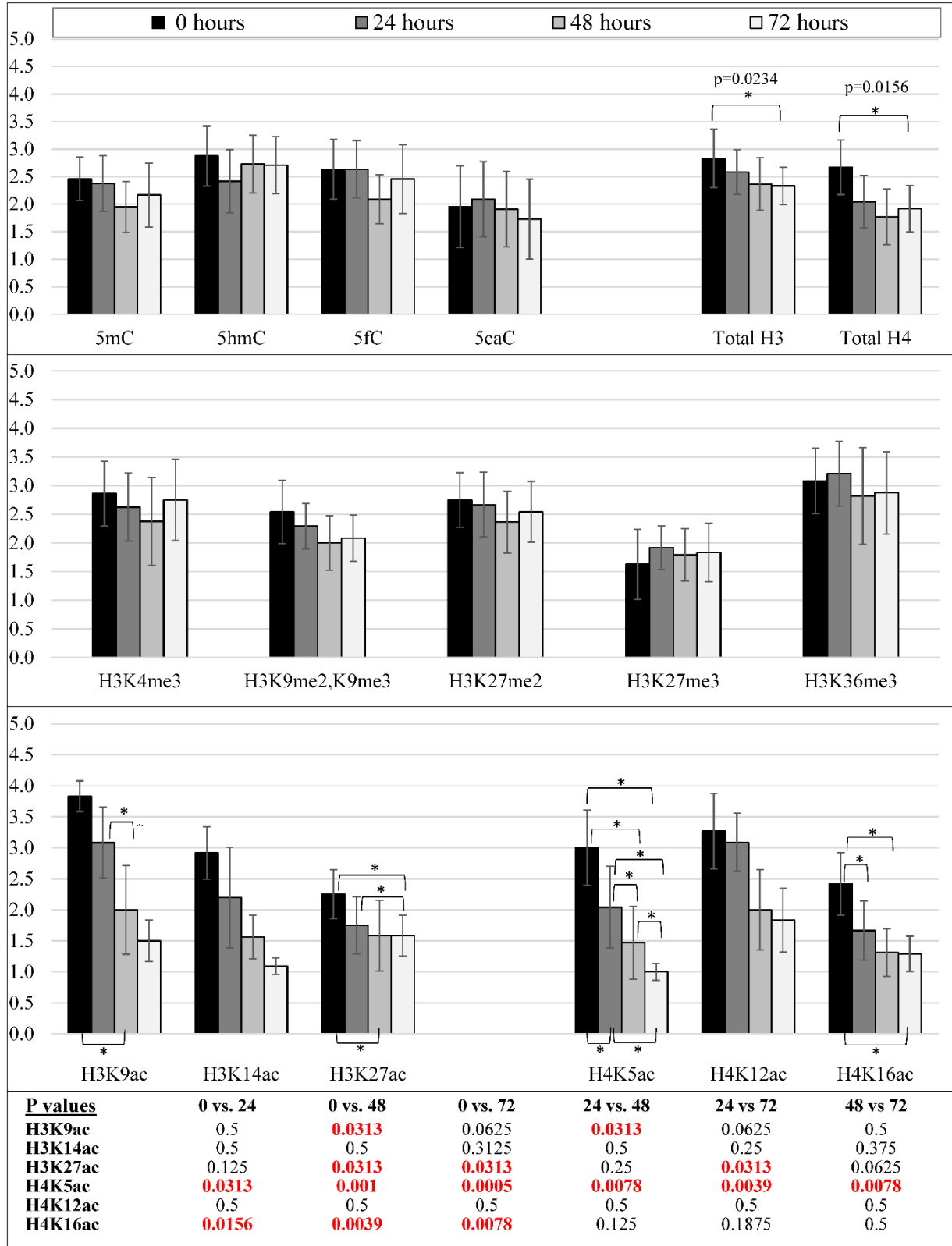
Table 4.13. Loss of epigenetic mark immunoreactivity among different cell types in young adult

mouse hippocampal dentate gyrus.

Epigenetic Modification	Observed change (time point)	Nuclear Morphology				
		Large	Intermediate	Small round	Small long / irregular	Endothelial / Smooth muscle
5mC	72 hour	minimal				
5hmC	72 hour					
5fC	72 hour					
5caC	72 hour	minimal				
H3K4me3	72 hour				minimal	minimal
H3K9me2, K9me3	72 hour	minimal			minimal	
H3K27me2	72 hour	moderate				
H3K27me3	72 hour	minimal			minimal	minimal
H3K36me3	72 hour				minimal	
H3K9ac	48 hour	moderate			minimal	
H3K14ac[A]	72 hour	minimal				minimal
H3K27ac	72 hour	minimal			minimal	
H4K5ac	48 hour	moderate				
H4K12ac	48 hour	moderate				
H4K16ac	48 hour	n/a				
Total H3	48 hour	minimal	minimal			
Total H4	72 hour	minimal	minimal		minimal	

[A] large nuclei were not positively stained at 0 hour
A blank cell represents no change

Figure 4.28: Representative immunohistochemical detection of epigenetic marks in human neocortex tissue microarray. Column A shows control temporal lobe obtained from a nonpathological surgical specimen that was fixed < 1 hour after devitalization. Column B shows a frontal lobe specimen from a person who survived in coma for 7 days after a severe hypoxic insult and whose autopsy (i.e. delay to fixation) was performed 31 hours after death. Column C shows a nonpathological frontal lobe specimen from a person who died immediately after trauma and whose autopsy was performed 4 days after death. For all antibodies shown, in the control tissue almost all nuclei (except for those of scattered endothelial cells) are immunoreactive. 5mC immunoreactivity (top row) was reduced in some hypoxic neurons (arrow) and some small nuclei after prolonged delay to fixation (arrowhead). H3K27me3 (second row) immunoreactivity was unchanged in hypoxic brain (although cell shapes were altered). After prolonged delay to fixation, a few small nuclei were negative (arrowhead). H3K14ac immunoreactivity was diminished in approximately half the cells in hypoxic brain (arrows) and many neurons in the delayed fixation brain (arrowheads). H4K5ac immunoreactivity was unchanged in hypoxic brain but showed diminished intensity in the delayed fixation brain (arrowheads). Images taken at 200x magnification. DAB detection of antibody (brown) and hematoxylin counterstain (blue).

242
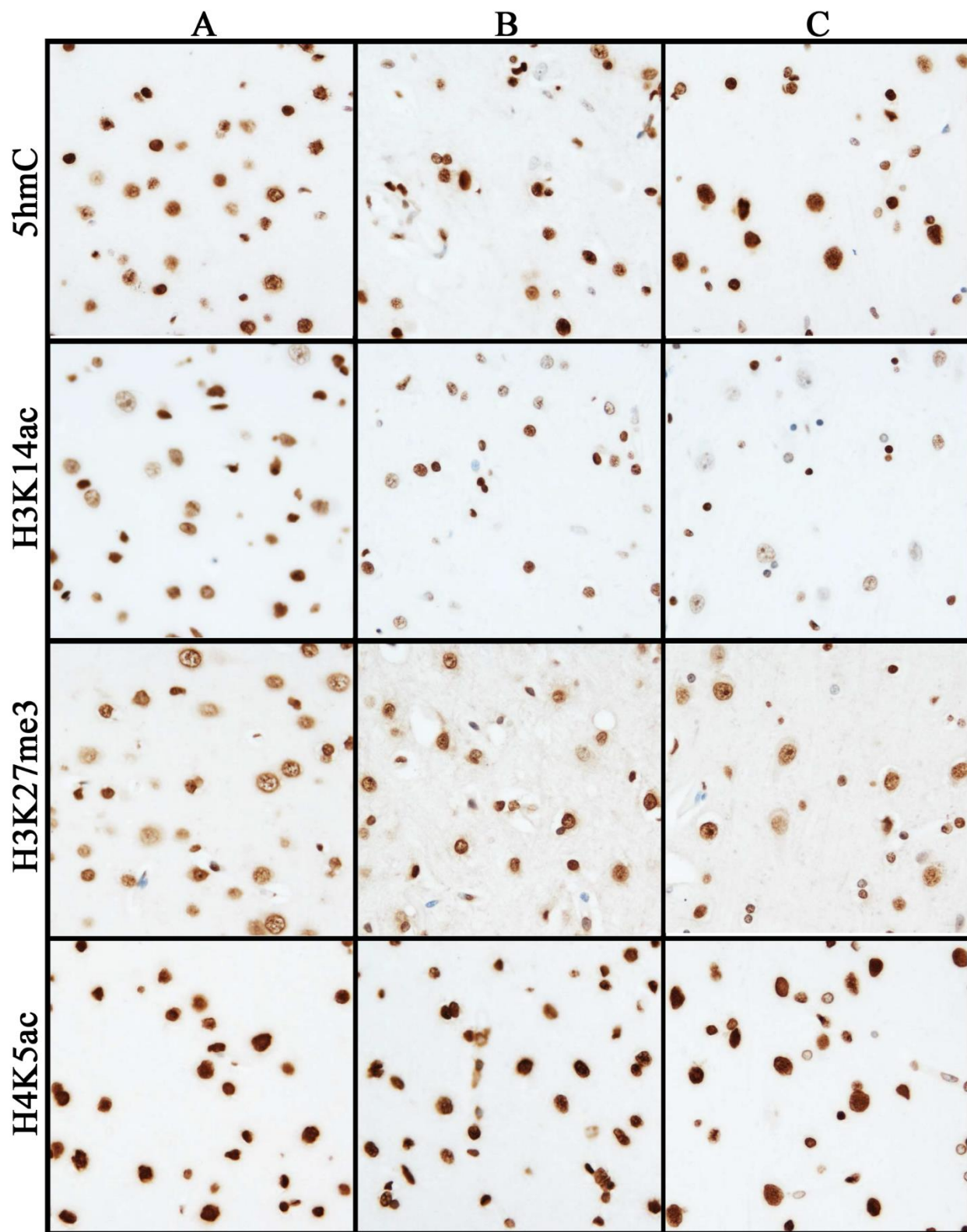
Table 4.14: Changes in epigenetic mark immunoreactivity - human neocortex tissue microarray samples.

	Normal			Subacute hypoxic changes
Epigenetic Modification	3 days post-mortem	4 days post-mortem	5 days post-mortem	31-43 hours post-mortem
5mC	No change	No change	No change	Cytoplasm leakage
5hmC	No change	No change	No change	Few (-) small nuclei
5fC	No change	No change	Moderate decrease; glial & neuronal	No change
5caC	No change	No change	Moderate decrease; neuronal	Few small nuclei are (-)
H3K4me3	Minor cytoplasmic labeling	Minor decrease, neuronal	Minor decrease, neuronal	Cytoplasm leakage
H3K27me3	No change	Few (-) glial cells	No change	No change
H3K36me3	No change	Minor decrease; glial & neuronal	Minor decrease; glial & neuronal	Minor decrease; neuronal
H3panAc	No change	Minor decrease; glial & neuronal	Minor decrease; glial & neuronal	Minor decrease; glial & neuronal
H3K9ac	No change	Minor decrease; glial	Minor decrease; glial & neuronal	Few small nuclei are (-)
H3K14ac	Minor decrease; glial & neuronal	Minor decrease; glial Moderate decrease; neuronal; few (-) neurons	Minor decrease; glial, Moderate decrease; neuronal; few (-) neurons	Minor to moderate decrease; glial & neuronal; few (-) neurons
H3K27ac	Minor decrease; glial	Few small nuclei are (-)	Few small nuclei are (-)	Few small nuclei are (-)
H4K5ac	No change	Moderate decrease; glial & neuronal	Few small nuclei are (-)	No change
H4K12ac	No change	No change	No change	No change

NOTE: There were no obvious differences between the specimens obtained surgically and fixed <1 hour after devitalization and the autopsy samples that were fixed ≤2 days after death, unless there were also changes due to hypoxic-ischemic brain damage.

Table 4.15: Summary of the immunoreactivity stability of histone acetylation, histone methylation, and DNA cytosine modifications in brain samples*.

Epigenetic Modification	IHC Human - Cx	IHC - Immunoreactivity		IHC – Proportion		IHC – Counts		Western blot
		Pig – Cx	Mouse - DG	Pig – Cx	Mouse - DG	Neurons	Glia	Pig – Cx
5mC	120	72	72	72	72	72	72	n/a
5hmC	120	72	72	72	72	-	-	n/a
5fC	96	72	72	72	72	-	-	n/a
5caC	96	72	72	72	72	-	-	n/a
H3K4me3	72	72	72	72	72	-	-	72
H3K9me2/K9me3	nd	72	72	72	72	nd**	nd**	No signal**
H3K27me$_3$	72	72	72	72	72	48	72	72
H3K36me$_3$	72	72	72	72	72	-	-	48
H3K9ac	72	48	48	24	24	24	72	Wrong mw
H3K14ac	53	72	72	72	72	72	48	Low signal
H3K27ac	53	24	24	24	24	48	72	Wrong mw
H4K5ac	72	72	48	24	<24	<24	24	<24
H4K12ac	120	24	24	72	72	48	72	24
H4K16ac	nd	24	24	24	<24	24	48	No signal
Total H3	nd	24	72	48	48	-	-	72h
Total H4	nd	72	72	72	48	-	-	72h
H3panAc	72	nd	nd	nd	nd	nd	nd	24h

Abbreviations: IHC = immunohistochemistry; Cx = neocortex; DG = dentate gyrus of hippocampus; nd = not done; n/a = not applicable; - = not counted; mw = molecular weight

* Numeric values represent hours post-mortem to formalin fixation (or freezing for Western blots) at which there are no differences compared to samples that were fixed or frozen immediately after death.

** H3K9me2,K9me3 antibody was discontinued; H3K9me2 replacement antibody could not be optimized

CHAPTER 5: MANUSCRIPT 3 - DNA METHYLATION AND HISTONE POST-TRANSLATIONAL MODIFICATIONS IN HUMAN AND NON-HUMAN PRIMATE BRAIN FOLLOWING PRENATAL ALCOHOL EXPOSURE

Authors: Jessica S. Jarmasz, Hannah Stirton, James R. Davie, Duaa Basalah, Sterling K. Clarren, Susan J. Astley, Marc R. Del Bigio

In preparation for submission to journal.

Preface

This publication was the result of the third research aim.

Authors' contributions: JSJ conducted almost all the research, put all results together, and wrote the manuscript. HS performed some of the Macaque immunostaining and imaging. DB analyzed oxidative changes in brain tissue (supplement with results to be included) and reprocessed the monkey brain tissue. SJA and SKC provided the Macaque brain samples and will be contributing to the discussion. JRD provided guidance over the selection of markers and will be contributing to the discussion. MRD planned the project, provided financial support, effectuated the statistical analysis and will finalize the manuscript.

ABSTRACT

The neurodevelopmental abnormalities associated with prenatal alcohol exposure

(PNAE) / fetal alcohol spectrum disorder have been attributed, at least in part, to epigenetic

modifications. There is considerable work in animals and several epigenetic analyses of non-

neural tissues in humans. However, there are no direct analyses of human brain tissue. PNAE

and age-, sex-, and post-mortem delay matched control fetuses and infants (n=18 pairs; 21 to

70.5 weeks post-conception) who had undergone autopsy, along with comparable tissue from a

macaque monkey model of PNAE (n=6 pairs), were assessed by immunohistochemical detection

of epigenetic markers. We focused on the temporal lobe including the ventricular and

subventricular zone, ependyma, temporal cortex, temporal white matter, dentate gyrus and CA1

neurons. We used antibodies targeting 4 DNA cytosine, 4 histone methylation, and 6 histone

acetylation modifications, and analyzed them semiquantitatively. Human PNAE demonstrated

statistically significant increases among epigenetic marks 5mC, 5fC, H3K27me3, H3K36me3,

H3K9ac, H3K14ac and H3K27ac in various brain regions. Statistically significant decreases

were seen among epigenetic marks 5mC, 5caC, H3K4me3, H3K27me3, H3K36me3, H3K9ac,

H3K14ac, H3K27ac, H4K5ac, H4K12ac, and H4K16ac. No statistically significant differences

were seen for epigenetic mark 5hmC. H3K4me3 (active transcriptional mark) was decreased in 5

of the 7 brain regions studied. In the macaques, PNAE was associated with statistically

significant decreases of epigenetic marks 5fC, 5caC, H3K9ac, H3K9me2/K9me3, and

H3K36me3 in the ependyma. Both the human infant and macaque PNAE brains showed overlap

in H3K9ac (ependyma) and in H3K36me3 (white matter), which demonstrated decreases.

These effects are region specific and appear to coincide with the development of neuronal

and glial cells. These results support the general hypothesis that PNAE is associated with an

overall decrease in DNA methylation, a decrease in histone methylation, and an increase in histone acetylation. However, interspecies comparisons are likely extremely difficult.

INTRODUCTION

An estimated 10-15% of women in North America consume alcohol (ethanol) during pregnancy (Popova, Lange, Probst, et al., 2017). Prenatal alcohol exposure (PNAE) is associated with spontaneous abortion, sudden unexplained death of an infant (SUDI), and Fetal Alcohol Spectrum Disorder (FASD). Individuals with FASD demonstrate neurodevelopmental malformations, cognitive deficits, as well as social and behavioural problems (Carson, Cox, Crane, et al., 2010; Reynolds, Weinberg, Clarren, et al., 2011). The global prevalence of FASD is 7.7 per 1,000 people (Lange, Probst, Gmel, et al., 2017).

Human neuroimaging studies (MRI) have demonstrated a wide range of brain abnormalities in individuals diagnosed with FASD including micrencephaly, abnormal gyral patterns, corpus callosum abnormalities, cortical thinning, and reductions in regional brain volume (e.g. basal ganglia, diencephalon, cerebellum) (Donald, Eastman, Howells, et al., 2015; Jacobson, Jacobson, Molteno, et al., 2017; Moore, Migliorini, Infante, et al., 2014; Nardelli, Lebel, Rasmussen, et al., 2011; Norman, Crocker, Mattson, et al., 2009). In our recent study of 174 human autopsy cases with PNAE or FASD (Jarmasz, Basalah, Chudley, et al., 2017), among the fetal, stillborn, and infant cases (n=116) we identified: micrencephaly in 18 cases, neural tube defects in 5, heterotopias in 4, hydrocephalus (only) in 4, hydrocephalus and partial agenesis of the corpus callosum in 1, and alobar holoprosencephaly in 1 (Jarmasz, Basalah, Chudley, et al., 2017).

The pathogenesis of PNAE / FASD-associated brain anomalies is not well understood. Many have suggested that epigenetic modifications are involved (Chater-Diehl, Laufer, & Singh, 2017; Lussier, Weinberg, & Kobor, 2017). Epigenetics includes a range of acquired and inheritable chemical modifications found within and surrounding (i.e. histones) the genome that

influence gene expression without direct changes to the nucleotide sequence of DNA (Feinberg, 2018). Epigenetics plays a substantial role in DNA replication and transcription, genomic imprinting, cellular differentiation, and cell death. Epigenetic processes include chromatin remodeling, RNA interference (micro RNAs), and covalent reversible chemical modifications to DNA (DNA cytosine modifications) or to histones (post-translational modifications - PTMs). Together this is dubbed the "epigenome" (Feinberg, 2018).

Within the central nervous system (CNS), differentiation of neural stem / precursor cells into neurons, astrocytes, and oligodendrocytes is epigenetically driven (Coskun, Tsoa, & Sun, 2012; Hirabayashi, & Gotoh, 2010; Liu, Moyon, Hernandez, et al., 2016). For example, neural genes are activated through histone acetylation, whereas pluripotent genes and non-neural genes are repressed through histone methylation and DNA methylation (Hirabayashi, & Gotoh, 2010). Recent reviews have summarized the epigenetic effects, mainly DNA methylation and histone PTMs, in brains of rodents exposed to alcohol in the pre- and post-natal (human third trimester equivalent) periods (Chater-Diehl, Laufer, & Singh, 2017; Laufer, Chater-Diehl, Kapalanga, et al., 2017; Lussier, Weinberg, & Kobor, 2017). For a summary of all epigenetic PNAE studies, please see **Table 5.1**, for DNA modifications, and **Table 5.2** for histone PTMs findings.

To the best of our knowledge, PNAE-associated epigenetic changes have not been directly assessed in human brain tissue. In this study, a cohort of 18 PNAE and matched control fetuses (20 to 41 weeks post-conception (PC)) and infants (43-70.5 weeks PC) who had undergone autopsy (Jarmasz, Basalah, Chudley, et al., 2017) were investigated by immunohistochemistry using antibodies targeting 4 DNA cytosine modifications, 4 histone methylation modifications, and 8 histone acetylation modifications. We focused on the temporal lobe including the hippocampus, due to its distinct and unambiguous cryoarchitecture. In

parallel, we studied the temporal lobe from macaques exposed *in utero* to alcohol (2.5 – 4.1g/kg

maternal bodyweight) or isocaloric sucrose (6 pairs total) between gestational weeks 5-24.

Offspring were sacrificed at 5.7 to 7.2 months of age (along with age- and sex-matched controls).

We hypothesized that PNAE is associated with epigenetic changes in brain cells that persist

postnatally.

METHODS

Human Autopsy Cases

Appropriate ethics approval was obtained from the University of Manitoba Research Ethics Board (#HS1311 – H2011:213). Details of the full PNAE / FASD autopsy cohort (N=174) were described previously (Chapter 3) (Jarmasz, Basalah, Chudley, et al., 2017). Because our hypothesis concerns epigenetic changes associated with PNAE, and because epigenetic changes can occur during postnatal life (Kundakovic, & Champagne, 2015), we restricted our study to fetuses and infants <1 year. Exclusion criteria were: no availability of formalin-fixed paraffin-embedded (FFPE) brain sample(s), extensive autolysis of brain tissue, severe hypoxic damage, cases dated <1988 (inconsistent FFPE), known gene mutations or chromosomal abnormalities, major brain malformations, bacterial meningitis, or post-mortem delay (PMD) >48 hours (which was determined to have adverse effects on histone acetylation marks in our recent study (Jarmasz, et al., 2018, accepted for publication, Chapter 4 manuscript). Age- and sex-matched controls were selected from the same autopsy database. Sex matching is important because there are documented differences in brain size, neurological disease prevalence, epigenetics, and stress response (Dekaban, 1978; Kigar, & Auger, 2013; Menger, Bettscheider, Murgatroyd, et al., 2010; Shen, Ahern, Cheung, et al., 2015). Inclusion criteria for age and sex-matched controls were: the case year had to be accrued within 10 years of the PNAE case, suffered little to no brain trauma, had no brain abnormalities, and have a PMD of ≤48 hours. A recent case not described in the previous publication was included because the documented PNAE exposure was high despite not meeting the ≤48 hour PMD inclusion criteria. The PNAE cohort consisted of 9 fetuses or premature births with gestational age <42 weeks and 9 infants age 43 to 70.5 weeks PC, along with controls. PNAE cohort epidemiologic and pathologic details are described in

Table 5.3. PNAE and control pairings are described in **Table 5.4**. FFPE medial temporal lobe blocks stored at the pathology department (Health Sciences Centre, MB) were cut by microtome (5-6μm thick) and mounted onto charged slides for immunohistochemistry.

Non-Human Primate PNAE Brains

The *Macaca nemestrina* model of PNAE was developed in the early 1980's (Bonthius, Bonthius, Napper, et al., 1996; Clarren, Astley, Bowden, et al., 1990; Clarren, Astley, & Bowden, 1988; Clarren, Bowden, & Astley, 1987; Sheller, Clarren, Astley, et al., 1988). Briefly, 48 pregnant adult female pig-tailed macaques received weekly nasogastric doses of alcohol ranging from 0.3 to 4.1 g/kg bodyweight of ethanol; the latter is roughly equivalent to 16 standard distilled liquor drinks in a human (i.e. a binge exposure). High doses (2.5, 3.3, and 4.1g/kg weekly) of alcohol were started at 33 to 46 days of gestation because of the high risk of spontaneous abortion (determined in a previous pilot study) (Clarren, Bowden, & Astley, 1987). Controls received isocaloric sucrose. Thirty-three viable infants were born and subsequently assessed for overall health and features of the Fetal Alcohol Syndrome (FAS) phenotype (Clarren, Astley, & Bowden, 1988). FAS (and relevant diagnostic criteria) was the primary diagnostic term at the time. The monkeys were killed at 5.7 to 7.2 months of age, which is the human brain development equivalent of 2.7 to 3.5 years of age (http://translatingtime.org/translate). A series of intramuscular injections of ketamine (10-15mg/kg body weight) as well as intravenous chloral hydrate (40mg/kg) administration through the saphenous vein were given until adequate sedation was achieved (Clarren, Astley, Bowden, et al., 1990). The entire dissection was completed in less than 8 minutes from the moment the calvarium was removed and the superior sagittal sinus was ruptured. The optic globes were

enucleated with the optic nerves and the brain was removed, weighed fresh and inspected for gross abnormalities. The cerebral hemispheres were bisected along the midsagittal plane and further dissected to produce multiple brain regions of interest for various studies. The right hemisphere was placed in 10% neutral buffered formalin for neuropathological study. After fixation (unknown duration), the hemisphere was sectioned into 5mm slices, examined, photographed and then processed and embedded in paraffin (Clarren, Astley, Bowden, et al., 1990). FFPE tissue blocks archived at the University of Washington were transferred to the senior author's (MDB) laboratory. The samples consisted of 6-8 coronal slices (each ~3mm thick) of one cerebral hemisphere extending from the occipital lobe tip to frontal lobe at the level of the posterior striatum. In all cases, at least one slice included temporal lobe, hippocampus, and nearby thalamus. The duration of the tissue immersion in formalin prior to paraffin embedding had not been documented and the paraffin was brittle. Therefore, tissue blocks of interest were heated at 60°C for 30 minutes and re-embedded in new paraffin. We utilized the three highest PNAE levels (2.5, 3.3 and 4.1g/kg; N=6) along with age- and sex-matched controls (sucrose exposure only; N=5; one male control was used twice) (see **Table 5.5**).

Antibodies to Epigenetic Modifications

We selected antibodies to epigenetic modifications that are known to occur in the brain, and / or have been reported to be affected by alcohol exposure in the prenatal, postnatal immature, or adult periods in either human brain cell lines or rodent brains (Chater-Diehl, Laufer, & Singh, 2017; Laufer, Chater-Diehl, Kapalanga, et al., 2017; Lussier, Weinberg, & Kobor, 2017). These include: 5-methylcytosine (5mC), 5-hydroxymethylcytosine (5hmC), 5-formylcytosine (5fC), 5-carboxycytosine (5caC), histone trimethylated at lysine 4 (H3K4me3),

H3K9me2/K9me3, H3K27me3, H3K36me3, histone acetylated at lysine 9 (H3K9ac), H3K14ac, H3K27ac, H4K5ac, H4K12ac, H4K16ac. We also included antibodies targeting total histone H3 and H4, as well as pan-acetyl H3 and H4. Rationale for inclusion of DNA / histone modifications in this study, as well as technical details of the antibodies are presented in **Table 5.6** and **Table 5.7**.

Immunohistochemistry

Human and macaque brain tissue sections (5-6 µm thickness) were subjected to immunohistochemistry which is previously described in greater detail in Chapter 4 manuscript (page 172). Optimal primary antibody concentration was determined by running a series of dilutions greater and less than the manufacturer's suggestions (see **Table 5.8** for specific immunostaining conditions). Briefly, paraffin was melted at ~60°C, and tissue samples were rehydrated through multiple xylenes and graded ethanol solutions (100, 90 and 75%). Slides were subjected to antigen retrieval, as well as endogenous peroxidase blocked before incubation with 10% serum. The primary antibody was applied, followed by application of the secondary antibody, followed by application of peroxidase-conjugated streptavidin (with multiple washes in between each application). DAB (3,3' diaminobenzidine) chromogen was used to develop the slides. The slides were counterstained with Harris hematoxylin solution, dehydrated through graded ethanol and multiple xylene solutions, coverslipped with Permount, and left to air dry overnight.

Imaging of Immunohistochemical Results

Slide images were captured at 40x, 200x, and 400x, using a standard upright microscope with digital camera (Olympus BX51TRF microscope; Qimaging 32-0110A-568 MicroPublisher 5.0, Model LH100HG) with QCapture software (v2.8.1, 2001-2005, Qimaging Corp.). The dentate gyrus (DG), CA1 neurons of the hippocampal formation, ependymal cells along the floor of the temporal horn of the lateral ventricle (TE), temporal neocortex (CX) in the parahippocampal gyrus, and temporal white matter (WM) were evaluated. In fetuses 34 weeks and younger, the germinal region along the roof of the lateral ventricle including the ventricular zone (VZ) and subventricular zones (SVZ) were also evaluated. Two semiquantitative scales were previously developed to estimate the proportion of immunoreactive nuclei (graded 4 to 0) (**Figure 4.7** in previous chapter) and the intensity of immunoreactivity (graded 3.5 to 0) (**Figure 4.8** in previous chapter) at 400x magnification. Morphologic features of nuclei were used as a surrogate for probable brain cell type (**Figure 4.9** in previous chapter). First, control cases were examined in order to establish a general developmental pattern of expression for the epigenetic marks. During the mid to late gestation fetal period (21-34 weeks PC), the brain morphology and anatomical distribution of immunoreactivity changed dramatically. Afterward (i.e. term birth to infancy), the pattern of expression remained relatively stable. Not all epigenetic marks were quantified in every single infant. For example, focal tissue damage or imperfections in the immunostaining would preclude proper evaluation. Thirteen of 18 controls (but not necessarily the same 13 pairs for all marks) were scored against matched PNAE pairs. The immunoreactivity scores (proportion and intensity) for every brain region was recorded in an Microsoft Excel spreadsheet. Cells representing cases that were not examined remained blank.

Images and Statistical Analysis

For the humans, images were acquired at either 20x, 200x or 400x magnifications for 13 antibodies in 7 brain regions: temporal cortex (parahippocampal gyrus) (CX), temporal lobe white matter (WM), ventricular zone in the roof of the temporal horn (VZ), subventricular zone (SVZ) in the roof of the temporal horn, ependyma on the floor of the temporal lateral ventricle (TE), CA1 neurons of the hippocampal formation (CA1), and dentate gyrus neurons (DG). Intensity score (3.5-0) and distribution score (4-0) were multiplied (maximum score of 14). Bar graphs were produced in Microsoft Excel using the control data (Y-axis = total multiplied rank, X-axis = post-conception age in weeks). Polynomial trendlines were added to depict the general pattern of developmental expression of each epigenetic mark (see **Figure 5.1**). PNAE data curves were included to visualize possible differences. Data were subjected to multiple comparisons: across all ages, within the fetal group and infant group separately, and within 4 age clusters (21-25 weeks PC fetuses, 31-40 weeks PC fetuses, 43-48.5 weeks PC infants, and 53-70.5 weeks PC infants. Paired t-test (two-tailed) was used to compare the overall group and the age subsets (JMP 13.0 statistical software; SAS Institute, Cary NC). Differences were considered statistically significant if $p<0.05$ and trends were noted if $p<0.075$.

For the macaque brains, images were acquired at 400x magnification for 13 antibodies in 5 brain regions: temporal cortex (parahippocampal gyrus; CX), temporal lobe white matter (WM), ependyma on the floor of the temporal lateral ventricle (TE), CA1 neurons of the hippocampal formation (CA1), and dentate gyrus (DG) neurons. Images were assigned an intensity score (3.5-0) and distribution score (4-0) (as described above in human tissue section of methods), which were then multiplied (maximum score of 14). Two tailed t-test was used to compare control and PNAE groups for each location and each antibody (JMP 13.0 statistical

software; SAS Institute, Cary NC). Statistically significant differences were considered at p<0.05 and trends were considered at p<0.075.

RESULTS

Graphical representation of the human control and PNAE results is shown in **Figures 5.2-5.6**. Polynomial curves were fit to the data to all location / epitope combinations because they provide a convenient way for visualizing and comparing the data sets. However, because the data actually represent two biologically different populations (i.e. stillborn fetuses with uncertain post-mortem *in utero* conditions vs. liveborn infants) a formal polynomial regression fit to compare the curves would not be valid. Statistically significant differences between human control and PNAE pairings are summarized in **Table 5.9** and statistically significant differences between monkey control and PNAE pairings are summarized in **Table 5.10**. Below we will describe main points concerning the developmental expression of epigenetic marks in control human temporal lobes.

Developmental Expression – Human Brain

General observations were made regarding certain cell types and brain regions. Most antibodies against epigenetic marks strongly labeled a narrow band of cells at the neocortical surface from the earliest age studied (21 weeks); the exceptions were moderate to faint immunoreactivity with anti-5mC and anti-5hmC (see **Figure 5.7**). As the human brain matured, marks that are expressed in the cortical mantle tended to progress with increasing depth from the surface. The VZ and SVZ were of particular interest because they give rise to most brain cell populations and FASD is considered to be a neurodevelopmental abnormality. Developmental expression of epigenetic marks in the VZ varied considerably; 7/13 epigenetic marks (5mC, 5hmC, H3K4me3, H3K36m3, H3K9ac, H3K14ac, H4K5ac) exhibited a 'U' shape curve prior to disappearance of the VZ at 31-34 weeks (**Figures 5.2-5.5, 5.8** and **5.9**). It is possible that this

pattern is an artifact of small sample size. In the SVZ, most marks started at low levels, and increased with increasing gestational age (5caC, H3K4me3, H3K36me3, H3K9ac, H4K5ac, H4K12ac) (**Figures 5.2-5.5**, and **5.9**). An anatomical gradient was evident for 5mC, H3K4me3, H3K36me3, H3K9ac, H3K14ac, H3K27ac, H4K5ac, H4K12ac, and H4K16ac, where the superficial SVZ adjacent to the VZ was initially positive with progression to involve the entire SVZ with maturation until it disappeared at 34 weeks gestation. Among the remaining brain regions (CX, WM, DG, CA1), 7 epigenetic modifications (5mC, 5hmC, H3K4me3, H3K27me3, H3K9ac, H4K5ac, H4K12ac) demonstrated the same developmental pattern, with a rapid increase from mid gestation, peaking at birth, followed by a minimal decrease with increasing age (inverted "U" patterns; **Figures 5.2-5.5**).

Some differences were observed with respect to the morphologic cell type. The epigenetic marks 5mC, 5caC, H3K4me3, H3K27me3, H3K36me3, H3K9ac, and H4K12ac were identified in essentially all cell types including neurons and glial cells. 5hmC was specific to hippocampal, white matter and large cortical neurons. 5fC and H4K16ac were preferentially expressed in smaller nuclei, presumed to be those of astroglial and / or oligodendroglial cells. The distribution of H3K14ac positive nuclei switched during development; immature neurons were mainly positive and became negative as they matured while glial cells became positive in infancy. For H3K27ac and H4K5ac, immunoreactivity among neurons and glial cells was equally strong from 21 weeks gestation to term, then after 1 month of age, neurons lost their intensity. For 5mC, 5hmC, H3K27me3, H3K36me3, H3K9ac, H4K16ac, the dentate neurons occasionally demonstrated a maturation gradient, where more mature nuclei distant from the germinal layer were positive while smaller less mature nuclei were negative. For H3K4me3, as

neurons matured, the proportion of positive nuclei was greater, but the intensity decreased with maturation.

With almost every antibody, vascular endothelial cells and arterial smooth muscle cells lining blood vessels were an apparently random mix of positive and negative cells; the exceptions were almost uniform negativity for 5mC and 5hmC (**Figure 5.10**). Almost every antibody labeled epithelial cells of the choroid plexus (**Figure 5.10**). Nuclei of the temporal horn ependyma were ~75% positive for most marks (**Figure 5.10**). However, there were changes in the epigenetic labeling pattern of ependymal cells in association with PNAE.

Technical Difficulties

For total histone H3 and H4 antibodies, we expected the antibodies to label virtually every nucleus at all stages of maturation. Surprisingly, this was not the case (**Figure 5.11**). Similarly, we expected that histone H3 and H4 pan-acetyl antibodies would label more cells than any antibody that targets a single acetylated lysine. However, some of the single histone acetylation antibodies labeled almost all nuclei (e.g. anti-H3K27ac, H4K12ac) but the proportion of cells labeled by anti-pan-acetyl histone was much less (**Figure 5.11**). Because these antibodies do not label what is expected, we did not undertake a detailed analysis.

Human and Macaque Control Versus PNAE Statistical Comparisons

Statistically significant differences between human control and PNAE pairings are summarized in **Table 5.9**. In association with PNAE in humans, increased levels of 4 different histone modifications (H3K9ac, H3K27ac, H3K27me3, H3K36me3) along with 5mC were observed in the SVZ, and decreased levels of 2 marks (5caC, H4K16ac) were observed.

Temporal cortex (a mix of neurons and glial cells), white matter (predominantly glial cells) (**Figure 5.12**), and ependymal cells exhibited decreases in several different histone modifications (5mC, H3K4me3, H3K36me3, H3K9ac, H3K14ac, H3K27ac, H4K5ac, H4K16ac). Ependymal cells also exhibited increases in 5fC and H3K36me3. In CA1 neurons, a similar spectrum of histone modification decreases (5mC, H3K4me3, H3K27ac) were observed. In the dentate gyrus neurons, a mix of decreased histone methylations (**Figure 5.13**) and increased histone acetylations were observed. H3K4me3 exhibited a decrease in 5 of the 7 brain regions studied (**Figures 5.12** and **5.13**).

Statistically significant differences between monkey control and PNAE groups are summarized in **Table 5.10**. H3K36me3 was significantly decreased in all 5 brain regions examined. In the CA1 neurons, H3K27me3 was decreased and H4K12ac was increased (**Figure 5.14**). The ependymal cells showed the statistically significant decreases in 6 different epigenetic marks (5fC, 5caC, H3K9ac, H3K9me3 / K9me2, H3K27me3; see **Figure 5.15**).

Comparison of the human infant and macaque brain findings shows overlap in H3K9ac temporal ependyma as well as in H3K36me3 white matter which both showed a decrease in immunoreactivity. 5hmC also showed no effect in both humans and macaques.

DISCUSSION

Epigenetic modifications play a substantial role in brain development, guiding the specification, differentiation, and maturation of neural progenitor cells (NPCs). NPCs in the mouse neural tube gain 5mC during specification, gain 5hmC during differentiation, and then lose 5mC in the later stages of maturation (Zhou, 2012). Similarly, in dentate granule neurons of the developing mouse hippocampus, a methylation gradient correlates with the outside-in pattern of neuronal maturation (Yuanyuan Chen, Ozturk, & Zhou, 2013). Studies in rat and mouse have demonstrated associations between brain development and histone PTM changes (Cho, Kim, Kim, et al., 2011; Hahn, Qiu, Wu, et al., 2013; Podobinska, Szablowska-Gadomska, Augustyniak, et al., 2017; Resendiz, Mason, Lo, et al., 2014; Zhang, Parvin, & Huang, 2012). In order for stem cells to change from totipotency to pluri- or multi-potency, active histone PTMs are present on gene promotors such as H3K27ac and H3K4me3. Once NPCs begin to differentiate, most gene promotors carry bivalent (poised state) histone PTMs such as H3K27me3 and H3K4me3, allowing them to rapidly turn on and off, which facilitates cell type commitment (e.g neuronal, glial, etc.). Once a brain cell has been fully differentiated, repressive histone PTMs such as H3K27me3 are typically present (Podobinska, Szablowska-Gadomska, Augustyniak, et al., 2017). This regulatory process is reflective in our developmental expression graphs, where the peak at birth might represent terminal differentiation of all neurons, and the general decrease after birth might represent continued maturation. In general, during neural specification, NPCs have varying levels of histone methylation marks, which decrease during differentiation. Conversely, H3K4me2 and histone acetylation levels increase during differentiation (Resendiz, Mason, Lo, et al., 2014). Compared to NPCs, mature mouse cortical neurons are enriched in histone acetylation marks (Cho, Kim, Kim, et al., 2011). Our analysis of

262

various epigenetic marks in human fetal and infant cases demonstrates the differential developmental patterns of expression, which correspond to these rodent findings. In the VZ, TC, WM, DG and CA1 regions, H3K27me3 demonstrates a gradual increase (NPC proliferation), peaks, and then begins to decrease (differentiation & maturation) as development progresses. In contract, H3K14ac demonstrated a gradual increase (**Figure 5.2** and **5.3**).

The VZ and SVZ, which collectively form the germinal matrix, give rise to glutamatergic and GABAergic interneurons respectively (Adle-Biassette, Harding, & Golden, 2018; ten Donkelaar, 2000). The SVZ also gives rise to precursors of astrocytes and oligodendrocytes. The size of the SVZ peaks between 23–25 weeks of gestation (Del Bigio, 2011), however NPC proliferation in the SVZ peaks between 20–26 weeks, and then begins to resolve by 30–32 weeks (Arshad, Vose, Vinukonda, et al., 2016). The cerebral SVZ largely involutes by approximately 32-34 weeks gestation, by which time most neuronal and glial cells have been generated. Ethanol has profound effects on the on survival and proliferation of NPCs (Boschen, & Klintsova, 2017; Resendiz, Mason, Lo, et al., 2014), and can cause apoptosis of brain cells (Smith, Garic, Flentke, et al., 2014; Wilhelm, & Guizzetti, 2016). This toxicity could account for the microcephaly in FASD as well as cortical dysgenesis and heterotopias (De La Monte, & Kril, 2014; Jarmasz, Basalah, Chudley, et al., 2017). Among our human fetuses, PNAE was associated with minimal changes in the VZ. However, in the SVZ, many changes were seen among epigenetic marks representative of active transcription (H3K9ac, H3K27ac, H3K36me3, H4K16ac), repressed transcription (5mC, H3K27me3), and active demethylation (5caC). Potential aberrant changes in gene expression could affect proliferation, survival, or migration of interneuron and glial cell precursors from the SVZ.

Within maturing brain regions, we observed many epigenetic mark changes in association with PNAE (**Table 5.9**). H3K4me3, which represents transcriptional activation, was decreased in almost all brain regions. H3K9ac, H3K27ac and H4K16ac, marks of active transcription, were decreased many of the brain regions studied. H3K36me3, a mark of active transcription increased in half of the brain regions studied. Most *in utero* and postnatal alcohol studies in animals demonstrate a decrease in DNA methylation, a decrease in histone methylation, and an increase in histone acetylation (See **Tables 5.1** and **5.2**) (Chater-Diehl, Laufer, & Singh, 2017; Laufer, Chater-Diehl, Kapalanga, et al., 2017; Lussier, Weinberg, & Kobor, 2017).

Because rodent brains are very immature at birth, many experiments use postnatal alcohol administration to model late gestation human *in utero* exposure. Hippocampal and neocortical tissue from mice and rats that received alcohol during postnatal days 1-11 had increases in global DNA methylation, H3K4me3, H3K9me2, H3K27me2, H3K27me3 (Chater-Diehl, Laufer, Castellani, et al., 2016; Otero, Thomas, Saski, et al., 2012; Subbanna, Nagre, Shivakumar, et al., 2014; Subbanna, Shivakumar, Umapathy, et al., 2013) and decreases in H3K9me2 and H3K27me2 (Subbanna, Shivakumar, Umapathy, et al., 2013). These results partially overlap with our findings. Differences may be species specific or because the maternal metabolism and placental transfer of alcohol was not present in these postnatal rodent experiments (Burd, Roberts, Olson, et al., 2007).

A major target in FASD research is identification of a DNA methylation pattern sufficiently characteristic to be used as a biomarker for early diagnosis in living children. This usually relies on whole genome methylation analysis of DNA extracted from leukocytes or buccal epithelium cells. In buccal cells from 12 males with FASD (3-6 years), 269 differentially methylated cytosine-phosphate-guanine (CpGs) were identified (including genes potentially

264

involved with glutamatergic synapses and Wnt / TGF-β signaling pathways) (Laufer, Kapalanga, Castellani, et al., 2015). In a cohort of 110 FASD and 96 control children (5-18 years), differentially methylated CpGs were found in 403 genes, many of which are related to neurons and brain diseases (e.g. autism, epilepsy, substance abuse). A separate cohort of children with FASD (24 FASD and 24 control; ages 3.5-18 years) was used to replicate the findings (Lussier, Morin, MacIsaac, et al., 2018); 82 hypermethylated and 79 hypomethylated genes, some the same as in the previous study. The common genes of interest relate to the dopaminergic system (*SLC6A3* and *DRD4*) (Lussier, Morin, MacIsaac, et al., 2018). Despite our small cohort, 5mC changes were identified in the SVZ, CX and CA1 of human PNAE.

We observed several changes in epigenetic marks, in the absence of overt morphologic abnormalities, within the mature ciliated ependymal epithelium (TE). In both human and macaque PNAE, 5fC and H3K36me3 were affected but in opposite directions. This layer serves several functions including acting as a barrier between cerebrospinal fluid (CSF) and brain extracellular space, facilitating movement of signaling molecules in the CSF, and providing a niche for mature brain subventricular zone (stem) cells (Del Bigio, 2010; Ohata, & Alvarez-Buylla, 2016). Nothing is known about epigenetic regulation in the mature ependymal layer. However, it is worth noting, although none of the cases studied here were hydrocephalic, that hydrocephalus due to aqueduct stenosis was one of the more frequent malformations encountered in our full PNAE / FASD autopsy study (Jarmasz, Basalah, Chudley, et al., 2017). Integrity of the ependymal lining along the cerebral aqueduct is necessary for maintaining patency (Sival, Guerra, den Dunnen, et al., 2011). We must consider the possibility that PNAE associated epigenetic changes might adversely affect barrier function of ependymal cells, which in turn may alter the health of the subjacent NPCs.

An unavoidable limitation to our study is the variability among human autopsy subjects. All but two cases did not have a comprehensive genetic (i.e. gene mutation) analysis, so we cannot be certain that abnormalities attributed to PNAE are, in fact, related to an unrecognized genetic disorder. We previously described many complex abnormalities and confounding factors in the autopsy cohort of PNAE / FASD cases (Jarmasz, Basalah, Chudley, et al., 2017). Here we avoided cases with severe malformations, restricting the analysis to brains of small size (micrencephaly). Hypoxic-ischemic stress frequently occurs prior to death of fetuses or children. This in itself could mask epigenetic changes caused by PNAE. Oxidative stress is postulated to be one of the contributors to the development of FASD (Brocardo, Gil-Mohapel, & Christie, 2011). However, in a partially overlapping cohort of human fetal and infant brains with a history of PNAE, we found no immunohistochemical evidence that oxidative changes in DNA, lipid, or protein differ from non-PNAE cases (Basalah, 2015). We also showed (Chapter 4 manuscript), that post-mortem delay could have an adverse effect on some histone acetylation marks, necessitating use post-mortem delay time as a factor to be controlled, which in turn, narrowed options for control cases. We hoped that inclusion of a non-human primate model of PNAE would assist in the interpretation of the human findings. However, those tissues required slightly different immunohistochemical techniques, possibly related to prolonged fixation in formalin, and often had labelling artifacts (e.g. patchy unstained tissue). A possible reason why our human and macaque results did not fully overlap is because of the differences between agonal states of between humans (dying from natural causes) and macaques (death by anesthetic overdose). Although some studies have demonstrated changes in epigenetics as a result of anesthetic exposure, none have really shown that this occurs after only a few minutes of exposure (Ju, Jia, Sun, et al., 2016; Mori, Iijima, Higo, et al., 2014; Pekny, Andersson, Wilhelmsson, et al., 2014).

Because epigenetic changes are modifiable during postnatal life, we restricted our human study cohort to the period of infancy (maximum age 7 months). However, the ~6-month-old macaque infants have an approximate human developmental equivalent of 2.7-3.5 years (http://translatingtime.org/translate), and therefore are not directly comparable. Regardless, the overlap in two histone PTMs (activation marks H3K9ac and H3K36me3) remains an avenue for future research. Preliminary analysis of the dentate gyrus in a single 22-month-old PNAE case (compared to matched control) demonstrated increases in 5mC, 5hmC, H3K4me3, H3K36me3, H3K9ac, H3K14ac, H3K27ac, and no changes in H4K16ac, H4K12ac, H4K5ac. Only H4K5ac results overlap with the macaque dentate gyrus results.

We hypothesized that epigenetic changes occur in association with PNAE, therefore the converse null hypothesis would be no change. The one-tailed t-test is typically calculated if differences in a particular direction are of interest or are expected. The two-tailed t-test is performed if differences in either direction are of interest. A type I error (false-positive) occurs if the null hypothesis is rejected but is actually true in the population. A type II error (false-negative) occurs if the null hypothesis is accepted but is actually false. A large sample size generally avoids type I and type II errors (Amitav Banerjee, Chitnis, Jadhav, et al., 2009). Our sample sizes (N=18 human pairs; N=6 macaque pairs) are small and, depending on the variability of the data, potentially subject to type 1. We calculated many different statistical comparisons which increases our risk for type I error however, we have reported changes that did not reach statistical significance (p<0.075).

In summary, we showed a variety of epigenetic changes in the nuclei of brain cells of human fetuses and infants with a history of PNAE. These partially align with prior PNAE rodent studies of epigenetic changes. Considerable variability in the expression of specific DNA

cytosine modifications and histone PTMs across ages, as well as the possibility of influence by the environment, makes it difficult to identify particular marks with the potential to act as biomarkers of PNAE. The overlap in histone PTM H3K36me3 may represent the level of PNAE. This is especially true for histone acetylation, which turns over quickly. However, in general our findings support the broad hypothesis that epigenetic changes occur in PNAE, particularly among those that are stable (e.g. methylation). These changes might contribute to the abnormalities in brain development that are associated with FASD. Future work will include more cases to increase sample size, detailed cell type analysis (e.g. with double label immunofluorescence) to confirm specific cell populations affected by PNAE, and eventually identification of modifications associated with specific genes. Then, the brain tissue changes might be correlated with genetic modifications identified in nonneural tissues (e.g. buccal epithelium from living FASD patients).

Table 5.1: Changes in DNA cytosine modifications and related enzymes following experimental *in utero* alcohol exposure.

DNA cytosine modification	Result of ethanol exposure	Animal & Age at Sacrifice	Ethanol exposure	Brain region studied	Method	Reference
Promotor methylation of Slc6a4	Higher Slc6a4 promoter CpG methylation at P55	Rat; G21 and P55	G1 - G21, ~12-15g ethanol per kg body weight per day	Hypothalamus	Bisulfite conversion, PCR and pyrosequencing	(Ngai, Sulistyoningrum, O'Neill, et al., 2015)
Methylation of CpG islands in Vmn2r64, Olfr110, Olfr601, Vpreb2	Vmn2r64 hypermethylated, Olfr110 hypo- and hyper-methylated, Olf601 hypomethylated, Vpreb2 hypomethylated	Inbred mice; P28 and P60	G0.5 – 8.5, 12g±2.6g ethanol per kg body weight per day	P28: hippocampus	Bisulfite conversion, PCR and sequencing	(Marjonen, Sierra, Nyman, et al., 2015)
CpG methylation of BDNF gene	increased CpG methylation	Sprague-Dawley rats	E1-E20, 6.0 g/kg alcohol daily by intragastric intubation	E21 granule cells of olfactory bulbs; P10 granule cells of olfactory bulbs	DNA digestion with methylation-sensitive enzyme *HpaII* followed by RT-PCR	(Maier, Cramer, West, et al., 1999)
CpG methylation of POMC gene	CpG methylation higher in F1 and F2 generations	Sprague-Dawley rats; both sexes	G7–G10 (1.7 to 5.0% v/v EtOH), then G11–G21 (6.7% v/v EtOH) (F1). FAE Offspring (F1) were bred again with controls on the opposite sex (F2).	Arcuate nucleus of the hypothalamus	DNA digestion with methylation-sensitive enzyme *HpaII* followed by RT-PCR; verified by pyrosequencing	(Govorko, Bekdash, Zhang, et al., 2012)
Dnmt1 5hmC	increased Dnmt1, decreased 5hmC (mRNA), increased 5hmC (IF)			Arcuate nucleus of the hypothalamus, β-endorphin-positive cells	Immunofluorescence (IF); mRNA levels	
Dnmt1 Dnmt3a MeCP2	Dnmt1 increased, Dnmt3a, increased (IF) but no change (mRNA), MeCP2 increased	Sprague-Dawley rats; males 60 to 65 days	G7 – G10 (1.7 to 5.0% v/v EtOH), then G11 – G21 (6.7% v/v EtOH)	β-endorphin-positive cells of the hypothalamus	mRNA levels & immunofluorescence	(Bekdash, Zhang, & Sarkar, 2013)

G – gestational day, P – postnatal day, IF – immunofluorescence, CpG – Cytosine phosphate guanine, 5hmC – 5-hydroxymethylcytosine, Dnmt – DNA methyltransferase, MeCP2 – Methyl binding protein, BDNF – brain derived neurotropic factor, POMC – Proopiomelano-cortin

Table 5.2: Changes in histone post-translational modifications and related enzymes following experimental in utero alcohol exposure.

Histone PTM	Result of Ethanol Exposure	Species & Age at Sacrifice	*In utero* ethanol exposure	Area Studied	Method	Reference
H3K9ac	decreased acetylation	Sprague-Dawley rats; Males 60 to 65 days old	G7 – G10 (1.7 to 5.0% v/v EtOH), then G11 – G21 (6.7% v/v EtOH)	β-Endorphin-positive cells of the hypothalamus	Immuno-fluorescence	(Bekdash, Zhang, & Sarkar, 2013)
	decreased acetylation	Sprague-Dawley Rats; both sexes	G7 – G10 (1.7 to 5.0% v/v EtOH), then G11 – G21 (6.7% v/v EtOH) (F1). FAE Offspring (F1) were bred again with controls on the opposite sex (F2).	Arcuate of the hypothalamus β-Endorphin-positive cells	Immuno-fluorescence,	(Govorko, Bekdash, Zhang, et al., 2012)
H3K4me2, K4me3	decrease methylation	Sprague-Dawley rats; Males 60 to 65 days old	G7 – G10 (1.7 to 5.0% v/v EtOH), then G11 – G21 (6.7% v/v EtOH)	β-Endorphin-positive cells of the hypothalamus	Immuno-fluorescence	(Bekdash, Zhang, & Sarkar, 2013)
	decreased methylation	Sprague-Dawley Rats; Both sexes 60 to 80 days old	G7 – G10 (1.7 to 5.0% v/v EtOH), then G11 – G21 (6.7% v/v EtOH) (F1). FAE Offspring (F1) were bred again with controls on the opposite sex (F2).	Arcuate of the hypothalamus β-Endorphin-positive cells	Immuno-fluorescence,	(Govorko, Bekdash, Zhang, et al., 2012)
H3K9me2	increased methylation	Sprague-Dawley rats; Males 60 to 65 days old	G7 – G10 (1.7 to 5.0% v/v EtOH), then G11 – G21 (6.7% v/v EtOH)	β-Endorphin-positive cells of the hypothalamus	Immuno-fluorescence	(Bekdash, Zhang, & Sarkar, 2013)
	increased methylation	Sprague-Dawley Rats; Both sexes 60 to 80 days old	G7 – G10 (1.7 to 5.0% v/v EtOH), then G11 – G21 (6.7% v/v EtOH) (F1). FAE Offspring (F1) were bred again with controls on the opposite sex (F2).	Arcuate of the hypothalamus β-Endorphin-positive cells	Immuno-fluorescence,	(Govorko, Bekdash, Zhang, et al., 2012)
Set7/9 G9a Setdb1	Set7/9 decreased, G9a, increased, Setbd1 increased	Sprague-Dawley rats; males 60 to 65 days old	G7 – G10 (1.7 to 5.0% v/v EtOH), then G11 – G21 (6.7% v/v EtOH)	β-Endorphin-positive cells of the hypothalamus	mRNA levels	(Bekdash, Zhang, & Sarkar, 2013)
Set7/9 G9a Setdb1 Hdac2	Set7/9 decreased, G9a, increased, Setbd1 increased Hdac2 increased	Sprague-Dawley Rats; Both sexes 60 to 80 days old	G7 – G10 (1.7 to 5.0% v/v EtOH), then G11 – G21 (6.7% v/v EtOH) (F1). FAE Offspring (F1) were bred again with controls on the opposite sex (F2).	Arcuate nucleus of hypothalamus	mRNA levels	(Govorko, Bekdash, Zhang, et al., 2012)

G – gestational day, Set – histone-lysine N-methyltransferase, G9a – Histone-lysine N-methyltransferase, HDAC – histone deacetylase

Table 5.3: Clinical details of human fetuses and infants with prenatal alcohol exposure.

Case #	Sex	Age	Cause of death	Brain weight (percentile)*	PNAE	Physical anomalies	Cardiac defects	Brain abnormalities
1	F	20 weeks gestation	Stillborn / intrauterine death	$\geq 10^{th}$ - $<50^{th}$	Mixed substance abuse	-	-	None
2	F	21.5 weeks gestation	Stillborn / intrauterine death	$<5^{th}$	Rubbing alcohol 2nd trimester	None	None	Micrencephaly
3	M	27 weeks gestation	Stillborn / intrauterine death	$\geq 10^{th}$ - $<50^{th}$	Alcohol abuse	Facial anomalies, low set ears, bilateral neck webbing	None	None
4	F	29 weeks gestation	Stillborn / intrauterine death	Not indicated	Alcohol abuse	Low set ears	None	None
5	M	34 weeks gestation	Stillborn / intrauterine death	$\geq 5^{th}$ - $<10^{th}$	Drank until pregnancy was determined	Low set ears, palmar creases unusual	None	Micrencephaly
6	F	34 weeks gestation	Intrapartum death with prematurity	$<5^{th}$	Drank heavily throughout pregnancy	Facial anomalies, bilateral club foot and partial webbing of toes	Absent superior vena cava, large ASD	Micrencephaly, ventricle wall fusion (partial), periventricular heterotopia (rare), retarded laminar development cerebral cortex and hippocampus, hypoplasia pons
7	M	36 weeks gestation	Stillborn / intrauterine death	$\geq 10^{th}$ - $<50^{th}$	Occasional alcohol during the first trimester	None	Right coronary ostium	None
8	F	40 weeks gestation	Stillborn / intrauterine death with placental abnormalities	$<5^{th}$	Drank heavily during the third trimester	None	None	Micrencephaly
9	M	41 weeks gestation	Stillborn / intrauterine death	$<5^{th}$	History of alcohol abuse	None	None	Micrencephaly

Case #	Sex	Age	Cause of death	Brain weight (percentile)*	PNAE	Physical anomalies	Cardiac defects	Brain abnormalities
10	M	21 days (43 weeks PC)	Bacterial + viral infection	<5th	Drank throughout pregnancy	None	None	Micrencephaly
11	F	23 days (43.5 weeks PC)	SUDI with unsafe sleeping environment	≥5th - <10th	Drank throughout pregnancy	None	None	Micrencephaly
12	M	6 weeks (46 weeks PC)	SUDI with congenital anomalies	≥10th - <50th	Drank during pregnancy (known alcoholic)	Thin upper lip	ASD with PDA	Recent mild hypoxic neuron change.
13	F	8 weeks (48 weeks PC)	SUDI with congenital anomalies	Not Indicated	Drank heavily during pregnancy	None	Small VSD	None
14	M	2 months (48.5 weeks PC)	SUDI with unsafe sleeping environment	≥10th - <50th	Drank during pregnancy	Low set ears	Subaortic VSD	None
15	M	3 months (53 weeks PC)	SUDI	≥10th - <50th	Binged during pregnancy	None	None	None
16	F	4 months (57.5 weeks PC)	SUDI	≥10th - <50th	Drank during the first and second trimester	None	None	Periventricular leukomalacia, subacute (small foci in parietal white matter)
17	F	6 months (66 weeks PC)	SUDI	≥50th - <90th	Fetal alcohol syndrome	None	None	Polygyria
18	M	7 months (70.5 weeks PC)	SUDI	>95th	Mother alcoholic	Facial anomalies	None	None

* according to (Maroun, & Graem, 2005; Phillips, Billson, & Forbes, 2009)

Abbreviations: SUDI - sudden unexpected death of an infant and PC - post-conception

Table 5.4: Alcohol-exposed human fetuses and infants with paired controls cases and controls.

Case #	Sex	Prenatal Alcohol Exposed			Age-, Sex- and PMD-Matched Controls		
		PMD (hours)	Age (PC weeks)	Cause of death	PMD (hours)	Age (PC weeks)	Cause of death
1	F	24	20 weeks	Stillborn / intrauterine death	<24	21 weeks	Stillborn / intrauterine death with placental abnormalities
2	F	24.5	21.5 weeks	Stillborn / intrauterine death	21.5	22 weeks*	Intrapartum death: prematurity
3	M	7-8.5	27 weeks	Stillborn / intrauterine death	22	25 weeks	Stillborn / intrauterine death with placental abnormalities
4	F	49	29 weeks	Stillborn / intrauterine death	~24	31 weeks	Stillborn / intrauterine death with placental abnormalities
5	M	~24	34 weeks	Stillborn/ intrauterine death with malformation(s)	56.5	33 weeks	Prematurity with pulmonary hypoplasia
6	F	107	34 weeks*	Intrapartum death: prematurity and malformation(s)	48	34 weeks*	Intrapartum death: prematurity and malformation(s)
7	M	48	36 weeks	Stillborn / intrauterine death	~1-5	37.5 weeks	Stillborn / intrauterine death
8	F	33	40 weeks	Stillborn / intrauterine death with placental abnormalities	32	38 weeks	Stillborn / intrauterine death
9	M	39	41 weeks	Stillborn / intrauterine death	~39-49	40 weeks	Stillborn / intrauterine death
10	M	28	43 weeks	Bacterial / viral infection	24-30	43 weeks	SUDI due to unsafe sleeping environment
11	F	20	43.5 weeks	SUDI due to unsafe sleeping environment	49	44 weeks	Asphyxiation due to accidental smothering
12	M	21	46 weeks	Malformations / congenital anomalies	26	46 weeks	SUDI due to unsafe sleeping environment
13	F	12	48 weeks	Malformations / congenital anomalies	24	48 weeks	SUDI
14	M	25-35	48.5 weeks	SUDI due to unsafe sleeping environment	47-53	48.5 weeks	SUDI due to unsafe sleeping environment
15	M	26	53 weeks	SUDI	36	53 weeks	SUDI
16	F	3.5-7.5	57.5 weeks	SUDI	~24	57.5 weeks	SUDI
17	F	8	66 weeks	SUDI	24-36	64 weeks	SUDI due to unsafe sleeping environment
18	M	19.5	70.5 weeks	SUDI	32-34	70.5 weeks	Accidental positional asphyxiation

*Liveborn; died within minutes to hours of birth
Abbreviations: Post-conception (PC), Female (F), Male (M), Post-mortem delay (PMD), Sudden unexplained death of an infant (SUDI)

Table 5.5: Alcohol-exposed and control macaque details.

Prenatal Alcohol Exposed Macaques						Age- & Sex-Matched Controls		
ID number	Sex	Age at sacrifice	Weekly dose of ethanol	Maternal peak plasma ethanol concentration	Abnormalities	ID number	Sex	Age at sacrifice
13077 / 29	F	5.7 months	2.5g/kg	264mg/dl	None	11023 / 2	F	5.7 months
13076 / 28	M	6.2 months	2.5g/kg	260mg/dl	Strabismus	13071* / 4	M	5.9 months
13078 / 30	F	5.8 months	3.3g/kg	420mg/dl	Significantly delayed learning, mild motor deficits	10512 / 1	F	5.8 months
13080 / 32	F	6 months	3.3g/kg	432mg/dl	Unusual auricles, metopic synostosis	10241 / 0	F	6.3 months
13079 / 31	M	6.1 months	3.3g/kg	432mg/dl	Motor deficits	13071* / 4	M	5.9 months
11019 / 33	M	7.2 months	4.1g/kg	540mg/dl	Strabismus, bilateral microphthalmia, significant growth deficiency, microcephaly, motor deficits	13072 / 5	M	6.1 months

Abbreviations: Female (F), Male (M), Grams per kilogram maternal bodyweight (g/kg), Milligrams per deciliter (mg/dl), Ethanol (EtOH)

The 5 digit ID number represents the neuropathological ID and the 2 digit number represents the publications ID (Clarren, Astley, & Bowden, 1988)

PNAE macaques received ethanol (EtOH) during gestational weeks 5 – 24; Controls received isocaloric sucrose on weeks 1-24

* this case was used twice for matching

Table 5.6: Epigenetic marks (DNA cytosine modifications, histone acetylation, and histone methylation) being investigated in PNAE human and macaque monkey brain samples. The enzymes responsible for the addition and removal of these modifications is also listed. Lysine demethylase (KDM) and methyltransferase (KMT) aliases have been listed (a full comprehensive list can be found in Black *et al.*, 2012).

Epigenetic mark	Role	Enzyme(s) responsible for modification	Removal of modification	Reference
5mC	Gene repression and genomic imprinting.	DNMT1, DNMT3A DNMT3B, DNMT3L	n/a	(Kellinger, Song, Chong, et al., 2012; Ndlovu, Denis, & Fuks, 2011; Wagner, Steinbacher, Kraus, et al., 2015; Lanfeng Wang, Zhou, Xu, et al., 2015)
5hmC	Promotes gene expression during active demethylation. Associated with transcription.	TET1, TET2, TET3	n/a	
5fC	Enriched at poised enhancers and other regulatory elements.	TET1, TET2, TET3	n/a	
5caC	Along with 5fC, cause increased pausing, backtracking, and reduced fidelity of RNAPII.	TET1, TET2, TET3	n/a	
H3K4me3	Associated with transcriptional start sites of actively transcribed genes. Enriched in gene promoters. Role in splicing. Regulates histone acetylation	SETD1A, SETD1B, PRDM9, MLL, MLL2-5, ASH1L	JARID1A-D, PHF8, JHDM1B, NO66	(Barth, & Imhof, 2010; Black, Van Rechem, & Whetstine, 2012; Campos, & Reinberg, 2009; Chater-Diehl, Laufer, & Singh, 2017; Zhang, Ho, Vega, et al., 2015)
H3K9me2, K9me3	Inactive gene promotors; associated with heterochromatin formation.	G9a, GLP, SETDB1, SETB2, SUV39H1, SUV39H2	LSD1, JMJD2A-D	
H3K27me2	Silences enhancers. Transcriptionally silenced gene regions. Associated with heterochromatin.	G9a, GLP, EZH1, EZH2, NSD1, NSD3	PHF8, JMJD3, UTX, JHDM1D	
H3K27me3	Inactive gene promoters. Enriched in gene promotors of developmentally regulated genes. Associated with facultative heterochromatin. Inhibits elongation.	EZH2, NSD3	JMJD3, UTX	
H3K36me3	Transcriptionally active promotors. Associated with transcribed downstream gene regions. Promotes elongation. Role in splicing. Regulates histone acetylation	NSD1-3, ASH1L, SMYD2, SETMAR, SETD2	JHDM1B, JMJD2A-D, NO66	
H3K9ac	Highly correlated with active promoters. Co-occurrence with H3K14ac and H3K4me3. Associated with active regulatory regions.	GCN5 (KAT2A), ELP3, CBP, P300	SIRT1, SIRT6, Any HDAC	(Barth, & Imhof, 2010; Chater-Diehl, Laufer, &

H3K14ac	Transcriptionally active chromatin / genes.	MYST3, GCN5 (KAT2A), CLOCK, NCOAT, GTF3C4	SIRT1, Any HDAC	Singh, 2017; Creyghton, Cheng, Welstead, et al., 2010; Hawkins, Hon, Yang, et al., 2011; Karmodiya, Krebs, Oulad-Abdelghani, et al., 2012; Zhibin Wang, Zang, Rosenfeld, et al., 2008; Yonggang Zhou, & Grummt, 2005)
H3K27ac	Associated with active regulatory regions and enhancers.	CBP, P300	Any HDAC	
H4K5ac	Transcriptionally active regions.	Tip60, CBP, p300, KAT2A, KAT5, MYST2, HAT1	Any HDAC	
H4K12ac	Transcriptionally active promotors.	TIP60, HAT1, CBP, KAT2A, KAT5, MYST2, p300,	Any HDAC,	
H4K16ac	Gene promoters with the highest transcriptional activity as well as a proposed role in repression. High order chromatin structure.	MOF, CBP, KAT2A, p300, MYST1	SIRT1, SIRT2, SIRT3, Any HDAC	

Table 5.7: Antibodies to epigenetic marks. Specificity and post-mortem stability of select antibodies was verified. The results can be found in Chapter 4 manuscript.

Antibody	Immunogen / target	Isotype	Species	Type	Company Details
5mC	Recognizes 5-methylcytidine in vertebrate DNA	IgG	Mouse	Monoclonal (clone 33D3)	Active Motif, #39649
5hmC	Raised against 5-hydroxymethylcytidine conjugated to KLH	Serum	Rabbit	Polyclonal	Active Motif, #39769
5fC	Raised against 5-formylcytidine conjugated to KLH	Serum	Rabbit	Polyclonal	Active Motif, #61223
5caC	Raised against 5-carboxylcytidine conjugated to KLH	Serum	Rabbit	Polyclonal	Active Motif, #61225
H3K4me3	Raised against a peptide including trimethyl-lysine 4 of histone H3.	Serum	Rabbit	Polyclonal	Active Motif, #39159
H3K9ac	Synthetic peptide corresponding to Human Histone H3 aa 1-100 (N terminal) (acetyl K9) conjugated to KLH	IgG	Rabbit	Polyclonal	Abcam, #ab10812
H3K9me2, K9me3	Synthetic peptide within human histone H3 aa1-100 (tri methyl K9); exact sequence is proprietary	IgG1	Mouse	Monoclonal (clone 6F12-H4)	Abcam, #ab71604
H3K14ac	Synthetic peptide within human histone H3 (acetyl K14); exact sequence is proprietary.	IgG	Rabbit	Monoclonal (clone EP964Y)	Abcam #ab52946
H3K27ac	Synthetic peptide corresponding to human histone H3 aa 1-100 (acetyl K27) conjugated to KLH	IgG	Rabbit	Polyclonal	Abcam, #ab4729
H3K27me3	Synthetic peptide within human histone H3 aa 1-100 (tri methyl K27) conjugated to KLH; exact sequence is proprietary	IgG	Mouse	Monoclonal (clone 6002)	Abcam, #ab6002
H3K36me3	Synthetic peptide within human histone H3 aa 1-100 (tri methyl K36) conjugated to KLH; exact sequence is proprietary	IgG	Rabbit	Polyclonal	Abcam, #ab9050
H4K5ac	Synthetic peptide within human histone H4 aa 1-100 (N terminal) (acetyl K5); exact sequence is proprietary	IgG	Rabbit	Monoclonal (clone EP1000Y)	Abcam, #ab51997
H4K12ac	Synthetic peptide corresponding to human histone H4 aa 10-15 (acetyl K12)	IgG	Rabbit	Polyclonal	Abcam, #ab61238
H4K16ac	Synthetic peptide corresponding to human histone H4 (acetyl K16); exact sequence is proprietary	IgG	Rabbit	Monoclonal (EPR1004)	Abcam, #ab109463
H3panAc	Peptide including acetyl-lysines contained in the N-terminal tail of human histone H3	IgG	Rabbit	Polyclonal	Active Motif, #61637
H4panAc	Peptide corresponding to amino acids 1- 24 of human histone H4 acetylated at lysines 5, 8, 12 and 16 (cross-reactivity with acetylated histone H2B)	IgG1k	Mouse	Monoclonal (clone 3HH4-2C2)	Active Motif #39967
Total H3	Peptide containing the N-terminus of histone H3.	IgG2b	Mouse	Monoclonal (clone MABIO3O1)	Active Motif, #39763
Total H4	Synthetic peptide containing human histone H4.	IgG2b	Mouse	Monoclonal (clone MABI0400)	Active Motif, #61521

KLH represents Keyhole limpet hemocyanin

Table 5.8: Procedural details of immunohistochemical labeling.

Antibody	Dilution	Duration (hours)	DAB Time	Dilution	Duration (hours)	DAB Time	Antigen Retrieval	Ab Diluent	Washing Buffer #1	Washing Buffer #2
5mC	1:500	1.5	5min	1:500	2hrs	5min	Sodium Citrate pH 6.0	1% BSA in PBS	1X PBS + 0.2% Triton-X-100	1X PBS
5hmC	1:3000	1.5	5min	1:4000*	2hrs	4min	Tris-EDTA pH 9.0	1% BSA in TBS	1X TBS + 0.1% Tween 20	1X TBS
5fC	1:400	1.5	6min	1:300	2.5hrs	6min	Tris-EDTA pH 9.0	1% BSA in TBS	1X TBS + 0.1% Tween 20	1X TBS
5caC	1:250	1.5	6min	1:200	2.5hrs	6min	Tris-EDTA pH 9.0	1% BSA in TBS	1X TBS + 0.1% Tween 20	1X TBS
H3K4me3	1:500	2	5min	1:200	2hrs	6min	Sodium Citrate pH 6.0	1% BSA in PBS	1X PBS + 0.2% Triton-X-100	1X PBS
H3K9ac	1:500	1.5	6min	1:300	2hrs	6min	Tris-EDTA pH 9.0	1% BSA in TBS	1X TBS + 0.1% Tween 20	1X TBS
H3K9me2, K9me3**		n/a		1:250	2.5hrs	5min	Sodium Citrate pH 6.0	1% BSA in PBS	1X PBS + 0.2% Triton-X-100	1X PBS
H3K14ac	1:150	1.5	5min		n/a		Sodium Citrate pH 6.0	1% BSA in PBS	1X PBS + 0.2% Triton-X-100	1X PBS
H3K27ac	1:500	1.5	5min	1:400	2hrs	5min	Sodium Citrate pH 6.0	1% BSA in PBS	1X PBS + 0.2% Triton-X-100	1X PBS
H3K27me3	1:150	1.5	5min	1:100	2.5hrs	6min	Sodium Citrate pH 6.0	1% BSA in PBS	1X PBS + 0.2% Triton-X-100	1X PBS
H3K36me3	1:100	1.5	5mins	1:250*	2hrs	5min	Tris-EDTA pH 9.0	1% BSA in TBS	1X TBS + 0.1% Tween 20	1X TBS
H4K5ac	1:350	1.5	5min	1:250	2hrs	5min	Tris-EDTA pH 9.0	1% BSA in TBS	1X TBS + 0.1% Tween 20	1X TBS
H4K12ac	1:250	1.5	5min	1:100	2hrs	5min	Tris-EDTA pH 9.0	1% BSA in TBS	1X TBS + 0.1% Tween 20	1X TBS
H4K16ac	1:100	1.5	6min		n/a		Sodium Citrate pH 6.0	1% BSA in PBS	1X PBS + 0.2% Triton-X-100	1X PBS
H3panAc	1.200	1.5	5min	1:150	2hrs	6min	Sodium Citrate pH 6.0	1% BSA in PBS	1X PBS + 0.2% Triton-X-100	1X PBS
H4panAc	1:150	2	5min		n/a		Sodium Citrate pH 6.0	1% BSA in PBS	1X PBS + 0.2% Triton-X-100	1X PBS
Total H3	1:300	1.5	6min	1:75	3hrs	6min	Sodium Citrate pH 6.0	1% BSA in PBS	1X PBS + 0.2% Triton-X-100	1X PBS
Total H4	1:1000	1.5	5min	1:800	2hrs	5min	Tris-EDTA pH 9.0	1% BSA in TBS	1X TBS + 0.1% Tween 20	1X TBS

*The original lot concentration differed
**The epigenetic mark H3K9me2/K9me3 was assessed in the macaques but this antibody was discontinued by the manufacturer and was not available for the human cohort. We purchased anti-H3K9me2 monoclonal antibody from the same manufacturer (#ab176882, Abcam) as an alternative. Despite being reported for use in immunohistochemistry, we did not succeed in getting it to work in the human PNAE samples after multiple attempts.
Note: among the macaques, anti-H3K14ac and anti-H4K16ac did not work via immunohistochemistry.

Figure 5.1: Examples of human control and PNAE immunostaining raw data with polynomial curve fit. The black solid curve (grey bars) represent controls and the red dotted curve (red bars) represent PNAE. The Y-axis is the product of intensity and distribution scores (maximum score of 14) and the X-axis is the post-conception age in weeks.
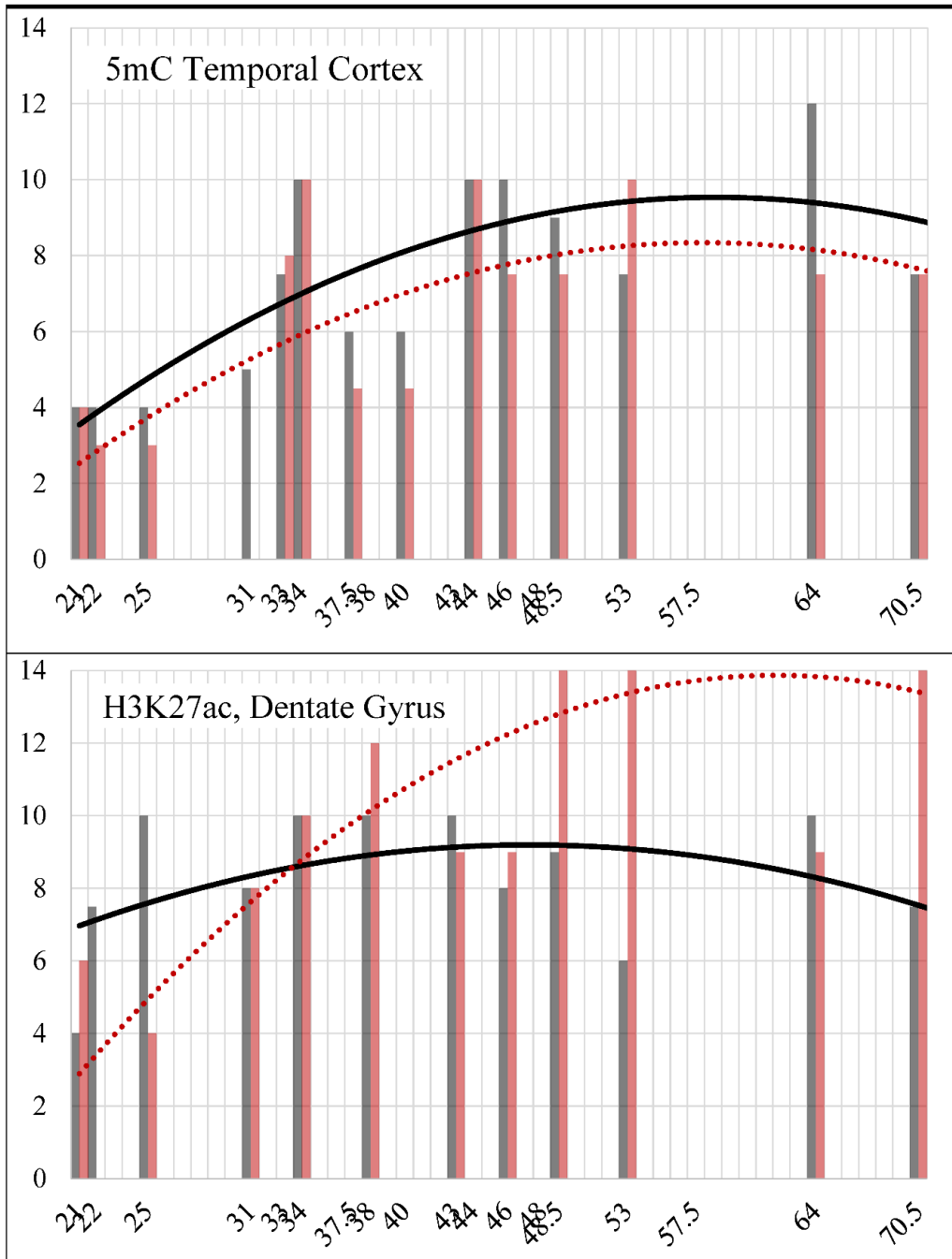
Figure 5.2: Graphic representation of semi-quantitative score values (maximum 14; Y-axis) for DNA cytosine modifications in the human brain regions assessed. The black curve represents the control cases and the red dotted curve represents PNAE. The X-axis represents the post-conception age in weeks (7m = 70.5 weeks post-conception). The ventricular and subventricular zones only show the fetal cases up to 34 weeks gestation because the structures are not present afterward.

	Ventricular Zone	Subventricular Zone	Temporal Cortex	White Matter	Dentate Gyrus	CA1
5mC						
5hmC						
5fC						
5caC						

281
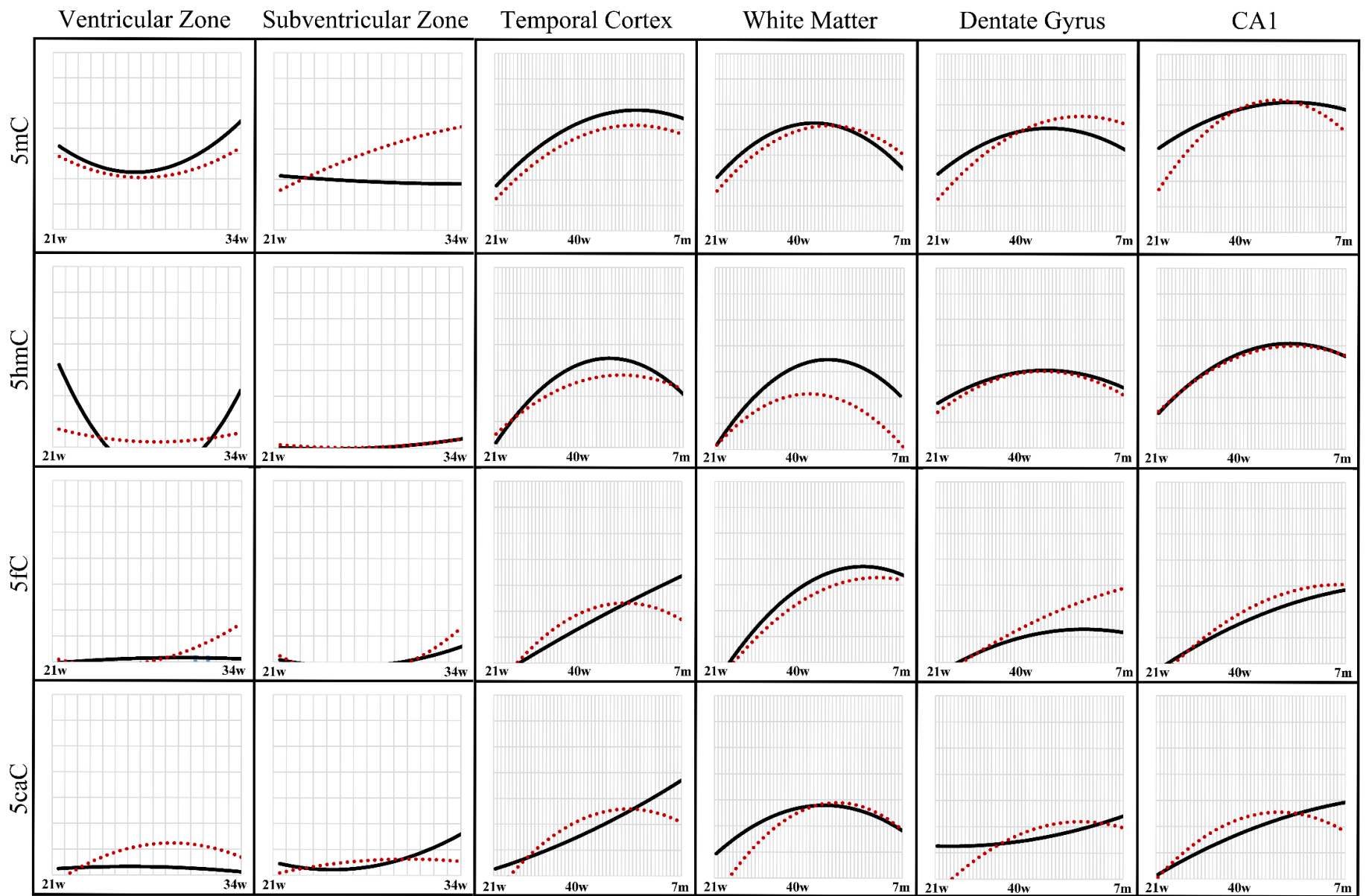
Figure 5.3: Graphic representation of semi-quantitative score values (maximum 14; Y-axis) for histone H3 methylation marks in the human brain regions assessed. The black curve represents the control cases and the red dotted curve represents PNAE. The X-axis represents the post-conception age in weeks (7m = 70.5 weeks post-conception). The ventricular and subventricular zones only show the fetal cases up to 34 weeks gestation because the structures are not present afterward.

	Ventricular Zone	Subventricular Zone	Temporal Cortex	White Matter	Dentate Gyrus	CA1
H3K4me3						
H3K27me3						
H3K36me3						

283
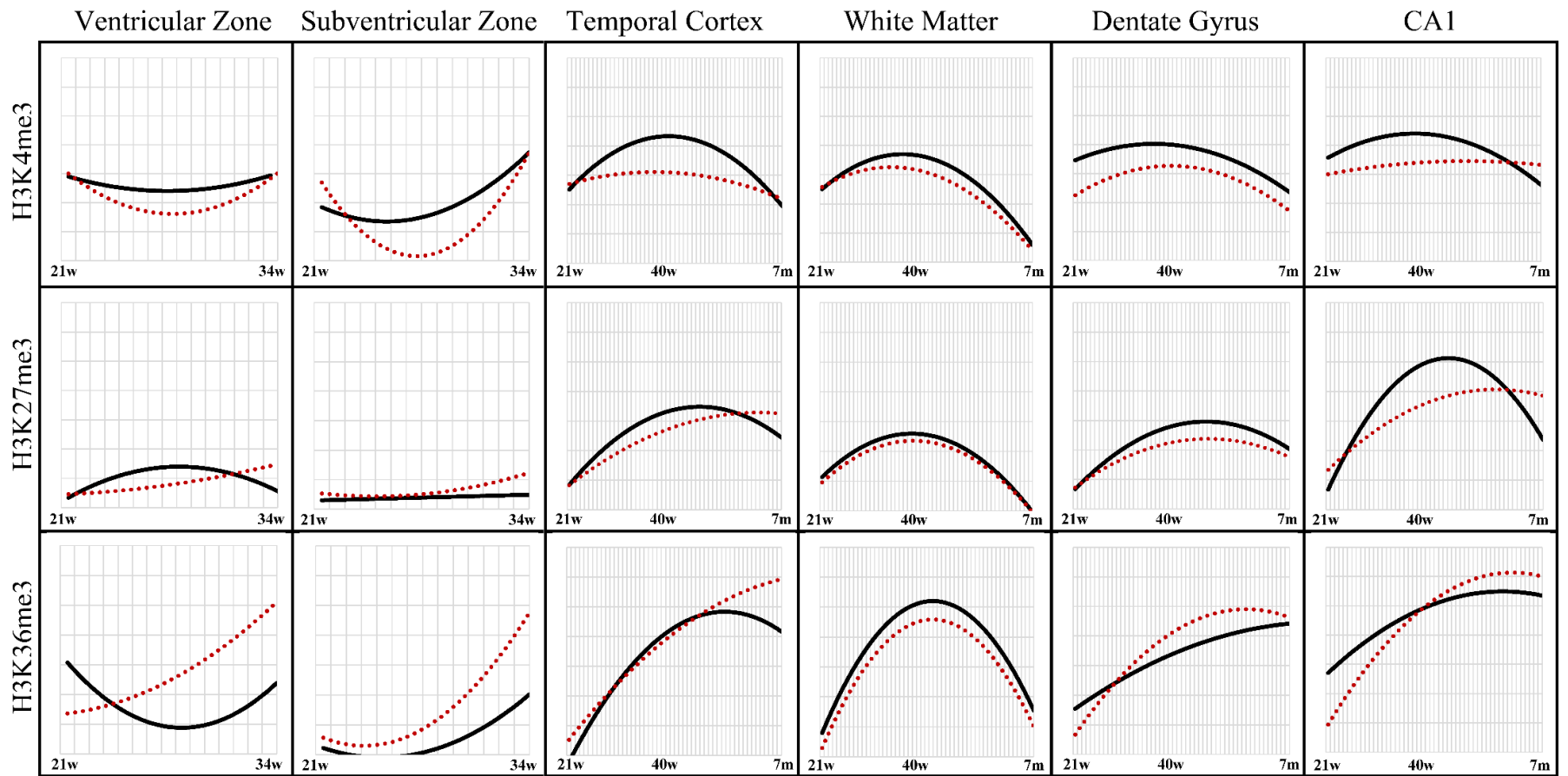
Figure 5.4: Graphic representation of semiquantitative score values (maximum 14; Y-axis) for histone H3 acetylation marks in the human brain regions assessed. The black curve represents the control cases and the red dotted curve represents PNAE. The X-axis represents the post-conception age in weeks (7m = 70.5 weeks post-conception). The ventricular and subventricular zones only show the fetal cases up to 34 weeks gestation because the structures are not present afterward.
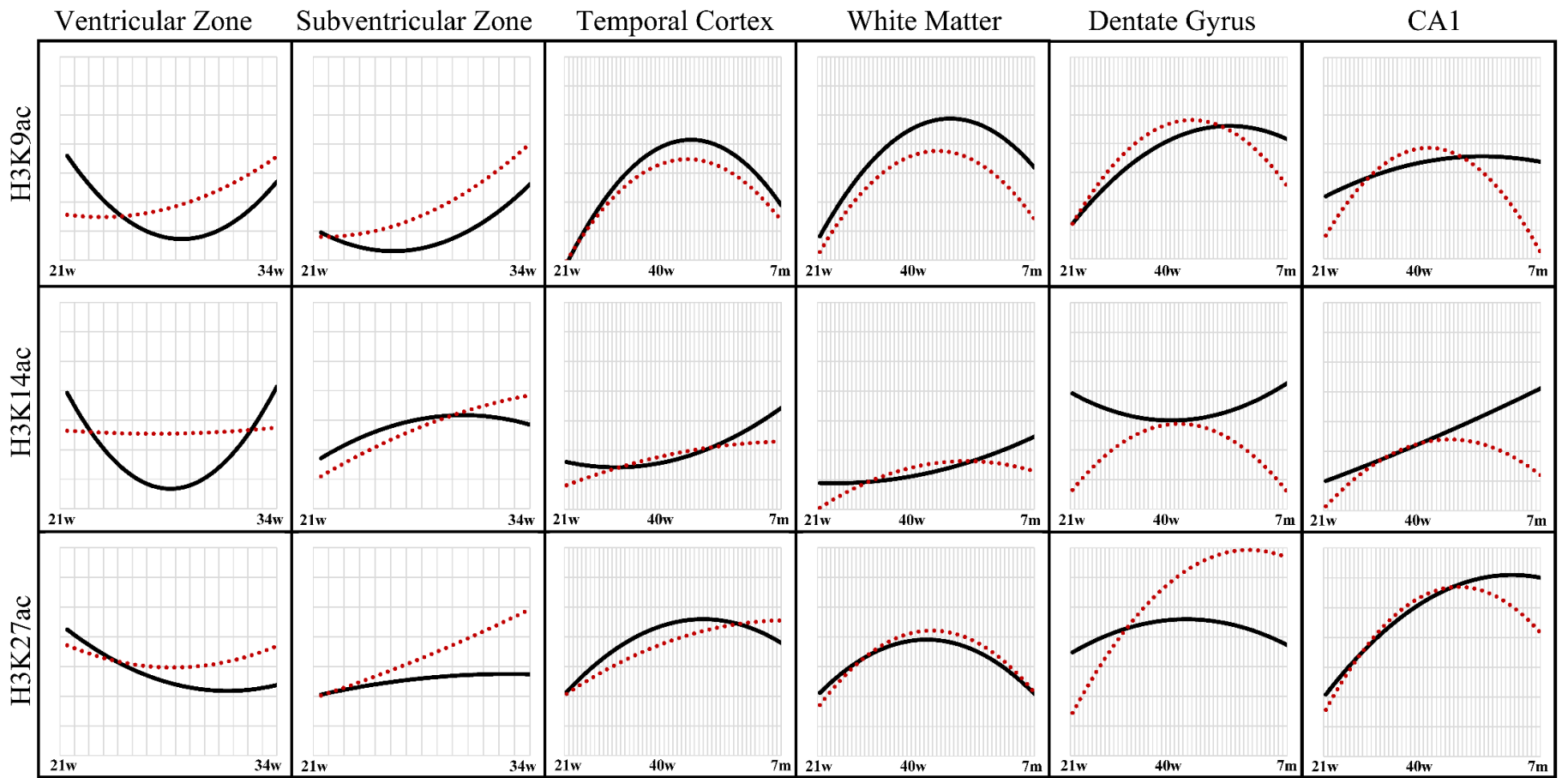
Figure 5.5: Graphic representation of semiquantitative score values (maximum 14; Y-axis) for histone H4 acetylation marks in the human brain regions assessed. The black curve represents the control cases and the red dotted curve represents PNAE. The X-axis represents the post-conception age in weeks (7m = 70.5 weeks post-conception). The ventricular and subventricular zones only show the fetal cases up to 34 weeks gestation because the structures are not present afterward.

| | Ventricular Zone | Subventricular Zone | Temporal Cortex | White Matter | Dentate Gyrus | CA1 |
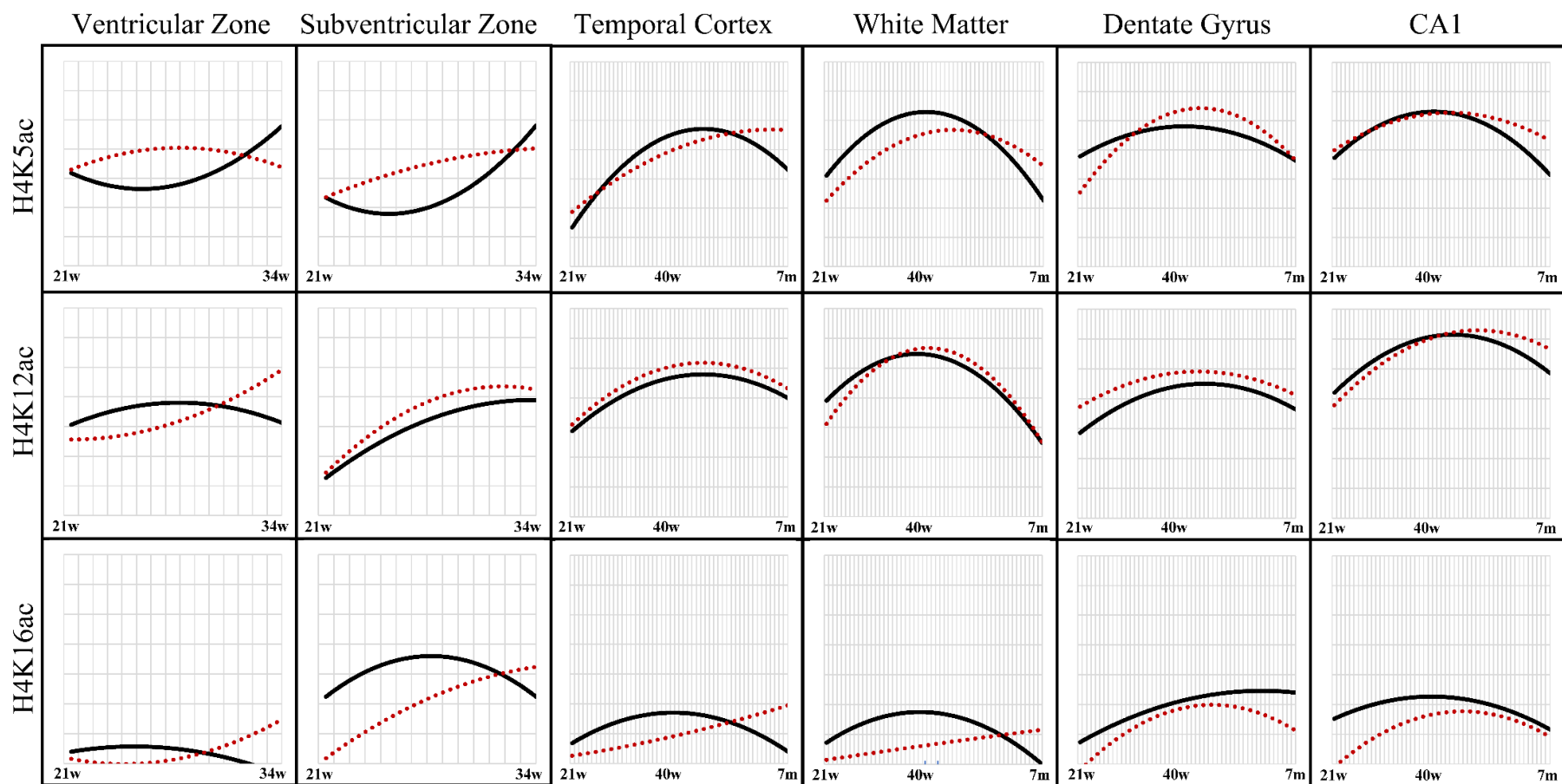
Figure 5.6: Graphic representation of semiquantitative score values (maximum 14; Y-axis) statistically significant epigenetic marks in the human temporal ependyma. The black curve represents the control cases and the red dotted curve represents PNAE. The X-axis represents the post-conception age in weeks (7m = 70.5 weeks post-conception).
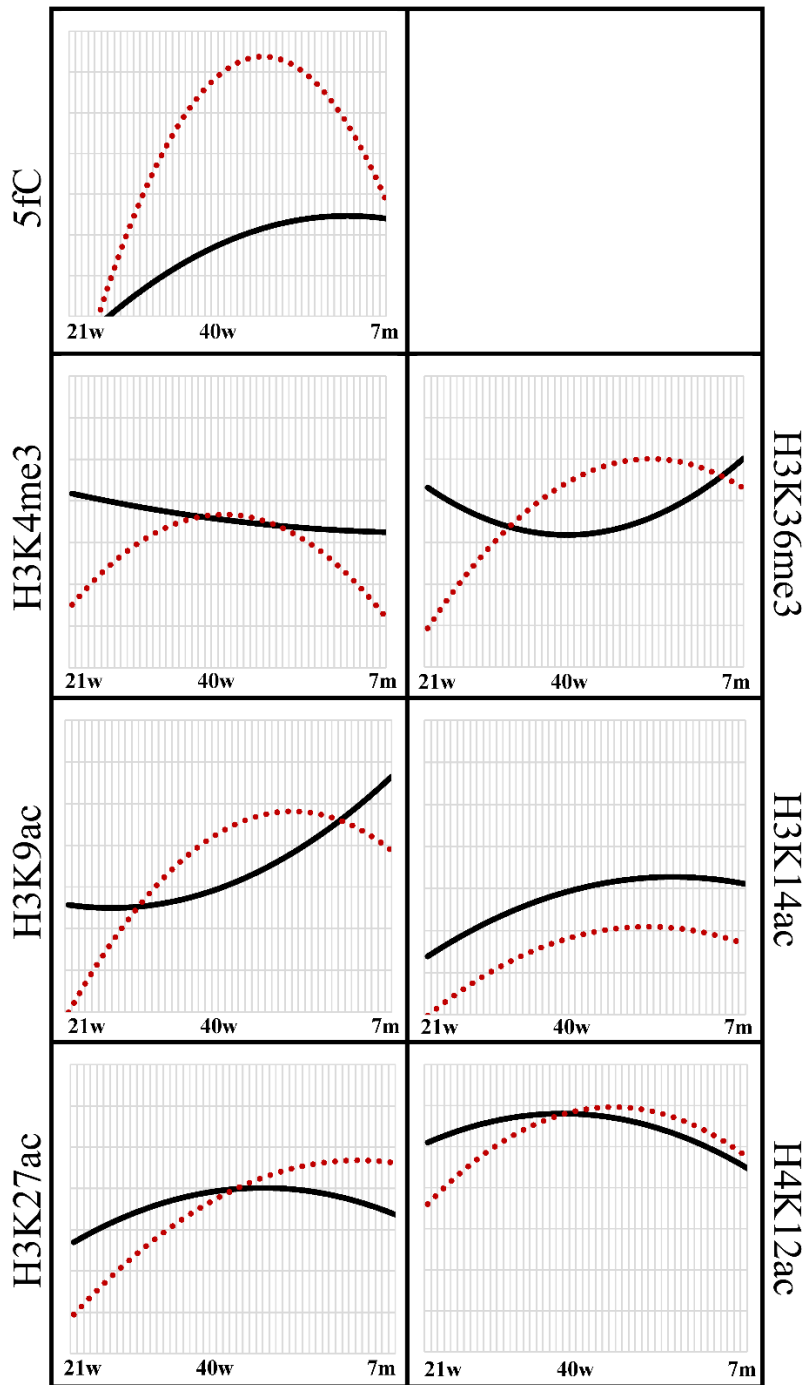
Table 5.9: Statistically significant results for human control and PNAE pairings (n=18 pairs).

Brain location	Age range in post-conception weeks	Increased in PNAE	Decreased in PNAE
Ventricular Zone	All ages (21-34)	-	-
	21-25	-	H4K12ac (p=0.0019)
	31-34	H3K9ac (p=0.0477)	-
Subventricular Zone	All ages (21-34)	H3K27me3 (p=0.0385)* H3K36me3 (p=0.0268) H3K9ac (p=0.0525) H3K27ac (p=0.0759)	-
	21-25	-	H4K16ac (p=0.0407)
	31-34	5mC (p=0.0477) H3K36me3 (p=0.0533) H3K9ac (p=0.0471) H3K27ac (p=0.0452)	5caC (p=0.0471)*
Temporal Ependyma	All ages (21-70)	5fC (p=0.0067)	H3K14ac (p=0.0118) H3K4me3 (p=0.0232)
	All fetuses	-	-
	21-25	-	H3K4me3 (p=0.0117) H3K9ac (p=0.0099) H3K27ac (p=0.0071)
	31-40	-	-
	All infants	5fC (p=0.0183) H3K36me3 (p=0.0361)	H3K14ac (p=0.0235) H4K12ac (p=0.0585)
	43-48.5	5fC (p=0.0436)	H3K14ac (p=0.0492)
	53-70.5	-	-
Temporal Cortex	All ages (21-70)	-	5mC (p=0.0269) H3K4me3 (p=0.0382) H4K16ac (p=0.0649)
	All fetuses	-	5mC (p=0.0451)
	21-25	-	H3K9ac (p=0.0407)*
	31-40	-	-
	All infants	-	5hmC (p=0.0585) H3K4me3 (p=0.0413) H3K9ac (p=0.0198)
	43-48.5	-	H3K4me3 (p=0.0357) H3K9ac (p=0.0101) H3K27ac (p=0.0114)
	53-70.5	-	-
White Matter	All ages (21-70)	-	H4K16ac (p=0.0073)
	All fetuses	-	H4K5ac (p=0.0431) H4K16ac (p=0.0141)
	21-25	-	H3K9ac (p=0.0189)*
	31-40	-	H4K16ac (p=0.0389)
	All infants	-	H3K36me3 (p=0.0296) H3K9ac (p=0.0673)
	43-48.5	-	-

Brain location	Age range in post-conception weeks	Increased in PNAE	Decreased in PNAE
	53-70	-	H3K4me3 (p=0.0286)* H3K9ac (p=0.0424)
Dentate Gyrus	All ages (21-70)	H3K14ac (p=0.0432) H4K12ac (p=0.0622)	H3K4me3 (p=0.0652)
	All fetuses	H4K12ac (p=0.0671)	5caC (p=0.0521)
	21-25	-	H4K5ac (p=0.0548)
	31-40	-	-
	All infants	H3K27ac (p=0.0505) H3K36me3 (p=0.0125)	H3K27me3 (p=0.0178) H3K4me3 (p=0.0500) H4K16ac (p=0.0118)
	43-48.5	-	H4K16ac (p=0.0170)
	53-70.5	-	-
CA1 Neurons	All ages (21-70)	-	H4K16ac (p=0.0625)
	All fetuses	-	-
	21-25	-	5mC (p=0.0099) H4K16ac (p=0.0730)
	31-40	-	-
	All infants	-	-
	43-48.5	-	H3K4me3 (p=0.0399)
	53-70.5	-	H3K27ac (p=0.0383)

p-values determined from two-tailed paired t test. p<0.05 is considered statistically significant, but trends with p<0.075 are also reported for discussion purposes because of the small sample sizes in some subgroups.
* indicates statistical difference with possibility of biologic irrelevance (e.g. small overall difference but small variance).
- no significant differences in pairing

Table 5.10: Immunohistochemical expression of epigenetic marks - comparison between control and PNAE macaque temporal lobes.

Epigenetic mark	Ependyma	Temporal Cortex	White Matter	Dentate Gyrus	CA1 Neurons
5mC	-	-	-	-	-
5hmC	-	-	-	-	-
5fC	↓ p=0.0007	-	-	-	- a
5caC	↓ p=0.0081	-	-	-	-
H3K4me3	-	-	-	-	-
H3K9me2,K9me3	↓ p=0.0423	-	-	-	- a
H3K27me3	↓ p=0.0526	-	-	-	↓ p=0.0071
H3K36me3	↓ p=0.0005	↓ p=0.0195	↓ p=0.0316	↓ p<0.0001	↓ p=0.0096
H3K9ac	↓ p=0.0115	- a	-	-	- a
H3K27ac	-	-	-	-	-
H4K5ac	-	-	-	- a	- a
H4K12ac	-	-	-	-	↑ p=0.0304

p-values determined from two-tailed t test. p<0.05 is considered statistically significant
- no significant differences
↓ - decreased in PNAE (n=6) relative to control (n=5)
↑ - increased in PNAE (n=6) relative to control (n=5)
a - minimal immunoreactivity

Figure 5.7: Photomicrographs of the human temporal neocortex surface (red arrows) for epigenetic marks 5mC, H3K4me3, H3K27ac, and H4K5ac. Red arrows point to the positively labelled narrow band of cells, with the exception of 5mC. Images were taken at 20x (upper panels) and 200x (lower panels) magnifications. DAB detection of antibody (brown) and hematoxylin counterstain (blue). The gestational age in weeks (w) is indicated for each panel.
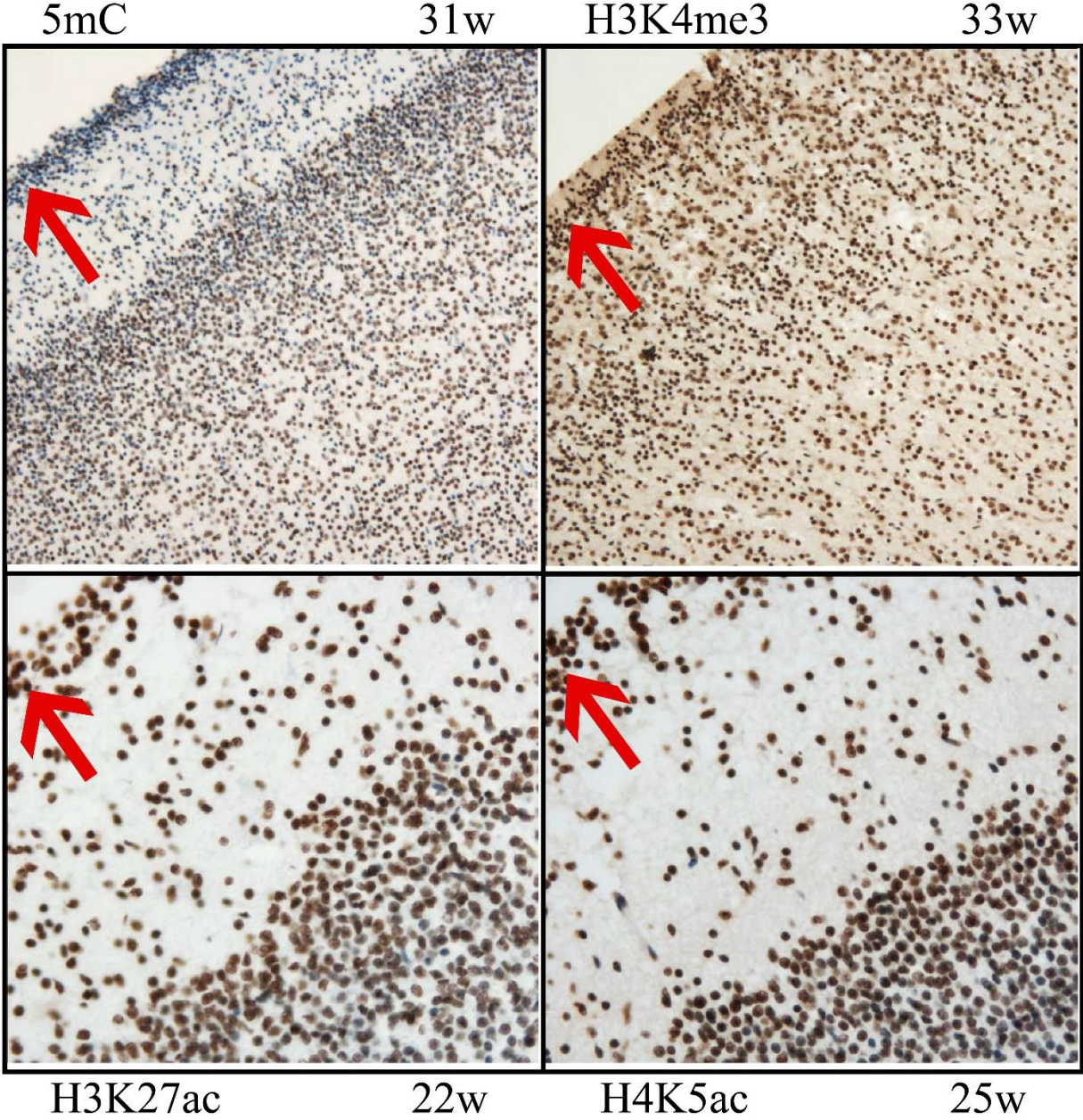
Figure 5.8: Photomicrograph of the human control ventricular (VZ) and subventricular zones (SVZ) for 5mC. The VZ is strong positive, decreases and then becomes strong positive before its disappearance at 31-34 weeks ('U' shape). The SVZ increased with increasing age. The observed increase in the SVZ was significant (p=0.0477) for PNAE. Images were taken at 200x magnification. DAB detection of antibody (brown) and hematoxylin counterstain (blue). The gestational age in weeks (w) is indicated for each panel. V= ventricle.

Control   PNAE

21w   20w

V   VZ   SVZ

25w   27w

31w   29w

33w   34w

294
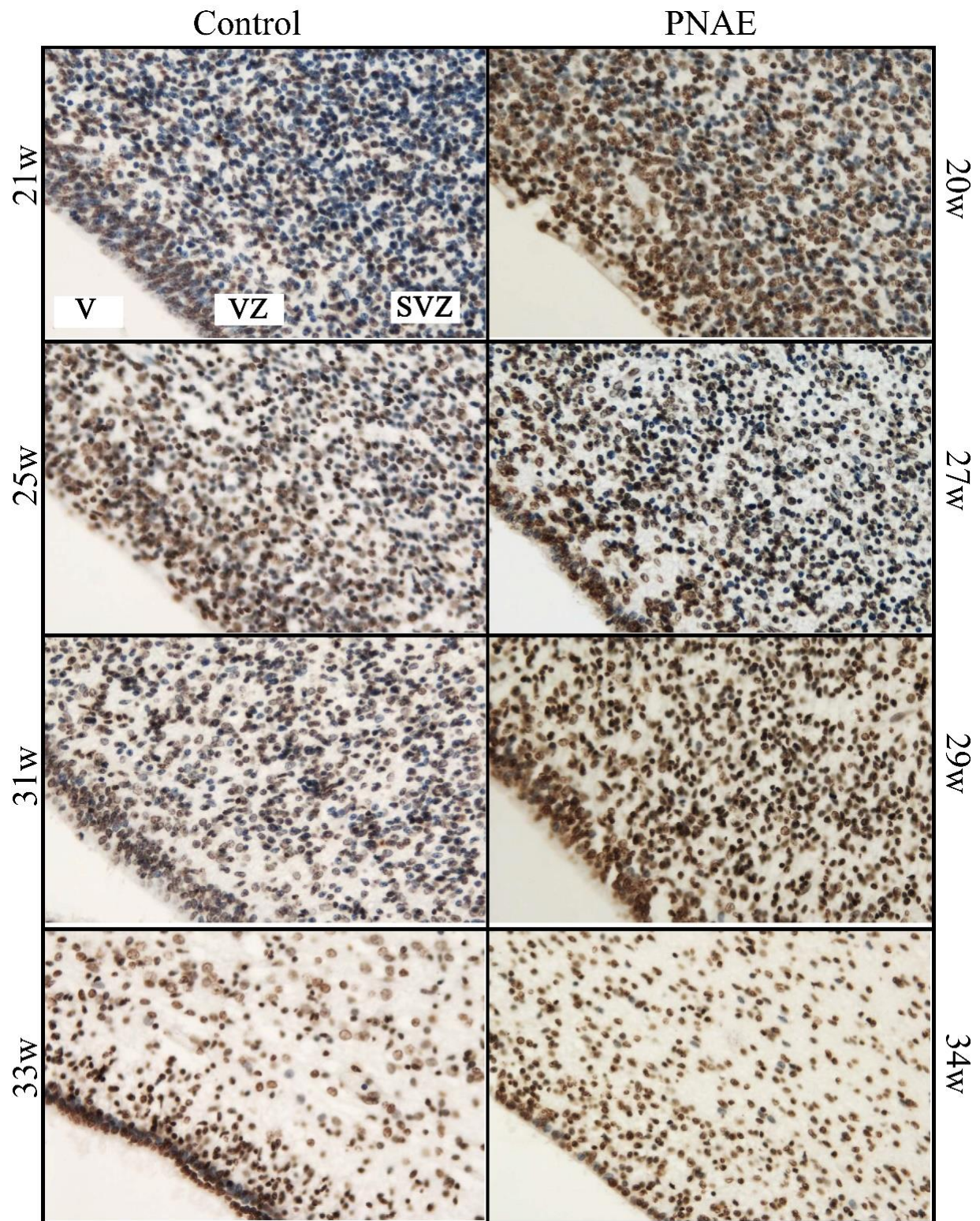
Figure 5.9: Photomicrograph of the human control ventricular (VZ) and subventricular zones (SVZ) for H3K36me3. In the VZ, the control case demonstrates strong immunoreactivity, decreases, then increases again ('U' shape) before its disappearance at 31-34 weeks PC. The SVZ increased with increasing age. The observed increase in PNAE SVZ was significant (p=0.0268 and p=0.0533). Images were taken at 200x magnification. DAB detection of antibody (brown) and hematoxylin counterstain (blue). The gestational age in weeks (w) is indicated for each panel. V= ventricle.

Control | PNAE

21w — 20w
25w — 27w
31w — 29w
33w — 34w

296
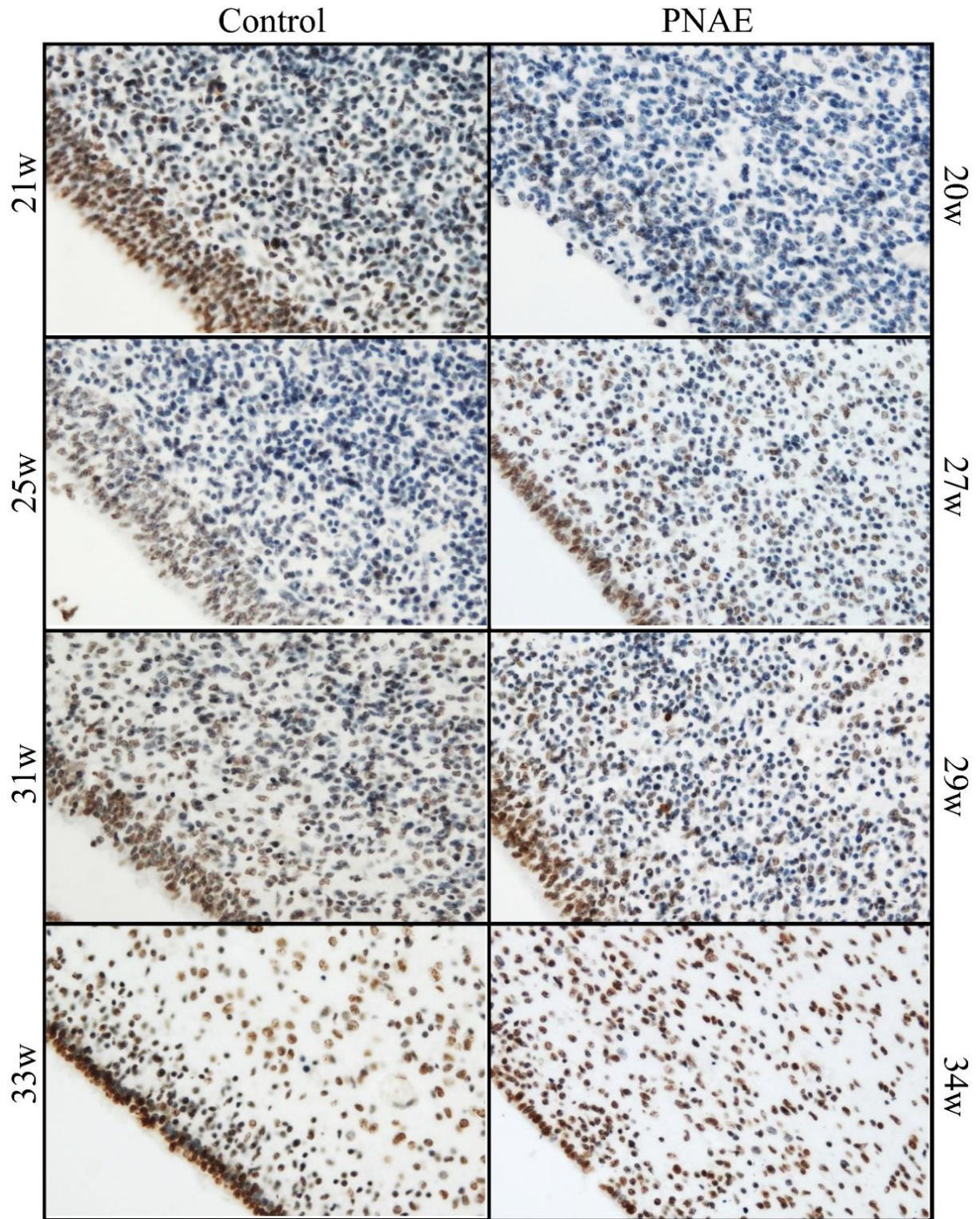
Figure 5.10: Photomicrographs of human control vascular endothelial cells, arterial smooth muscle cells lining blood vessels, and epithelial cells of the choroid plexus. a) H3K9ac (41 post-conception weeks (w). b) 5mC (20w). c) H3K27ac (43w). d) H4K5ac (57.5w). e) H3K4me3 (66w). f) H3K36me3 (66w). Note that the endothelial and smooth muscle nuclei are typically a mix of positive and negative, while the choroid plexus cells tend to be more uniformly positive. Images were taken at 400x magnification. DAB detection of antibody (brown) and hematoxylin counterstain (blue).
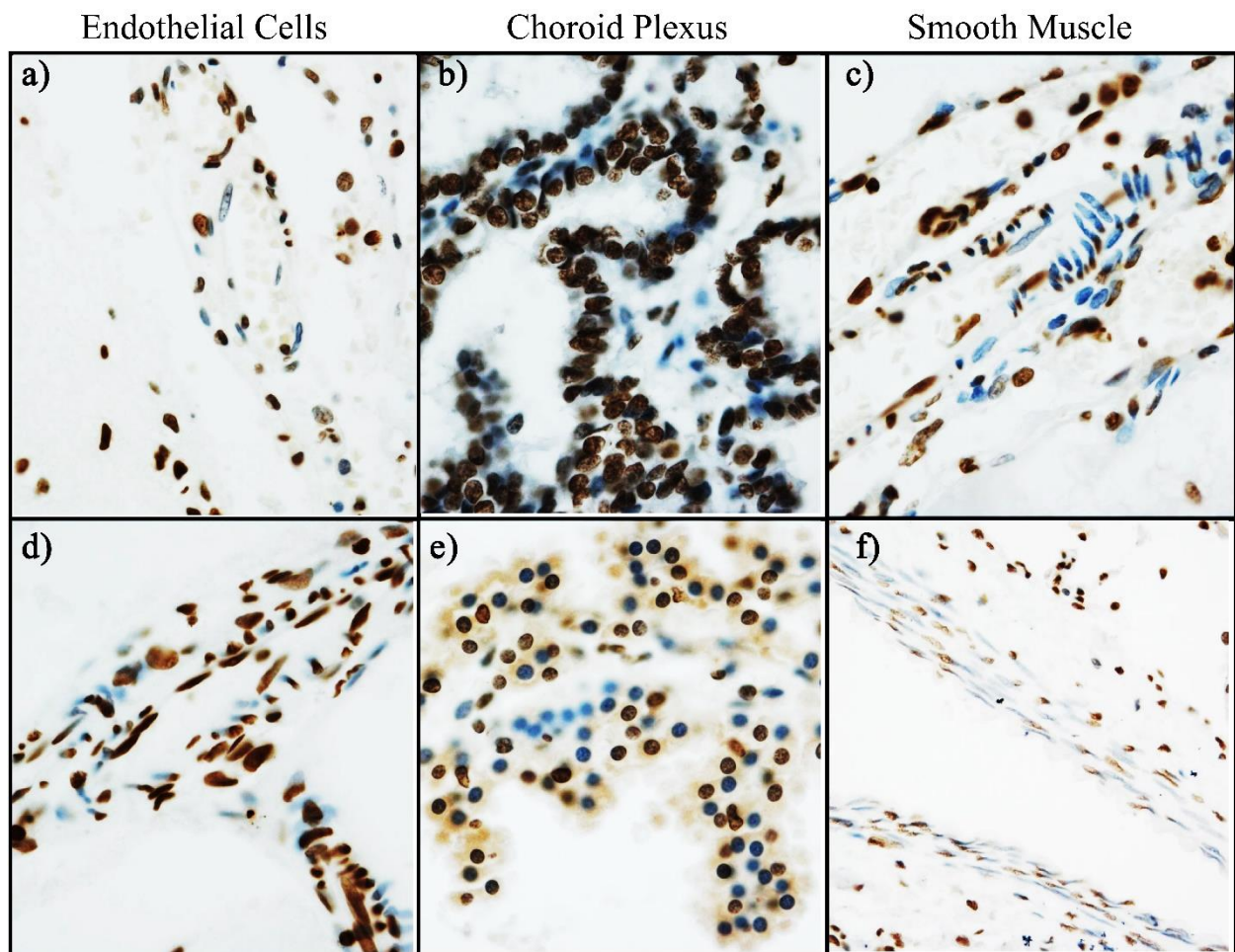
Figure 5.11: Photomicrographs of human control temporal neocortex showing discrepancies between selective and total histone antibodies. Red arrows depict the difference in intensity and blue arrows point at negative nuclei primarily in the background. Antibodies to total histone H3, total histone H4, H3 pan acetyl, and H4 pan acetyl do not necessarily show more widespread immunoreactivity than corresponding more selective antibodies to H3K27ac and H4K12ac. Images were taken at 400x magnifications. DAB detection of antibody (brown) and hematoxylin counterstain (blue).
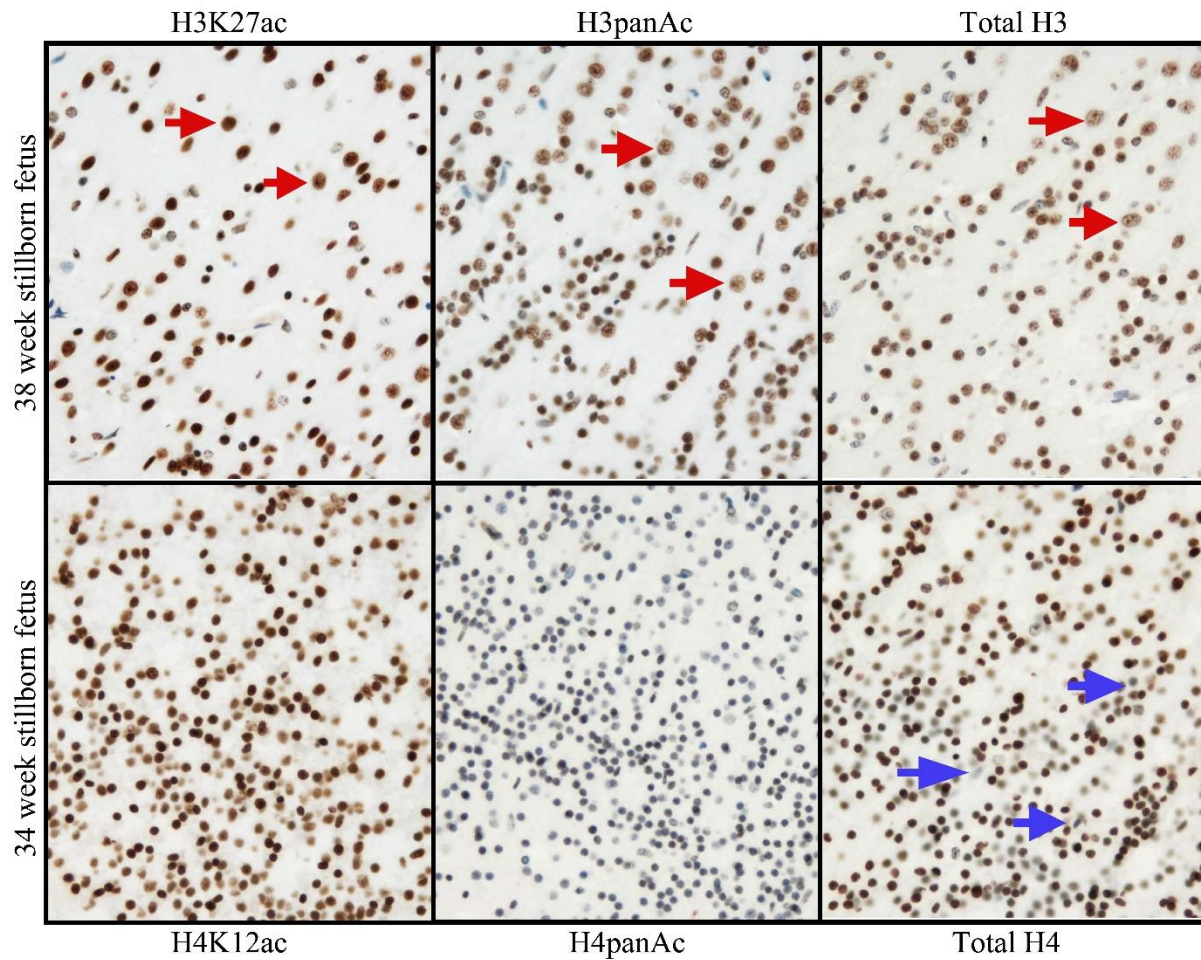
Figure 5.12: Photomicrographs of human control and PNAE human temporal neocortex (CX) and white matter (WM) for H3K4me3 and H3K9ac (respectively). Among PNAE, H3K4me3 was significantly decreased (p=0.0382; all ages) as well as H3K9ac (p=0.0673; infants). Post-conception ages in weeks (w) are shown. Images were taken at 200x magnification. DAB detection of antibody (brown) and hematoxylin counterstain (blue).
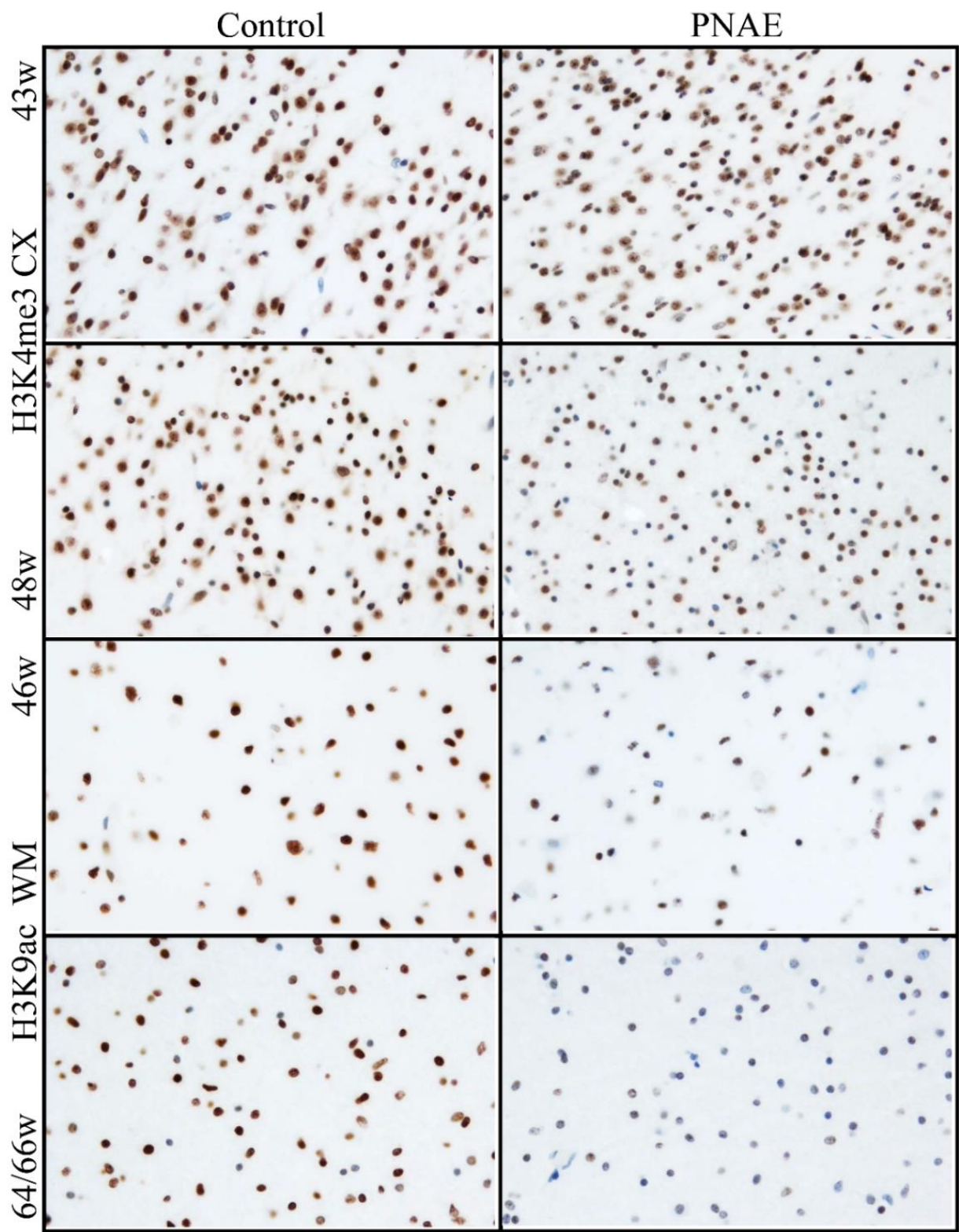
Figure 5.13: Photomicrographs of the human control and PNAE dentate gyrus for H3K4me3. PNAE significantly decreased (p=0.050; all infants) and a trend was seen among all ages (p=0.0652). Post-conception ages in weeks (w) are shown. Images were taken at 400x magnification. DAB detection of antibody (brown) and hematoxylin counterstain (blue).

Control   PNAE

25w   27w

46w   46w

70.5w   70.5w
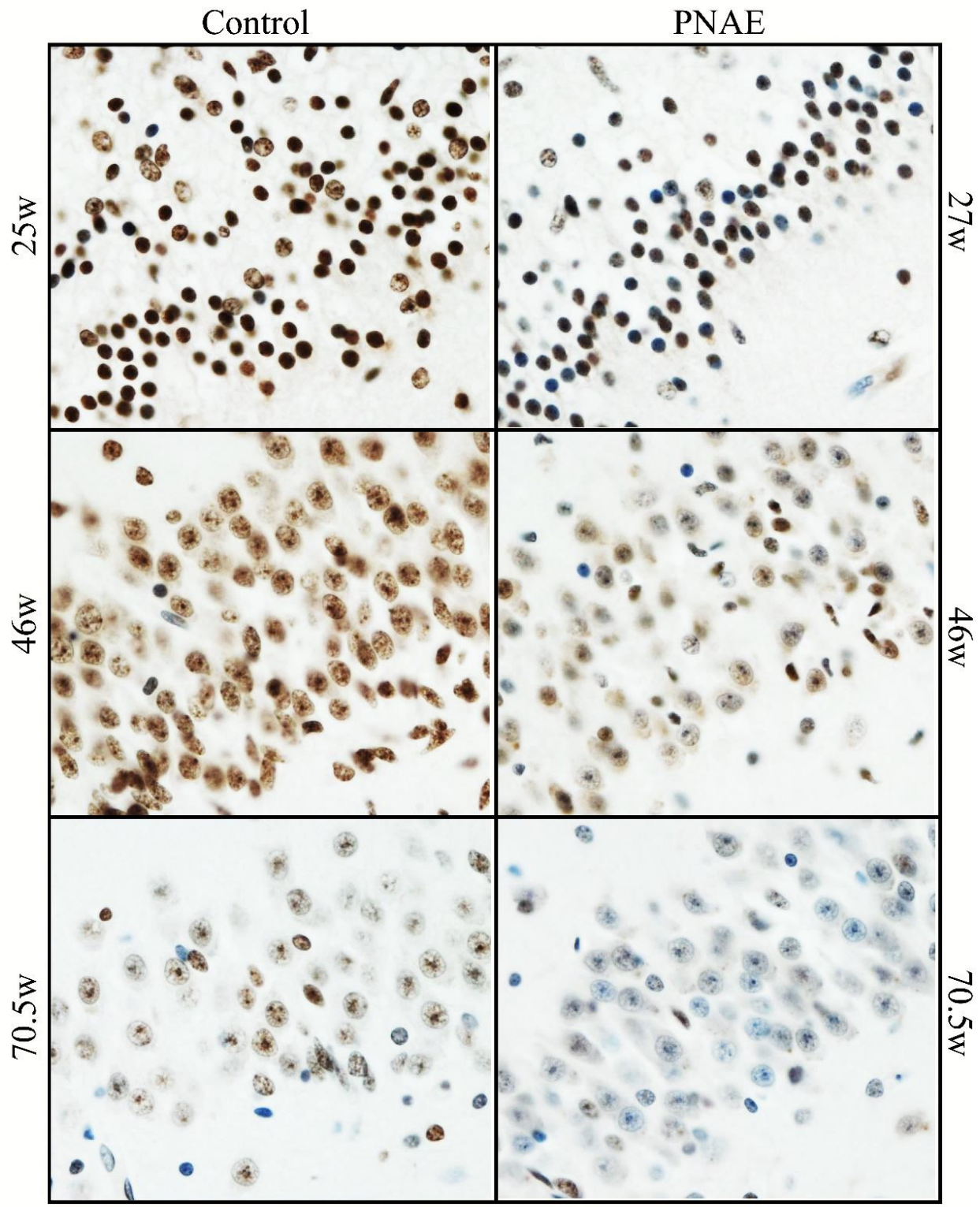
Figure 5.14: Photomicrographs of control and PNAE macaque dentate gyrus (DG) for H3K36me3, and CA1 neurons for H3K36me3, H3K27me3, and H4K12ac. PNAE was significantly lower for H3K36me3 (DG p<0.001, CA1 p=0.0096) and H3K27me3 (p=0.0071), and significantly higher for H4K12ac (p=0.0304). *In utero* exposure to 3.3g/kg ethanol (H3K36me3), 2.5g/kg (H3K27me3), and 4.1g/kg (H4K12ac). Images were taken at 400x magnifications. DAB detection of antibody (brown) and hematoxylin counterstain (blue).
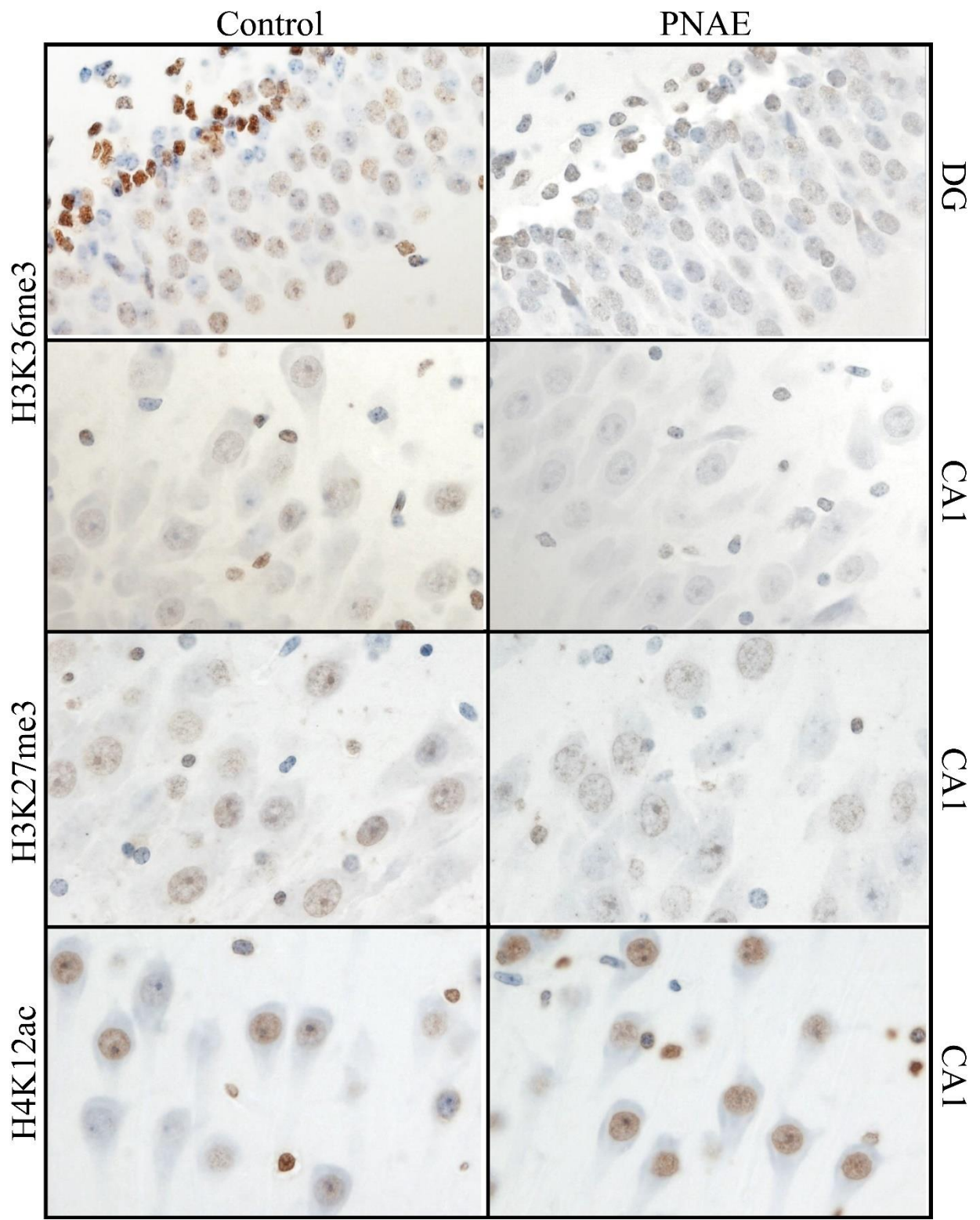
Figure 5.15: Photomicrographs of control and PNAE macaque temporal horn ependyma for 5fC and H3K27me3. The decrease among PNAE for 5fC was statistically significant (p=0.0313), and a trend was observed for H3K27me3 (p=0.0625). Prenatal alcohol exposure is also shown in g/kg maternal body weight. Images were taken at 400x magnifications. DAB detection of antibody (brown) and hematoxylin counterstain (blue).
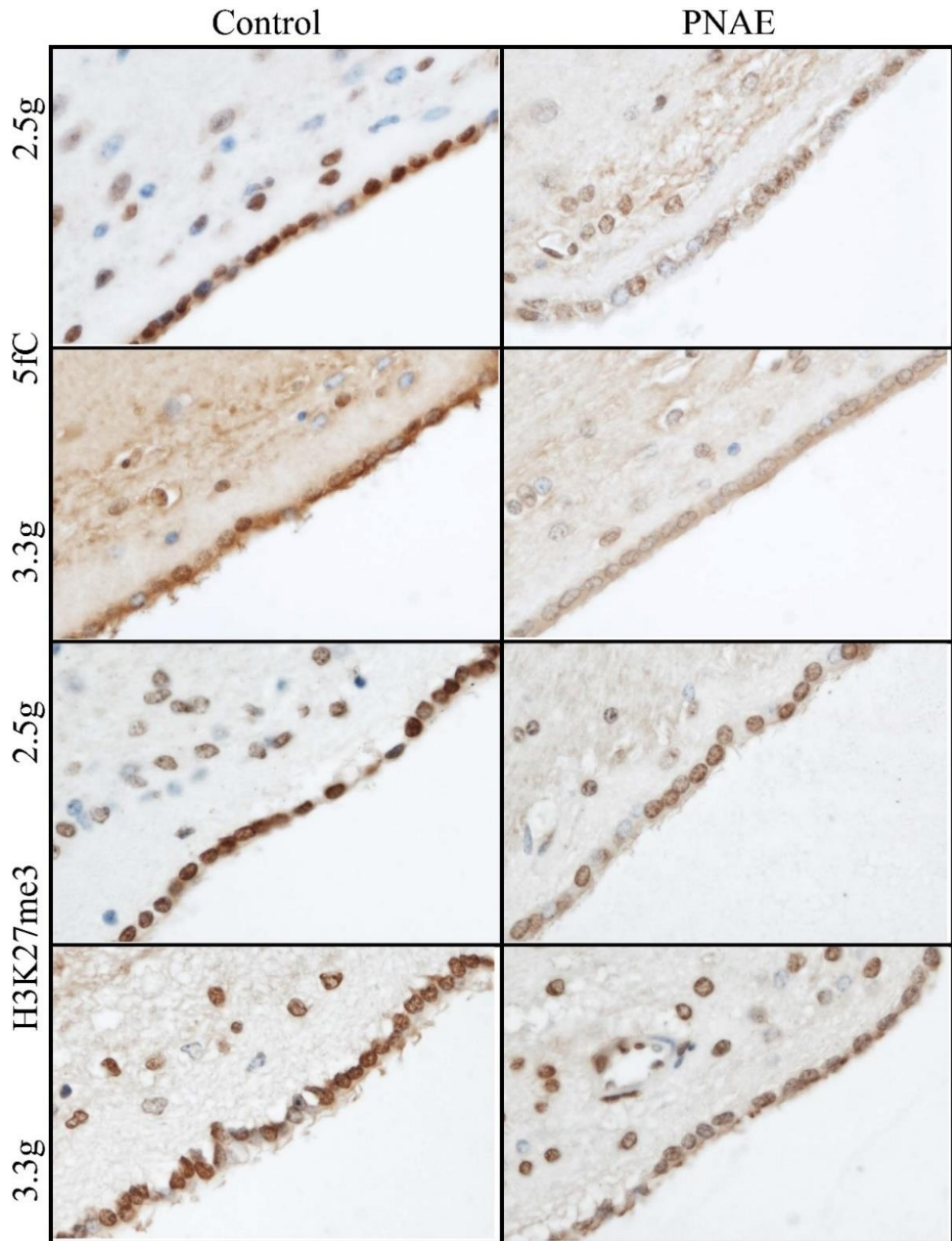
CHAPTER 6: SUMMARY OF DISCUSSION

Conclusions

I have described the largest collection of human brains with documented prenatal alcohol exposure (PNAE) or a diagnosis of Fetal Alcohol Spectrum Disorder (FASD) in the medical literature. I have demonstrated that epigenetic studies utilizing immunohistochemistry on human autopsy brain tissue are feasible. One must be cautious when interpreting histone acetylation results because many are prone to post-mortem degradation (e.g. H4K5ac). I hypothesized that PNAE is associated with epigenetic changes that persist in neuronal and glial cell populations. Based on the findings, I accept my hypothesis. Statistically significant changes were seen among multiple epigenetic marks in the temporal lobe, including hippocampus, of human fetuses and infants. Some of them correspond with changes in a non-human primate FASD model. These epigenetic modifications might be involved in the pathogenesis of the neurodevelopmental defect in FASD, however a cause-effect relationship could not be determined.

Summary of Study Limitations

No study is without limitations. The human PNAE / FASD cohort of 174 cases had many confounding variables. Maternal histories and alcohol use details were inconsistently reported. Therefore, my classification of PNAE is at best an estimate. We were not able to specify ethnicity; it has been shown that processing of alcohol differs between ethnic groups. Among the older age groups where an FASD diagnosis was made, FASD diagnostic criteria were likely not applied uniformly, because these cases spanned several decades. There was likely a referral and ascertainment bias, particularly among the teenage and adult age groups. Brain sampling also varied because several different neuropathologists conducted the post-mortem examinations.

Micrencephaly (i.e. small brain) is the most common abnormality associated with FASD. The circumstances before death (e.g. brain swelling) could have affected brain weight at death, therefore, reliance on the brain weight could mask the presence of pre-existing micrencephaly. Because the majority of our cases did not undergo comprehensive genetic analysis, we cannot absolutely exclude the possibility that documented brain abnormalities are due to an unrecognized genetic disorder rather than PNAE.

Our post-mortem delay study had several technical limitations. Most antibody specification sheets documented the immunogen and made claims about recognition of certain antigens. However, cross reactivity among all species is seldom documented. In particular, the use on pig tissue is non-standard. Antibodies may not work equally well in all methods (e.g. immunohistochemistry on paraffin embedded tissue vs. Western blots vs. dot blots, etc.). I observed discrepancies in the apparent post-mortem stability of histone PTMs between immunohistochemical detection and Western blotting methods. I did not test all of the anti-histone antibodies with all possible peptides to fully evaluate blocking in immunohistochemistry and sensitivity in dot blot. I expected total histone antibodies to show more widespread immunoreactivity than antibodies targeting specific histone marks. However, this was not the case. Therefore, the use of "total histone" H3 or H4 antibodies to normalize the Western blots might not be entirely reliable.

My final study also had a few limitations, the most important being small sample sizes. I cannot exclude the possibility of type 1 errors (false negative) in the statistical analysis. In both the PMD study and my final study, I was forced to group males and females despite known epigenetic differences (e.g. histone modifications are sexually dimorphic in the developing mouse hippocampus (Tsai, Grant, & Rissman, 2009)) as well as brain differences (functional and

behavioural, generally as a result of hormones (Choleris, Galea, Sohrabji, et al., 2018; Marrocco, & McEwen, 2016)) between sexes. The original intent was to have males and females ungrouped, since there is an underrepresentation of females (due to male bias) among neuroscience-based research. Some of the analyses showed statistically significant differences, but the polynomial curves appeared to overlap. This could reflect the situation where a small biologically irrelevant difference is consistent and gives a false positive. Our age-, sex- and PMD-matched controls were not matched with regard to ethnicity. As mentioned previously, there are genetic differences among race with regard to metabolic enzymes (Wall, Luczak, & Hiller-Sturmhöfel, 2016; Zakhari, 2006). A global genomic DNA methylation study in humans was able to distinguish people by their ethnicity through distinct DNA methylation patterns (Zhang, Cardarelli, Carroll, et al., 2011). The macaque brain samples were over-fixed, and the paraffin blocks were brittle, possibly allowing oxidation of exposed tissue during the approximate 30 years storage. Despite having re-embedded the tissues, the results must be interpreted with caution because immunoreactivity was greatly reduced and many sections showed various artefacts (patches of unstained tissue). However, these artefacts did not greatly interfere with our analysis, because the hippocampus is medially located within the temporal lobe and most artefacts were located around the edges of the samples.

Future Directions

In our autopsy cohort, most mothers smoked cigarettes and many abused other drugs like marijuana or cocaine during pregnancy in combination with alcohol. Very few animal models have investigated combinational *in utero* drug exposure (Bhattacharya, Majrashi, Ramesh, et al., 2018; Church, Holmes, Overbeck, et al., 1991; Martin, Martin, Chao, et al., 1982; Mitchell,

Keller, & Snyder-Keller, 2002; Morris, Dinieri, Szutorisz, et al., 2011; Wells, Bhatia, Drake, et al., 2016). Nicotine is a vasoconstrictor, thereby decreasing blood flow to the placenta (Behnke, & Smith, 2013). In addition, nicotine has been postulated to reduce blood alcohol levels (Chabenne, Moon, Ojo, et al., 2014). Therefore, studies combining nicotine and alcohol exposure *in utero* and evaluate the effects on the developing brain are suggested. Bhattacharya *et al.* developed a nicotine-PNAE model where pregnant rats received a subcutaneous dose of nicotine while consuming 10% alcohol in tap water (Bhattacharya, Majrashi, Ramesh, et al., 2018). At 6 weeks of age the cerebellum of offspring showed greater deleterious effects than alcohol alone (ROS production, lipid peroxidation, glutathione content, caspase and catalase activity) (Bhattacharya, Majrashi, Ramesh, et al., 2018). With legalization of marijuana in Canada, the instances of multi-drug exposure may continue to rise. An investigation into these multi-drug effects *in utero* is merited in rodents and is more reflective of the human condition.

I did not use immunohistochemical double labeling to specifically identify brain cell types in the human PNAE cohort. I based the identity of neurons, astrocytes, and oligodendrocytes by cell morphology, which is standard practice in diagnostic neuropathology but is subjective. For example, in the hippocampus and cortex, the large neurons can be easily identified but the smaller interneurons would need labeling in order to distinguish them from glial cells. Some epigenetic marks are claimed to be cell-type specific (e.g. 5hmC for neurons) (Jang, Shin, Lee, et al., 2017). Therefore, it would be ideal to verify the epigenetic changes in specific brain cells.

One outstanding question that remains is why not every nucleus is labeled with antibodies targeting "total" histone. Every cell has a nucleus with chromatin within the nucleolus. The covalent cross-linking reaction of formaldehyde is almost completely reversed

with antigen retrieval methods, yet endothelial cells in particular are almost always ~50% positive. Beyond the technical question about the antibody specificity, there might be an interesting biological question concerning, for example, endothelial proliferation.

With regard to the stability of epigenetic modifications, it would be of interest to study the enzymes responsible for removing these epigenetic modifications. In particular, histone deacetylase (HDACs) and histone lysine acetylase (KATs) enzymes might be able to function temporarily in a hypoxic environment after death. This could explain why histone acetylation stability is variable.

Whole genome DNA methylation studies are becoming popular for biomarker identification at the tissue and individual cell level. Identifying characteristic methylome signatures in disorders like FASD and autism would be useful, but has been challenging (Farré, Jones, Meaney, et al., 2015; Lussier, Morin, MacIsaac, et al., 2018). Conventional methylation arrays like the Illumina do not actually distinguish between 5-methylcytosine and 5-hydroxymethylcytosine. Bisulfite sequencing (MethylC-Seq) followed by Tet-assisted bisulfite sequencing (TAB-Seq) can enable the distinction (Yu, Hon, Szulwach, et al., 2012; Zhang, Keown, Wen, et al., 2018). Direct investigation of brain tissue is not possible in living humans but might point to parallel changes in accessible cell populations (i.e. buccal epithelium). Therefore, it would be ideal to correlate our FASD brain epigenetic findings with other routinely sampled tissue (at autopsy) from the oral cavity / throat (i.e. tongue, larynx, oesophagus, etc.), which are possibly reflective of buccal epithelium. Also emerging are studies showing signatures among the enzymes responsible for epigenetic modifications (Butcher, Cytrynbaum, Turinsky, et al., 2017). If the epigenetic machinery itself is being epigenetically modified, this could explain some of the heterogeneity in the FASD phenotype.

While conducting the descriptive epidemiology component of the thesis work, it became apparent that the inconsistent reporting of clinical histories in autopsy reports should be standardized. This a more a recommendation than a future direction. The information and level of detail reported in autopsy reports is inconsistent. This inconsistency may be as a result of the case itself, the reason behind the request to conduct an autopsy, or practice of the pathologist involved. Perhaps a standard could be applied when reporting clinical histories. A general outline is typically followed when it comes to the reporting of gross and microscopic findings in organs including brain, but the clinical history section lacks required fields and organization. With the possible increased use of utilizing human autopsy material to conduct epigenetic studies, detailed clinical histories would enable proper sample selection and may possibly allow for the reduction of multiple confounding variables.

REFERENCE LIST

Abbott, C. W., Rohac, D. J., Bottom, R. T., Patadia, S., & Huffman, K. J. (2017). Prenatal Ethanol Exposure and Neocortical Development: A Transgenerational Model of FASD. *Cerebral Cortex*. July;1–14.

Abdel-Misih, S. R. Z., & Bloomston, M. (2014). Liver Anatomy. *Surg Clin North Am*. 90(4);643–653.

Abel, E. L. (2004). Paternal contribution to fetal alcohol syndrome. *Addiction Biology*. 9(2);127–133.

Abel, E. L., & Bilitzke, P. (1990). Paternal alcohol exposure: paradoxical effect in mice and rats. *Psychopharmacology*. 100(2);159–164.

Adle-Biassette, H., Harding, B., & Golden, J. (Eds.). (2018). *Developmental Neuropathology* (Second.) John Wiley & Sons Ltd.

Alabert, C., Barth, T. K., Reverón-Gómez, N., Sidoli, S., Schmidt, A., Jensen, O., Imhof, A., & Groth, A. (2015). Two distinct modes for propagation of histone PTMs across the cell cycle. *Genes and Development*. 29(6);585–590.

Alfonso-Loeches, S., & Guerri, C. (2011). Molecular and behavioral aspects of the actions of alcohol on the adult and developing brain. *Critical Reviews in Clinical Laboratory Sciences*. 48(1);19–47.

Andeen, N. K., Bowman, R., Baullinger, T., Brooks, J. M., & Tretiakova, M. S. (2017). Epitope preservation methods for tissue microarrays. *American Journal of Clinical Pathology*. 148(5);380–389.

Anderson, K. W., Chen, J., Wang, M., Mast, N., & Pikuleva, I. A. (2015). Quantification of histone deacetylase isoforms in human frontal cortex, human retina, and mouse brain. *PlOS One*. 10(5);1–16.

Ardekani, A. M., & Naeini, M. M. (2010). The role of microRNAs in human diseases. *Avicenna Journal of Medical Biotechnology*. 2(4);161–179.

Arias-Carrión, O., Stamelou, M., Murillo-Rodríguez, E., Menéndez-González, M., & Pöppel, E. (2010). Dopaminergic reward system: a short integrative review. *International Archives of Medicine*. 3;24.

Arnold, S. E., & Trojanowski, J. Q. (1996). Human Fetal Hippocampal Development : and Neuronal Morphologic Features. *Journal of Comparative Neurology*. 367;274–292.

Arshad, A., Vose, L. R., Vinukonda, G., Hu, F., Yoshikawa, K., Csiszar, A., Brumberg, J. C., & Ballabh, P. (2016). Extended Production of Cortical Interneurons into the Third Trimester of Human Gestation. *Cerebral Cortex*. 26(5);2242–2256.

Auclair, G., & Weber, M. (2012). Mechanisms of DNA methylation and demethylation in mammals. *Biochimie*. 94(11);2202–11.

Avery, S. N., Clauss, J. A., Winder, D. G., Woodward, N., Heckers, S., & Blackford, J. U. (2014). BNST neurocircuitry in humans. *NeuroImage*. 91;311–23.

Babenko, O., Kovalchuk, I., & Metz, G. A. S. (2015). Stress-induced perinatal and transgenerational epigenetic programming of brain development and mental health. *Neuroscience and Biobehavioral Reviews*. 48;70–91.

Bager, H., Christensen, L. P., Husby, S., & Bjerregaard, L. (2017). Biomarkers for the Detection of Prenatal Alcohol Exposure: A Review. *Alcoholism: Clinical and Experimental Research*. 41(2);251–261.

Bailey, B. A., & Sokol, R. J. (2011). Prenatal Alcohol Exposure and Miscarriage, Stillbirth, Preterm Delivery and Sudden Infant Death Syndrome. *Alcohol Research & Health*. 34(1);86–91.

Bak, S. T., Staunstrup, N. H., Starnawska, A., Daugaard, T. F., Nyengaard, J. R., Nyegaard, M., Børglum, A., Mors, O., Dorph-Petersen, K. A., & Nielsen, A. L. (2018). Evaluating the feasibility of DNA methylation analyses using long-term archived brain formalin-fixed paraffin-embedded samples. *Molecular Neurobiology*. 55;668–681.

Bakhireva, L. N., Garrison, L., Shrestha, S., Sharkis, J., Miranda, R., & Rogers, K. (2018). Challenges of diagnosing fetal alcohol spectrum disorders in foster and adopted children. *Alcohol (Fayetteville, N.Y.)*. 67;37–43.

Ballard, M. S., Sun, M., & Ko, J. (2012). Vitamin A, folate, and choline as a possible preventive intervention to fetal alcohol syndrome. *Medical Hypotheses*. 78(4);489–493.

Baltan, S. (2012). Histone deacetylase inhibitors preserve function in aging axons. *J Neurochem*. 123(Suppl 2);108–115.

Baltan, S., Bachleda, A., Morrison, R. S., & Murphy, S. P. (2011). Expression of histone deacetylases in cellular compartments of the mouse brain and the effects of ischemia. *Translational Stroke Research*. 2(3);411–23.

Banerjee, A., Chitnis, U., Jadhav, S., Bhawalkar, J., & Chaudhury, S. (2009). Hypothesis testing, type I and type II errors. *Industrial Psychiatry Journal*. 18(2);127.

Banerjee, N. (2014). Neurotransmitters in alcoholism: A review of neurobiological and genetic studies. *Indian Journal of Human Genetics*. 20(1);20–31.

Barau, J., Teissandier, A., Zamudio, N., Roy, S., Nalesso, V., Hérault, Y., Guillou, F., & Bourc'his, D. (2016). The DNA methyltransferase DNMT3C protects male germ cells from transposon activity. *Science*. 354(6314);909–912.

Barrachina, M., & Ferrer, I. (2009). DNA methylation of Alzheimer disease and tauopathy-related genes in postmortem brain. *Journal of Neuropathology and Experimental Neurology*. 68(8);880–91.

Barrachina, M., Moreno, J., Villar-Menéndez, I., Juvés, S., & Ferrer, I. (2012). Histone tail acetylation in brain occurs in an unpredictable fashion after death. *Cell and Tissue Banking*. 13(4);597–606.

Barth, T. K., & Imhof, A. (2010). Fast signals and slow marks: the dynamics of histone modifications. *Trends in Biochemical Sciences*. 35(11);618–626.

Bartolomei, M. S., & Ferguson-Smith, A. C. (2011). Mammalian genomic imprinting. *Cold Spring Harbor Perspectives in Biology*. 3(7);1–18.

Basalah, D. A. (2015). *Oxidative Stress and Neuronal Changes Associated with Prenatal Ethanol Exposure in Human and Monkey Brains*. University of Manitoba.

Basavarajappa, B., & Subbanna, S. (2016). Epigenetic Mechanisms in Developmental Alcohol-Induced Neurobehavioral Deficits. *Brain Sciences*. 6(2);12.

Baserga, R. (1974). Non-histone chromosomal proteins in normal and abnormal growth. *Life Sciences*. 15(5);1057–1071.

Beaulieu, J.-M., & Gainetdinov, R. R. (2011). The physiology, signaling, and pharmacology of dopamine receptors. *Pharmacological Reviews*. 63(1);182–217.

Becker, H. C., Diaz-Granados, J. L., & Randall, C. L. (1996). Teratogenic actions of ethanol in the mouse: a minireview. *Pharmacology, Biochemistry, and Behavior*. 55(4);501–513.

Behnke, M., & Smith, V. C. (2013). Prenatal substance abuse: short- and long-term effects on the exposed fetus. *Pediatrics*. 131(3);e1009-24.

Bekdash, R. A., Zhang, C., & Sarkar, D. K. (2013). Gestational choline supplementation normalized fetal alcohol-induced alterations in histone modifications, DNA methylation, and proopiomelanocortin (POMC) gene expression in β-endorphin-producing POMC neurons of the hypothalamus. *Alcoholism, Clinical and Experimental Research*. 37(7);1133–42.

315

Bernier, B. E., Whitaker, L. R., & Morikawa, H. (2011). Previous ethanol experience enhances synaptic plasticity of NMDA receptors in the ventral tegmental area. *The Journal of Neuroscience : The Official Journal of the Society for Neuroscience*. 31(14);5205–12.

Bhattacharya, D., Majrashi, M., Ramesh, S., Govindarajulu, M., Bloemer, J., Fujihashi, A., Crump, B. R., Hightower, H., Bhattacharya, S., Moore, T., Suppiramaniam, V., & Dhanasekaran, M. (2018). Assessment of the cerebellar neurotoxic effects of nicotine in prenatal alcohol exposure in rats. *Life Sciences*. 194(December 2017);177–184.

Biggio, G., Concas, A., Follesa, P., Sanna, E., & Serra, M. (2007). Stress, ethanol, and neuroactive steroids. *Pharmacology & Therapeutics*. 116(1);140–71.

Bishop, D. V. M. (2010). Which neurodevelopmental disorders get researched and why? *PloS One*. 5(11);e15112.

Biswal, S., Das, D., Barhwal, K., Kumar, A., Nag, T. C., Thakur, M. K., Hota, S. K., & Kumar, B. (2017). Epigenetic regulation of SNAP25 prevents progressive glutamate excitotoxicty in hypoxic CA3 neurons. *Molecular Neurobiology*. 54(8);6133–6147.

Black, J. C., Van Rechem, C., & Whetstine, J. R. (2012). Histone Lysine Methylation Dynamics: Establishment, Regulation, and Biological Impact. *Molecular Cell*. 48(4);491–507.

Blaschke, K., Ebata, K. T., Karimi, M. M., Zepeda-Martínez, J. a, Goyal, P., Mahapatra, S., Tam, A., Laird, D. J., Hirst, M., Rao, A., Lorincz, M. C., & Ramalho-Santos, M. (2013). Vitamin C induces Tet-dependent DNA demethylation and a blastocyst-like state in ES cells. *Nature*. 500(7461);222–6.

Bönnemann, C., & Meinecke, P. (1990). Holoprosencephaly as a possible embryonic alcohol effect: another observation. *American Journal of Medical Genetics*. 37(3);431–2.

Bonthius, D. J., Bonthius, N. E., Napper, R. M., Astley, S. J., Clarren, S. K., & West, J. R. (1996). Purkinje cell deficits in nonhuman primates following weekly exposure to ethanol during gestation. *Teratology*. 53(4);230–6.

Boronat, S., Sanchez-Montanez, A., Gomez-Barros, N., Jacas, C., Martinez-Ribot, L., Vazquez, E., & Del Campo, M. (2017). Correlation between morphological MRI findings and specific diagnostic categories in fetal alcohol spectrum disorders. *European Journal of Medical Genetics*. 60(1);65–71.

Boschen, K. E., & Klintsova, A. Y. (2017). Disruptions to hippocampal adult neurogenesis in rodent models of fetal alcohol spectrum disorders. *Neurogenesis*. 4(1);e1324259.

Brady, K. T., & Back, S. E. (2012). Childhood trauma, posttraumatic stress disorder, and alcohol dependence. *Alcohol Research : Current Reviews*. 34(4);408–13.

Breton, C. V., Byun, H. M., Wenten, M., Pan, F., Yang, A., & Gilliland, F. D. (2009). Prenatal tobacco smoke exposure affects global and gene-specific DNA methylation. *American Journal of Respiratory and Critical Care Medicine*. 180(5);462–467.

Brocardo, P. S., Gil-Mohapel, J., & Christie, B. R. (2011). The role of oxidative stress in fetal alcohol spectrum disorders. *Brain Research Reviews*. 67(1–2);209–25.

Broide, R. S., Redwine, J. M., Aftahi, N., Young, W., Bloom, F. E., & Winrow, C. J. (2007). Distribution of histone deacetylases 1 – 11 in the rat brain. *Journal of Molecular Neuroscience*. 31;47–58.

Brownell, M., Chartier, M., Au, W., MacWilliam, L., Schultz, J., Guenette, W., & Valdivia, J. (2015). *The Educational Outcomes of Children in Care in Manitoba* Winnipeg, MB. Winnipeg, MB. Available at: http://mchp-appserv.cpe.umanitoba.ca/reference/CIC_report_web.pdf. Accessed: February 13, 2018.

Brzezinski, M. R., Boutelet-Bochan, H., Person, R. E., Fantel, A. G., & Juchau, M. R. (1999). Catalytic activity and quantitation of cytochrome P-450 2E1 in prenatal human brain. *The Journal of Pharmacology and Experimental Therapeutics*. 289(3);1648–1653.

Budhavarapu, V. N., Chavez, M., & Tyler, J. K. (2013). How is epigenetic information maintained through DNA replication? *Epigenetics and Chromatin*. 6(1);1.

Buesa, C., Maes, T., Subirada, F., Barrachina, M., & Ferrer, I. (2004). DNA Chip Technology in Brain Banks : Confronting a Degrading World. *Journal of Neuropathology and Experimental Neurology*. 63(10);1003–1014.

Burd, L., Klug, M. G., Bueling, R., Martsolf, J., Olson, M., & Kerbeshian, J. (2008). Mortality rates in subjects with fetal alcohol spectrum disorders and their siblings. *Birth Defects Research. Part A, Clinical and Molecular Teratology*. 82(4);217–223.

Burd, L., Roberts, D., Olson, M., & Odendaal, H. (2007). Ethanol and the placenta: A review. *Journal of Maternal-Fetal and Neonatal Medicine*. 20(5);361–375.

Burd, L., & Wilson, H. (2004). Fetal, infant, and child mortality in a context of alcohol use. *American Journal of Medical Genetics. Part C, Seminars in Medical Genetics*. 127C(1);51–58.

Butcher, D. T., Cytrynbaum, C., Turinsky, A. L., Siu, M. T., Inbar-Feigenberg, M., Mendoza-Londono, R., Chitayat, D., Walker, S., Machado, J., Caluseriu, O., Dupuis, L., Grafodatskaya,

D., Reardon, W., Gilbert-Dussardier, B., Verloes, A., Bilan, F., Milunsky, J. M., … Weksberg, R. (2017). CHARGE and Kabuki Syndromes: Gene-Specific DNA Methylation Signatures Identify Epigenetic Mechanisms Linking These Clinically Overlapping Conditions. *American Journal of Human Genetics*. 100(5);773–788.

Byard, R. W. (2009, December). SUDI or "undetermined": does it matter? *Forensic Science, Medicine, and Pathology*.

Campos, E. I., & Reinberg, D. (2009). Histones: annotating chromatin. *Annual Review of Genetics*. 43;559–99.

Carson, G., Cox, L. V., Crane, J., Croteau, P., Graves, L., Kluka, S., Koren, G., Martel, M.-J., Midmer, D., Nulman, I., Poole, N., Senikas, V., Wood, R., & Society of Obstetricians and Gynaecologists of Canada. (2010). Alcohol use and pregnancy consensus clinical guidelines. *Journal of Obstetrics and Gynaecology Canada : JOGC*. 32(8 Suppl 3);S1-31.

Carter, R. C., Wainwright, H., Molteno, C. D., Georgieff, M. K., Dodge, N. C., Warton, F., Meintjes, E. M., Jacobson, J. L., & Jacobson, S. W. (2016). Alcohol, Methamphetamine, and Marijuana Exposure Have Distinct Effects on the Human Placenta. *Alcoholism: Clinical and Experimental Research*. 40(4);753–764.

Cederbaum, A. I. (2012). Alcohol metabolism. *Clinics in Liver Disease*. 16(4);667–85.

Chabenne, A., Moon, C., Ojo, C., Khogali, A., Nepal, B., & Sharma, S. (2014). Biomarkers in fetal alcohol syndrome. *Biomarkers and Genomic Medicine*. 6(1);12–22.

Chandana, R., Mythri, R. B., Mahadevan, A., Shankar, S. K., & Bharath, M. M. S. (2009). Biochemical analysis of protein stability in human brain collected at different post-mortem intervals. *Indian J Med Res*. (February);189–199.

Charness, M. E., Riley, E. P., & Sowell, E. R. (2016). Drinking During Pregnancy and the Developing Brain: Is Any Amount Safe? *Trends in Cognitive Sciences*. 20(2);80–82.

Chater-Diehl, E. J., Laufer, B. I., Castellani, C. A., Alberry, B. L., & Singh, S. M. (2016). Alteration of gene expression, DNA methylation, and histone methylation in free radical scavenging networks in adult mouse hippocampus following fetal alcohol exposure. *PLoS ONE*. 11(5);1–25.

Chater-Diehl, E. J., Laufer, B. I., & Singh, S. M. (2017). Changes to histone modifications following prenatal alcohol exposure: An emerging picture. *Alcohol*. 60;41–52.

Chatterton, Z., Hartley, B. J., Seok, M. H., Mendelev, N., Chen, S., Milekic, M., Rosoklija, G.,

Stankov, A., Trencevsja-Ivanovska, I., Brennand, K., Ge, Y., Dwork, A. J., & Haghighi, F. (2017). In utero exposure to maternal smoking is associated with DNA methylation alterations and reduced neuronal content in the developing fetal brain. *Epigenetics and Chromatin*. 10(1);1–11.

Chen, C.-P. (2008). Syndromes, Disorders and Maternal Risk Factors Associated With Neural Tube Defects (VI). *Taiwanese Journal of Obstetrics and Gynecology*. 47(3);267–275.

Chen, W.-J. A., Maier, S. E., Parnell, S. E., & West, J. R. (2003). Alcohol and the developing brain: neuroanatomical studies. *Alcohol Research & Health : The Journal of the National Institute on Alcohol Abuse and Alcoholism*. 27(2);174–80.

Chen, W. A., & Maier, S. E. (2011). Combination drug use and risk for fetal harm. *Alcohol Research & Health : The Journal of the National Institute on Alcohol Abuse and Alcoholism*. 34(1);27–28.

Chen, W., & Qin, C. (2015). General hallmarks of microRNAs in brain evolution and development. *RNA Biology*. 12(7);701–8.

Chen, Y., Damayanti, N. P., Irudayaraj, J., Dunn, K., & Zhou, F. C. (2014). Diversity of two forms of DNA methylation in the brain. *Frontiers in Genetics*. 5(MAR);1–13.

Chen, Y., Ozturk, N. C., & Zhou, F. C. (2013). DNA Methylation Program in Developing Hippocampus and Its Alteration by Alcohol. *PLoS ONE*. 8(3);1–11.

Chernoff, G. F. (1977). The Fetal Alcohol Syndrome in Mice: An Animal Model. *Teratology*. 15;223–230.

Chevyreva, I., Faull, R. L. M., Green, C. R., & Nicholson, L. F. B. (2008). Assessing RNA quality in postmortem human brain tissue. *Experimental and Molecular Pathology*. 84(1);71–7.

Cho, B., Kim, H. J., Kim, H., & Sun, W. (2011). Changes in the Histone Acetylation Patterns during the Development of the Nervous System. *Experimental Neurobiology*. 20(2);81.

Choleris, E., Galea, L. A. M., Sohrabji, F., & Frick, K. M. (2018). Sex differences in the brain: Implications for behavioral and biomedical research. *Neuroscience and Biobehavioral Reviews*. 85(January 2017);126–145.

Choudhary, C., Weinert, B. T., Nishida, Y., Verdin, E., & Mann, M. (2014). The growing landscape of lysine acetylation links metabolism and cell signalling. *Nature Reviews Molecular Cell Biology*. 15(8);536–550.

Christopher, M. A., Kyle, S. M., & Katz, D. J. (2017). Neuroepigenetic mechanisms in disease.

Epigenetics and Chromatin. 10(1);1–18.

Chudley, A. E. (2018). Diagnosis of fetal alcohol spectrum disorder: current practices and future considerations. *Biochemistry and Cell Biology*. 96;231–236.

Chudley, A. E., Conry, J., Cook, J. L., Loock, C., Rosales, T., & Leblanc, N. (2005). Fetal Alcohol Spectrum Disorder: Canadian Guidelines for Diagnosis. *Canadian Medical Association Journal*. 172(5 suppl);S1-21.

Chudley, A. E., Kilgour, A. R., Cranston, M., & Edwards, M. (2007). Challenges of diagnosis in fetal alcohol syndrome and fetal alcohol spectrum disorder in the adult. *American Journal of Medical Genetics. Part C, Seminars in Medical Genetics*. 145C(3);261–72.

Church, M. W., Holmes, P. A., Overbeck, G. W., Tilak, J. P., & Zajac, C. S. (1991). Interactive effects of prenatal alcohol and cocaine exposures on postnatal mortality, development and behavior in the Long Evans rat. *Neurotoxicol Teratol*. 13(4);377–386.

Clapp, P., Bhave, S. V., & Hoffman, P. L. (2008). How Adaptation of the Brain to Alcohol Leads to Dependence. *Alcohol Research & Health*. 31(4);310.

Clarren, S. K. (1977). Central Nervous System Malformations in Two Offspring of alcoholic women. *Birth Defects*. XIII(3D);151–153.

Clarren, S. K. (1981). Recognition of fetal alcohol syndrome. *Journal of the American Medical Association*. 245(23);2436–2439.

Clarren, S. K. (1986). Neuropathology in Fetal Alcohol yndrome. In J. R. West (Ed.), *Neuropathology in Fetal Alcohol Syndrome* Oxford University Press. New York.

Clarren, S. K., Alvord, E. C., Sumi, S. M., Streissguth, a P., & Smith, D. W. (1978). Brain malformations related to prenatal exposure to ethanol. *The Journal of Pediatrics*. 92(1);64–67.

Clarren, S. K., Astley, S. J., & Bowden, D. M. (1988). Physical Anomalies and Developmental Delays in Nonhuman Primate Infants Exposed to Weekly Doses of Ethanol During Gestation. *Teratology*. 37;561–569.

Clarren, S. K., Astley, S. J., Bowden, D. M., Lai, H., Milam, A. H., Rudeen, P. K., & Shoemaker, W. J. (1990). Neuroanatomic and Neurochemical Abnormalities in Non-human Primate Infants Exposed to Weekly Doses of Ethanol during Gestation. *Alcoholism: Clinical and Experimental Research*. 14(5);674–683.

Clarren, S. K., & Bowden, D. M. (1982). Fetal alcohol syndrome: A new primate model for binge drinking and its relevance to human ethanol teratogenesis. *The Journal of Pediatrics*.

101(5);819–824.

Clarren, S. K., & Bowden, D. M. (1984). Measures of alcohol damage in utero in the pigtailed macaque (Macaca nemestrina). *Ciba Foundation*. Symposium(157);172.

Clarren, S. K., Bowden, D. M., & Astley, S. J. (1987). Pregnancy Outcomes After Weekly Oral Administration of Ethanol During Gestation in the Pig-Tailed Macaque (Macaca nemestrina). *Teratology*. 35;345–354.

Clugston, R. D., & Blaner, W. S. (2012). The adverse effects of alcohol on vitamin A metabolism. *Nutrients*. 4(5);356–371.

Coles, C. D., Gailey, A. R., Mulle, J. G., Kable, J. A., Lynch, M. E., & Jones, K. L. (2016). A Comparison Among 5 Methods for the Clinical Diagnosis of Fetal Alcohol Spectrum Disorders. *Alcoholism, Clinical and Experimental Research*. 40(5);1000–1009.

Collins, S. E. (2016). Associations Between Socioeconomic Factors and Alcohol Outcomes. *Alcohol Research : Current Reviews*. 38(1);83–94.

Committee on Understanding Premature Birth and Assuring Healthy Outcomes, & Board on Health Sciences Policy. (2007). *Preterm Birth: Causes, Consequences and Prevention*. (R. E. Behrman & A. S. Butler, Eds.) National Academies Press. Washington, DC.

Cook, J. L., Green, C. R., Lilley, C. M., Anderson, S. M., Baldwin, M. E., Chudley, A. E., Conry, J. L., LeBlanc, N., Loock, C. A., Lutke, J., Mallon, B. F., McFarlane, A. A., Temple, V. K., & Rosales, T. (2016). Fetal alcohol spectrum disorder: a guideline for diagnosis across the lifespan. *Canadian Medical Association Journal*. 188(3);191–197.

Coriale, G., Fiorentino, D., Di Lauro, F., Marchitelli, R., Scalese, B., Fiore, M., Maviglia, M., & Ceccanti, M. (2013). Fetal Alcohol Spectrum Disorder (FASD): Neurobehavioral profile, indications for diagnosis and treatment. *Rivista Di Psichiatria*. 48(5);359–369.

Coskun, V., Tsoa, R., & Sun, Y. E. (2012). Epigenetic regulation of stem cells differentiating along the neural lineage. *Current Opinion in Neurobiology*. 22(5);762–767.

Coulter, C. L., Leech, R. W., Schaefer, G. B., Scheithauer, B. W., & Brumback, R. A. (1993). Midline cerebral dysgenesis, dysfunction of the hypothalamic-pituitary axis, and fetal alcohol effects. *Archives of Neurology*. 50(7);771–5.

CPHO. (2015). *The Chief Public Health Officer's Report on the State of Public Health in Canada 2015 - Alcohol Consumption in Canada*. Ottawa, ON. Available at: http://healthycanadians.gc.ca/publications/department-ministere/state-public-health-alcohol-

2015-etat-sante-publique-alcool/alt/state-phac-alcohol-2015-etat-aspc-alcool-eng.pdf. Accessed: February 19, 2018.

Crabbe, J. C., Harris, R. A., & Koob, G. F. (2011). Preclinical studies of alcohol binge drinking. *Annals of the New York Academy of Sciences*. 1216(1);24–40.

Crecelius, A., Götz, A., Arzberger, T., Fröhlich, T., Arnold, G. J., Ferrer, I., & Kretzschmar, H. (2008). Assessing quantitative post-mortem changes in the gray matter of the human frontal cortex proteome by 2-D DIGE. *Proteomics*. 8(6);1276–91.

Creeley, C. E., & Olney, J. W. (2013). Drug-Induced Apoptosis: Mechanism by which Alcohol and Many Other Drugs Can Disrupt Brain Development. *Brain Sciences*. 3(3);1153–1181.

Creyghton, M. P., Cheng, A. W., Welstead, G. G., Kooistra, T., Carey, B. W., Steine, E. J., Hanna, J., Lodato, M., Frampton, G. M., Sharp, P., Boyer, L., Young, R., & Jaenisch, R. (2010). Histone H3K27ac separates active from poised enhancers and predicts developmental state. *Proceedings of the National Academy of Sciences of the United States of America*. 107(50);21931–6.

D'Addario, C., Johansson, S., Candeletti, S., Romualdi, P., Ögren, S. O., Terenius, L., & Ekström, T. J. (2011). Ethanol and acetaldehyde exposure induces specific epigenetic modifications in the prodynorphin gene promoter in a human neuroblastoma cell line. *FASEB Journal : Official Publication of the Federation of American Societies for Experimental Biology*. 25(3);1069–75.

Dambska, M., Wisniewski, K. E., & Sher, J. H. (1986). Marginal glioneuronal heterotopias in nine cases with and without cortical abnormalities. *Journal of Child Neurology*. 1(2);149–57.

Davie, J. R., Drobic, B., Perez-Cadahia, B., He, S., Espino, P. S., Sun, J.-M., Chen, H. Y., Dunn, K. L., Wark, L., Mai, S., Khan, D. H., Davie, S. N., Lu, S., Peltier, C. P., & Delcuve, G. P. (2010). Nucleosomal response, immediate-early gene expression and cell transformation. *Advances in Enzyme Regulation*. 50(1);135–45.

Davis-Anderson, K. L., Berger, S., Lunde-Young, E. R., Naik, V. D., Seo, H., Johnson, G. A., Steen, H., & Ramadoss, J. (2017). Placental Proteomics Reveal Insights into Fetal Alcohol Spectrum Disorders. *Alcoholism: Clinical and Experimental Research*. 41(9);1551–1558.

Dawson, D. A., Goldstein, R. B., Saha, T. D., & Grant, B. F. (2015). Changes in alcohol consumption: United States, 2001–2002 to 2012–2013. *Drug and Alcohol Dependence*. 148;2001–2002.

De La Monte, S. M., & Kril, J. J. (2014). Human alcohol-related neuropathology. *Acta Neuropathologica*. 127(1);71–90.

Dekaban, A. S. (1978). Changes in brain weights during the span of human life: relation of brain weights to body heights and body weights. *Annals of Neurology*. 4(4);345–56.

Del Bigio, M. R. (2010). Ependymal cells: biology and pathology. *Acta Neuropathologica*. 119(1);55–73.

Del Bigio, M. R. (2011). Cell proliferation in human ganglionic eminence and suppression after prematurity-associated haemorrhage. *Brain : A Journal of Neurology*. 134(Pt 5);1344–61.

Del Campo, M., & Jones, K. L. (2017). A review of the physical features of the fetal alcohol spectrum disorders. *European Journal of Medical Genetics*. 60(1);55–64.

Dibley, M. J., & Jeacocke, D. A. (2001). Safety and toxicity of vitamin A supplements in pregnancy. *Food and Nutrition Bulletin*. 22(3);248–266.

Dinieri, J. A., Wang, X., Szutorisz, H., Spano, S. M., Kaur, J., Casaccia, P., Dow-Edwards, D., & Hurd, Y. L. (2011). Maternal cannabis use alters ventral striatal dopamine D2 gene regulation in the offspring. *Biological Psychiatry*. 70(8);763–769.

Donald, K. A., Eastman, E., Howells, F. M., Adnams, C., Riley, E. P., Woods, R. P., Narr, K. L., & Stein, D. J. (2015). Neuroimaging effects of prenatal alcohol exposure on the developing human brain: A magnetic resonance imaging review. *Acta Neuropsychiatrica*. 27(5);251–269.

Donczo, B., & Guttman, A. (2018). Biomedical analysis of formalin-fixed, paraffin-embedded tissue samples: The Holy Grail for molecular diagnostics. *Journal of Pharmaceutical and Biomedical Analysis*. 155;125–134.

Dong, L., Yang, K.-Q., Fu, W.-Y., Shang, Z.-H., Zhang, Q.-Y., Jing, F.-M., Li, L.-L., Xin, H., & Wang, X.-J. (2014). Gypenosides protected the neural stem cells in the subventricular zone of neonatal rats that were prenatally exposed to ethanol. *International Journal of Molecular Sciences*. 15(12);21967–79.

Dorrie, N., Focker, M., Freunscht, I., & Hebebrand, J. (2014). Fetal alcohol spectrum disorders. *European Child & Adolescent Psychiatry*. 23(10);863–875.

Downing, C., Johnson, T. E., Larson, C., Leakey, T. I., Siegfried, R. N., Rafferty, T. M., & Cooney, C. A. (2011). Subtle decreases in DNA methylation and gene expression at the mouse Igf2 locus following prenatal alcohol exposure: Effects of a methyl-supplemented diet. *Alcohol*. 45(1);65–71.

Drew, P. D., & Kane, C. J. M. (2014). *Fetal alcohol spectrum disorders and neuroimmune changes*. *International Review of Neurobiology* (1st ed., Vol. 118) Elsevier Inc.

Du, J., Johnson, L. M., Jacobsen, S. E., & Patel, D. J. (2015). DNA methylation pathways and their crosstalk with histone methylation. *Nature Reviews. Molecular Cell Biology*. 16(9);519–32.

du Plessis, L., Jacobson, J. L., Jacobson, S. W., Hess, A. T., van der Kouwe, A., Avison, M. J., Molteno, C. D., Stanton, M. E., Stanley, J. A., Peterson, B. S., & Meintjes, E. M. (2014). An In Vivo 1 H Magnetic Resonance Spectroscopy Study of the Deep Cerebellar Nuclei in Children with Fetal Alcohol Spectrum Disorders. *Alcoholism: Clinical and Experimental Research*. 38(5);1330–1338.

Duester, G. (2008). Retinoic Acid Synthesis and Signaling during Early Organogenesis. *Cell*. 134(6);921–931.

Dukes, K. A., Burd, L., Elliott, A. J., Fifer, W. P., Folkerth, R. D., Hankins, G. D. V., Hereld, D., Hoffman, H. J., Myers, M. M., Odendaal, H. J., Signore, C., Sullivan, L. M., Willinger, M., Wright, C., & Kinney, H. C. (2014). The safe passage study: Design, methods, recruitment, and follow-up approach. *Paediatric and Perinatal Epidemiology*. 28(5);455–465.

Durrenberger, P. F., Fernando, S., Kashefi, S. N., Ferrer, I., Hauw, J.-J., Seilhean, D., Smith, C., Walker, R., Al-Sarraj, S., Troakes, C., Palkovits, M., Kasztner, M., Huitinga, I., Arzberger, T., Dexter, D. T., Kretzschmar, H., & Reynolds, R. (2010). Effects of antemortem and postmortem variables on human brain mRNA quality: a BrainNet Europe study. *Journal of Neuropathology and Experimental Neurology*. 69(1);70–81.

Eberhart, J. K., & Parnell, S. E. (2016). The Genetics of Fetal Alcohol Spectrum Disorders. *Alcoholism: Clinical and Experimental Research*. (1980);1–12.

Ehrlich, M., & Lacey, M. (2013). Epigenetic Alterations in Oncogenesis. In A. R. Karpf (Ed.), *Epigenetic Alterations in Oncogenesis, Advances in Experimental 31 Medicine and Biology* (Vol. 754, pp. 31–56) Springer New York. New York, NY.

Ek, C. J., Dziegielewska, K. M., Habgood, M. D., & Saunders, N. R. (2012). Barriers in the developing brain and Neurotoxicology. *NeuroToxicology*. 33(3);586–604.

Enoch, M.-A. (2008). The role of GABA(A) receptors in the development of alcoholism. *Pharmacology, Biochemistry, and Behavior*. 90(1);95–104.

Enoch, M.-A., Zhou, Z., Kimura, M., Mash, D. C., Yuan, Q., & Goldman, D. (2012). GABAergic gene expression in postmortem hippocampus from alcoholics and cocaine addicts; corresponding findings in alcohol-naïve P and NP rats. *PloS One*. 7(1);e29369.

Ernst, C. (2016). Proliferation and Differentiation Deficits are a Major Convergence Point for

Neurodevelopmental Disorders. *Trends in Neurosciences*. 39(5);290–299.

Famy, C., Streissguth, A. P., & Unis, A. S. (1998). Mental illness in adults with fetal alcohol syndrome or fetal alcohol effects. *The American Journal of Psychiatry*. 155(4);552–554.

Faraco, G., Pancani, T., Formentini, L., Mascagni, P., Fossati, G., Leoni, F., Moroni, F., & Chiarugi, A. (2006). Pharmacological Inhibition of Histone Deacetylases by Suberoylanilide Hydroxamic Acid Specifically Alters Gene Expression and Reduces Ischemic Injury in the Mouse Brain. *Molecular Pharmacology*. 70(6);1876–1884.

Farag, M. (2014). Diagnostic issues affecting the epidemiology of fetal alcohol spectrum disorders. *Journal of Population Therapeutics and Clinical Pharmacology*. 21(1);e153-8.

Farré, P., Jones, M. J., Meaney, M. J., Emberly, E., Turecki, G., & Kobor, M. S. (2015). Concordant and discordant DNA methylation signatures of aging in human blood and brain. *Epigenetics & Chromatin*. 8;19.

Feduccia, A. a, Chatterjee, S., & Bartlett, S. E. (2012). Neuronal nicotinic acetylcholine receptors: neuroplastic changes underlying alcohol and nicotine addictions. *Frontiers in Molecular Neuroscience*. 5(August);83.

Feinberg, A. P. (2018). The Key Role of Epigenetics in Human Disease Prevention and Mitigation. *New England Journal of Medicine*. 378(14);1323–1334.

Feltes, B. C., de Faria Poloni, J., Nunes, I. J. G., & Bonatto, D. (2014). Fetal Alcohol Syndrome, Chemo-Biology and OMICS: Ethanol Effects on Vitamin Metabolism During Neurodevelopment as Measured by Systems Biology Analysis. *OMICS: A Journal of Integrative Biology*. 18(6);344–363.

Ferdous, J., Mukherjee, R., Ahmed, K. T., & Ali, D. W. (2017). Retinoic acid prevents synaptic deficiencies induced by alcohol exposure during gastrulation in zebrafish embryos. *Neurotoxicology*. 62;100–110.

Féré, C. (1895). Etudes experimentales sur l'influence tératogène ou dégénérative des alcools et des essences sur l'embryon de poulet. *Journal de Anatomie et de La Physiologie*. 31;161–186.

Féré, C. (1898). Presentation de poulets vivants provenant d'oeufs ayant subi des injections d'alcool éthylique dans l'albumen. *C.R de La Soc Biol.* 46;646.

Féré, C. (1899). Influence du repos sur les effects de l'exposition préalable aux vapeurs d'alcool avant l'incubation de l'oeuf de poule. *C.R de La Soc Biol.* 51;806.

Ferrer, I., Armstrong, J., Capellari, S., Parchi, P., Arzberger, T., Bell, J., Budka, H., Ströbel, T.,

Giaccone, G., Rossi, G., Bogdanovic, N., Fakai, P., Schmitt, A., Riederers, P., Al-Sarraj, S., Ravid, R., & Kretzschmar, H. (2007). Effects of formalin fixation, paraffin embedding, and time of storage on DNA preservation in brain tissue: a BrainNet Europe study. *Brain Pathology*. 17(3);297–303.

Ferrer, I., & Galofré, E. (1987). Dendritic spine anomalies in fetal alcohol syndrome. *Neuropediatrics*. 18(3);161–3.

Ferrer, I., Martinez, A., Boluda, S., Parchi, P., & Barrachina, M. (2008). Brain banks: benefits, limitations and cautions concerning the use of post-mortem brain tissue for molecular studies. *Cell and Tissue Banking*. 9(3);181–94.

Ferrer, I., Santpere, G., Arzberger, T., Bell, J., Blanco, R., Boluda, S., Budka, H., Carmona, M., Giaccone, G., Krebs, B., Limido, L., Parchi, P., Puig, B., Strammiello, R., Stro, T., Kretzschmar, H., & Ströbel, T. (2007). Brain protein preservation largely depends on the postmortem storage temperature: implications for study of proteins in human neurologic diseases and management of brain banks: a BrainNet Europe Study. *Journal of Neuropathology and Experimental Neurology*. 66(1);35–46.

Finegersh, A., & Homanics, G. E. (2014). Paternal alcohol exposure reduces alcohol drinking and increases behavioral sensitivity to alcohol selectively in male offspring. *PLoS ONE*. 9(6).

Finegersh, A., Rompala, G. R., Martin, D. I. K., & Homanics, G. E. (2015). Drinking beyong a lifetime: New and emerging insights into paternal alcohol exposure on subsequent generations. *Alcohol*. 49(5);461–470.

Fox, C. H., Johnson, F. B., Whiting, J., & Roller, P. P. (1985). Formaldehyde Fixation. *The Journal of Histochemistry and Cytochemistry*. 33(8);845–853.

Fracasso, T., Vennemann, M., Pfeiffer, H., & Bajanowski, T. (2009). Organ weights in cases of sudden infant death syndrome: a German study. *The American Journal of Forensic Medicine and Pathology*. 30(3);231–4.

Frankel, A. (2012). Formalin fixation in the "-omics" era: A primer for the surgeon-scientist. *ANZ Journal of Surgery*. 82(6);395–402.

Funabashi, K. S., Barcelos, D., Visoná, I., e Silva, M. S., e Sousa, M. L. A. P. O., de Franco, M. F., & Iwamura, E. S. M. (2012). DNA extraction and molecular analysis of non-tumoral liver, spleen, and brain from autopsy samples: the effect of formalin fixation and paraffin embedding. *Pathology, Research and Practice*. 208(10);584–91.

Garro, A. J., McBeth, D. L., Lima, V., & Lieber, C. S. (1991). Ethanol consumption inhibits fetal DNA methylation in mice: implications for the fetal alcohol syndrome. *Alcohol Clin Exp Res*. 15(3);395–398.

Gassmann, M., & Bettler, B. (2012). Regulation of neuronal GABA(B) receptor functions by subunit composition. *Nature Reviews. Neuroscience*. 13(6);380–94.

Gemma, S., Vichi, S., & Testai, E. (2007). Metabolic and genetic factors contributing to alcohol induced effects and fetal alcohol syndrome. *Neuroscience and Biobehavioral Reviews*. 31(2);221–229.

Geschwind, D. H., & Rakic, P. (2013). Cortical evolution: Judge the brain by its cover. *Neuron*. 80(3);633–647.

Gibson, A., Woodside, J. V, Young, I. S., Sharpe, P. C., Mercer, C., Patterson, C. C., McKinley, M. C., Kluijtmans, L. A. J., Whitehead, A. S., & Evans, A. (2008). Alcohol increases homocysteine and reduces B vitamin concentration in healthy male volunteers - A randomized, crossover intervention study. *Qjm*. 101(11);881–887.

Globisch, D., Münzel, M., Müller, M., Michalakis, S., Wagner, M., Koch, S., Brückl, T., Biel, M., & Carell, T. (2010). Tissue distribution of 5-hydroxymethylcytosine and search for active demethylation intermediates. *PLoS ONE*. 5(12);1–9.

Goasdoué, K., Miller, S. M., Colditz, P. B., & Björkman, S. T. (2017). Review: The blood-brain barrier; protecting the developing fetal brain. *Placenta*. 54;111–116.

González-Maeso, J., Torre, I., Rodríguez-Puertas, R., García-Sevilla, J. A., Guimón, J., & Meana, J. J. (2002). Effects of Age , Postmortem Delay and Storage Time on Receptor-mediated Activation of G-proteins in Human Brain. *Neuropsychopharmacology*. 26(4);468–478.

Gordillo, M., Evans, T., & Gouon-Evans, V. (2015). Orchestrating liver development. *Development*. 142(12);2094–2108.

Govorko, D., Bekdash, R. a, Zhang, C., & Sarkar, D. K. (2012). Male germline transmits fetal alcohol adverse effect on hypothalamic proopiomelanocortin gene across generations. *Biological Psychiatry*. 72(5);378–88.

Gräff, J., Dohoon, K., Dobbin, M. M., & Tsai, L.-H. (2011). Epigenetic Regulation of Gene Expression in Physiological and Pathological Brain Processes. *Physiology Reviews*. 91;603–649.

Gräff, J., & Mansuy, I. M. (2008). Epigenetic codes in cognition and behaviour. *Behavioural Brain*

Research. 192(1);70–87.

Grucza, R. A., Norberg, K. E., & Bierut, L. J. (2009). Binge drinking among youths and young adults in the united states: 1979-2006. *Journal of the American Academy of Child and Adolescent Psychiatry*. 48(7);692–702.

Gude, N. M., Roberts, C. T., Kalionis, B., & King, R. G. (2004). Growth and function of the normal human placenta. *Thrombosis Research*. 114(5–6);397–407.

Guerri, C., & Renau-piqueras, J. (1997). Alcohol, Astroglia, and Brain Development. *Molecular Neurobiology*. 15(1);65–81.

Guo, J. U., Su, Y., Shin, J. H., Shin, J., Li, H., Xie, B., Zhong, C., Hu, S., Le, T., Fan, G., Zhu, H., Chang, Q., Gao, Y., Ming, G., & Song, H. (2013). Distribution, recognition and regulation of non-CpG methylation in the adult mammalian brain. *Nature Neuroscience*. 17(2);215–222.

Guo, J. U., Su, Y., Zhong, C., Ming, G., & Song, H. (2011a). Emerging roles of TET proteins and 5-hydroxymethylcytosines in active DNA demethylation and beyond. *Cell Cycle*. 10(16);2662–2668.

Guo, J. U., Su, Y., Zhong, C., Ming, G., & Song, H. (2011b). Hydroxylation of 5-methylcytosine by TET1 promotes active DNA demethylation in the adult brain. *Cell*. 145(3);423–34.

Guo, W., Crossey, E. L., Zhang, L., Zucca, S., George, O. L., Valenzuela, C. F., & Zhao, X. (2011). Alcohol exposure decreases CREB binding protein expression and histone acetylation in the developing cerebellum. *PloS One*. 6(5);e19351.

Guyard, A., Boyez, A., Pujals, A., Robe, C., Tran Van Nhieu, J., Allory, Y., Moroch, J., Georges, O., Fournet, J.-C., Zafrani, E.-S., & Leroy, K. (2017). DNA degrades during storage in formalin-fixed and paraffin-embedded tissue blocks. *Virchows Archiv : An International Journal of Pathology*. 471(4);491–500.

Gyetvai, B., Simonyi, A., Oros, M., Saito, M., Smiley, J., & Vadász, C. (2011). mGluR7 genetics and alcohol: intersection yields clues for addiction. *Neurochemical Research*. 36(6);1087–100.

Hackett, J. A., Sengupta, R., Zylicz, J. J., Murakami, K., Lee, C., Down, T. A., & Surani, M. A. (2013). Germline DNA demethylation dynamics and imprint erasure through 5-hydroxymethylcytosine. *Science*. 339(6118);448–52.

Hahn, M. A., Qiu, R., Wu, X., Li, A. X., Zhang, H., Wang, J., Jui, J., Jin, S. G., Jiang, Y., Pfeifer, G. P., & Lu, Q. (2013). Dynamics of 5-Hydroxymethylcytosine and Chromatin Marks in Mammalian Neurogenesis. *Cell Reports*. 3(2);291–300.

Haig, D. (2012). Commentary: The epidemiology of epigenetics. *International Journal of Epidemiology*. 41(1);13–16.

Haile, S., Pandoh, P., McDonald, H., Corbett, R. D., Tsao, P., Kirk, H., MacLeod, T., Jones, M., Bilobram, S., Brooks, D., Smailus, D., Steidl, C., Scott, D. W., Bala, M., Hirst, M., Miller, D., Moore, R. A., … Marra, M. A. (2017). Automated high throughput nucleic acid purification from formalin-fixed paraffin-embedded tissue samples for next generation sequence analysis. *PloS One*. 12(6);e0178706.

Haluskova, J. (2010). Epigenetic studies in human diseases. *Folia Biol (Praha)*. 56(3);83–96.

Han, X., Li, M., Zhang, X., Xue, Z., & Cang, J. (2014). Single sevoflurane exposure increases methyl-CpG island binding protein 2 phosphorylation in the hippocampus of developing mice. *Molecular Medicine Reports*.

Hannuksela, M. L., Liisanantti, M. K., & Savolainen, M. J. (2002). Effect of alcohol on lipids and lipoproteins in relation to atherosclerosis. *Critical Reviews in Clinical Laboratory Sciences*. 39(May);225–283.

Hanson, D. J. (2013). Historical Evolution of Alcohol Consumption in Society. In P. Boyle, P. Boffetta, A. B. Lowenfels, H. Burns, O. Brawley, W. Zatonski, & J. Rehm (Eds.), *Alcohol: Science, Policy and Public Health* Oxford Scholarship Online.

Harikumar, A., & Meshorer, E. (2015). Chromatin remodeling and bivalent histone modifications in embryonic stem cells. *EMBO Reports*. 16(12);1609–1619.

Hawkins, R. D., Hon, G. C., Yang, C., Antosiewicz-Bourget, J. E., Lee, L. K., Ngo, Q.-M., Klugman, S., Ching, K., Edsall, L. E., Ye, Z., Kuan, S., Yu, P., Liu, H., Zhang, X., Green, R. D., Lobanenkov, V. V, Stewart, R., … Ren, B. (2011). Dynamic chromatin states in human ES cells reveal potential regulatory sequences and genes involved in pluripotency. *Cell Research*. 21(10);1393–409.

Haycock, P. C., & Ramsay, M. (2009). Exposure of Mouse Embryos to Ethanol During Preimplantation Development: Effect on DNA Methylation in the H19 Imprinting Control Region1. *Biology of Reproduction*. 81(4);618–627.

He, X., Lu, J., Dong, W., Jiao, Z., Zhang, C., Yu, Y., Zhang, Z., Wang, H., & Xu, D. (2017). Prenatal nicotine exposure induces HPA axis-hypersensitivity in offspring rats via the intrauterine programming of up-regulation of hippocampal GAD67. *Archives of Toxicology*. 91(12);3945–3946.

Heberlein, A., Leggio, L., Stichtenoth, D., & Hillemacher, T. (2012). The treatment of alcohol and opioid dependence in pregnant women. *Current Opinion in Psychiatry*. 25(6);559–64.

Hendrickson, T. J., Mueller, B. A., Sowell, E. R., Mattson, S. N., Coles, C. D., Kable, J. A., Jones, K. L., Boys, C. J., Lim, K. O., Riley, E. P., & Wozniak, J. R. (2017). Cortical gyrification is abnormal in children with prenatal alcohol exposure. *NeuroImage. Clinical*. 15;391–400.

Herculano-Houzel, S. (2009). The human brain in numbers: a linearly scaled-up primate brain. *Frontiers in Human Neuroscience*. 3(31);1–11.

Hicks, S. D., Middleton, F. A., & Miller, M. W. (2010). Ethanol-induced methylation of cell cycle genes in neural stem cells. *Journal of Neurochemistry*. 114(6);1767–1780.

Hilbig, H., Bidmon, H.-J., Till Oppermann, O., & Remmerbach, T. (2004). Influence of post-mortem delay and storage temperature on the immunohistochemical detection of antigens in the CNS of mice. *Experimental and Toxicologic Pathology*. 56(3);159–171.

Hines, R. N. (2007). Ontogeny of human hepatic cytochromes P450. *Journal of Biochemical and Molecular Toxicology*. 21(4);169–175.

Hirabayashi, Y., & Gotoh, Y. (2010). Epigenetic control of neural precursor cell fate during development. *Nature Reviews Neuroscience*. 11(6);377–388.

Hodyl, N. A., Aboustate, N., Bianco-Miotto, T., Roberts, C. T., Clifton, V. L., & Stark, M. J. (2017). Child neurodevelopmental outcomes following preterm and term birth: What can the placenta tell us? *Placenta*. 57;79–86.

Hoek, J. B., Cahill, A., & Pastorino, J. G. (2002). Alcohol and mitochondria: A dysfunctional relationship. *Gastroenterology*. 122(7);2049–2063.

Hotchkiss, R. D. (1948). The quantitative separation of purines, pyrimidines, and nucleosides by paper chromatography. *J. Biol. Chem*. 175;315–332.

Hou, N., Gong, M., Bi, Y., Zhang, Y., Tan, B., Liu, Y., Wei, X., Chen, J., & Li, T. (2014). Spatiotemporal expression of HDAC2 during the postnatal development of the rat hippocampus. *International Journal of Medical Sciences*. 11(8);788–95.

Hoyme, H. E., Kalberg, W. O., Elliott, A. J., Blankenship, J., Buckley, D., Marais, A.-S., Manning, M. A., Robinson, L. K., Adam, M. P., Abdul-Rahman, O., Jewett, T., Coles, C. D., Chambers, C., Jones, K. L., Adnams, C. M., Shah, P. E., Riley, E. P., … May, P. A. (2016). Updated Clinical Guidelines for Diagnosing Fetal Alcohol Spectrum Disorders. *Pediatrics*. 138(2).

Hsieh, J., & Gage, F. H. (2004). Epigenetic control of neural stem cell fate. *Current Opinion in*

Genetics & Development. 14(5);461–9.

Huang, H.-S., Matevossian, A., Jiang, Y., & Akbarian, S. (2006). Chromatin immunoprecipitation in postmortem brain. *Journal of Neuroscience Methods*. 156(1–2);284–92.

Huang, H., Sabari, B. R., Garcia, B., Allis, C. D., & Zhao, Y. (2014). SnapShot: Histone Modifications. *Cell*. 159(2);458–458.e1.

Hunsucker, S. W., Solomon, B., Gawryluk, J., Geiger, J. D., Vacano, G. N., Duncan, M. W., & Patterson, D. (2008). Assessment of post-mortem-induced changes to the mouse brain proteome. *Journal of Neurochemistry*. 105(3);725–37.

Huppertz, B. (2008). The anatomy of the normal placenta. *Journal of Clinical Pathology*. 61(12);1296–1302.

Iida, K., Hirano, S., Takashima, S., & Miyahara, S. (1994). Developmental study of leptomeningeal glioneuronal heterotopia. *Pediatric Neurology*. 10(4);295–298.

Incerti, M., Vink, J., Roberson, R., Benassou, I., Abebe, D., & Spong, C. Y. (2010). Prevention of the alcohol-induced changes in brain-derived neurotrophic factor expression using neuroprotective peptides in a model of fetal alcohol syndrome. *American Journal of Obstetrics and Gynecology*. 202(5);457.e1-457.e4.

Inouye, R. N., Kokich, V. G., Clarren, S. K., & Bowden, D. M. (1985). Fetal Alcohol Syndrome: An Examination of Craniofacial Dysmorphology. *J. Med. Primatol.* 14;35–48.

Irner, T. B. (2012). Substance exposure in utero and developmental consequences in adolescence: a systematic review. *Child Neuropsychology : A Journal on Normal and Abnormal Development in Childhood and Adolescence*. 18(6);521–49.

Israel, Y., Rivera-Meza, M., Karahanian, E., Quintanilla, M. E., Tampier, L., Morales, P., & Herrera-Marschitz, M. (2013). Gene specific modifications unravel ethanol and acetaldehyde actions. *Frontiers in Behavioral Neuroscience*. 7(July);80.

Ito, S., Shen, L., Dai, Q., Wu, S. C., Collins, L. B., Swenberg, J. A., He, C., & Zhang, Y. (2011). Tet proteins can convert 5-methylcytosine to 5-formylcytosine and 5-carboxylcytosine. *Science*. 333(6047);1300–3.

Itzhak, Y., Ergui, I., & Young, J. I. (2015). Long-term parental methamphetamine exposure of mice influences behavior and hippocampal DNA methylation of the offspring. *Molecular Psychiatry*. 20(2);252–262.

Jacobson, S. W., Jacobson, J. L., Molteno, C. D., Warton, C. M. R., Wintermark, P., Hoyme, H. E.,

De Jong, G., Taylor, P., Warton, F., Lindinger, N. M., Carter, R. C., Dodge, N. C., Grant, E., Warfield, S. K., Zöllei, L., van der Kouwe, A. J. W., & Meintjes, E. M. (2017). Heavy Prenatal Alcohol Exposure is Related to Smaller Corpus Callosum in Newborn MRI Scans. *Alcoholism: Clinical and Experimental Research*. 41(5);965–975.

Jakovcevski, M., & Akbarian, S. (2012). Epigenetic mechanisms in neurological disease. *Nature Medicine*. 18(8);1194–204.

Jang, H. S., Shin, W. J., Lee, J. E., & Do, J. T. (2017). CpG and non-CpG methylation in epigenetic gene regulation and brain function. *Genes*. 8(6);2–20.

Jarmasz, J. S., Basalah, D. A., Chudley, A. E., & Del Bigio, M. R. (2017). Human Brain Abnormalities Associated With Prenatal Alcohol Exposure and Fetal Alcohol Spectrum Disorder. *Journal of Neuropathology and Experimental Neurology*. 76(9);813–833.

Jégou, S., El Ghazi, F., de Lendeu, P. K., Marret, S., Laudenbach, V., Uguen, A., Marcorelles, P., Roy, V., Laquerrière, A., & Gonzalez, B. J. (2012). Prenatal alcohol exposure affects vasculature development in the neonatal brain. *Annals of Neurology*. 72(6);952–60.

Johnson, A. B., Denko, N., & Barton, M. C. (2008). Global repression of transcription. *Mutat Res*. 640(713);174–179.

Jones, K. L. (1975). Aberrant neuronal migration in the fetal alcohol syndrome. *Birth Defects Original Article Series*. 11(7);131–2.

Jones, K. L., & Smith, D. W. (1973). Recognition of the Fetal Alcohol Syndrome in Early Infancy. *The Lancet*. (November);999–1001.

Jones, K., Smith, D., Ulleland, C., & Streissguth, A. (1973). Pattern of Malformation in Offspring of Chronic Alcoholic Mothers. *The Lancet*. 301(7815);1267–1271.

Jonsson, E., Salmon, A., & Warren, K. R. (2014). The international charter on prevention of fetal alcohol spectrum disorder. *The Lancet. Global Health*. 2(3);e135-7.

Joubert, B. R., Håberg, S. E., Nilsen, R. M., Wang, X., Vollset, S. E., Murphy, S. K., Nystad, W., Bell, D. A., Peddada, S. D., & London, S. J. (2012). 450K Epigenome-Wide Scan Identifies Differential DNA Methylation in Newborns Related to Maternal Smoking during Pregnancy. *Environmental Health Perspectives*. 120(10);1425–1432.

Joya, X., Friguls, B., Ortigosa, S., Papaseit, E., Martínez, S. E., Manich, A., Garcia-Algar, O., Pacifici, R., Vall, O., & Pichini, S. (2012). Determination of maternal-fetal biomarkers of prenatal exposure to ethanol: A review. *Journal of Pharmaceutical and Biomedical Analysis*.

69;209–222.

Ju, L., Jia, M., Sun, J., Sun, X., Zhang, H., Ji, M., Yang, J., & Wang, Z. (2016). Hypermethylation of hippocampal synaptic plasticity-related genes is involved in neonatal sevoflurane exposure-induced cognitive impairments in rats. *Neurotoxicity Research*. 29(2);243–55.

Jung, Y., Hsieh, L. S., Lee, A. M., Zhou, Z., Coman, D., Heath, C. J., Hyder, F., Mineur, Y. S., Yuan, Q., Goldman, D., Bordey, A., & Picciotto, M. R. (2016). An epigenetic mechanism mediates developmental nicotine effects on neuronal structure and behavior. *Nature Neuroscience*. 19(7);905–914.

Kabir, Z. D., Kennedy, B., Katzman, A., Lahvis, G. P., & Kosofsky, B. E. (2014). Effects of prenatal cocaine exposure on social development in mice. *Developmental Neuroscience*. 36(3–4);338–346.

Kable, J. A., & Mukherjee, R. A. S. S. (2017). Neurodevelopmental disorder associated with prenatal exposure to alcohol (ND-PAE): A proposed diagnostic method of capturing the neurocognitive phenotype of FASD. *European Journal of Medical Genetics*. 60(1);49–54.

Karmodiya, K., Krebs, A. R., Oulad-Abdelghani, M., Kimura, H., & Tora, L. (2012). H3K9 and H3K14 acetylation co-occur at many gene regulatory elements, while H3K14ac marks a subset of inactive inducible promoters in mouse embryonic stem cells. *BMC Genomics*. 13;424.

Kellinger, M. W., Song, C.-X., Chong, J., Lu, X.-Y., He, C., & Wang, D. (2012). 5-formylcytosine and 5-carboxylcytosine reduce the rate and substrate specificity of RNA polymerase II transcription. *Nature Structural & Molecular Biology*. 19(8);831–3.

Kelly, S. J., Goodlett, C. R., & Hannigan, J. H. (2009). Animal models of fetal alcohol spectrum disorders: Impact of the social environment. *Developmental Disabilities Research Reviews*. 15(3);200–208.

Kernohan, K. D., & Bérubé, N. G. (2010). Genetic and epigenetic dysregulation of imprinted genes in the brain R eview. *Epigenomics*. 2(6);743–763.

Khalid, O., Kim, J. J., Kim, H. S., Hoang, M., Tu, T. G., Elie, O., Lee, C., Vu, C., Horvath, S., Spigelman, I., & Kim, Y. (2014). Gene expression signatures affected by alcohol-induced DNA methylomic deregulation in human embryonic stem cells. *Stem Cell Research*. 12(3);791–806.

Kigar, S. L., & Auger, A. P. (2013). Epigenetic mechanisms may underlie the aetiology of sex differences in mental health risk and resilience. *Journal of Neuroendocrinology*. 25(11);1141–1150.

Kilgour, A. R., & Chudley, A. E. (2012). Fetal Alcohol Spectrum Disorder. In J. C. Verster, K. Brady, M. Galanter, & P. Conrod (Eds.), *Drug Abuse and Addiction in Medical Illness: Causes, Consequences and Treatment* (pp. 443–452) Springer Science+Business Media.

Kim, H., Wang, X., & Jin, P. (2018). Developing DNA methylation-based diagnostic biomarkers. *Journal of Genetics and Genomics*. 45(2);87–97.

Kim, J.-S., & Shukla, S. D. (2005). Histone H3 modifications in rat hepatic stellate cells by ethanol. *Alcohol and Alcoholism*. 40(5);367–72.

Kim, J.-S., & Shukla, S. D. (2006). Acute in vivo effect of ethanol (binge drinking) on histone H3 modifications in rat tissues. *Alcohol and Alcoholism*. 41(2);126–32.

Kinde, B., Gabel, H. W., Gilbert, C. S., Griffith, E. C., & Greenberg, M. E. (2015). Reading the unique DNA methylation landscape of the brain: Non-CpG methylation, hydroxymethylation, and MeCP2. *Proceedings of the National Academy of Sciences*. 112(22);6800–6806.

Kinney, H., Faix, R., & Brazy, J. (1980). The Fetal Alcohol Syndrome and Neuroblastoma. *Pediatrics*. 66(1);130–132.

Knezovich, J. G., & Ramsay, M. (2012). The effect of preconception paternal alcohol exposure on epigenetic remodeling of the H19 and Rasgrf1 imprinting control regions in mouse offspring. *Frontiers in Genetics*. 3(FEB);1–10.

Knight, A. (2007). Systematic reviews of animal experiments demonstrate poor human clinical and toxicological utility. *ATLA Alternatives to Laboratory Animals*. 35(6);641–659.

Kobor, M. S., & Weinberg, J. (2011). Focus on: epigenetics and fetal alcohol spectrum disorders. *Alcohol Research & Health : The Journal of the National Institute on Alcohol Abuse and Alcoholism*. 34(1);29–37.

Kodydková, J., Vávrová, L., Kocík, M., & Žák, A. (2014). Human catalase, its polymorphisms, regulation and changes of Its activity in different diseases. *Folia Biologica (Czech Republic)*. 60(4);153–167.

Kohlmeier, K. A. (2014). Nicotine during pregnancy: Changes induced in neurotransmission, which could heighten proclivity to addict and induce maladaptive control of attention. *Journal of Developmental Origins of Health and Disease*. 6(3);169–181.

Kong, X., Ouyang, S., Liang, Z., Lu, J., Chen, L., Shen, B., Li, D., Zheng, M., Li, K. K., Luo, C., & Jiang, H. (2011). Catalytic mechanism investigation of lysine-specific demethylase 1 (LSD1): a computational study. *PloS One*. 6(9);e25444.

Konovalov, G. N., Kovetskiĭ, N. S., Solonskiĭ, A. V, & Mokhovikov, A. N. (1988). [Disorders of brain development in embryos obtained from mothers who abused alcohol]. *Zhurnal Nevropatologii i Psikhiatrii Imeni S.S. Korsakova (Moscow, Russia : 1952)*. 88(7);60–6.

Konovalov, H. V, Kovetsky, N. S., Bobryshev, Y. V, & Ashwell, K. W. (1997). Disorders of brain development in the progeny of mothers who used alcohol during pregnancy. *Early Human Development*. 48(1–2);153–66.

Koren, G. (2012). The first description of fetal alcohol syndrome by French pediatrician Paul Lemoine. *Journal of Population Therapeutics and Clinical Pharmacology*. 19(2);2012.

Kot-Leibovich, H., & Fainsod, A. (2009). Ethanol induces embryonic malformations by competing for retinaldehyde dehydrogenase activity during vertebrate gastrulation. *Disease Models & Mechanisms*. 2(5–6);295–305.

Kotch, L., & Sulik, K. (1992). Experimental Fetal Alcohol Syndrome Facial and Brain anomalies mice. *American Journal of Medical Genetics*. 44;168–176.

Kovetskiĭ, N. S. (1989a). [Disorders of the cerebellar development in alcoholic embryopathy]. *Zhurnal Nevropatologii i Psikhiatrii Imeni S.S. Korsakova (Moscow, Russia : 1952)*. 89(7);45–9.

Kovetskiĭ, N. S. (1989b). [Etiology of porencephalia and other developmental disorders of the brain in alcoholic embryopathy]. *Zhurnal Nevropatologii i Psikhiatrii Imeni S.S. Korsakova (Moscow, Russia : 1952)*. 89(2);117–22.

Kovetskiĭ, N. S. (1991). [Neural tube dysraphia at the level of the midbrain in alcoholic embryopathy]. *Zhurnal Nevropatologii i Psikhiatrii Imeni S.S. Korsakova (Moscow, Russia : 1952)*. 91(3);79–83.

Kovetskiĭ, N. S., Konovalov, G. V, Orlovskaia, D. D., Semke, V. I., & Solonskiĭ, A. V. (1991). [Dysontogenesis of the brain of the progeny born to mothers drinking alcohol during pregnancy]. *Zhurnal Nevropatologii i Psikhiatrii Imeni S.S. Korsakova (Moscow, Russia : 1952)*. 91(10);57–63.

Kovetskiĭ, N. S., Solonskiĭ, A. V, & Moiseeva, T. L. (1995). [The dynamics of developmental disorders of the brain in fetuses obtained from mothers consuming alcohol during pregnancy (14- to 15-week-old fetuses)]. *Zhurnal Nevrologii i Psikhiatrii Imeni S.S. Korsakova*. 95(3);58–62.

Kowlessar, D. L. (1997). *An Examination of the Effects of Prenatal Alcool Exposure on School-Age*

Children In Manitoba First Nation Community. A Study of Fetal Alcohol Syndrome Prevalence and Dysmorphology. University of Manitoba.

Kriaucionis, S., & Heintz, N. (2009). The nuclear DNA base 5-hydroxymethylcytosine is present in Purkinje neurons and the brain. *Science*. 324(5929);929–930.

Kruman, I. I., & Fowler, A. K. (2014). Impaired one carbon metabolism and DNA methylation in alcohol toxicity. *Journal of Neurochemistry*. 129(5);770–780.

Kundakovic, M., & Champagne, F. A. (2015). Early-life experience, Epigenetics, and the developing brain. *Neuropsychopharmacology*. 40(1);141–153.

Kundakovic, M., Jiang, Y., Kavanagh, D. H., Dincer, A., Brown, L., Pothula, V., Zharovsky, E., Park, R., Jacobov, R., Magro, I., Kassim, B., Wiseman, J., Dang, K., Sieberts, S. K., Roussos, P., Fromer, M., Harris, B., … Akbarian, S. (2017). Practical guidelines for high-resolution epigenomic profiling of nucleosomal histones in postmortem human brain tissue. *Biological Psychiatry*. 81(2);162–170.

Lalwani, V., Surekha, R., Vanishree, M., Koneru, A., Hunasgi, S., & Ravikumar, S. (2015). Honey as an alternative fixative for oral tissue: An evaluation of processed and unprocessed honey. *Journal of Oral and Maxillofacial Pathology : JOMFP*. 19(3);342–347.

Lange, S., Probst, C., Gmel, G., Rehm, J., Burd, L., & Popova, S. (2017). Global prevalence of fetal alcohol spectrum disorder among children and youth: A systematic review and meta-analysis. *JAMA Pediatrics*. 171(10);948–956.

Lange, S., Shield, K., Koren, G., Rehm, J., & Popova, S. (2014). A comparison of the prevalence of prenatal alcohol exposure obtained via maternal self-reports versus meconium testing: a systematic literature review and meta-analysis. *BMC Pregnancy and Childbirth*. 14(1);127.

Laufer, B. I., Chater-Diehl, E. J., Kapalanga, J., & Singh, S. M. (2017). Long-term alterations to DNA methylation as a biomarker of prenatal alcohol exposure: From mouse models to human children with fetal alcohol spectrum disorders. *Alcohol*. 60;67–75.

Laufer, B. I., Kapalanga, J., Castellani, C. A., Diehl, E. J., Yan, L., & Singh, S. M. (2015). Associative DNA methylation changes in children with prenatal alcohol exposure. *Epigenomics*. 7(8);1259–1274.

Laufer, B. I., Mantha, K., Kleiber, M. L., Diehl, E. J., Addison, S. M. F., & Singh, S. M. (2013). Long-lasting alterations to DNA methylation and ncRNAs could underlie the effects of fetal alcohol exposure in mice. *Disease Models & Mechanisms*. 6(4);977–992.

Lecuyer, M., Laquerrière, A., Bekri, S., Lesueur, C., Ramdani, Y., Jégou, S., Uguen, A., Marcorelles, P., Marret, S., & Gonzalez, B. J. (2017). PLGF, a placental marker of fetal brain defects after in utero alcohol exposure. *Acta Neuropathologica Communications*. 5(1);44.

Lehman, L. L., & Rivkin, M. J. (2014). Perinatal arterial ischemic stroke: presentation, risk factors, evaluation, and outcome. *Pediatric Neurology*. 51(6);760–768.

Leibson, T., Neuman, G., Chudley, A. E., & Koren, G. (2014). The differential diagnosis of fetal alcohol spectrum disorder. *Journal of Population Therapeutics and Clinical Pharmacology*. 21(1);e1–e30.

Lemoine, P., Harousseau, H., Borteyru, J. P., & Menuet, J. C. (2003). Children of alcoholic parents--observed anomalies: discussion of 127 cases. *Therapeutic Drug Monitoring*. 25(2);132–136.

Levenson, V. V. (2010). DNA methylation as a universal biomarker. *Expert Review of Molecular Diagnostics*. 10(4);481–488.

Li, D., Wu, H., & Lu, Q. (2015). TET Family of Dioxygenases: Crucial Roles and Underlying Mechanisms. *Cytogenet Genome Res*. 146;171–180.

Li, J. Z., Vawter, M. P., Walsh, D. M., Tomita, H., Evans, S. J., Choudary, P. V, Lopez, J. F., Avelar, A., Shokoohi, V., Chung, T., Mesarwi, O., Jones, E. G., Watson, S. J., Akil, H., Bunney, W. E., & Myers, R. M. (2004). Systematic changes in gene expression in postmortem human brains associated with tissue pH and terminal medical conditions. *Human Molecular Genetics*. 13(6);609–16.

Li, S., & Mason, C. E. (2014). The Pivotal Regulatory Landscape of RNA Modifications. *Annual Review of Genomics and Human Genetics*. 15(1);127–150.

Liang, F., Diao, L., Liu, J., Jiang, N., Zhang, J., Wang, H., Zhou, W., Huang, G., & Ma, D. (2014). Paternal ethanol exposure and behavioral abnormities in offspring: Associated alterations in imprinted gene methylation. *Neuropharmacology*. 81;126–133.

Lipinski, R. J., Hammond, P., O'Leary-Moore, S. K., Ament, J. J., Pecevich, S. J., Jiang, Y., Budin, F., Parnell, S. E., Suttie, M., Godin, E. a, Everson, J. L., Dehart, D. B., Oguz, I., Holloway, H. T., Styner, M. a, Johnson, G. A., & Sulik, K. K. (2012). Ethanol-induced face-brain dysmorphology patterns are correlative and exposure-stage dependent. *PloS One*. 7(8);e43067.

Lister, R., Mukamel, E. A., Nery, J. R., Urich, M., Puddifoot, C. A., Johnson, N. D., Lucero, J., Huang, Y., Dwork, A. J., Schultz, M. D., Yu, M., Tonti-Filippini, J., Heyn, H., Hu, S., Wu, J. C., Rao, A., Esteller, M., … Ecker, J. R. (2013). Global Epigenomic Reconfiguration During

Mammalian Brain Development. *Science*. 341(6146);1237905–1237905.

Lister, R., Pelizzola, M., Dowen, R. H., Hawkins, R. D., Hon, G., Tonti-Filippini, J., Nery, J. R., Lee, L., Ye, Z., Ngo, Q.-M., Edsall, L., Antosiewicz-Bourget, J., Stewart, R., Ruotti, V., Millar, A. H., Thomson, J. A., Ren, B., & Ecker, J. R. (2009). Human DNA methylomes at base resolution show widespread epigenomic differences. *Nature*. 462;315–322.

Liu, J., Moyon, S., Hernandez, M., & Casaccia, P. (2016). Epigenetic control of oligodendrocyte development: Adding new players to old keepers. *Current Opinion in Neurobiology*. 39;133–138.

Liu, Y., Balaraman, Y., Wang, G., Nephew, K. P., & Zhou, F. C. (2009). Alcohol exposure alters DNA methylation profiles in mouse embryos at early neurulation. *Epigenetics : Official Journal of the DNA Methylation Society*. 4(7);500–11.

Livy, D. J., Miller, E. K., Maier, S. E., & West, J. R. (2003). Fetal alcohol exposure and temporal vulnerability: Effects of binge-like alcohol exposure on the developing rat hippocampus. *Neurotoxicology and Teratology*. 25(4);447–458.

Liyanage, V. R. B., Curtis, K., Zachariah, R. M., Chudley, A. E., & Rastegar, M. (2017). Overview of the Genetic Basis and Epigenetic Mechanisms that Contribute to FASD Pathobiology. *Current Topics in Medicinal Chemistry*. 17(7);808–828.

Liyanage, V. R. B., Jarmasz, J. S., Murugeshan, N., Del Bigio, M. R., Rastegar, M., & Davie, J. R. (2014). DNA modifications: function and applications in normal and disease States. *Biology*. 3(4);670–723 [Liyanage & Jarmasz are Co–first authors].

Llamas, B., Holland, M. L., Chen, K., Cropley, J. E., Cooper, A., & Suter, C. M. (2012). High-resolution analysis of cytosine methylation in ancient DNA. *PLoS ONE*. 7(1).

Lo, J. O., Schabel, M. C., Roberts, V. H. J., Wang, X., Lewandowski, K. S., Grant, K. A., Frias, A. E., & Kroenke, C. D. (2017). First trimester alcohol exposure alters placental perfusion and fetal oxygen availability affecting fetal growth and development in a non-human primate model. *American Journal of Obstetrics and Gynecology*. 216(3);302.e1-302.e8.

Lu, Y.-L., & Richardson, H. N. (2014). Alcohol, stress hormones, and the prefrontal cortex: a proposed pathway to the dark side of addiction. *Neuroscience*. 277;139–51.

Lussier, A. A., Morin, A. M., MacIsaac, J. L., Salmon, J., Weinberg, J., Reynolds, J. N., Pavlidis, P., Chudley, A. E., & Kobor, M. S. (2018). DNA methylation as a predictor of fetal alcohol spectrum disorder. *Clinical Epigenetics*. 10(1);1–14.

Lussier, A. A., Weinberg, J., & Kobor, S. (2017). Epigenetics studies of fetal alcohol spectrum disorder: where are we now? *Epigenomics*. 9(3);291–311.

Lyko, F. (2018). The DNA methyltransferase family: A versatile toolkit for epigenetic regulation. *Nature Reviews Genetics*. 19(2);81–92.

Maccani, J. Z., Koestler, D. C., Houseman, E. A., Marsit, C. J., & Kelsey, K. T. (2013). Placental DNA methylation alterations associated with maternal tobacco smoking at the RUNX3 gene are also associated with gestational age. *Epigenomics*. 5(6);619–630.

MacDonald, J. L., & Roskams, A. J. (2008). Histone deacetylases 1 and 2 are expressed at distinct stages of neuro-glial development. *Developmental Dynamics : An Official Publication of the American Association of Anatomists*. 237(8);2256–67.

Maier, S. E., Chen, W. J., Miller, J. a, & West, J. R. (1997). Fetal alcohol exposure and temporal vulnerability regional differences in alcohol-induced microencephaly as a function of the timing of binge-like alcohol exposure during rat brain development. *Alcoholism, Clinical and Experimental Research*. 21(8);1418–28.

Maier, S. E., Cramer, J. A., West, J. R., & Sohrabji, F. (1999). Alcohol exposure during the first two trimesters equivalent alters granule cell number and neurotrophin expression in the developing rat olfactory bulb. *Journal of Neurobiology*. 41(3);414–423.

Majewski, F. (1981). Alcohol embryopathy: some facts and speculations about pathogenesis. *Neurobehavioral Toxicology and Teratology*. 3(2);129–44.

Majewski, F., Fischbach, H., Peiffer, J., & Bierich, J. R. (1978). [Interruption of pregnancy in alcoholic women]. *Deutsche Medizinische Wochenschrift (1946)*. 103(21);895–8.

Manzo-Avalos, S., & Saavedra-Molina, A. (2010). Cellular and mitochondrial effects of alcohol consumption. *International Journal of Environmental Research and Public Health*. 7(12);4281–4304.

Marceau, G., Gallot, D., Lemery, D., & Sapin, V. (2007). Metabolism of Retinol During Mammalian Placental and Embryonic Development. *Vitamins and Hormones*. 75(06);97–115.

Mariani, C. J., Vasanthakumar, A., Madzo, J., Yesilkanal, A., Bhagat, T., Yu, Y., Bhattacharyya, S., Wenger, R. H., Cohn, S. L., Nanduri, J., Verma, A., Prabhakar, N. R., & Godley, L. A. (2014). TET1-mediated hydroxymethylation facilitates hypoxic gene induction in neuroblastoma. *Cell Reports*. 7(5);1343–1352.

Marjonen, H., Sierra, A., Nyman, A., Rogojin, V., Gröhn, O., Linden, A. M., Hautaniemi, S., &

Kaminen-Ahola, N. (2015). Early maternal alcohol consumption alters hippocampal DNA methylation, gene expression and volume in a mouse model. *PLoS ONE*. 10(5);1–20.

Marmorstein, R., & Zhou, M. (2014). Writers and readers of histone acetylation: structure, mechanism, and inhibition. *Cold Spring Harbor Perspectives in Biology*. 6(7);a018762.

Maroun, L. L., & Graem, N. (2005). Autopsy standards of body parameters and fresh organ weights in nonmacerated and macerated human fetuses. *Pediatric and Developmental Pathology : The Official Journal of the Society for Pediatric Pathology and the Paediatric Pathology Society*. 8(2);204–17.

Marquardt, K., & Brigman, J. L. (2016). The impact of prenatal alcohol exposure on social, cognitive and affective behavioral domains: Insights from rodent models. *Alcohol*. 51;1–15.

Marrocco, J., & McEwen, B. S. (2016). Sex in the brain: Hormones and sex differences. *Dialogues in Clinical Neuroscience*. 18(4);373–383.

Martin, J., Martin, D., Chao, S., & Shores, P. (1982). Interactive effects of chronic maternal ethanol and nicotine exposure upon offspring development and function. *Neurobehav Toxicol Teratol*. 4(3);293–298.

Mato, S., & Pazos, A. (2004). Influence of age, postmortem delay and freezing storage period on cannabinoid receptor density and functionality in human brain. *Neuropharmacology*. 46(5);716–26.

May, P. A., Gossage, J. P., Kalberg, W. O., Robinson, L. K., Buckley, D., Manning, M., & Hoyme, H. E. (2009). Prevalence and epidemiologic characteristics of FASD from various research methods with an emphasis on recent in-school studies. *Developmental Disabilities Research Reviews*. 15(3);176–92.

Maze, I., Noh, K.-M., Soshnev, A. a, & Allis, C. D. (2014). Every amino acid matters: essential contributions of histone variants to mammalian development and disease. *Nature Reviews. Genetics*. 15(4);259–71.

McCarthy, D. M., Mueller, K. A., Cannon, E. N., Huizenga, M. N., Darnell, S. B., Bhide, P. G., & Sadri-Vakili, G. (2017). Prenatal Cocaine Exposure Alters BDNF-TrkB Signaling in the Embryonic and Adult Brain. *Developmental Neuroscience*. 38(5);365–374.

McDonald, S. W., Hicks, M., Rasmussen, C., Nagulesapillai, T., Cook, J., & Tough, S. C. (2014). Characteristics of Women Who Consume Alcohol Before and After Pregnancy Recognition in a Canadian Sample: A Prospective Cohort Study. *Alcoholism, Clinical and Experimental*

Research. 38(12);3008–3016.

McGee, C. L., & Riley, E. P. (2006). Brain imaging and fetal alcohol spectrum disorders. *Annali Dell'Istituto Superiore Di Sanità*. 42(1);46–52.

Mead, E. A., & Sarkar, D. K. (2014). Fetal alcohol spectrum disorders and their transmission through genetic and epigenetic mechanisms. *Frontiers in Genetics*. 5;154.

Melamed, P., Yosefzon, Y., David, C., Tsukerman, A., & Pnueli, L. (2018). Tet Enzymes, Variants, and Differential Effects on Function. *Frontiers in Cell and Developmental Biology*. 6(March);1–6.

Meldrum, B. S. (2000). Glutamate as a Neurotransmitter in the Brain : Review of Physiology and Pathology. *Journal of Nutrition*. 130(4S);1007–1015.

Méndez, C., & Rey, M. (2015). Characterization of polymorphisms of genes ADH2, ADH3, ALDH2 and CYP2E1 and relationship to the alcoholism in a Colombian population. *Colombia Médica*. 46(4);176–182.

Menger, Y., Bettscheider, M., Murgatroyd, C., & Spengler, D. (2010). Sex differences in brain epigenetics. *Epigenomics*. 2(6);807–21.

Merrick, J., Merrick, E., Morad, M., & Kandel, I. (2006). Fetal alcohol syndrome and its long-term effects. *Minerva Pediatrics*. 58;211–218.

Miao, Z., He, Y., Xin, N., Sun, M., Chen, L., Lin, L., Li, J., Kong, J., Jin, P., & Xu, X. (2015). Altering 5-hydroxymethylcytosine modification impacts ischemic brain injury. *Human Molecular Genetics*. 24(20);5855–5866.

Michishita, E., Park, J. Y., Burneskis, J. M., Barrett, J. C., & Izumi, H. (2005). Evolutionarily conserved and nonconserved cellular localizations and functions of human SIRT proteins. *Molecular Biology of the Cell*. 16;4623–4635.

Miller, M. W., Astley, S. J., & Clarren, S. K. (1999). Number of axons in the corpus callosum of the Mature macaca nemestrina: increases caused by prenatal exposure to ethanol. *The Journal of Comparative Neurology*. 412(1);123–31.

Mitchell, E. S., Keller, R. W., & Snyder-Keller, A. (2002). Immediate-early gene expression in concurrent prenatal ethanol- and/or cocaine-exposed rat pups: Intrauterine differences in cocaine levels and Fos expression. *Developmental Brain Research*. 133(2);141–149.

Monoranu, C. M., Apfelbacher, M., Grünblatt, E., Puppe, B., Alafuzoff, I., Ferrer, I., Al-Saraj, S., Keyvani, K., Schmitt, A., Falkai, P., Schittenhelm, J., Halliday, G., Kril, J., Harper, C., McLean,

C., Riederer, P., & Roggendorf, W. (2009). pH measurement as quality control on human post mortem brain tissue: a study of the BrainNet Europe consortium. *Neuropathology and Applied Neurobiology*. 35(3);329–37.

Monoranu, C. M., Grünblatt, E., Bartl, J., Meyer, A., Apfelbacher, M., Keller, D., Michel, T. M., Al-Saraj, S., Schmitt, A., Falkai, P., Roggendorf, W., Deckert, J., Ferrer, I., & Riederer, P. (2011). Methyl- and acetyltransferases are stable epigenetic markers postmortem. *Cell and Tissue Banking*. 12(4);289–97.

Moonat, S., Starkman, B. G., Sakharkar, A., & Pandey, S. C. (2010). Neuroscience of alcoholism: molecular and cellular mechanisms. *Cellular and Molecular Life Sciences : CMLS*. 67(1);73–88.

Moore, E. M., Migliorini, R., Infante, M. A., & Riley, E. P. (2014). Fetal Alcohol Spectrum Disorders: Recent Neuroimaging Findings. *Current Developmental Disorders Reports*. 1(3);161–172.

Moore, K. L., Agur, A. M. R., & Dalley, A. F. (2011). *Essential Clinical Anatomy* (Fourth.) Wolters Kluwer Lippincott Williams & Wilkins. Philadelphia, PA.

Moore, K. L., Persaud, T. V. N., & Torchia, M. G. (2015). *The Developing Human* (10th ed.) Sauders.

Moore, S. P. G., Toomire, K. J., & Strauss, P. R. (2013). DNA modifications repaired by base excision repair are epigenetic. *DNA Repair*. 12(12);1152–8.

Moosavi, A., & Ardekani, A. M. (2016). Role of epigenetics in biology and human diseases. *Iranian Biomedical Journal*. 20(5);246–258.

Mori, K., Iijima, N., Higo, S., Aikawa, S., Matsuo, I., Takumi, K., Sakamoto, A., & Ozawa, H. (2014). Epigenetic suppression of mouse Per2 expression in the suprachiasmatic nucleus by the inhalational anesthetic, sevoflurane. *PloS One*. 9(1);e87319.

Morris, M. J., & Monteggia, L. M. (2013). Unique functional roles for class I and class II histone deacetylases in central nervous system development and function. *International Journal of Developmental Neuroscience : The Official Journal of the International Society for Developmental Neuroscience*. 31(6);370–81.

Morris, C. V, Dinieri, J. A., Szutorisz, H., & Hurd, Y. L. (2011). Molecular mechanisms of maternal cannabis and cigarette use on human neurodevelopment. *European Journal of Neuroscience*. 34(10);1574–1583.

Muckle, G., Laflamme, D., Gagnon, J., Boucher, O., Jacobson, J. L., & Jacobson, S. W. (2011). Alcohol, smoking, and drug use among Inuit women of childbearing age during pregnancy and the risk to children. *Alcoholism, Clinical and Experimental Research*. 35(6);1081–91.

Münzel, M., Globisch, D., Brückl, T., Wagner, M., Welzmiller, V., Michalakis, S., Müller, M., Biel, M., & Carell, T. (2010). Quantification of the sixth DNA base hydroxymethylcytosine in the brain. *Angewandte Chemie - International Edition*. 49(31);5375–5377.

Muralidharan, P., Sarmah, S., Zhou, F. C., & Marrs, J. A. (2013). Fetal Alcohol Spectrum Disorder (FASD) Associated Neural Defects: Complex Mechanisms and Potential Therapeutic Targets. *Brain Sciences*. 3(2);964–991.

Murko, C., Lagger, S., Steiner, M., Seiser, C., Schoefer, C., & Pusch, O. (2010). Expression of class I histone deacetylases during chick and mouse development. *The International Journal of Developmental Biology*. 54(10);1527–37.

Mychasiuk, R., & Metz, G. A. S. (2016). Epigenetic and gene expression changes in the adolescent brain: What have we learned from animal models? *Neuroscience and Biobehavioral Reviews*. 70;189–197.

Myren, M., Mose, T., Mathiesen, L., & Knudsen, L. E. (2007). The human placenta - An alternative for studying foetal exposure. *Toxicology in Vitro*. 21(7);1332–1340.

Nanney, D. L. (1958). Epigenetic control systems. *Proceedings of the National Academy of Sciences of the United States of America*. 44(7);712–7.

Naoi, M., Maruyama, W., & Nagy, G. M. (2004). Dopamine-Derived Salsolinol Derivatives as Endogenous Monoamine Oxidase Inhibitors: Occurrence, Metabolism and Function in Human Brains. *NeuroToxicology*. 25(1–2);193–204.

Nardelli, A., Lebel, C., Rasmussen, C., Andrew, G., & Beaulieu, C. (2011). Extensive deep gray matter volume reductions in children and adolescents with fetal alcohol spectrum disorders. *Alcoholism, Clinical and Experimental Research*. 35(8);1404–17.

Ndlovu, M. N., Denis, H., & Fuks, F. (2011). Exposing the DNA methylome iceberg. *Trends in Biochemical Sciences*. 36(7);381–7.

Ngai, Y. F., Sulistyoningrum, D. C., O'Neill, R., Innis, S. M., Weinberg, J., & Devlin, A. M. (2015). Prenatal alcohol exposure alters methyl metabolism and programs serotonin transporter and glucocorticoid receptor expression in brain. *American Journal of Physiology - Regulatory, Integrative and Comparative Physiology*. 309(5);R613–R622.

Niciu, M. J., Kelmendi, B., & Sanacora, G. (2012). Overview of glutamatergic neurotransmission in the nervous system. *Pharmacology, Biochemistry, and Behavior*. 100(4);656–64.

Norman, A. L., Crocker, N., Mattson, S. N., & Riley, E. P. (2009). Neuroimaging and fetal alcohol spectrum disorders. *Developmental Disabilities Research Reviews*. 15(3);209–217.

Norman, M. G., McGillivray, B. C., Kalousek, D. K., Hill, A., & Poskitt, K. J. (1995). *Congenital Malformations of the Brain. Pathologic, Embryologic, Clinical, Radiologic and Genetic Aspects* Oxford University Press. New York.

Novikova, S. I., He, F., Bai, J., Cutrufello, N. J., Lidow, M. S., & Undieh, A. S. (2008). Maternal cocaine administration in mice alters DNA methylation and gene expression in hippocampal neurons of neonatal and prepubertal offspring. *PloS One*. 3(4);e1919.

Nuñez, S. C., Roussotte, F., & Sowell, E. R. (2011). Focus On: Structural and Functional Brain Abnormalities in Fetal Alcohol Spectrum Disorders. *Alcohol Research & Health*. 34(1);121–131.

O'Keeffe, L. M., Kearney, P. M., McCarthy, F. P., Khashan, A. S., Greene, R. a, North, R. a, Poston, L., McCowan, L. M. E., Baker, P. N., Dekker, G. a, Walker, J. J., Taylor, R., & Kenny, L. C. (2015). Prevalence and predictors of alcohol use during pregnancy: findings from international multicentre cohort studies. *BMJ Open*. 5(7).

O'Leary, C., Jacoby, P., D'Antoine, H., Bartu, A., & Bower, C. (2012). Heavy prenatal alcohol exposure and increased risk of stillbirth. *BJOG : An International Journal of Obstetrics and Gynaecology*. 119(8);945–952.

O'Shea, K. S., & Kaufman, M. H. (1979). The teratogenic effect of acetaldehyde: implications for the study of the fetal alcohol syndrome. *J Anat*. 128(Pt 1);65–76.

Ohata, S., & Alvarez-Buylla, A. (2016). Planar Organization of Multiciliated Ependymal (E1) Cells in the Brain Ventricular Epithelium. *Trends in Neurosciences*. 39(8);543–551.

Ornoy, A., Reece, E. A., Pavlinkova, G., Kappen, C., & Miller, R. K. (2015). Effect of maternal diabetes on the embryo, fetus, and children: congenital anomalies, genetic and epigenetic changes and developmental outcomes. *Birth Defects Research. Part C, Embryo Today : Reviews*. 105(1);53–72.

Osna, N. A., Donohue, T. M. J., & Kharbanda, K. K. (2017). Alcoholic Liver Disease: Pathogenesis and Current Management. *Alcohol Research : Current Reviews*. 38(2);147–161.

Ospina, M., & Dennett, L. (2013). *Systematic review on the prevalence of Fetal Alcohol Spectrum*

Disorders. Institute of Health Economics. Available at: http://fasd.alberta.ca/documents/Systematic_Prevalence_Report_FASD.pdf. Accessed: March 4, 2018.

Otero, N. K. H., Thomas, J. D., Saski, C. A., Xia, X., & Kelly, S. J. (2012). Choline Supplementation and DNA Methylation in the Hippocampus and Prefrontal Cortex of Rats Exposed to Alcohol During Development. *Alcoholism: Clinical and Experimental Research*. 36(10);1701–1709.

Ouko, L. A., Shantikumar, K., Knezovich, J., Haycock, P., Schnugh, D. J., & Ramsay, M. (2009). Effect of alcohol consumption on CpG methylation in the differentially methylated regions of H19 and IG-DMR in male gametes - Implications for fetal alcohol spectrum disorders. *Alcoholism: Clinical and Experimental Research*. 33(9);1615–1627.

Pacey, M. (2009). *Fetal alcohol syndrome and fetal alcohol spectrum disorder among Aboriginal Peoples: A review of prevalence*. Available at: https://www.ccnsa-nccah.ca/docs/health/RPT-FASDAboriginalReviewPrevalence-Pacey-EN.pdf. Accessed: February 27, 2018.

Park, P.-H., Miller, R., & Shukla, S. D. (2003). Acetylation of histone H3 at lysine 9 by ethanol in rat hepatocytes. *Biochemical and Biophysical Research Communications*. 306(2);501–504.

Paus, T., Nawazkhan, I., Leonard, G., Perron, M., Pike, G. B., Pitiot, A., Richer, L., Veillette, S., & Pausova, Z. (2008). Corpus callosum in adolescent offspring exposed prenatally to maternal cigarette smoking. *NeuroImage*. 40(2);435–441.

Pava, M. J., & Woodward, J. J. (2012). A review of the interactions between alcohol and the endocannabinoid system: implications for alcohol dependence and future directions for research. *Alcohol*. 46(3);185–204.

Pei, J., Denys, K., Hughes, J., & Rasmussen, C. (2011). Mental health issues in fetal alcohol spectrum disorder. *Journal of Mental Health*. 20(5);473–483.

Peiffer, J., Majewski, F., Fischbach, H., Bierich, J. R., & Volk, B. (1979). Alcohol embryo- and fetopathy. *Journal of the Neurological Sciences*. 41(2);125–137.

Pekny, T., Andersson, D., Wilhelmsson, U., Pekna, M., & Pekny, M. (2014). Short general anaesthesia induces prolonged changes in gene expression in the mouse hippocampus. *Acta Anaesthesiologica Scandinavica*. 58(9);1127–33.

Pereira, R. D., De Long, N. E., Wang, R. C., Yazdi, F. T., Holloway, A. C., & Raha, S. (2015). Angiogenesis in the placenta: The role of reactive oxygen species signaling. *BioMed Research International*. 2015.

Perreault, S. (2016). *Impaired driving in Canada, 2015*. Available at: https://www150.statcan.gc.ca/n1/en/pub/85-002-x/2016001/article/14679-eng.pdf?st=w-g9kEBK. Accessed: July 25, 2018.

Petrelli, B., Weinberg, J., & Hicks, G. G. (2018). Effects of Prenatal Alcohol Exposure (PAE): Insights into FASD using PAE Mouse Models. *Biochemistry and Cell Biology*.

Phelan, S. (2014). Smoking cessation in pregnancy. *Obstetrics and Gynecology Clinics of North America*. 41(2);255–266.

Phillips, J. B., Billson, V. R., & Forbes, A. B. (2009). Autopsy standards for fetal lengths and organ weights of an Australian perinatal population. *Pathology*. 41(6);515–26.

Pinney, S. (2014). Mammalian Non-CpG Methylation: Stem Cells and Beyond. *Biology*. 3(4);739–751.

Plemenitas, A., Kastelic, M., Porcelli, S., Serretti, A., Rus Makovec, M., Kores Plesnicar, B., & Dolžan, V. (2015). Genetic variability in CYP2E1 and catalase gene among currently and formerly alcohol-dependent male subjects. *Alcohol and Alcoholism*. 50(2);140–145.

Podobinska, M., Szablowska-Gadomska, I., Augustyniak, J., Sandvig, I., Sandvig, A., & Buzanska, L. (2017). Epigenetic Modulation of Stem Cells in Neurodevelopment: The Role of Methylation and Acetylation. *Frontiers in Cellular Neuroscience*. 11(February);1–16.

Pollack, Y., Stein, R., Razin, A., & Cedar, H. (1980). Methylation of foreign DNA sequences in eukaryotic cells. *Proc Natl Acad Sci USA*. 77(11);6463–7.

Popova, S., Lange, S., Burd, L., Chudley, A. E., Clarren, S. K., & Rehm, J. (2013). Cost of fetal alcohol spectrum disorder diagnosis in Canada. *PloS One*. 8(4);e60434.

Popova, S., Lange, S., Burd, L., & Rehm, J. (2016). The Economic Burden of Fetal Alcohol Spectrum Disorder in Canada in 2013. *Alcohol and Alcoholism*. 51(3);367–75.

Popova, S., Lange, S., Chudley, A. E., Reynolds, J. N., Rehm, J., & Centre for Addiction and Mental Health. (2018). *World Health Organization International Study on the Prevalence of Fetal Alcohol Spectrum Disorder (FASD) Canadian Component*. Available at: http://www.camh.ca/en/research/news_and_publications/reports_and_books/Documents/WHO-FASD-Report-English-April2018.pdf. Accessed: March 2, 2018.

Popova, S., Lange, S., Probst, C., Parunashvili, N., & Rehm, J. (2017). Prevalence of alcohol consumption during pregnancy and Fetal Alcohol Spectrum Disorders among the general and Aboriginal populations in Canada and the United States. *European Journal of Medical*

Genetics. 60(1);32–48.

Popova, S., Lange, S., Probst, C., Shield, K., Kraicer-Melamed, H., Ferreira-Borges, C., & Rehm, J. (2016). Actual and predicted prevalence of alcohol consumption during pregnancy in the WHO African Region. *Tropical Medicine & International Health : TM & IH*. 21(10);1209–1239.

Popova, S., Lange, S., Shield, K., Mihic, A., Chudley, A. E., Mukherjee, R. A. S., Bekmuradov, D., & Rehm, J. (2016). Comorbidity of fetal alcohol spectrum disorder: a systematic review and meta-analysis. *The Lancet*. 6736(15);1–10.

Portales-Casamar, E., Lussier, A. A., Jones, M. J., MacIsaac, J. L., Edgar, R. D., Mah, S. M., Barhdadi, A., Provost, S., Lemieux-Perreault, L.-P., Cynader, M. S., Chudley, A. E., Dubé, M.-P., Reynolds, J. N., Pavlidis, P., & Kobor, M. S. (2016). DNA methylation signature of human fetal alcohol spectrum disorder. *Epigenetics & Chromatin*. 9(1);25.

Pratt, O. E., & Doshi, R. (1984). Range of alcohol-induced damage in the developing central nervous system. *Ciba Foundation Symposium*. 105;142–56.

Proctor, W. R., Diao, L., Freund, R. K., Browning, M. D., & Wu, P. H. (2006). Synaptic GABAergic and glutamatergic mechanisms underlying alcohol sensitivity in mouse hippocampal neurons. *The Journal of Physiology*. 575(Pt 1);145–59.

Public Health Agency of Canada. (2005). *Fetal alcohol spectrum disorder (FASD)*. Available at: http://www.publichealth.gc.ca/fasd. Accessed: February 18, 2018.

Purves, D., Augustine, G. J., Fitzpatrick, D., Hall, W. C., LaMantia, A.-S., McNamara, J. O., & Williams, S. M. (2004). *Neuroscience* (3rd ed.) Sinauer Associates Inc. Sunderland.

Quenneville, S., Verde, G., Corsinotti, A., Kapopoulou, A., Jakobsson, J., Offner, S., Baglivo, I., Pedone, P. V., Grimaldi, G., Riccio, A., & Trono, D. (2011). In embryonic stem cells, ZFP57/KAP1 recognize a methylated hexanucleotide to affect chromatin and DNA methylation of imprinting control regions. *Molecular Cell*. 44(3);361–372.

Rajagopalan, V., Scott, J., Habas, P. A., Kim, K., Corbett-Detig, J., Rousseau, F., Barkovich, A. J., Glenn, O. A., & Studholme, C. (2011). Local Tissue Growth Patterns Underlying Normal Fetal Human Brain Gyrification Quantified In Utero. *Journal of Neuroscience*. 31(8);2878–2887.

Rakic, P., & Yakovlev, P. I. (1968). Development of the corpus callosum and cavum septi in man. *The Journal of Comparative Neurology*. 132(1);45–72.

Ratna, A., & Mandrekar, P. (2017). Alcohol and cancer: Mechanisms and therapies. *Biomolecules*. 7(3);1–20.

Razin, a, & Cedar, H. (1977). Distribution of 5-methylcytosine in chromatin. *Proceedings of the National Academy of Sciences of the United States of America*. 74(7);2725–2728.

Reik W, Dean W, W. J. (2001). Epigenetic reprogramming in mammalian development. *Science*. 293;19–25.

Resendiz, M., Mason, S., Lo, C. L., & Zhou, F. C. (2014). Epigenetic regulation of the neural transcriptome and alcohol interference during development. *Frontiers in Genetics*. 5(AUG);1–15.

Reynolds, J. N., Weinberg, J., Clarren, S., Beaulieu, C., Rasmussen, C., Kobor, M., Dube, M.-P., & Goldowitz, D. (2011). Fetal alcohol spectrum disorders: gene-environment interactions, predictive biomarkers, and the relationship between structural alterations in the brain and functional outcomes. *Seminars in Pediatric Neurology*. 18(1);49–55.

Rhein, M., Hagemeier, L., Klintschar, M., Muschler, M., Bleich, S., & Frieling, H. (2015). DNA methylation results depend on DNA integrity-role of post mortem interval. *Frontiers in Genetics*. 6(MAY);1–7.

Ring, J. A., Ghabrial, H., Ching, M. S., Smallwood, R. A., & Morgan, D. J. (1999). Fetal hepatic drug elimination. *Pharmacology & Therapeutics*. 84(3);429–45.

Risau, W., & Wolburg, H. (1990). Development of the blood-brain barrier. *Trends Neurosci*. 13(5);174–178.

Roebuck, T. M., Mattson, S. N., & Riley, E. P. (1998). A review of the neuroanatomical findings in children with fetal alcohol syndrome or prenatal exposure to alcohol. *Alcoholism, Clinical and Experimental Research*. 22(2);339–44.

Ronen, G. M., & Andrews, W. L. (1991). Holoprosencephaly as a possible embryonic alcohol effect. *American Journal of Medical Genetics*. 40(2);151–4.

Roozen, S., Peters, G.-J. Y., Kok, G., Townend, D., Nijhuis, J., & Curfs, L. (2016). Worldwide Prevalence of Fetal Alcohol Spectrum Disorders: A Systematic Literature Review Including Meta-Analysis. *Alcoholism, Clinical and Experimental Research*. 40(1);18–32.

Rose, N. R., & Klose, R. J. (2014). Understanding the relationship between DNA methylation and histone lysine methylation. *Biochimica et Biophysica Acta*. 1839(12);1362–72.

Rosenfeld, C. S. (2010). Animal models to study environmental epigenetics. *Biology of Reproduction*. 82(3);473–88.

Ross, C. P., & Persaud, T. V. (1989). Neural tube defects in early rat embryos following maternal

treatment with ethanol and caffeine. *Anatomischer Anzeiger*. 169(4);247–252.

Ryan, S. H., Williams, J. K., & Thomas, J. D. (2008). Choline supplementation attenuates learning deficits associated with neonatal alcohol exposure in the rat: Effects of varying the timing of choline administration. *Brain Research*. 1237;91–100.

Sadler, T. W. (2005). Embryology of neural tube development. *American Journal of Medical Genetics - Seminars in Medical Genetics*. 135 C(1);2–8.

Sakata-Haga, H., Sawada, K., Ohnishi, T., & Fukui, Y. (2004). Hydrocephalus following prenatal exposure to ethanol. *Acta Neuropathologica*. 108(5);393–398.

Salihu, H. M., Kornosky, J. L., Lynch, O., Alio, A. P., August, E. M., & Marty, P. J. (2011). Impact of prenatal alcohol consumption on placenta-associated syndromes. *Alcohol*. 45(1);73–79.

Sanders, J. L. (2009). Were our Forebears Aware of Prenatal Alcohol Exposure and Its Effects ? A Review of the History of Fetal Alcohol Spectrum Disorder. *Can J Clin Pharmacol*. 16(2);288–295.

Sarkar, D. K. (2016). Male germline transmits fetal alcohol epigenetic marks for multiple generations: A review. *Addiction Biology*. 21(1);23–34.

Sarnat, H. B., Philippart, M., Flores-Sarnat, L., & Wei, X.-C. (2015). Timing in neural maturation: arrest, delay, precociousness, and temporal determination of malformations. *Pediatric Neurology*. 52(5);473–86.

Saunders, N. R., Liddelow, S. A., & Dziegielewska, K. M. (2012). Barrier mechanisms in the developing brain. *Frontiers in Pharmacology*. 3(46);1–18.

Schneider, M. L., Moore, C. F., & Adkins, M. M. (2011). The effects of prenatal alcohol exposure on behavior: Rodent and primate studies. *Neuropsychology Review*. 21(2);186–203.

Schweizer, S., Meisel, A., & Märschenz, S. (2013). Epigenetic mechanisms in cerebral ischemia. *Journal of Cerebral Blood Flow & Metabolism*. 33(9);1335–1346.

Scott-Goodwin, A. C., Puerto, M., & Moreno, I. (2016). Toxic effects of prenatal exposure to alcohol, tobacco and other drugs. *Reproductive Toxicology*. 61;120–130.

Senturias, Y. S. N. (2014). Fetal alcohol spectrum disorders: An overview for pediatric and adolescent care providers. *Current Problems in Pediatric and Adolescent Health Care*. 44(4);74–81.

Serrano, M., Han, M., Brinez, P., & Linask, K. K. (2010). Fetal alcohol syndrome: cardiac birth defects in mice and prevention with folate. *American Journal of Obstetrics and Gynecology*.

203(1);75.e7-75.e15.

Shabihkhani, M., Lucey, G. M., Wei, B., Mareninov, S., Lou, J. J., Vinters, H. V, Singer, E. J., Cloughesy, T. F., & Yong, W. H. (2014). The procurement, storage, and quality assurance of frozen blood and tissue biospecimens in pathology, biorepository, and biobank settings. *Clinical Biochemistry*. 47(4–5);258–66.

Shabtai, Y., & Fainsod, A. (2018). Competition between ethanol clearance and retinoic acid biosynthesis in the induction of fetal alcohol syndrome. *Biochemistry and Cell Biology*. 96(2);148–160.

Sharma, S., De Carvalho, D. D., Jeong, S., Jones, P. a, & Liang, G. (2011). Nucleosomes containing methylated DNA stabilize DNA methyltransferases 3A/3B and ensure faithful epigenetic inheritance. *PLoS Genetics*. 7(2);e1001286.

Sheller, B., Clarren, S. K., Astley, S. J., & Sampson, P. D. (1988). Morphometric Analysis of Macaca nemestrina Exposed to Ethanol During Gestation. *Teratology*. 38;411–417.

Shen, E. Y., Ahern, T. H., Cheung, I., Straubhaar, J., Dincer, A., Houston, I., de Vries, G. J., Akbarian, S., & Forger, N. G. (2015). Epigenetics and sex differences in the brain: A genome-wide comparison of histone-3 lysine-4 trimethylation (H3K4me3) in male and female mice. *Experimental Neurology*. 268;21–9.

Shiraishi, K., Shindo, A., Harada, A., Kurumizaka, H., Kimura, H., Ohkawa, Y., & Matsuyama, H. (2018). Roles of histone H3.5 in human spermatogenesis and spermatogenic disorders. *Andrology*. 6(1);158–165.

Shukla, P. K., Sittig, L. J., Ullmann, T. M., & Redei, E. E. (2011). Candidate placental biomarkers for intrauterine alcohol exposure. *Alcoholism, Clinical and Experimental Research*. 35(3);559–65.

Shukla, S. D., Velazquez, J., French, S. W., Lu, S. C., Ticku, M. K., & Zakhari, S. (2008). Emerging role of epigenetics in the actions of alcohol. *Alcoholism, Clinical and Experimental Research*. 32(9);1525–34.

Siew, L. K., Love, S., Dawbarn, D., Wilcock, G. K., & Allen, S. J. (2004). Measurement of pre- and post-synaptic proteins in cerebral cortex: effects of post-mortem delay. *Journal of Neuroscience Methods*. 139(2);153–9.

Sikarwar, A. S., Hinton, M., Santhosh, K. T., Chelikani, P., & Dakshinamurti, S. (2014). Palmitoylation of Gαq determines its association with the thromboxane receptor in hypoxic

pulmonary hypertension. *American Journal of Respiratory Cell and Molecular Biology*. 50(1);135–143.

Simon, L., Jolley, S. E., & Molina, P. E. (2017). Alcoholic Myopathy: Pathophysiologic Mechanisms and Clinical Implications. *Alcohol Research: Current Reviews*. 38(2);e-1-e-11.

Singal, D., Brownell, M., Hanlon-Dearman, A., Chateau, D., Longstaffe, S., & Roos, L. L. (2016). Manitoba mothers and fetal alcohol spectrum disorders study (MBMomsFASD): protocol for a population-based cohort study using linked administrative data. *BMJ Open*. 6(9);e013330.

Sival, D. A., Guerra, M., den Dunnen, W. F. A., Bátiz, L. F., Alvial, G., Castañeyra-Perdomo, A., & Rodríguez, E. M. (2011). Neuroependymal denudation is in progress in full-term human foetal spina bifida aperta. *Brain Pathology*. 21(2);163–79.

Sjöholm, L. K., Ransome, Y., Ekström, T. J., & Karlsson, O. (2017). Evaluation of post-mortem effects on global brain DNA methylation and hydroxymethylation. *Basic & Clinical Pharmacology & Toxicology*. 122;208–213.

Smith, H. S. (2009). Opioid metabolism. *Mayo Clinic Proceedings*. 84(7);613–24.

Smith, S. M., Garic, A., Flentke, G. R., & Berres, M. E. (2014). Neural crest development in fetal alcohol syndrome. *Birth Defects Research. Part C, Embryo Today : Reviews*. 102(3);210–20.

Söderpalm, B., & Ericson, M. (2013). Neurocircuitry Involved in the Development of Alcohol Addiction : The Dopamine System and its Access Points. *Current Topics in Behavioural Neuroscience*. 13;127–161.

Solonskiĭ, A. V, & Kovetskiĭ, N. S. (1989). [Ultrastructural characteristics of embryonic brain cells in the offspring of alcoholic mothers]. *Zhurnal Nevropatologii i Psikhiatrii Imeni S.S. Korsakova (Moscow, Russia : 1952)*. 89(7);41–5.

Solonskiĭ, A. V, Kovetskiĭ, N. S., & Iarygina, E. G. (1991). [Development of embryonal brain synapses in the normal state and in maternal alcoholism]. *Zhurnal Nevropatologii i Psikhiatrii Imeni S.S. Korsakova (Moscow, Russia : 1952)*. 91(2);91–3.

Solonskiĭ, A. V, Logvinov, S. V, & Ketepova, N. A. (2007). [Development of brain vessels in human embryos and fetuses subjected to prenatal exposure to alcohol]. *Morfologiia (Saint Petersburg, Russia)*. 131(2);63–6.

Solonskii, A. V, Logvinov, S. V, & Kutepova, N. A. (2008). Development of brain vessels in human embryos and fetuses in conditions of prenatal exposure to alcohol. *Neuroscience and Behavioral Physiology*. 38(4);373–6.

Sorrells, S. F., Paredes, M. F., Cebrian-Silla, A., Sandoval, K., Qi, D., Kelley, K. W., James, D., Mayer, S., Chang, J., Auguste, K. I., Chang, E. F., Gutierrez, A. J., Kriegstein, A. R., Mathern, G. W., Oldham, M. C., Huang, E. J., Garcia-Verdugo, J. M., … Alvarez-Buylla, A. (2018). Human hippocampal neurogenesis drops sharply in children to undetectable levels in adults. *Nature*. 555(7696);377–381.

Spadoni, A. D., Mcgee, C. L., Fryer, S. L., & Riley, E. P. (2007). Neuroimaging and Fetal Alcohol Spectrum Disorders. *Neuroscience and Behavioural Reviews*. 31(2);239–245.

Spanagel, R. (2003). Alcohol addiction research : from animal models to clinics. *Best Practice and Research Cilinical Gastroenterology*. 17(4);507–518.

Spiegler, E., Kim, Y. K., Wassef, L., Shete, V., & Quadro, L. (2012). Maternal-fetal transfer and metabolism of vitamin A and its precursor β-carotene in the developing tissues. *Biochimica et Biophysica Acta - Molecular and Cell Biology of Lipids*. 1821(1);88–98.

Sprow, G. M., & Thiele, T. E. (2012). The neurobiology of binge-like ethanol drinking: Evidence from rodent models. *Physiology and Behavior*. 106(3);325–331.

Srinivasan, M., Sedmak, D., & Jewell, S. (2002). Effect of fixatives and tissue processing on the content and integrity of nucleic acids. *The American Journal of Pathology*. 161(6);1961–71.

St John, J. C., Facucho-Oliveira, J., Jiang, Y., Kelly, R., & Salah, R. (2010). Mitochondrial DNA transmission, replication and inheritance: a journey from the gamete through the embryo and into offspring and embryonic stem cells. *Human Reproduction Update*. 16(5);488–509.

Stadler, F., Kolb, G., Rubusch, L., Baker, S. P., Jones, E. G., & Akbarian, S. (2005). Histone methylation at gene promoters is associated with developmental regulation and region-specific expression of ionotropic and metabotropic glutamate receptors in human brain. *Journal of Neurochemistry*. 94(2);324–36.

Stan, A. D., Ghose, S., Gao, X.-M., Roberts, R. C., Lewis-Amezcua, K., Hatanpaa, K. J., & Tamminga, C. A. (2006). Human postmortem tissue: what quality markers matter? *Brain Research*. 1123(1);1–11.

Stånge, L., Carlström, K., & Eriksson, M. (1978). Hypervitaminosis a in early human pregnancy and malformations of the central nervous system. *Acta Obstetricia et Gynecologica Scandinavica*. 57(3);289–91.

Statistics Canada. (2017). CANSIM table 102-0552: Age-standardized mortality rates by selected causes, by sex (Both sexes).

Stephens, M. A. C., & Wand, G. (2012). Stress and the HPA Axis: Role of Glucocorticoid. *The Journal of the National Institute on Alcohol Abuse and Alcoholism*. 34(4);468–483.

Stiles, J., & Jernigan, T. L. (2010). The basics of brain development. *Neuropsychology Review*. 20(4);327–48.

Stockard, C. R. (1914). A study of further generations of mammals from ancestors. *Proceedings of the Society for Experimental Biology and Medicine*. xi;136–139.

Stoos, C., Nelsen, L., Schissler, K. A., Elliott, A. J., & Kinney, H. C. (2015). Fetal Alcohol Syndrome and Secondary Schizophrenia: A Unique Neuropathologic Study. *Journal of Child Neurology*. 30(5);601–605.

Stuppia, L., Franzago, M., Ballerini, P., Gatta, V., & Antonucci, I. (2015). Epigenetics and male reproduction: the consequences of paternal lifestyle on fertility, embryo development, and children lifetime health. *Clinical Epigenetics*. 7(1);120.

Subbanna, S., & Basavarajappa, B. S. (2014). Pre-administration of G9a/GLP inhibitor during synaptogenesis prevents postnatal ethanol-induced LTP deficits and neurobehavioral abnormalities in adult mice. *Experimental Neurology*. 261;34–43.

Subbanna, S., Nagre, N. N., Shivakumar, M., Umapathy, N. S., Psychoyos, D., & Basavarajappa, B. S. (2014). Ethanol induced acetylation of histone at G9a exon1 and G9a-mediated histone H3 dimethylation leads to neurodegeneration in neonatal mice. *Neuroscience*. 258;422–432.

Subbanna, S., Nagre, N. N., Umapathy, N. S., Pace, B. S., & Basavarajappa, B. S. (2015). Ethanol exposure induces neonatal neurodegeneration by enhancing CB1R Exon1 Histone H4K8 acetylation and up-regulating CB1R function causing neurobehavioral abnormalities in adult mice. *International Journal of Neuropsychopharmacology*. 18(5);1–15.

Subbanna, S., Shivakumar, M., Umapathy, N. S., Saito, M., Mohan, P. S., Kumar, A., Nixon, R. A., Verin, A. D., Psychoyos, D., & Basavarajappa, B. S. (2013). G9a-mediated histone methylation regulates ethanol-induced neurodegeneration in the neonatal mouse brain. *Neurobiology of Disease*. 54;475–85.

Summers, B. L., Rofe, A. M., & Coyle, P. (2009). Dietary zinc supplementation throughout pregnancy protects against fetal dysmorphology and improves postnatal survival after prenatal ethanol exposure in mice. *Alcoholism: Clinical and Experimental Research*. 33(4);591–600.

Sun, E., & Shi, Y. (2015). MicroRNAs: Small molecules with big roles in neurodevelopment and diseases. *Experimental Neurology*. 268;46–53.

Swift, R., & Davidson, D. (1998). Alcohol Hangover - Mechanisms and Mediators. *Alcohol Health and Research World*. 22(1);54–60.

Szutorisz, H., & Hurd, Y. L. (2016). Epigenetic effects of cannabis exposure. *Biological Psychiatry*. 79(7);586–594.

Taanman, J. W. (1999). The mitochondrial genome: structure, transcription, translation and replication. *Biochimica et Biophysica Acta*. 1410(2);103–23.

Tai, M., Piskorski, A., Kao, J. C. W., Hess, L. A., M de la Monte, S., & Gundogan, F. (2017). Placental Morphology in Fetal Alcohol Spectrum Disorders. *Alcohol and Alcoholism*. 52(2);138–144.

Tanabe, K., Liu, J., Kato, D., Kurumizaka, H., Yamatsugu, K., Kanai, M., & Kawashima, S. A. (2018). LC-MS/MS-based quantitative study of the acyl group- and site-selectivity of human sirtuins to acylated nucleosomes. *Scientific Reports*. 8(1);2656.

Tangsermkijsakul, A. (2016). Fetal Alcohol Syndrome in Sudden Unexpected Death in Infancy. *The American Journal of Forensic Medicine and Pathology*. 37(1);9–13.

Taniura, H., Sng, J. C. G., & Yoneda, Y. (2007). Histone modifications in the brain. *Neurochemistry International*. 51(2–4);85–91.

ten Donkelaar, H. J. (2000). Major Events in the Development of the Forebrain. *European Journal of Morphology*. 38(5);301–308.

ten Donkelaar, H. J., Lammens, M., Wesseling, P., Thijssen, H. O., & Renier, W. O. (2003). Development and developmental disorders of the human cerebellum. *Journal of Neurology*. 250(9);1025–1036.

Thanh, N. X., & Jonsson, E. (2015). Costs of Fetal Alcohol Spectrum Disorder in the Canadian Criminal Justice System. *Journal of Population Therapeutics and Clinical Pharmacology*. 22(1);e125-31.

Thinnes, C. C., England, K. S., Kawamura, A., Chowdhury, R., Schofield, C. J., & Hopkinson, R. J. (2014). Targeting histone lysine demethylases - Progress, challenges, and the future. *Biochimica et Biophysica Acta*. 1839(12);1416–1432.

Thirlwell, C., Eymard, M., Feber, A., Teschendorff, A., Pearce, K., Lechner, M., Widschwendter, M., & Beck, S. (2010). Genome-wide DNA methylation analysis of archival formalin-fixed paraffin-embedded tissue using the Illumina Infinium HumanMethylation27 BeadChip. *Methods*. 52(3);248–54.

Thomas, J. D., Biane, J. S., O'Bryan, K. A., O'Neill, T. M., & Dominguez, H. D. (2007). Choline supplementation following third-trimester-equivalent alcohol exposure attenuates behavioral alterations in rats. *Behavioral Neuroscience*. 121(1);120–130.

Thompson, A., Hackman, D., & Burd, L. (2014). Mortality in Fetal Alcohol Spectrum Disorders. *Open Journal of Pediatrics*. 4(1);21–33.

Thomson, A. (2000). Mechanisms of vitamin deficiency in chronic alcohol misusers and the development of the Wernicke-Korsakoff syndrome. *Alcohol and Alcoholism*. 35(1);2–7.

Treit, S., Chen, Z., Zhou, D., Baugh, L., Rasmussen, C., Andrew, G., Pei, J., & Beaulieu, C. (2017). Sexual dimorphism of volume reduction but not cognitive deficit in fetal alcohol spectrum disorders: A combined diffusion tensor imaging, cortical thickness and brain volume study. *NeuroImage. Clinical*. 15;284–297.

Treit, S., Zhou, D., Chudley, A. E., Andrew, G., Rasmussen, C., Nikkel, S. M., Samdup, D., Hanlon-Dearman, A., Loock, C., & Beaulieu, C. (2016). Relationships between Head Circumference, Brain Volume and Cognition in Children with Prenatal Alcohol Exposure. *PloS One*. 11(2);e0150370.

Trigo, J. M., Martin-García, E., Berrendero, F., Robledo, P., & Maldonado, R. (2010). The endogenous opioid system: a common substrate in drug addiction. *Drug and Alcohol Dependence*. 108(3);183–94.

Tsai, H., Grant, P. A., & Rissman, E. F. (2009). Sex differences in histone modifications in the neonatal mouse brain. *Epigenetics*. 4(1);47–53.

Turner, B. M. (1991). Histone acetylation and control of gene expression. *J. Cell Sci.* 99;13–20.

Vallés, S., Pitarch, J., Renau-Piqueras, J., & Guerri, C. (1997). Ethanol exposure affects glial fibrillary acidic protein gene expression and transcription during rat brain development. *Journal of Neurochemistry*. 69(6);2484–2493.

van der Wijst, M. G. P., van Tilburg, A. Y., Ruiters, M. H. J., & Rots, M. G. (2017). Experimental mitochondria-targeted DNA methylation identifies GpC methylation, not CpG methylation, as potential regulator of mitochondrial gene expression. *Scientific Reports*. 7(1);177.

Van Heertum, K., & Rossi, B. (2017). Alcohol and fertility: how much is too much? *Fertility Research and Practice*. 3(1);10.

van Rensburg, L. J. (1981). Major skeletal defects in the fetal alcohol syndrome. A case report. *South African Medical Journal*. 59(19);687–8.

Vassoler, F. M., White, S. L., Schmidt, H. D., Sadri-Vakili, G., & Christopher Pierce, R. (2013). Epigenetic inheritance of a cocaine-resistance phenotype. *Nature Neuroscience*. 16(1);42–47.

Veazey, K. J., Parnell, S. E., Miranda, R. C., & Golding, M. C. (2015). Dose-dependent alcohol-induced alterations in chromatin structure persist beyond the window of exposure and correlate with fetal alcohol syndrome birth defects. *Epigenetics & Chromatin*. 8(1);39.

Venters, B. J., & Pugh, B. F. (2009). How eukaryotic genes are transcribed. *Critical Reviews in Biochemistry and Molecular Biology*. 44(2–3);117–141.

Viteri, O. A., Soto, E. E., Bahado-Singh, R. O., Christensen, C. W., Chauhan, S. P., & Sibai, B. M. (2015). Fetal anomalies and long-term effects associated with substance abuse in pregnancy: a literature review. *American Journal of Perinatology*. 32(5);405–416.

Vlachou, S., & Markou, A. (2010). GABAB receptors in reward processes. *Advances in Pharmacology*. 58(10);315–71.

Voigt, P., Tee, W. W., & Reinberg, D. (2013). A double take on bivalent promoters. *Genes and Development*. 27(12);1318–1338.

Volpe, J. J. (2000). Overview: Normal and Abnormal Human Brain Development. *Mental Retardation and Developmental Disabilities Research Reviews*. 6(1);1–5.

Waddington, C. H. (1942). The Epigenotpye. *Endeavour*. ;18–20.

Waddington, C. H. (2012). The epigenotype. 1942. *International Journal of Epidemiology*. 41(1);10–3.

Wagner, M., Steinbacher, J., Kraus, T. F. J., Michalakis, S., Hackner, B., Pfaffeneder, T., Perera, A., Müller, M., Giese, A., Kretzschmar, H. a., & Carell, T. (2015). Age-Dependent Levels of 5-Methyl-, 5-Hydroxymethyl-, and 5-Formylcytosine in Human and Mouse Brain Tissues. *Angewandte Chemie International Edition*. 54;1–5.

Walker, D., Fisher, C., Sherman, A., Wybrecht, B., & Kyndely, K. (2005). Fetal alcohol spectrum disorders prevention: an exploratory study of women's use of, attitudes toward, and knowledge about alcohol. *Journal of the American Academy of Nurse Practitioners*. 17(5);187–193.

Wall, T. L., Carr, L. G., & Ehlers, C. L. (2003). Protective association of genetic variation in alcohol dehydrogenase with alcohol dependence in Native American Mission Indians. *American Journal of Psychiatry*. 160(1);41–46.

Wall, T. L., Luczak, S. E., & Hiller-Sturmhöfel, S. (2016). Biology, Genetics, and Environment - Underlying Factors Influencing Alcohol Metabolism. *Alcohol Research: Current Reviews*.

38(1);59–68.

Wang, L., Zhou, Y., Xu, L., Xiao, R., Lu, X., Chen, L., Chong, J., Li, H., He, C., Fu, X.-D., & Wang, D. (2015). Molecular basis for 5-carboxycytosine recognition by RNA polymerase II elongation complex. *Nature*.

Wang, N., Tikellis, G., Sun, C., Pezic, A., Wang, L., Wells, J. C. K., Cochrane, J., Ponsonby, A. L., & Dwyer, T. (2014). The effect of maternal prenatal smoking and alcohol consumption on the placenta-to-birth weight ratio. *Placenta*. 35(7);437–441.

Wang, Y., TesFaye, E., Yasuda, R. P., Mash, D. C., Armstrong, D. M., & Wolfe, B. B. (2000). Effects of post-mortem delay on subunits of ionotropic glutamate receptors in human brain. *Brain Research. Molecular Brain Research*. 80(2);123–31.

Wang, Z., Zang, C., Rosenfeld, J. a, Schones, D. E., Barski, A., Cuddapah, S., Cui, K., Roh, T.-Y., Peng, W., Zhang, M. Q., & Zhao, K. (2008). Combinatorial patterns of histone acetylations and methylations in the human genome. *Nature Genetics*. 40(7);897–903.

Warren, K. R. (2015). A Review of the History of Attitudes Toward Drinking in Pregnancy. *Alcoholism, Clinical and Experimental Research*. 39(7);1110–1117.

Watari, H., Born, D. E., & Gleason, C. A. (2006). Effects of first trimester binge alcohol exposure on developing white matter in fetal sheep. *Pediatric Research*. 59(4 Pt 1);560–564.

Wells, P. G., Bhatia, S., Drake, D. M., & Miller-Pinsler, L. (2016). Fetal oxidative stress mechanisms of neurodevelopmental deficits and exacerbation by ethanol and methamphetamine. *Birth Defects Research Part C - Embryo Today: Reviews*. 108(2);108–130.

Wen, L., & Tang, F. (2014). Genomic distribution and possible functions of DNA hydroxymethylation in the brain. *Genomics*. 104(5);341–6.

Weng, Y.-L., An, R., Shin, J., Song, H., & Ming, G. (2013). DNA modifications and neurological disorders. *Neurotherapeutics : The Journal of the American Society for Experimental NeuroTherapeutics*. 10(4);556–67.

West, J. R., Goodlett, C. R., Bonthius, D. J., Hamre, K. M., & Marcussen, B. L. (1990). Cell population depletion associated with fetal alcohol brain damage: Mechanisms of BAC-dependent cell loss. *Alcoholism: Clinical and Experimental Research*. 14(6);813–818.

Whiteman, V. E., Salemi, J. L., Mogos, M. F., Cain, M. A., Aliyu, M. H., & Salihu, H. M. (2014). Maternal opioid drug use during pregnancy and its impact on perinatal morbidity, mortality, and the costs of medical care in the United States. *Journal of Pregnancy*. (Article ID 906723);1–8.

Wilhelm, C. J., & Guizzetti, M. (2016). Fetal Alcohol Spectrum Disorders: An Overview from the Glia Perspective. *Frontiers in Integrative Neuroscience*. 9(January);1–16.

Wills, T. A., & Winder, D. G. (2013). Ethanol Effects on N -Methyl- D -Aspartate Receptors in the Bed Nucleus of the Stria Terminalis. *Cold Spring Harbor Perspective in Medicine*. 3;a012161.

Wilsnack, S. C., Wilsnack, R. W., Kantor, L. W., Dawson, D. A., Goldstein, R. B., Saha, T. D., & Grant, B. F. (2013). Focus on: women and the costs of alcohol use. *Alcohol Research : Current Reviews*. 148(2);2001–2002.

Wisniewski, K. (1983). A Clinical Neuropathological Study of the Fetal Alcohol Syndrome. *Neuropediatrics*. 14;197–201.

Woo, N. D., & Persaud, T. V. (1988). Rat embryogenesis following exposure to alcohol and nicotine. *Acta Anatomica*. 131(2);122–126.

World Health Organization. (2014). *Global status report on alcohol and health 2014* Geneva. Geneva. Available at: http://www.who.int/iris/bitstream/10665/112736/1/9789240692763_eng.pdf?ua=1. Accessed: March 8, 2018.

Wyatt, G. R. (1950). Occurrence of 5-Methyl-Cytosine in Nucleic Acids. *Nature*. 166;237–238.

Xi, J., & Yang, Z. (2008). Expression of RALDHs Xi(ALDH1As) and CYP26s in human tissues and during the neural differentiation of P19 embryonal carcinoma stem cell. *Gene Expression Patterns*. 8(6);438–442.

Xia, X., Lemieux, M. E., Li, W., Carroll, J. S., Brown, M., Liu, X. S., & Kung, A. L. (2009). Integrative analysis of HIF binding and transactivation reveals its role in maintaining histone methylation homeostasis. *Proceedings of the National Academy of Sciences*. 106(11);4260–4265.

Xu, B., Karayiorgou, M., & Gogos, J. A. (2010). MicroRNAs in psychiatric and neurodevelopmental disorders. *Brain Research*. 1338;78–88.

Yakovleva, A., Plieskatt, J. L., Jensen, S., Humeida, R., Lang, J., Li, G., Bracci, P., Silver, S., & Bethony, J. M. (2017). Fit for genomic and proteomic purposes: Sampling the fitness of nucleic acid and protein derivatives from formalin fixed paraffin embedded tissue. *PloS One*. 12(7);e0181756.

Yamaguchi, S., Hong, K., Liu, R., Inoue, A., Shen, L., Zhang, K., & Zhang, Y. (2013). Dynamics of 5-methylcytosine and 5-hydroxymethylcytosine during germ cell reprogramming. *Cell*

Research. 23(3);329–39.

Yang, P., Zhang, J., Shi, H., Zhang, J., Xu, X., Xiao, X., & Liu, Y. (2014). Developmental profile of neurogenesis in prenatal human hippocampus: An immunohistochemical study. *International Journal of Developmental Neuroscience*. 38;1–9.

Yang, Y., Phillips, O. R., Kan, E., Sulik, K. K., Mattson, S. N., Riley, E. P., Jones, K. L., Adnams, C. M., May, P. A., O'Connor, M. J., Narr, K. L., & Sowell, E. R. (2012). Callosal Thickness Reductions Relate to Facial Dysmorphology in Fetal Alcohol Spectrum Disorders. *Alcoholism: Clinical and Experimental Research*. 36(5);798–806.

Yang, Y., Roussotte, F., Kan, E., Sulik, K. K., Mattson, S. N., Riley, E. P., Jones, K. L., Adnams, C. M., May, P. A., O'Connor, M. J., Narr, K. L., & Sowell, E. R. (2012). Abnormal cortical thickness alterations in fetal alcohol spectrum disorders and their relationships with facial dysmorphology. *Cerebral Cortex*. 22(5);1170–1179.

Yigazu, P., Kalra, V., & Altinok, D. (2014). Brainstem disconnection in a late preterm neonate with classic features of fetal alcohol syndrome. *Pediatric Neurology*. 51(5);745–6.

Yohn, N. L., Bartolomei, M. S., & Blendy, J. A. (2015). Multigenerational and transgenerational inheritance of drug exposure: The effects of alcohol, opiates, cocaine, marijuana, andnicotine. *Progress in Biophysics and Molecular Biology*. 118(1–2);21–33.

Young, J. K., Giesbrecht, H. E., Eskin, M. N., Aliani, M., & Suh, M. (2014). Nutrition implications for fetal alcohol spectrum disorder. *Advances in Nutrition (Bethesda, Md.)*. 5(6);675–692.

Yu, M., Hon, G. C., Szulwach, K. E., Song, C.-X., Jin, P., Ren, B., & He, C. (2012). Tet-assisted bisulfite sequencing of 5-hydroxymethylcytosine. *Nature Protocols*. 7(12);2159–70.

Yue, Y., Liu, J., & He, C. (2015). RNA N6-methyladenosine methylation in post-transcriptional gene expression regulation. *Genes and Development*. 29(13);1343–1355.

Yun, M., Wu, J., Workman, J. L., & Li, B. (2011). Readers of histone modifications. *Cell Research*. 21(4);564–578.

Zakhari, S. (2006). Overview: how is alcohol metabolized by the body? *Alcohol Research & Health : The Journal of the National Institute on Alcohol Abuse and Alcoholism*. 29(4);245–254.

Zakhari, S. (2013). Alcohol Metabolism and Epigenetics Changes. *Alcohol Research : Current Reviews*. 35(1);6–16.

Zakhary, S. M., Ayubcha, D., Dileo, J. N., Jose, R., Leheste, J. R., Horowitz, J. M., & Torres, G. (2010). Distribution analysis of deacetylase SIRT1 in rodent and human nervous systems.

Anatomical Record. 293(6);1024–32.

Zampieri, M., Ciccarone, F., Calabrese, R., Franceschi, C., Bürkle, A., & Caiafa, P. (2015). Reconfiguration of DNA methylation in aging. *Mechanisms of Ageing and Development*. 151;1–11.

Zhang, C. R., Ho, M. F., Vega, M. C. S., Burne, T. H. J., & Chong, S. (2015). Prenatal ethanol exposure alters adult hippocampal VGLUT2 expression with concomitant changes in promoter DNA methylation, H3K4 trimethylation and miR-467b-5p levels. *Epigenetics and Chromatin*. 8(1);1–12.

Zhang, F. F., Cardarelli, R., Carroll, J., Fulda, K. G., Kaur, M., Gonzalez, K., Vishwanatha, J. K., Santella, R. M., & Morabia, A. (2011). Significant differences in global genomic DNA methylation by gender and race/ethnicity in peripheral blood. *Epigenetics*. 6(5);623–9.

Zhang, J., Parvin, J., & Huang, K. (2012). Redistribution of H3K4me2 on neural tissue specific genes during mouse brain development. *BMC Genomics*. 13(Suppl 8);S5.

Zhang, T.-Y., Keown, C. L., Wen, X., Li, J., Vousden, D. A., Anacker, C., Bhattacharyya, U., Ryan, R., Diorio, J., O'Toole, N., Lerch, J. P., Mukamel, E. A., & Meaney, M. J. (2018). Environmental enrichment increases transcriptional and epigenetic differentiation between mouse dorsal and ventral dentate gyrus. *Nature Communications*. 9(1);298.

Zheng, J., Li, X., Shan, D., Zhang, H., & Guan, D. (2012). DNA degradation within mouse brain and dental pulp cells 72 hours postmortem. *Neural Regeneration Research*. 7(4);290–4.

Zhou, F. C. (2012). DNA methylation program during development. *Frontiers in Biology*. 7(6);485–494.

Zhou, F. C., Balaraman, Y., Teng, M., Liu, Y., Singh, R. P., & Nephew, K. P. (2011). Alcohol Alters DNA Methylation Patterns and Inhibits Neural Stem Cell Differentiation. *Alcoholism: Clinical and Experimental Research*. 35(4);735–746.

Zhou, Y., & Grummt, I. (2005). The PHD finger/bromodomain of NoRC interacts with acetylated histone H4K16 and is sufficient for rDNA silencing. *Current Biology : CB*. 15(15);1434–8.

Zhou, Z., Enoch, M.-A., & Goldman, D. (2014). Gene expression in the addicted brain. *International Review of Neurobiology*. 116;251–73.

Zimmerberg, B., & Scalzi, L. V. (1989). Commissural size in neonatal rats: effects of sex and prenatal alcohol exposure. *International Journal of Developmental Neuroscience : The Official Journal of the International Society for Developmental Neuroscience*. 7(1);81–86.

Zindel, L. R., & Kranzler, H. R. (2014). Pharmacotherapy of Alcohol Use Disorders : Seventy-Five Years of Progress. *Journal of Studies on Alcohol and Drugs*. 75(Supplement 17);79–88.

Zoghbi, H. Y., & Beaudet, A. L. (2016). Epigenetics and Human Disease. *Cold Spring Harb Perspect Biol*. 8;1–29.

Zuo, X., Sheng, J., Lau, H. T., McDonald, C. M., Andrade, M., Cullen, D. E., Bell, F. T., Iacovino, M., Kyba, M., Xu, G., & Li, X. (2012). Zinc finger protein ZFP57 requires its co-factor to recruit DNA methyltransferases and maintains DNA methylation imprint in embryonic stem cells via its transcriptional repression domain. *Journal of Biological Chemistry*. 287(3);2107–2118.